Faithful DNA Repair of 7,8-dihydro-8-oxo-guanine Lesions by Human Enzymes

Dissertation

zur

Erlangung der naturwissenschaftlichen Doktorwürde (Dr.sc.nat.)

volgelegt der

Mathematisch-naturwissenschaftlichen Fakultät

der

Universität Zürich

von

Barbara van Loon

aus

Kroatien

Promotionskomitee

Prof. Dr. Ulrich Hübscher (Vorsitz)

Prof. Dr. Michael Hengartner

Prof. Dr. Eugenia Dogliotti

Zürich, 2010

1. TABLE OF CONTENTS

Page

2. ABSTRACT

Reactive oxygen species (ROS) attack DNA and induce, among other lesions, about 1,000 7,8-dihydro-8-oxo-guanine (8-oxo-G) alterations per cell/per day. The presence of 8-oxo-G on the replicating strand leads to frequent (10-75%) misincorporation of adenine (A) opposite a lesion (formation of A:8-oxo-G mispairs). In contrary to many other DNA damages, the A:8-oxo-G mispair is not detected by the 3'→5' exonuclease proofreading activity of replicative DNA polymerases (pols) δ and ε, thus resulting in C:G to A:T transversion mutations. The subsequent repair mechanism allowing the removal of A and formation of C:8-oxo-G base pair is essential to prevent C:G to A:T transversion mutations. The MutY glycosylase homologue (MUTYH) is initiating the repair by recognizing A:8-oxo-G mispair and removing the A. During subsequent BER, a specialized repair DNA pol that will catalyze with high preference the accurate (incorporation of dCTP) bypass of 8-oxo-G is needed. Our laboratory has recently shown that the BER enzyme DNA pol λ, together with the auxiliary proteins replication protein A (RP-A) and proliferating cell nuclear antigen (PCNA), has the unique ability among human DNA pols to efficiently incorporate a C opposite an 8-oxo-G, with error frequencies in the range of 10^{-3}. Although these data implicated that DNA pol λ plays a key role in the repair of oxidative damage, its function in the MUTYH initiated BER has not been explored so far.

In the present work an accurate BER pathway for the repair of A:8-oxo-G mispairs coordinated by MUTYH and DNA pol λ is proposed. Immunofluorescence experiments, in the cells exposed to ROS, suggest the involvement of MUTYH and DNA pol λ in the 8-oxo-G repair. Additionally, upon treatment of the cells with H_2O_2, a dramatic increase in protein levels of MUTYH and DNA pol λ is observed, directly indicating the activation of MUTYH/DNA pol λ-dependent repair pathway.

The cross-linking assay with human whole cell extracts provides and evidence, that MUTYH, DNA pol λ, PCNA, flap endonuclease 1 (FEN1) and DNA ligases I and III are the crucial components of A:8-oxo-G repair pathway. Moreover, by using a novel 8-oxo-G specificity assay and recombinant human

proteins each individual step of this repair pathway is characterized. In particular these steps are:

i. the replicative enzyme DNA pol δ incorporates an incorrect dATP opposite 8-oxo-G;
ii. MUTYH recognizes the A from the miscoded replication product;
iii. apurinic endonuclease 1 (APE1) incises the apurinic site;
iv. DNA pol λ in the presence of PCNA and RP-A efficiently incorporates the correct dCTP opposite a lesion and upon strand displacement adds an additional nucleotide;
v. FEN1 cuts one nucleotide flap;
vi. DNA ligase I preferentially seals the accurate (C:8-oxo-G), but not inaccurate (A:8-oxo-G) product.

In summary, the data presented in this thesis suggest the existence of novel cellular response pathway to ROS, important to prevent C:G to A:T mutations formation and thereby to sustain genomic stability.

3. ZUSAMMENFASSUNG

Die DNS wird ständig durch reaktive Sauerstoffradikale (ROS) attackiert, welche unter anderem zur Entstehung von etwa 1'000 sogenannten 7,8-dihydro-8-oxo-Guanin (8-oxo-G) Schäden pro Zelle und Tag führen. Ein 8-oxo-G auf dem zu replizierenden DNS Strang führt häufig zum Fehleinbau von Adenin gegenüber dem 8-oxo-G Schaden, also zu A:8-oxo-G Basenpaaren. Im Gegensatz zu vielen anderen DNS Schäden wird die A:8-oxo-G Fehlpaarung nicht durch die exonukleolytische Korrekturlesefunktion der replikativen DNA-Polymerasen (pols) δ und ε erkannt, was zur Entstehung von C:G zu A:T Transversionen führen kann. Der Reparaturmechanismus, der die Entfernung von A gegenüber 8-oxo-G erlaubt, ist von höchster Wichtigkeit, um die Entstehung solcher C:G zu A:T Transversionen zu verhindern. Dieser Mechanismus wird durch die MutY Glycosylase (MUTYH) initiiert, welche das fehlgepaarte A gegenüber von 8-oxo-G erkennt und entfernt. In der daraufhin folgenden Basenexzisionsreparatur (BER) wird eine auf die DNS-Reparatur spezialisierte DNA pol, die eine hohe Präferenz für den Einbau der korrekten Base C gegenüber 8-oxo-G aufweist, gebraucht. Unser Labor hat kürzlich gezeigt, dass das BER Enzym DNA pol λ in Zusammenarbeit mit den Kofaktoren Replikations Protein A (RP-A) und dem Kenrantigen aus proliferierenen Zellen (PCNA), eine einzigartig hohe Präferenz für den Einbau des korrekten C gegenüber von 8-oxo-G aufweist. Die Fehlerrate von pol λ beim Einbau gegenüber von 8-oxo-G liegt im Bereich von 10^{-3}. Obwohl diese Daten dafür sprechen, dass DNA pol λ eine Schlüsselrolle in der Reparatur von oxidativen Schäden spielt, wurde ihre Rolle in der durch MUTYH initiierten BER bisher noch nicht im Detail erforscht.

In der vorliegenden Dissertationsarbeit wird das Vorhandensein einer exakten BER-Maschinerie für die Reparatur von A:8-oxo-G Fehlpaarungen, die durch MUTYH und DNA pol λ koordiniert wird, vorgeschlagen. Immunfluoreszenz-Experimente in Zellen, die ROS ausgesetzt wurden, weisen auf eine Involvierung von MUTYH und DNA pol λ in der Reparatur von 8-oxo-G hin. Zusätzlich wurde eine dramatische Erhöhung der Proteinmengen von

MUTYH und DNA pol λ in H_2O_2 behandelten Zellen beobachtet, was direkt auf die Aktivierung einer MUTYH/DNA pol λ-abhängigen Reparaturmaschinerie hinweist.

Ein Experiment, in dem Proteine mit der DNS verknüpft werden zeigt, dass MUTYH, DNA pol λ, PCNA, flap endonuklease 1 (FEN1) und die DNA ligase I und III wichtige Komponenten der A:8-oxo-G Reparaturmaschinerie darstellen. Des Weiteren wurde jeder einzelne Schritt dieses Reparaturmechanismus mit Hilfe von rekombinanten menschlichen Proteinen und mittels eines neuartigen 8-oxo-G Spezifitäts-Assays charakterisiert. Im Detail sind dies die folgenden Schritte.

i. Die replikative DNA pol δ inkorporiert ein inkorrektes dATP gegenüber von 8-oxo-G;
ii. MUTYH erkennt und entfernt die fehlgepaarte Base A;
iii. Apurinische endonuklease 1 (APE1) schneidet die apurinische Stelle ein
iv. DNA pol λ inkorporiert in Zusammenarbeit mit PCNA und RP-A effizient ein korrektes C gegenüber dem Schaden und fügt nach darauf folgender Strangdislokation noch ein weiteres Nukleotid ein;
v. FEN1 schneidet den um 1 Nukleotid überstehenden Strang ab;
vi. DNA ligase I versiegelt bevorzugt das korrekte (C:8-oxo-G), aber nicht das inkorrekte (A:8-oxo-G) Produkt.

Zusammenfassend weisen die Daten in der vorgelegten Dissertation auf die Existenz einer neuartigen zellulären Antwort auf ROS hin, welche wichtig ist, um C:G zu A:T Transversionen zu verhindern und somit die genomische Stabilität zu erhalten.

4. ABBREVIATIONS

A	adenine
AP	apurinic/apyrimidinic
APC	adenomatous polyposis coli
APE1	apurinic/apyrimidinic endonuclease 1
BER	base excision repair
BRCT	BRAC1 (breast-cancer-susceptibility protein-1) C-terminal domain
C	cytosine
CDK	cyclin dependent kinase
CPD	cyclobutane pyrimidine dimer
dATP	deoxyadenosine triphosphate
dCTP	deoxycytidine triphosphate
DHU	5,6-dihydrouracil
DNA	deoxyribonucleic acid
DNA pol	DNA polymerase
dNTP	deoxyribonucleotide triphosphate
ds	double strand
εA	ethenoadenine
DSBR	double strand break repair
faPyG	2,6-diamino-4-hydroxy-5-N-methylformamidopyrimidine
FEN1	flap endonuclease 1
G	guanine
HhH	helix-hairpin-helix
H_2O_2	hydrogen peroxid
IR	ionising radiation
kDa	kilodalton
LP-BER	long patch base excision repair
M	molar (concentration)
MAP	MUTYH-associated polyposis
mol	mole(s)
MTH1	8-oxo-G dGTPase
MUTYH	MutY glycosylase homologue
NEIL	endonuclease VIII (Nei)-like protein
NER	nucleotide excision repair
NHEJ	non-homologous end-joining
nt	nucleotide
NTase	nucleotidyltransferase
O6-mG	O^6-methylguanine
$\cdot O_2$	peroxide radical
·OH	hydroxyl radical
PCNA	proliferating cell nuclear antigen
PNK	polynucleotide kinase
Ref-1	redox factor
RF-C	replication factor C
ROS	reactive oxygen species
RP-A	replication protein A

SP-BER	short patch base excision repair
ss	single strand
SSB	single strand binding protein
T	thymine
TG	thymidine glycol
UNG	uracil DNA glycosylase
WCE	whole cell extract
XRCC1	X-ray repair cross complementing 1 protein
1-mA	1- methlyadenine
3-mA	3- methlyadenine
5'dRp	deoxyribose-5'-phosphate
5-foU	5-formyluracil
5-ohC	5-hydroxycytosine
6-4 PD	6-4 pyrimidine dimer
8-oxo-G	7,8-dihydro-8-oxo-guanine

5. INTRODUCTION

5.1. DNA Base Damage

DNA is a dynamic structure, subjected to a constant changes. Some of these changes are alterations in the chemistry of the normal nucleotides, also known as DNA damage (1). Depending on the source, DNA damage can be classified in two major classes: (i) spontaneous and (ii) environmental (2).

Three out of four bases normally present in the DNA, cytosine (C), adenine (A) and guanine (G), contain amino groups. The loss of these groups can occur spontaneously in pH- and temperature-dependent reactions of DNA. The result is the conversion of affected bases to uracil, hypoxanthine, xanthine and thymine (T) (Figure 1), respectively. Products of deamination present lesions that can during DNA synthesis result in altered base pairing and lead to mutations (3,4).

One of the most frequent types of endogenous damage are apurinic/apyrimidinic (AP) sites (1). The AP sites can arise at a substantial rate during spontaneous hydrolytic DNA depurination or depyrimidination. AP sites are also present as the central intermediates during base excision repair (BER). These sites are dangerous lesions, that block normal DNA replication, with cytotoxic and mutagenic consequences (5). Oxidative damage to DNA, produces structurally distinct abasic sites, known as oxidized AP sites. Such sites are 2-deoxyribonolactone and lesions at DNA strand breaks, such as 3'phosphoglycolate esters.

Enzymatic methylation of DNA bases, predominantly C, plays an important role in gene regulation. However, the nonenzymatic alkylation from endogenous sources or exposure to DNA alkylating agents leads to the formation of cytotoxic and mutagenic products (6,7). Methyl groups bound covalently to DNA bases result frequently in formation of mutagenic lesions, such as 3-methyladenine, O^6-methylguanine, 1-methlyadenine and *N*-methylated-2,6-diamino-4-hydroxy-5-formamidopyrimidine (Figure 1).

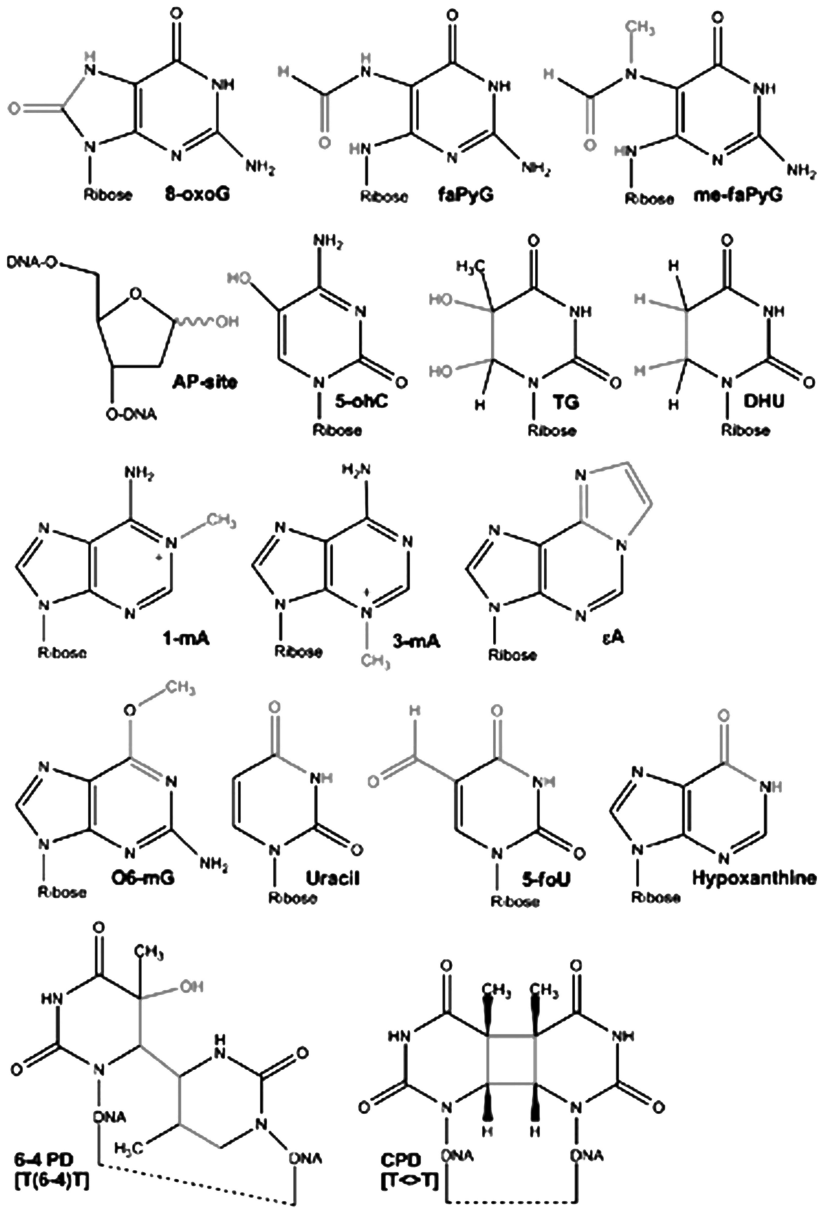

Figure 1. Examples of common base damages in genomic DNA. 8-oxo-G, 7,8-dihydro-8-oxo-guanine; faPyG, 2,6-diamino-4-hydroxy-5-N-methylformamidopyrimidine; AP site, apurinic/apyrimidinic site; 5-ohC, 5-hydroxycytosine; TG, thymidine glycol; DHU, 5,6-dihydrouracil; 1-mA, 1- methlyadenine; 3-mA, 3- methlyadenine; εA, ethenoadenine; O6-mG, O^6-methylguanine; 5-foU, 5-formyluracil; 6-4 PD, 6-4 pyrimidine dimer (here, thymine-thymine dimer [T(6-4)T]); CPD, cyclobutane pyrimidine dimer (here thymine-thymine dimer [T<>T]). Adopted from: Dalhus, B., Laerdahl, J. K., Backe, P. H. & Bjoras, M. (2009). DNA base repair - recognition and initiation of catalysis. *FEMS Microbiol Rev* (ahead of print).

Besides deamination, spontaneous hydrolysis and nonenzymatic methylation, exposure to the reactive oxygen species (ROS) is considered to be the major source of spontaneous damage. ROS damage vital cellular

macromolecules such as, proteins, lipids and DNA (8). In the cells, oxygen radicals are probably the result of leakage associated with the reduction of oxygen to water during mitochondrial respiration. During this process singlet oxygen, peroxide radicals ($\cdot O_2$), hydrogen peroxide (H_2O_2) and hydroxyl radicals ($\cdot OH$) are formed. The ROS can also be produced as a consequence of ionising radiation (IR), chemotherapeutic drugs and environmental exposure to transition metal and chemical oxidants (9,10). When ROS react with DNA, oxidized bases are generated (11). The most frequent oxidative lesions are 7,8-dihydro-8-oxo-guanine (8-oxo-G), formamidopyrimidine, 2,6-diamino-4-hydroxy-5-formamidopyrimidine and 4,6-diamino-5-formamidopyrimidine (12). Other important oxidative lesions include several premutagenic oxidized pyrimidines such as thymidine glycol, 5-hydroxycytosine, dihydrothymine and dihydrouracil (Figure 1). Persistence of oxidative DNA lesions in the genome can lead to point mutations.

DNA damage can also be caused by UV radiation. At the wave lengths (~260nm) that approach DNA absorption maximum, the adjacent pyrimidines become covalently linked. The structure formed by this photochemical cycloaddition is referred to as a cyclobutane dipyrimidine or pyrimidine dimer. The toxic effects of these unrepaired DNA lesions are commonly associated with transcription blockage and in addition, there is increasing evidence supporting a role for replication blockage as an apoptosis-inducing signal (13).

The variety of DNA damages must therefore be efficiently corrected by different DNA repair mechanisms in order for the genome to be faithfully reproduced, with a low rate of mutations, thus preventing cell death or an altered phenotype that can lead to cancer.

5.2. Base Excision Repair

In order to repair DNA, cells have evolved different mechanisms. The BER pathway is the primary repair system involved in the removal of damaged DNA bases. In addition, several enzymes that remove endogenous damage by damage-specific endonuclease or by direct reversal activity, such as methyl transferases, photolyases and dioxygenases, complement the BER pathway.

A) Short-patch BER

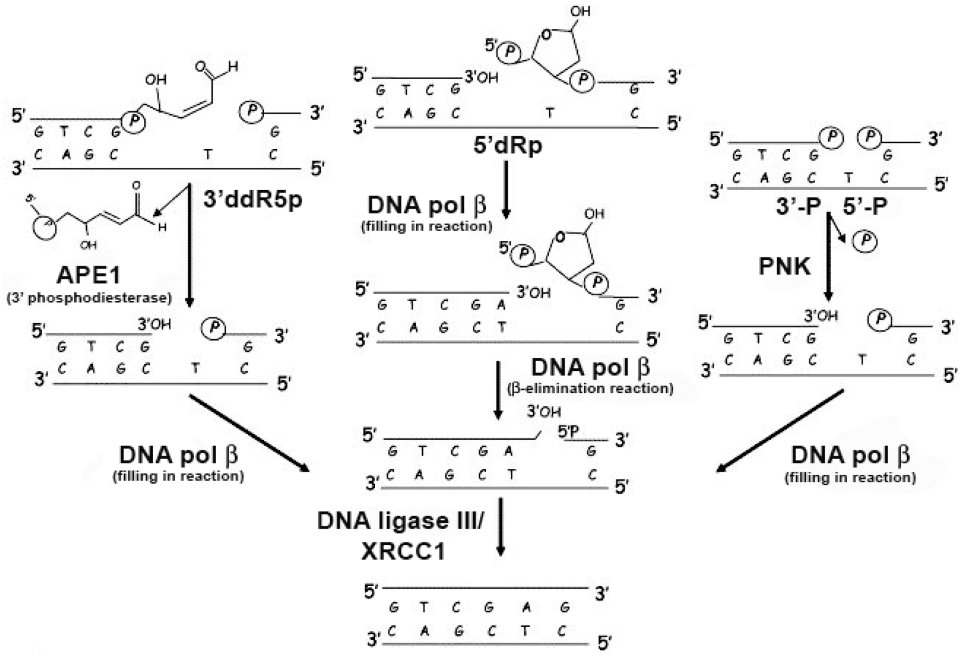

B) Long-patch BER

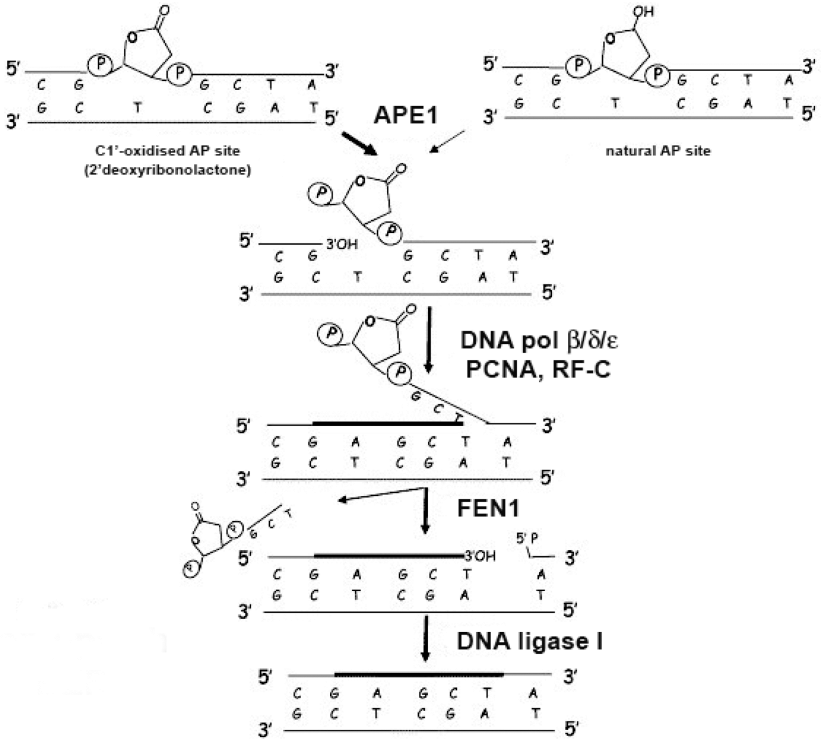

Figure 2. Different base excision repair (BER) sub-pathways. A) Short-patch BER. **B)** Long-patch BER. For more details see the text. Adopted from: Fortini, P. & Dogliotti, E. (2007). Base damage and single strand break repair: mechanisms and functional significance of short- and long-patch repair subpathways. *DNA Repair (Amst)* **6**, 398-409.

The BER pathway (Figure 2) is initiated by DNA glycosylases that recognize nucleotide lesions and excise the damaged DNA bases, by cleaving of the *N*-glycosylic bond between the 2'-deoxyribose and the damaged base (6,14,15). All organisms possess several DNA glycosylases that recognize and remove different DNA damages. The specificity of the BER pathway is determined by the type of glycosylase, that initiates it (6). DNA glycosylases are classified as mono- or bifunctional based on their reaction mechanism.

The monofunctional DNA glycosylases attack the anomeric carbon of the damaged base with an activated water molecule, thereby creating a free base and an AP site. The major 5' AP endonuclease, apurinic/apyrimidinic endonuclease 1 (APE1) utilizes the AP site and generates a DNA repair intermediate that contains a single strand (ss) break with 3'-hydroxyl and 5'-deoxyribose-5'-phosphate (5'dRp) termini (16). The 5'dRp terminus is next excised by the dRp lyase activity of DNA polymerase (pol) β and a single nucleotide gap is created. The bifunctional DNA glycosylases, upon recognition and excision of the damaged base, incise, by an associated AP lyase activity (β elimination activity), the strand 3' of the AP site. The remaining unsaturated 3' abasic fragment becomes a substrate for the APE1 and thus a single nucleotide gap is produced.

Further DNA repair is achieved through at least two distinct BER subpathways (i) short-patch BER (SP-BER) (Figure 2A) and (ii) long-patch BER (LP-BER) (Figure 2B). Distinct feature of these two subpathways is the size of the repair patch synthesized by repair DNA pol: (i) one nucleotide in the case of SP-BER (17), and (ii) two to twelve nucleotides in the case of LP-BER (18,19). DNA pol β is the major repair polymerase in SP-BER. However, in the LP-BER DNA pol β most likely incorporates the first nucleotide (20) and the elongation step is carried out by replicative DNA pol δ or ε. Additional players in LP-BER are (i) replication factor C (RF-C) that is required to load proliferating cell nuclear antigen (PCNA) onto the DNA, (ii) PCNA is the sliding clamp for DNA pols and (iii) flap endonuclease 1 (FEN1), a structure specific nuclease that excises the displaced oligonucleotide (21). The final ligation step is in SP-BER coordinated by DNA ligase III/X-ray repair cross complementing 1 protein (XRCC1) complex (22) and in LP-BER by DNA ligase I (23).

Recently an APE1-independent BER pathway has been described (24). Upon base excision, the endonuclease VIII (Nei)-like proteins, NEIL1 and NEIL2, cleave DNA at the AP site by βδ elimination leaving at 3' phosphate that is then removed by polynucleotide kinase (PNK) (Figure 2A, right track).

It is important to notice that the mechanisms described above and presented in Figure 2 are the result of studies carried out *in vitro* by using mammalian extracts or purified proteins on synthetic DNA molecules containing single lesions.

The importance of the proper functioning of the BER pathways is illustrated in the phenotypes seen in mouse knockout strains. BER defects appear to be incompatible with life. Mouse knockouts of genes coding for the core BER proteins; APE1 (25), DNA pol β (26), XRCC1 (27), FEN1 (28) and DNA ligase I (29), are embryonic lethal. So far, the targeted disruption of DNA glycosylases in the mouse genome has produced either an absent or a mild phenotype. This is likely due to the broad and partially overlapped substrate specificity of the different DNA glycosylases. Genetic diseases caused by mutations in BER genes are less common than those caused by mutations in other DNA repair pathway genes. However, 30% of all human tumours examined have variant (30) or misregulated DNA pol β proteins (31).

5.3. The Special Problem of 8-oxo-guanine

DNA bases are particularly susceptible to oxidation mediated by ROS. The low redox potential of G makes this base especially vulnerable (32). The 8-oxo-G is the most often generated oxidation product of G, arising by the introduction of oxo group on the carbon at position 8 (C8) and a hydrogen atom on the nitrogen at the position 7 (N7). The estimated steady-state level of 8-oxo-G lesions is about 10^3 per cell/per day in normal tissues and up to 10^5 lesions per cell/per day in cancer tissues (33). The presence of 8-oxo-G is often used as a cellular biomarker to indicate the extent of oxidative stress (34). The 8-oxo-G in *syn* conformation is particularly mutagenic because of its strong ability to functionally mimic T (Figure 3). In contrast to many other types of DNA damage, this structural feature allows the efficient, but inaccurate, bypass of 8-oxo-G by replicative DNA pols (35), resulting in a formation of

stable A(*anti*):8-oxo-G(*syn*) Hoogsteen mispair. These mispairs mimic normal base pairs and are not detected by the 3'→5' exonuclease proofreading activity of the replicative DNA pols. In contrast, the formation of C(*anti*):8-oxo-G(*anti*) base pair during DNA replication induces template and DNA pol distortions similar to those seen when the active site of DNA pol encounters mismatches.

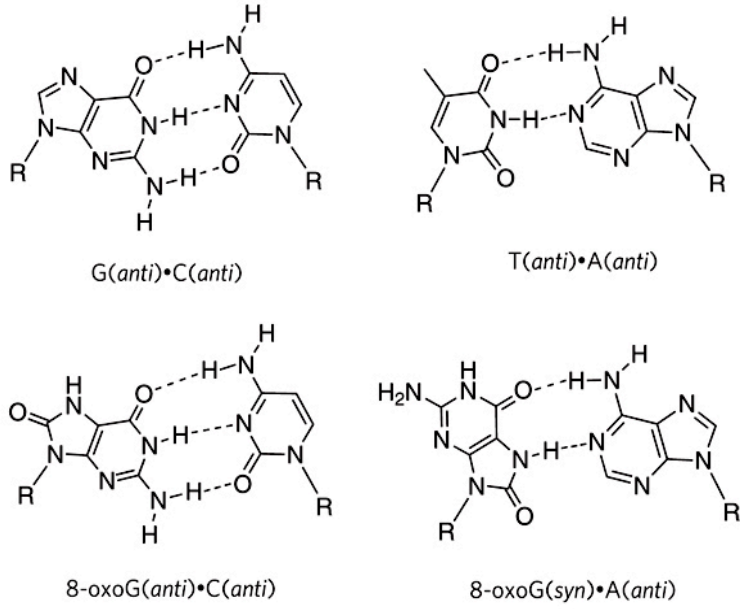

Figure 3. Structure of 8-oxo-G containing base pairs. The structures of the C:G and A:T base pairs (top) are compared with those of C:8-oxo-G and A:8-oxo-G. 8-oxo-G (bottom) differs from G by an oxo croup at C8 and an NH at N7. This subtle change allows 8-oxo-G to base pair easily with either A or C. Adopted from: David, S. S., O'Shea, V. L. & Kundu, S. (2007). Base-excision repair of oxidative DNA damage. *Nature* **447**, 941-50.

Failure to remove 8-oxo-G before replication leads to C:G to A:T transversion mutations. To reduce the mutagenic effect of 8-oxo-G, many organisms developed a three-component enzyme system (termed the 'GO system' after 8-oxo-G). In humans this system consists of the (i) 8-oxo-dGTPase (MTH1), and the two BER proteins (ii) 8-oxo-G DNA glycosylase (OGG1) and (iii) the MutY glycosylase homologue (MUTYH) (36). MTH1 hydrolyses 8-oxo-dGTP, thus removing it from the nucleotide pool so that it cannot be incorporated by DNA pols. OGG1 targets the C:8-oxo-G mispair, removes the lesion and in subsequent processing by other enzymes of the BER pathway, the C:G base pair is restored (Figure 4). However those 8-oxo-

G lesions that stay undetected or those formed during the S-phase become a substrate for replicative DNA pols and inaccurate bypass of 8-oxo-G occurs. The resultant A:8-oxo-G mispair is recognized by MUTYH and A is removed (Figure 4). During subsequent BER, a specialized repair DNA pol that will catalyze with high preference the accurate (incorporation of dCTP) bypass of 8-oxo-G is required. However, if a repair DNA pol is not faithful, inaccurate repair (formation of A:8-oxo-G mispair) might occur. Thus upon presence of 8-oxo-G in DNA, there are two possible processes which can lead to C:G to A:T transversion mutations, (i) DNA replication and (ii) inaccurate DNA repair (Figure 4).

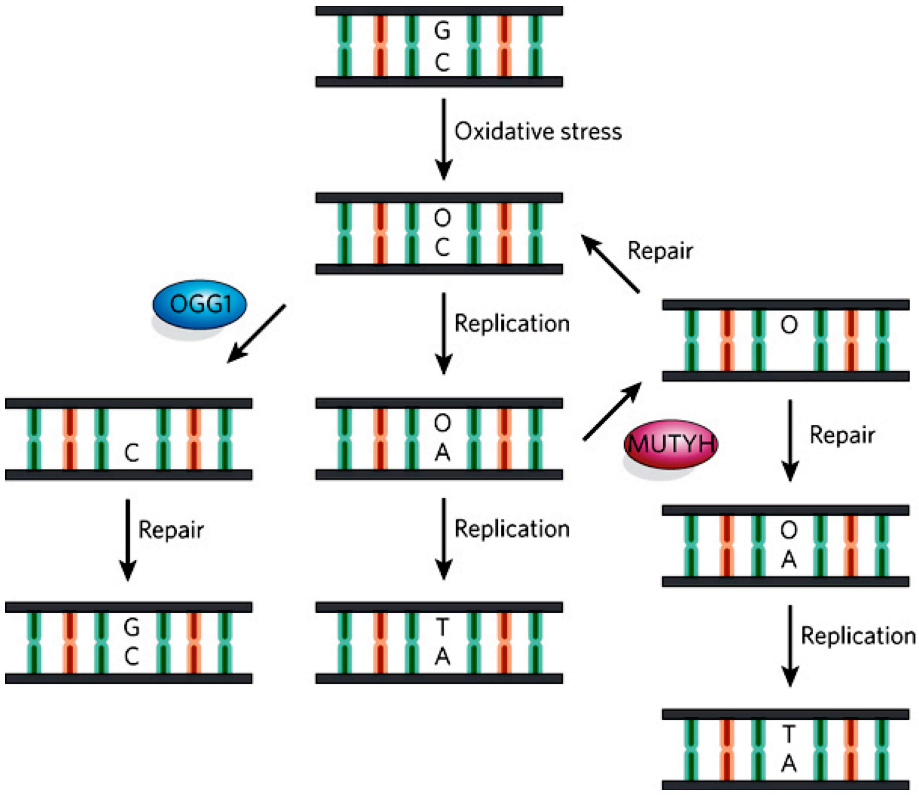

Figure 4. The 8-oxo-G base excision repair. The presence of 8-oxo-G (O) in DNA is a cause of C:G to A:T transversion mutations during (i) DNA replication – central pathway or (ii) inaccurate DNA repair – right side pathway. Human DNA glycosylases OGG1 and MUTYH are involved in the excision of bases from the DNA. OGG1 removes 8-oxo-G from C:8-oxo-G base pair, and MUTYH removes A from A:8-oxo-G mispair, both generating AP sites in DNA. The steps labelled ´repair` summarize the actions of AP endonuclease, deoxyribophosphate lyase, DNA polymerase and DNA ligase. Modified after: David, S. S., O'Shea, V. L. & Kundu, S. (2007). Base-excision repair of oxidative DNA damage. *Nature* **447**, 941-50.

5.4. Proteins Involved in the Repair of A:8-oxo-guanine Mispairs

5.4.1. Key Players

5.4.1.1. MutY Glycosylase Homologue

The *Escherichia coli* adenine DNA glycosylase, MutY is a member of helix-hairpin-helix (HhH) glycosylase family. MutY is an enzyme with mainly monofunctional DNA glycosylase and only week and fully uncoupled AP lyase activities (37). This glycosylase mediates removal of A paired with 8-oxo-G, G, faPyG, 5-hydroxyuracil or C.

Human MUTYH is encoded by the *MUTYH* gene, located on the short arm of chromosome 1 (1p32.1-p34.3). MUTYH is significantly larger than the bacterial protein (Figure 5) and consists of catalytic core domain with an [4-Fe-4S] iron sulfur cluster in N-terminus (38,39), followed by an additional C-terminal MutT-like domain (35). The extended N-terminal domain is involved in mitochondrial targeting of MUTYH and interaction with replication protein A (RP-A) while the C-terminal domain contains the nuclear localization sequence and the PCNA interacting motif (40-45). There are at least three types of MUTYH protein: a mitochondrial (57kDa) and two nuclear (52kDa and 53kDa) forms (40).

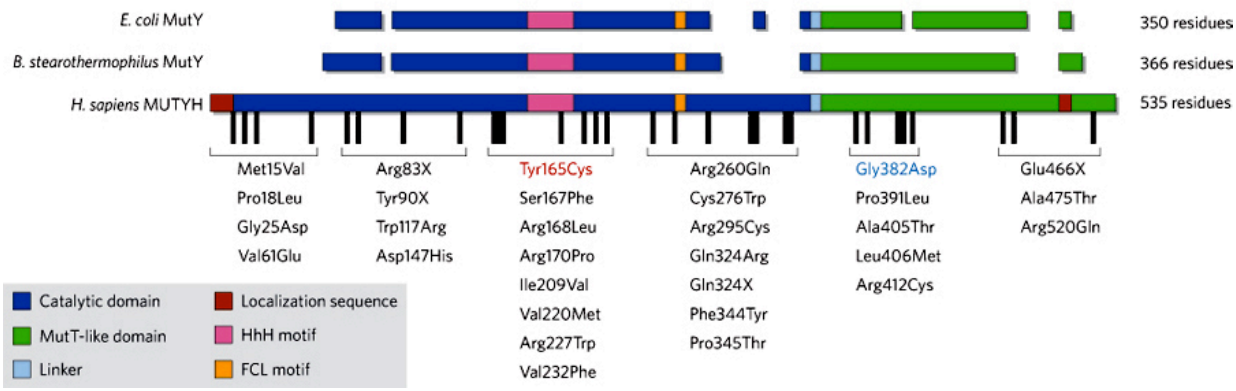

Figure 5. Adenine DNA glycosylase, MUTYH. Alignment of *E. coli* MutY, *B. stearothermophilus* MutY and human MUTYH. Representative mutations that have been observed in individuals with MUTYH-associated polyposis are indicated. Modified after: David, S. S., O'Shea, V. L. & Kundu, S. (2007). Base-excision repair of oxidative DNA damage. *Nature* **447**, 941-50.

The full-length structure of MutY cross-linked to DNA containing an A:8-oxo-G mispair has helped to understand how the protein recognizes both A and 8-oxo-G (Figure 6A and B) (39). The catalytic core and the MutT-like domains, both encircle the DNA, individually making close contacts to the appropriate DNA strand. The A is than flipped out into a deep pocket, similarly to other HhH type glycosylase-DNA complex structures and the 8-oxo-G stays in the base stack. The MutT-like domain establishes extensive contacts with 8-oxo-G, which in *anti* conformation gets stabilized in the MutY complex structure. Interestingly, when mispaired opposite A, the 8-oxo-G in *syn* conformation is the energetically favoured conformer.

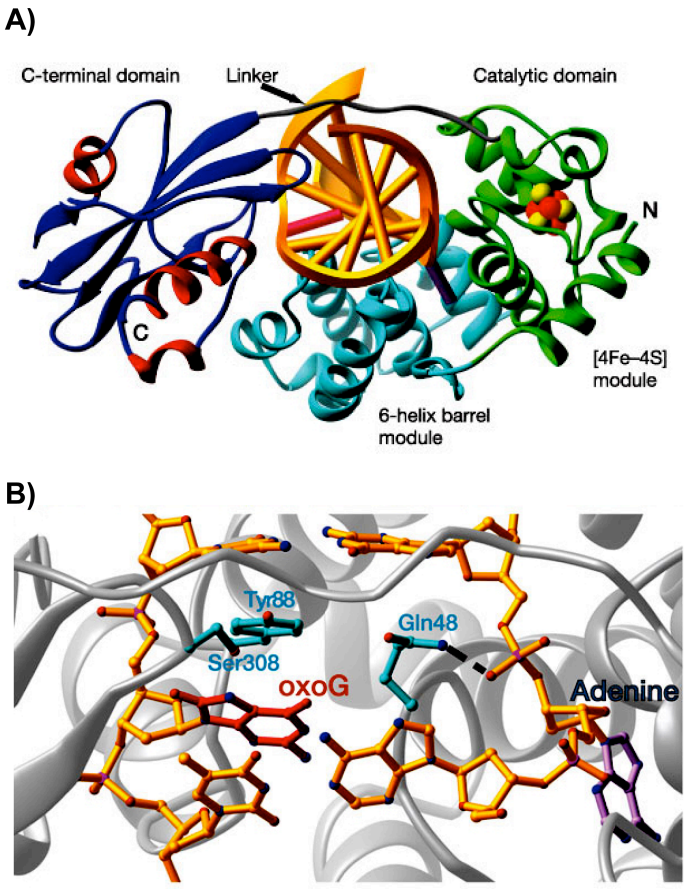

Figure 6. Recognition of A:8-oxo-G mispairs by MutY. A) Ribbon trace of the MutY-DNA complex. **B)** Ball-and-stick representation of the MutY-DNA interface and 8-oxo-G recognition. DNA is shown in gold, 8-oxo-G in magneta, the substrate A in purple, the [4Fe-4S] cluster in green and the six-helix domain in cyan. The C-terminal domain is coloured by secondary structure (β-strands, blue; helices, red). The sulphur and iron atoms of the [4Fe-4S] cluster are yellow and orange, respectively. Modified after: Fromme, J. C., Banerjee, A., Huang, S. J. & Verdine, G. L. (2004). Structural basis for removal of A mispaired with 8-oxoguanine by MutY adenine DNA glycosylase. *Nature* **427**, 652-6.

The MUTYH activity can be modulated through interaction with other proteins. APE1 physically interacts with MUTYH (43) and enhances the MUTYH glycosylase activity (46). Interestingly, this effect is independent of the APE1 endonuclease activity (46). MUTYH also directly associates with both PCNA and RP-A (43). This is of great importance, since in order to prevent mutations during DNA replication the MUTYH activity must be directed to the newly synthesized strand. Indeed, it was shown that DNA replication stimulates the MUTYH initiated repair of A:8-oxo-G mispairs *in vivo* and interaction between MUTYH and PCNA is critical for this repair to occur (47). In addition, MUTYH efficiently colocalizes with PCNA at replication foci (48).

Biallelic germ-line mutations in the *MUTYH* gene are associated with the recessive inheritance of multiple colorectal adenomas and carcinoma (49-53). This genetic predisposition is referred to as MUTYH-associated polyposis (MAP). Mutations in MUTYH cause a reduced capacity to initiate the repair of A:8-oxo-G mispairs, which probably leads to C:G to A:T transversion mutations in adenomatous polyposis coli (*APC*), *K-ras* and other genes that control cellular proliferation in the colon (49,54). The mutations in *APC* gene found in MAP occur at hot spots containing GAA sequence (49). More than 20 mutations in the human MUTYH gene have been indentified in MAP patients (Figure 5).

5.4.1.2. DNA Polymerase λ

DNA pols are enzymes that incorporate correctly base-paired deoxyribonucleside 5'-triphosphate onto the growing primer/template DNA. Based on their amino acid sequence similarity, the sixteen DNA pols have been categorized in seven DNA-pol families – A, B, C, D, X, Y and reverse transcriptase (55). The eukaryotic DNA pols are members of the A-family (DNA pols γ, θ and ν), the B-family (DNA pols α, δ, ε and ζ), the X-family (DNA pols β, λ, μ and deoxyribonucleotidyltransferase), the Y-family (DNA pols η, ι, κ and Rev1) and the reverse transcriptase family (telomerase) (56).

X-family DNA pols are distributive enzymes and are involved in the synthesis of short segments of DNA (57). DNA pol λ is the only member of the DNA pol X-family, whose homologues are encoded in the genomes of many

prokaryotes (58) and all eukaryotes except, protostomes (Figure 7A) (59). Finally the African swine fever virus contains beside a replicative DNA pol, also a repair X-family DNA pol (60). Thus, it is likely that DNA pol λ is most similar to the ancestor of the X-family DNA pols. It is suggested that the other X-family DNA pols (β, μ, σ and deoxyribonucleotidyltransferase) diverged from a DNA pol λ-type ancestor (59).

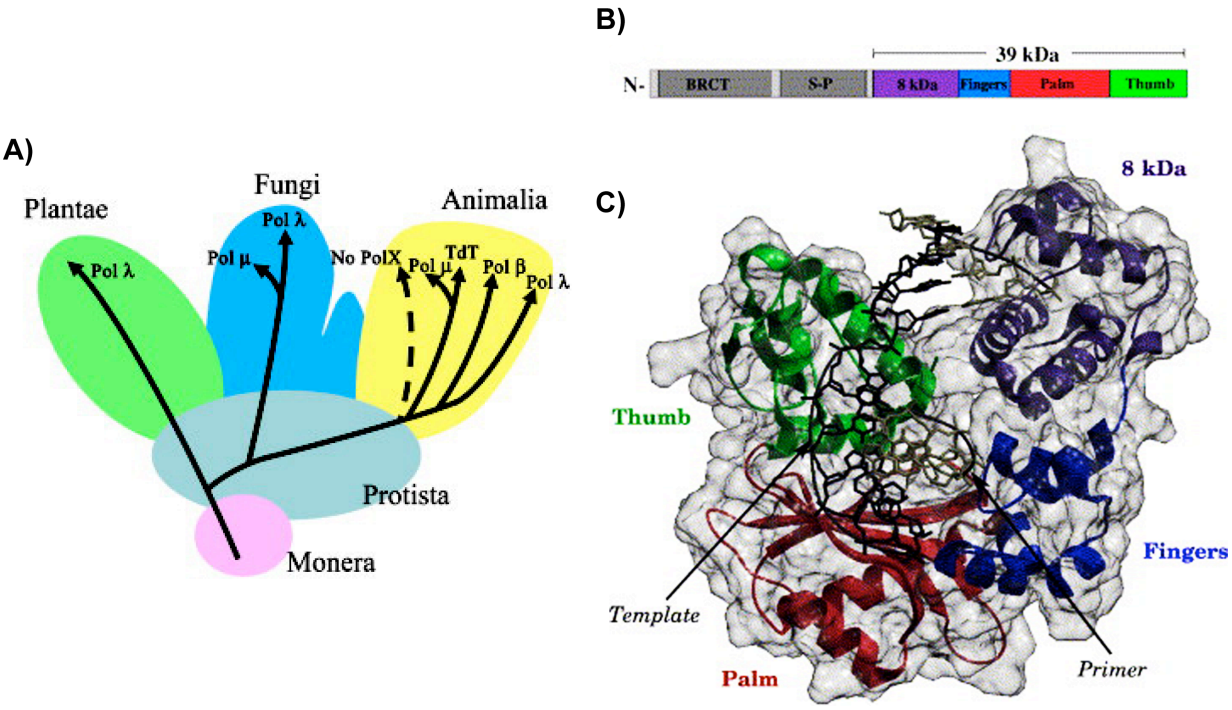

Figure 7. The divergence of X-family DNA polymerases in each kingdom and the domain structure of its most distributed member, DNA polymerase λ. A) DNA pol λ homologues are encoded in the genomes of all eukaryotes except protostomes (designated as "No PolX"). Adopted from: Uchiyama, Y., Takeuchi, R., Kodera, H. & Sakaguchi, K. (2009). Distribution and roles of X-family DNA polymerases in eukaryotes. *Biochimie* **91**, 165-70. **B)** Linear diagram indicating the different domains that compose the full-length DNA pol λ protein: BRCT, BRAC1 (breast-cancer-susceptibility protein-1) C-terminal domain; Serine-Proline rich domain (S-P); 8kDa domain and the DNA polymerase catalytic domain, composed of Fingers, Palm and Thumb subdomains. **C)** Ribbon representation of the 39kDa catalytic core of DNA pol λ in the complex with a two-nucleotide gap (the DNA is shown in stick representation). The molecular surface is shown in transparent gray. The different subdomains are colour coded as in B). Adopted from: Garcia-Diaz, M., Bebenek, K., Gao, G., Pedersen, L. C., London, R. E. & Kunkel, T. A. (2005). Structure-function studies of DNA polymerase lambda. *DNA Repair (Amst)* **4**, 1358-67.

Human DNA pol λ is a 68kDa protein that is encoded by the *POLL* gene on the chromosome 10q23. It is expressed at the highest level in testis, ovary

(61) and fetal liver (62). Like other X-family pols, DNA pol λ is a single subunit enzyme. The 575 amino acid polypeptide of human DNA pol λ comprises of N-terminal BRAC1 (breast-cancer-susceptibility protein-1) C-terminal (BRCT) domain, believed to mediate protein-protein interactions; the catalytic core and a serine-proline rich region connecting the two (Figure 7B). The serine-proline rich region has been sugested to be a target for posttranslational modifications (61). The 39kDa catalytic core of DNA pol λ shares the organization characteristic of X-family enzymes (Figure 7B). The catalytic core is composed of an N-terminal 8kDa domain and the polymerase domain, including fingers, palm and the thumb subdomains.

The X-ray crystal structure of the 39kDa catalytic domain of human DNA pol λ in complex with primer/template containing a two nucleotide gap (Figure 7C) shows that DNA pol λ has two DNA binding sites that bend DNA, thereby exposing the 3' primer terminus (63). The polymerase domain binds the primer terminal base pair and the upstream duplex, while the 8kDa domain binds the DNA down stream of the gap. The interactions between the polymerase domain and the duplex DNA upstream of the primer 3' terminus are not extensive (63). Furthermore, the template-binding groove in DNA pol λ is not as positively charged as in DNA pol β, suggesting weaker interactions with the template strand (57). However, the binding of the DNA downstream of the gap is predominantly mediated via the interaction of 5' terminus of the gap with the positively charged residues of the 8kDa domain. This binding is further enhanced by the presence of 5' terminal phosphate, which at the same time stimulates the DNA pol λ polymerase activity on gapped substrate (57). Very recent crystal structure revealed, that DNA pol λ, upon binding to 2nt gapped double stranded (ds) DNA, scrunches the template strand and binds the additional uncopied template base in an extrahelical position within a highly conserved binding pocket (64). Mutation of the amino acids within this pocket, into alanine, results in less processive gap filling and less efficient DNA repair (64). Thus, scrunching of the template strand by DNA pol λ occurs during gap filling DNA synthesis and is associated with DNA repair.

DNA pol λ is a DNA template dependent polymerase (54). It also possesses a terminal transferase, dRp lyase activities and can synthesize

DNA *de novo* (55,65-69). In an *in vitro* system, that contains human nuclear extract, DNA pol λ (specifically its BRCT domain), was found to be responsible for gap filling in non-homologous end-joining (NHEJ) (70). The DNA template dependent and template independent synthesis mode used by DNA pol λ to repair double strand breaks (DSB), as well as its ability to fill the short gaps in DNA, further supports with its role in NHEJ (66,69). The dRp lyase activity implicates a possible role of DNA pol λ in BER. In addition, DNA pol λ can efficiently repair uracil-containing DNA in an *in vitr*o reconstituted BER reaction (65). Finally, DNA pol λ could be also a template dependent RNA polymerase (U., Hubscher & K. Ramadan, unpublished data).

Upon treatment of mammalian cells with DNA damaging agents (UV, γ-irradiation and H_2O_2) mRNA levels of DNA pol λ are down-regulated (62). The group of Reynaud obtained knock out DNA pol $\lambda^{-/-}$ mice in which males were fertile, and homozygous breeding has been performed up to third generation without a noticeable problem (71), suggesting that this enzyme is not essential for mouse development. In addition, DNA pol λ is dispensable for Ig gene hypermutation. Recently, in our laboratory it was shown that DNA pol λ is very efficient in accurate bypass of 8-oxo-G lesion both on primed and 1 nucleotide (nt) gapped DNA templates (72,73). Human DNA pols α, δ and η, on the other hand, show a much lower efficiency than DNA pol λ and as expected preferentially incorporate dATP (72). Moreover, the two auxiliary proteins PCNA and RP-A are able to additionally promote accurate gap filling by DNA pol λ. In the presence of RP-A and PCNA, DNA pol λ incorporates dCTP opposite 8-oxo-G on a 1nt gapped template 750-fold better than dATP (73). At the same time, these two auxiliary proteins prevent binding of DNA pol β to 1nt gapped 8-oxo-G template. Overall, the presence of RP-A and PCNA results in a 145-fold more efficient DNA pol λ than DNA pol β incorporation of dCTP opposite 8-oxo-G on 1nt gaps (73). The experiments with DNA pol $\lambda^{-/-}$ cells reveal a high hypersensitivity to oxidative DNA damaging agents (74), further supporting the major role of this enzyme in the accurate pathway for 8-oxo-G. This is important to prevent the deleterious consequences of oxidative damage.

DNA pol λ exists mainly in a hypophosphorylated state during S phase, but is exclusively hyperphosphorylated during G2/M (76). Cyclin dependent kinase 2 (CDK2)/Cyclin A interacts directly with DNA pol λ and phosphrylates it. DNA pol λ is phosphorylated on several sites (77). The experiments with phosphorylation-defective mutants suggest that phosphorylation of threonine 553 is important for DNA pol λ stability (77). In particular DNA pol λ is stabilized in late S and G2 phases (77). This most likely allows DNA pol λ to correctly conduct DNA repair of damaged DNA during S phase. DNA pol λ interacts also directly with PCNA (75) and RP-A (73). Interaction with PCNA stimulates not only bypass of 8-oxo-G by DNA pol λ, but also the bypass of AP sites with subsequent extension. Phosphorylation of DNA pol λ by CDK2/Cyclin A results in decreased association with PCNA (76). Thus, DNA pol λ likely interacts with PCNA during S-phase, where it could participate in lesion bypass, perhaps at the replication fork.

5.4.2. Apurinic/Apyrimidinic Endonuclease 1

Human APE1 is a multifunctional enzyme. It is coded by the *APE1* gene located on the chromosome 14. APE1 has a molecular weight of 35.5kDa (78-80). As indicated above, APE1 is involved in BER pathway, which eliminates base lesions and spontaneous AP sites. According to some estimation 10,000 AP sites are generated per day in mammalian cells, mostly as a result of purine losses (81). APE1 cleaves DNA 5' of AP site to generate a ss break with 3'-OH and 5'-dRp (82). Apart from its endonuclease activity APE1 possesses 3'-phosphodiesterase, 3'-phosphatase and 3'→5' exonuclease activities (83). Moreover, APE1 was identified also as a redox factor (Ref-1). This function of APE1 is independent of its function in DNA repair (79,81). As a Ref-1, APE1 regulates gene expression by activating transcription factors such as nuclear NF-κB, Jun and Fos (78,84,85).

Apart from endonuclease and 3'-phosphodiesterase role in BER, APE1 could presumably act as a BER coordinator. APE1 interacts and stimulates mouse MUTYH glycosylase (44). At the same time APE1 also increases the affinity of MUTYH for A:8-oxo-G mispairs compared with A:G base pairs (46). On an AP site, APE1 facilitates the binding of DNA pol β to the non-cleaved

AP site and stimulates its dRp lyase activity (86). When DNA pol β and APE1 are in excess over substrate DNA, APE1 stimulates strand displacement by DNA pol β. In addition, APE1 can influence the LP-BER. The enzymatic activity of LP-BER proteins, FEN1 and DNA ligase I, increases in the presence of APE1 (87). The role of APE1 in stimulating the DNA glycosylase, dRp lyase, DNA polymerase, flap endonuclease and DNA ligase activities of repair enzymes suggests that individual steps of DNA repair are coordinated to ensure maximal efficiency.

5.4.3. Proliferating Cell Nuclear Antigen and Replication Factor C

PCNA belongs to the family of DNA sliding clamps (β clamps), which are structurally and functionally conserved (88). Although there is barely any sequence similarity between the β clamps in all branches of life, crystallographic studies have shown that they have almost super-imposable three-dimensional structures (89). PCNA is a homotrimeric ring-shaped protein with a molecular mass of 29kDa for each monomer that occupies 120° in the ring (90). PCNA is loaded on DNA by the conserved RF-C complex (91). RF-C is a composed of five similarly structured essential proteins (AAA+ type ATPases). RF-C specifically recognizes the primer/template 3' terminus and loads PCNA on these sites. ATP binding is required for the formation of a stable PCNA/RF-C complex. While encircling the DNA strand, PCNA does not make a direct contact with it (92).

The PCNA ring, tethers DNA pols firmly to DNA making the sliding clamp an essential cofactor for DNA synthesis. Early *in vitro* studies have shown that the presence of PCNA increases the processivity of DNA pols ten up to thousand fold (90). Although most PCNA interactions occur directly at the replication fork of replicating chromosomes, PCNA plays a role in different processes (Figure 8), such as gap-filling repair DNA synthesis and has other functions that are often linked to DNA repair (88).

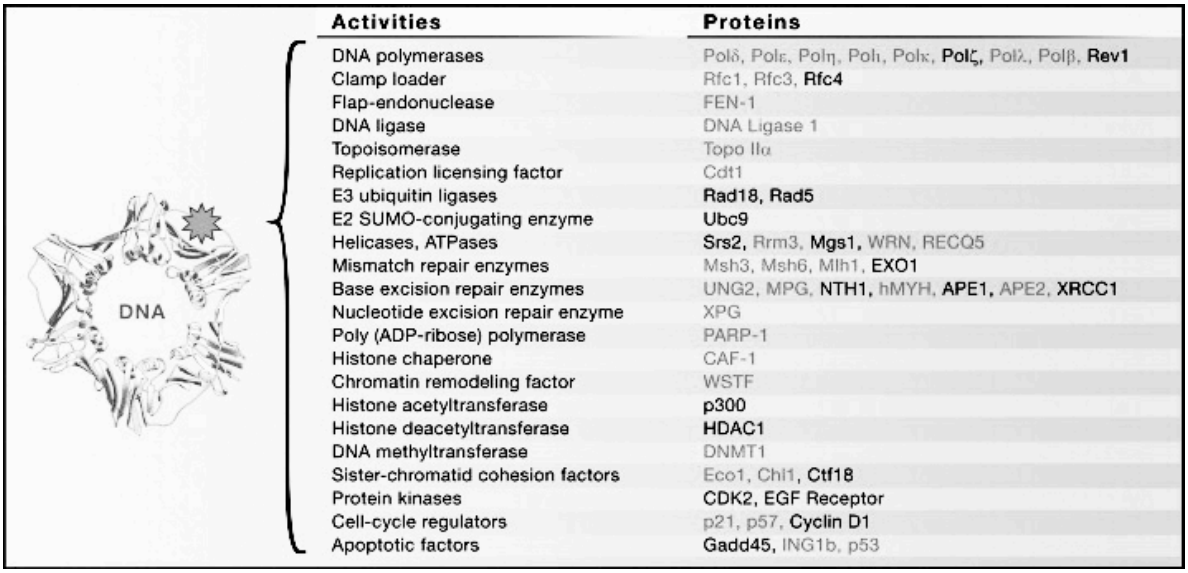

Figure 8. PCNA binding proteins. PCNA interacts with a host of proteins involved in many different cellular processes. Listed are a selection of key PCNA-dependent activities and the corresponding PCNA-interacting proteins. Proteins in gray are known to contain PIP-box sequences, which bind to a groove in PCNA (gray star) buried underneath the interdomain connecting loop. Adopted from: U Moldovan, G. L., Pfander, B. & Jentsch, S. (2007). PCNA, the maestro of the replication fork. *Cell* **129**, 665-79.

5.4.4. Replication Protein A

RP-A is a ss DNA binding heterotrimeric protein complex. It is composed of a large (70kDa), a middle (32kDa) and a small (14kDa) subunit (93). Functionally, RP-A corresponds to an alternative form of a bacterial ss DNA binding protein (SSB). RP-A is required for almost all aspects of cellular DNA metabolism, such as DNA replication, recombination, DNA damage checkpoints, and all major types of DNA repair, including BER. RP-A plays a role in activation of pre-replication complex. During strand elongation in DNA replication and DNA repair, RP-A stimulates the action of DNA pols α, δ, ε, λ and κ (56,94-96). RP-A participates in diverse pathways through its ability to interact with DNA and numerous proteins. Physical association of RP-A with DNA glycosylases; MUTYH, NEIL3 and uracil DNA glycosylase (UNG) has been reported (44,97,98). Very recently our laboratory showed that RP-A can interact with both DNA pols β and λ (73). In addition RP-A has been shown to

greatly enhance the activity of DNA ligase I (99), although no physical interaction has been reported between these two proteins.

5.4.5. Flap Endonuclease 1

FEN1 is a multifunctional and structure specific nuclease involved in nucleic acid processing pathways. It belongs to the family of RAD52 nucleases, which are conserved among bacteriophages, bacteria and eukaryotes (100). The RAD52 family proteins have a conserved core, which consists of the N-terminal and central domains. Human FEN1 is a 43kDa protein with 5' endonuclease and 5'→3' exonuclease activities (101). Both of these activities are strongly specific for the substrate structure. Acting as endonuclease FEN1 recognizes DNA duplexes with a gap and break, or a recessed 5' end and removes the nucleotide from the 5' end of the break or from the recessed 5' end. The natural substrate of FEN1 is a so-called 5' flap structure, consisting of three DNA strands. One is continuous, while the other two form a break (or a gap), with the 5' flanking strand having an overhanging 5' end (a flap). Such structures arise upon Okazaki fragment synthesis and DNA strand displacement. FEN1 processes flap structures during DNA replication. Moreover it is also involved in LP-BER and DNA recombination. FEN1 was very recently found to posses an additional gap endonuclease activity (102,103), possibly important for apoptotic DNA fragmentation. FEN1 interacts with a number of proteins, thereby affecting their activities. Some of its interaction partners are: PCNA (105,105), RP-A (106,107), APE1 (87) and DNA pol β (108,109). These protein-protein interactions improve the efficiency of replication and repair, thus FEN1 has an essential role in those processes.

5.4.6. DNA Ligases I and III

DNA ligases are nucleotidyltransferases (NTases) that utilize a high-energy cofactor, either NAD^+ or ATP, to catalyze phosphodiester bond formation in a three-step reaction mechanism (110). DNA ligases are essential for variety of DNA processes, such as DNA replication, repair and recombination. DNA ligases change their conformation during the DNA joining

reaction in order to accommodate multiple reactions with the nucleotide and DNA substrates (111). The multidomain architecture of these enzymes provides the necessary flexibility and probably enables loading on and off of the DNA. All eukaryotic DNA ligases are ATP dependent, whereas both ATP- and NAD^+- dependent DNA ligases have been identified in bacteria, archaea and viruses (111). The DNA ligases encoded by the human genes *LIG1*, *LIG3* and *LIG4* serve as the prototypic members of the three families of eukaryotic DNA ligases. Homologues of *LIG1* and *LIG4* appear to be present in all eukaryotes. In contrast the *LIG3* gene appears to be restricted to vertebrates.

DNA ligase I activity is high in proliferating cells (112,113) and the level correlates with the rate of cell proliferation (114). In accord with its expected role in DNA replication, the DNA ligase $I^{-/-}$ exhibit a marked defect in Okazaki fragment joining, but unexpectedly, this does not have an obvious effect on cell proliferation (115,116). In addition, DNA ligase I was shown to function in BER and nucleotide excision repair (NER) (117,118). Mouse embryos harbouring homozygous deletions of the DNA ligase I develop normally until midgestation (119), after which they die. The only known case of a human DNA ligase deficiency caused by an inherited mutant *lig1* allele was diagnosed in patient with recurrent infections (120,121). Thus, it appears that the DNA replication defect caused by DNA ligase I deficiency in mammals results in delayed growth and increased cancer incidence because of genomic instability. This proliferation defect also appears to underline abnormalities in hematopoiesis and lymphopoiesis (121).

Several DNA ligase I interacting proteins have been identified. The interaction with PCNA is primarily mediated by the conserved PCNA binding motif (122,123). This interaction is important for targeting of DNA ligase I to the sites of DNA replication (124). DNA ligase I interacts also with heterotrimeric hRad9-hRad1-hHus1 (9-1-1) complex. The 9-1-1 clamp very efficiently stimulates catalytic activity of DNA ligase I (125, 126). In addition DNA ligase I interacts with RFC p140 and hRad17 (123).

The *LIG3* gene of higher eukaryotes generates three distinct DNA ligase polypeptides: (i) nuclear and (ii) mitochondrial DNA ligase IIIα, and (iii) DNA ligase IIIβ. DNA ligase IIIα through its BRCT domain interacts with DNA

repair protein XRCC1, resulting in a formation of DNA ligase IIIα/XRCC1 complex (127-129). This interaction is important for the stabilization of DNA ligase IIIα. Findings from biochemical and cell biology studies indicated that the nuclear DNA ligase IIIα/XRCC1 is involved in the SP-BER (18), as well as ss break repair (SSBR) (130,131). In addition, it has been shown that the nuclear DNA ligase IIIα/XRCC1 complex plays a crucial role in NER (132). Deletion of either the *XRCC1* or the *LIG3* gene in mouse, results in early embryonic lethality (133,134).

The XRCC1, in addition to DNA ligase IIIα, interacts with several other proteins involved in BER and SSBR, suggesting that XRCC1 may act as a scaffold for the assembly of multiprotein repair complexes (111). By interacting with the OGG1 (135), APE1 (136) and DNA pol β (137), in addition to DNA ligase IIIα, XRCC1 potentially contributes to every step of the SP-BER.

5.5. Other Proteins Used in this Work

5.5.1. DNA Polymerase δ

The eukaryotic replicative DNA pols (DNA pol α, DNA pol δ and DNA pol ε) belong to the B-family and the mitochondrial DNA pol γ to A-family DNA pols. DNA pol δ exists as a heterotetrameric enzyme with subunits of 125kDa, 66kDa, 50kDa and 12kDa and possesses a wide range of functions. It is required (i) in DNA replication (lagging strand), (ii) in several DNA repair events (LP-BER, NER, mismatch repair), (iii) in translesion synthesis, (iv) in cell cycle control, as well as (v) in meiotic recombination (138). DNA pol δ synthesizes DNA with high accuracy, thus keeping the rate of mutations low. An incorrect nucleotide is incorporated only once in ~10^5 bases replicated. In addition the mispaired nucleotide can be removed by the polymerase's 3'→5' exonuclease domain, which provides additional ~10-60-fold increase in the level of accuracy (139-141). Very recent structural data obtained in studies using yeast *Saccharomyces cerevisiae*, indicated that high fidelity of DNA pol δ is determined primarily by the shape of Pol3 (catalytic subunit of DNA pol δ) pocket accommodating the nascent Watson-Crick base pair (142). The B-

family DNA pol kinetic evidence suggests that dNTP diffuses directly to the active site to provide a more direct check on correct versus incorrect base pairing (143). The binding pocket in Pol3 is composed of residues: Asn705, Ser706, Tyr708 and Gly709 from the fingers domain and Tyr613 from the palm domain; all of which are conserved in B-family DNA pols (142). The Pol3 binding pocket is largely devoid of contacts with the major groove. In purine-pyrimidine mismatches, the purine is displaced toward the minor groove and the pyrimidine toward the major groove (144-146). Thus given the shape of Pol3 binding pocket, the purine would sterically clash with Tyr708-Gly709 in the minor groove, and the pyrimidine would lose some of the favourable van der Waals and electrostatic interactions (142). In contrast, in purine-purine or pyrimidine-pyrimidine mismatches, the bases are displaced primarily toward the major groove, where there is little steric hindrance (146-148). Pol3 interacts with the bases as far away as the T_5-P_5 positions, mostly in the minor groove and involving direct or water-mediated hydrogen bonds (142). Loss of these hydrogen bonds at mismatches could shift the balance for binding of the template primer from the polymerase to the exonuclease domain. DNA pol δ slows down upon incorporation of an incorrect nucleotide, which can provides a time window for the switch between polymerase and exonuclease domain to occur. Accordingly, Tyr613 and Tyr708 in Pol3 help to shape the binding pocket for nucleotide insertion and check for a mismatch at the T_1-P_1 position (142).

The 3'→5' exonuclease activity of DNA pol δ besides acting as a proofreader has additional biological roles in Okazaki fragment maturation and mismatch repair. Point mutations and single-nucleotide deletions have also been identified in human POL3 in several cancer cell lines and sporadic colon cancers (149,150).

5.5.2. DNA Polymerase β

DNA pol β is a 39kDa single subunit protein, which through proteolytic cleavage can be separated into two domains: (i) the N-terminal 8kDa and (ii) the C-terminal 31kDa PolX domain. DNA pol β synthesizes DNA in a template-directed manner and can bind to a variety of DNA structures. It is the main

DNA pol of the BER pathways, where it is very well suited due to: (i) its DNA synthesis specificity for short gaps; (ii) its associated dRPlyase activity; and (iii) its ability to associate with other BER enzymes, such as DNA ligase I, APE1, DNA ligase III/XRCC1, RP-A and PCNA (151). Beside its role in BER, DNA pol β is involved in translesion synthesis since it efficiency bypasses cisplatin and oxaliplatin adducts (152). Lesion bypass by DNA pol β occurs predominantly by "skipping over" the lesion, by insertion of a nucleotide complementary to an adjacent downstream template site (151). Misalignment incorporation for DNA pol β occurs by the "dNTP-stabilized" mechanism resulting in both deletion and base substitution errors (153).

DNA pol β is constitutively expressed in most tissues, with the highest expression observed in testis, brain, thymus and spleen (154). DNA pol $\beta^{-/-}$ embryonic cells survive in culture, but are severely compromised in their ability to carry out SP-BER, resulting in their hypersensitivity to alkylating cancer agents (26). Interestingly, high levels of DNA pol β have been detected at the transcriptional level in many cancer tissues, mostly solid tumors (e.g. prostate, breast, colon, ovarian) as well as in chronic myeloid leukemia (30, 155). Its up-regulation probably contributes to genomic instability and tumourigenesis.

5.6. Aim of the Thesis

One of the predominant oxidative DNA lesions, upon exposure of the cells to ROS is 8-oxo-G. The 8-oxo-G in *syn* conformation is particularly deleterious because of its strong ability to functionally mimic T, thereby forming a stable A(anti):8-oxo-G(syn) Hoogsteen base pair during DNA replication. In contrast to many other DNA damages, this mispair is not detected by the 3'→5' exonuclease proofreading activity of the replicative DNA pols δ and ε, thus subsequently resulting in C:G to A:T transversion mutations. These mutations are one of the most predominant somatic mutations in lung, breast, ovarian, gastric and colorectal cancers. Human cells require a BER pathway ensuring correct and efficient repair of A:8-oxo-G mismatches, in order to reduce the mutational burden of ROS. The repair is initiated by MUTYH glycosylase that recognizes A:8-oxo-G mispair and removes the A. During subsequent BER, a specialized repair DNA pol that will catalyze with high preference the accurate bypass of 8-oxo-G is needed. Our laboratory recently showed that DNA pol λ is very efficient in the accurate bypass of 8-oxo-G lesion both on primed (72) and 1nt gapped DNA templates (73). Moreover, the two auxiliary proteins PCNA and RP-A additionally promote accurate gap filling by DNA pol λ. In the presence of the RP-A and PCNA, DNA pol λ incorporates dCTP opposite 8-oxo-G on a 1nt gapped template 750-fold better than dATP. At the same time, these two auxiliary proteins prevent binding of DNA pol β to 1nt gapped 8-oxo-G template. Overall the presence of RP-A and PCNA results in a 145-fold more efficient DNA pol λ than DNA pol β incorporation of dCTP opposite 8-oxo-G on 1nt gaps. Though these data implicate that DNA pol λ could play an important role, the mechanism ensuring accurate and efficient repair of A:8-oxo-G mismatches in human cells stays to be elucidated.

The aim of this thesis was to: (i) identify the role of DNA pol λ in MUTYH initiated repair of A:8-oxo-G mispairs, and (ii) to determine whether this repair is mediated via SP-BER or LP-BER pathway.

6. ORIGINAL RESEARCH ARTICLES

6.1. An 8-oxo-guanine Repair Pathway Coordinated by MUTYH Glycosylase and DNA Polymerase λ

Reprinted from *Proceedings of National Academy of Sciences USA* (2009) **106**, 18201-6.

An 8-oxo-guanine repair pathway coordinated by MUTYH glycosylase and DNA polymerase λ

Barbara van Loon and Ulrich Hübscher[1]

Institute of Veterinary Biochemistry and Molecular Biology, University of Zurich, Winterthurerstrasse 190, CH-8057 Zurich, Switzerland

Edited by Philip C. Hanawalt, Stanford University, Stanford, CA, and approved August 31, 2009 (received for review June 30, 2009)

Reactive oxygen species (ROS) interact with DNA, frequently generating highly mutagenic 7,8-dihydro-8-oxoguanine (8-oxo-G) lesions. Replicative DNA polymerases (pols) often misincorporate adenine opposite 8-oxo-G. The subsequent repair mechanism allowing the removal of adenine and formation of C:8-oxo-G base pair is essential to prevent C:G to A:T transversion mutations. Here, we show by immunofluorescence experiments, in cells exposed to ROS, the involvement of MutY glycosylase homologue (MUTYH) and DNA pol λ in the repair of A:8-oxo-G mispairs. We observe specific recruitment of MUTYH, DNA pol λ, proliferating cell nuclear antigen (PCNA), flap endonuclease 1 (FEN1) and DNA ligases I and III from human cell extracts to A:8-oxo-G DNA, but not to undamaged DNA. Using purified human proteins and a DNA template, we reconstitute the full pathway for the faithful repair of A:8-oxo-G mispairs involving MUTYH, DNA pol λ, FEN1, and DNA ligase I. These results reveal a cellular response pathway to ROS, important to sustain genomic stability and modulate carcinogenesis.

base excision repair | DNA ligase I | DNA ligase III | oxidation damage

One of the often generated oxidative DNA lesions, upon exposure of the cells to reactive oxygen species (ROS) is 7,8-dihydro-8-oxoguanine (8-oxo-G). The estimated steady-state level of 8-oxo-G lesions is $\approx 10^3$ per cell/per day in normal tissues and up to 10^5 lesions per cell/per day in cancer tissues (1). The presence of 8-oxo-G on the replicating strand leads to frequent (10–75%) misincorporations of adenine opposite a lesion (formation of A:8-oxo-G mispairs), subsequently resulting in C:G to A:T transversion mutations (2). These mutations are one of the most predominant somatic mutations in lung, breast, ovarian, gastric, and colorectal cancers (3). Thus, human cells require a base excision repair (BER) pathway ensuring correct and efficient repair of A:8-oxo-G mismatches to reduce the mutational burden of ROS. MutY glycosylase homologue (MUTYH) is initiating this repair by recognizing A:8-oxo-G mispair and removing the A (4, 5). During subsequent BER, a specialized repair DNA polymerase (pol) that will catalyze with high preference the accurate (incorporation of dCTP) bypass of 8-oxo-G is needed. In vitro studies have indicated that several DNA pols may be implicated in BER (6–8). DNA pol β, a member of DNA pol family X, was shown to be the major enzyme involved in gap filling (9–11), thus playing a central role in BER (12, 13). Another member of the DNA pol family X, DNA pol λ (14) has been implicated in BER (6, 15), nonhomologues end joining (16, 17) and translesion synthesis (18–20). We have recently shown (18, 21) that DNA pol λ is very efficient in the accurate bypass of 8-oxo-G lesion both on primed and 1-nucleotide (nt) gapped DNA templates. In the presence of the auxiliary proteins, replication protein A (RP-A) and proliferating cell nuclear antigen (PCNA), DNA pol λ incorporates dATP opposite 8-oxo-G with a very low frequency (10^{-3}). At the same time, these two auxiliary proteins prevent binding of DNA pol β to 1-nt gapped 8-oxo-G template. Overall the presence of RP-A and PCNA results in a 145-fold more efficient DNA pol λ than DNA pol β incorporation of dCTP opposite 8-oxo-G on 1-nt gaps (21). Although these data implicate that DNA pol λ could play an important role, the mechanism ensuring accurate and efficient repair of A:8-oxo-G mismatches in human cells stays to be elucidated.

In the present work we show a key role of MUTYH and DNA pol λ in the repair of 8-oxo-G. Additionally we identify the critical repair components, by specific recruitment of MUTYH, DNA pol λ, PCNA, flap endonuclease 1 (FEN1), and DNA ligases I and III from human whole cell extracts (WCEs) to A:8-oxo-G DNA. Using purified human proteins and an 8-oxo-G specificity assay, we prove that DNA pol δ preferentially forms A:8-oxo-G mispair during replication and that MUTYH recognizes this mispair thereby generating an apurinic (AP) site, subsequently processed by apurinic endonuclease 1 (APE1). We show that on the newly formed 1-nt gapped template, in the presence of auxiliary proteins RP-A and PCNA, DNA pol λ preferentially incorporates dCTP opposite 8-oxo-G and additionally elongates by adding 1 nt, thereby creating a short 1-nt flap. Interestingly, no elongation occurs when in the rare cases DNA pol λ synthesizes an A:8-oxo-G mispair. Finally, we find that DNA ligase I in the presence of flap endonuclease 1 (FEN1) ligates 2-fold better a correct C:8-oxo-G product of DNA pol λ repair synthesis than an incorrect A:8-oxo-G product. In summary, our findings provide a mechanism for the accurate repair of highly mutagenic A:8-oxo-G mispairs, important to prevent mutagenesis and sustain genomic stability.

Results

Exposure to ROS Leads to the Colocalization of MUTYH and DNA Polymerase λ with the Sites of Oxidative DNA Damage and to the Increase in Their Protein Levels. We introduced oxidative DNA damage in synchronized HeLa cells (Fig. S1*A*), by UVA laser microirradiation (Fig. 1*A* and *B*) or H_2O_2 treatment (Fig. 1*C* and Fig. S1), and tested whether MUTYH and DNA pol λ accumulate at the sites of damage. Immunofluorescence analysis revealed that both MUTYH (Fig. 1*A* and Fig. S1*C*) and DNA pol λ (Fig. 1*B* and Fig. S1*E*) efficiently colocalize with the sites of oxidative DNA damage, such as 8-oxo-G lesion sites. Recently recruitment of FEN1, X-ray repair cross-complementing 1 protein (XRCC1) and PCNA was reported in a similar experimental setup (22). Additionally, H_2O_2 treatment of HeLa cells caused a dramatic increase in the protein levels of MUTYH and DNA pol λ (Fig. 1*C*). These data clearly suggest activation of MUTYH/DNA pol λ-dependent repair pathway upon induction of oxidative DNA damage.

MUTYH, DNA Polymerase λ, PCNA, FEN1, and DNA Ligases I and III Are Specifically Recruited to DNA Containing A:8-oxo-G Mispair. To identify BER proteins directly involved in the repair of A:8-oxo-G mispairs, we used a reversible cross-linking approach (23). The 3′-biotin-

Author contributions: B.v.L. and U.H. designed research; B.v.L. performed research; B.v.L. and U.H. contributed new reagents/analytic tools; B.v.L. and U.H. analyzed data; and B.v.L. and U.H. wrote the paper.

The authors declare no conflict of interest.

This article is a PNAS Direct Submission.

[1]To whom correspondence should be addressed. E-mail: hubscher@vetbio.unizh.ch.

This article contains supporting information online at www.pnas.org/cgi/content/full/0907280106/DCSupplemental.

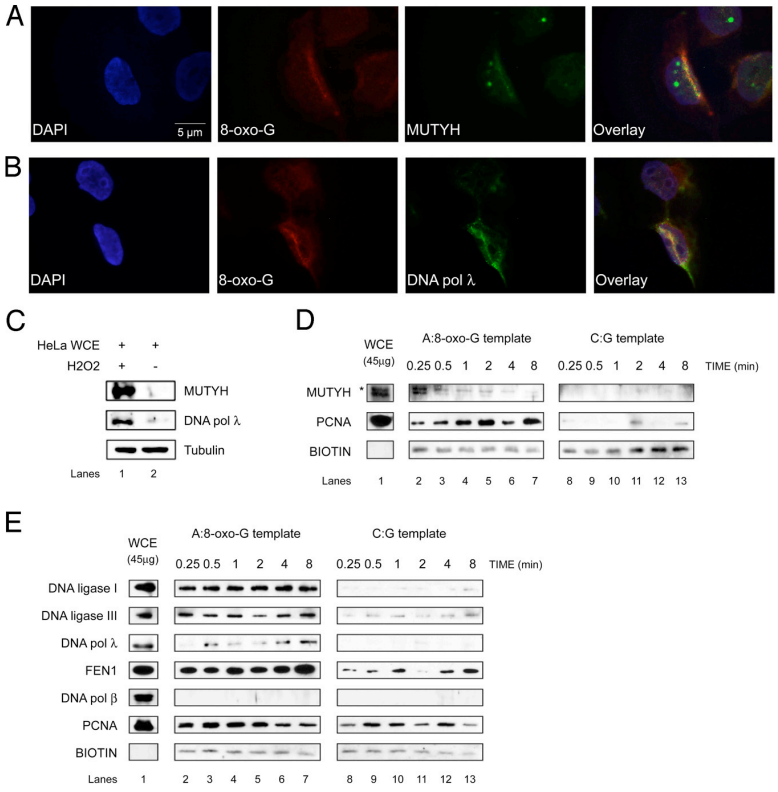

Fig. 1. Recruitment of BER proteins to the sites of oxidative DNA damage. The experiments were done under the conditions as specified in *Materials and Methods*. (*A* and *B*) Fluorescent microscope images of 355-nm laser-irradiated HeLa cells synchronized in G1/S phase and stained with antibodies against 8-oxo-G and MUTYH (*A*) or DNA pol λ (*B*). Colocalization was observed in 50% of the analyzed cells. (*C*) Immunoblot analysis of MUTYH and DNA pol λ protein level, 5 h upon recovery, in HeLa whole cell extract (WCE) treated with and without H_2O_2. (*D* and *E*) Protein recruitment assay using A:8-oxo-G (*Left*) or C:G (*Right*) biotinylated hairpin substrate and HeLa WCE in the absence (*D*) or presence (*E*) of Mg^{2+} for the times indicated (*, the higher molecular weight band corresponds to MUTYH localized in mitochondria). Only proteins that bind to hairpin substrate can be cross-linked and visualized by immunoblotting.

ylated oligonucleotides containing a hairpin loop and a single A:8-oxo-G mispair or C:G base pair (Fig. S2) were incubated with HeLa WCE in the presence of a cross-linking agent. Bound proteins were released, separated and detected by immunoblotting. During incubation of the A:8-oxo-G substrate with WCE, MUTYH, removes A from the substrate DNA, and APE1 incises the AP site, creating a 1-nt gap. This can be further processed by DNA pols β or λ and DNA ligase IIIα/XRCC1 or FEN1 and DNA ligase I. Because the recruitment of glycosylases to DNA is considered to be very fast, we first omitted Mg^{2+} from the reactions and observed a rapid recruitment (within 0.25 min of incubation) of MUTYH and a slower, but very robust recruitment of PCNA (Fig. 1*D*). Cross-linking of hairpin DNA substrates with WCE in the presence of Mg^{2+} resulted in a strong damage-specific recruitment of DNA ligases I and III, FEN1, as well as DNA pol λ (Fig. 1*E*). Interestingly, under the same conditions we were not able to detect the recruitment of DNA pol β to either A:8-oxo-G or to a control undamaged DNA substrate, although the protein was present in the WCE (Fig. 1*E*). Recruitment of PCNA in the presence of Mg^{2+} was damage-unspecific, which was expected because PCNA plays a role in variety of cellular processes besides DNA repair (24, 25). These results indicated a direct role of MUTYH, DNA pol λ, PCNA, FEN1, and DNA ligases I and III in the repair of A:8-oxo-G mispairs.

The Replicative DNA Polymerase δ Preferentially Incorporates dATP Opposite 8-oxo-G and This Mispair Is Specifically Cut by MUTYH. Next, we addressed the mechanism of A:8-oxo-G repair by developing an 8-oxo-G specificity assay (Fig. S3*A*). This assay enables accurate determination of DNA pols fidelity, based on a specific DNA sequence of the template strand (Fig. S3*B*). During DNA polymerization reaction on such template, dATP or dCTP can be incorporated only opposite a single 8-oxo-G lesion present on the template. Thus, a direct correlation can be made between the amount of dATP or dCTP incorporated opposite 8-oxo-G and the quantified signal intensity of the polymerization reaction products separated on a polyacrylamide gel. Compared with the generally used single nucleotide incorporation assays, the 8-oxo-G specificity assay more accurately reflects the physiological situation where replicative DNA pols synthesize longer stretches of DNA. Because in the 8-oxo-G specificity assay direct competition between dATP and dCTP within the same reaction is not possible, we first tested the fidelity of DNA pol δ under identical conditions in two experimental setups: (i) containing unlabeled primer/template and all 4 dNTPs when either dATP (Fig. S4*A*, lanes 2–5) or dCTP (Fig. S4*A*, lanes 6–9) were radioactively labeled; and (ii) containing labeled primer/template, dGTP, dTTP, and dATP (Fig. S4*B*, lanes 2–5) or dCTP (Fig. S4*B*, lanes 6–9). Independently whether in the reactions all four or only three dNTPs were present, DNA pol δ preferentially and with similar efficiencies incorporated dATP opposite 8-oxo-G lesion. The same effect was observed when PCNA was titrated in the reaction (Fig. S4*C*). Next we checked whether the product of the DNA pol δ polymerization reaction containing A:8-oxo-G mispair could be recognized as a substrate by MUTYH. For this MUTYH was titrated into the reactions in the presence of DNA pol δ and APE1. MUTYH efficiently removed A from A:8-oxo-G product synthesized by DNA pol δ, and together with APE1 created a 1-nt gap opposite the lesion (Fig. 2*A*, lanes 5 and 6). As expected, MUTYH was not able to act on C:8-oxo-G product of DNA pol δ (Fig. 2*A*, lanes 11 and 12).

DNA Polymerase λ Physically Interacts with MUTYH and Preferentially Incorporates the Correct dCTP Opposite 8-oxo-G on a 1-nt Gapped Substrate. It has been shown that MUTYH interacts with the components of long patch (LP) BER, such as APE1, PCNA, and

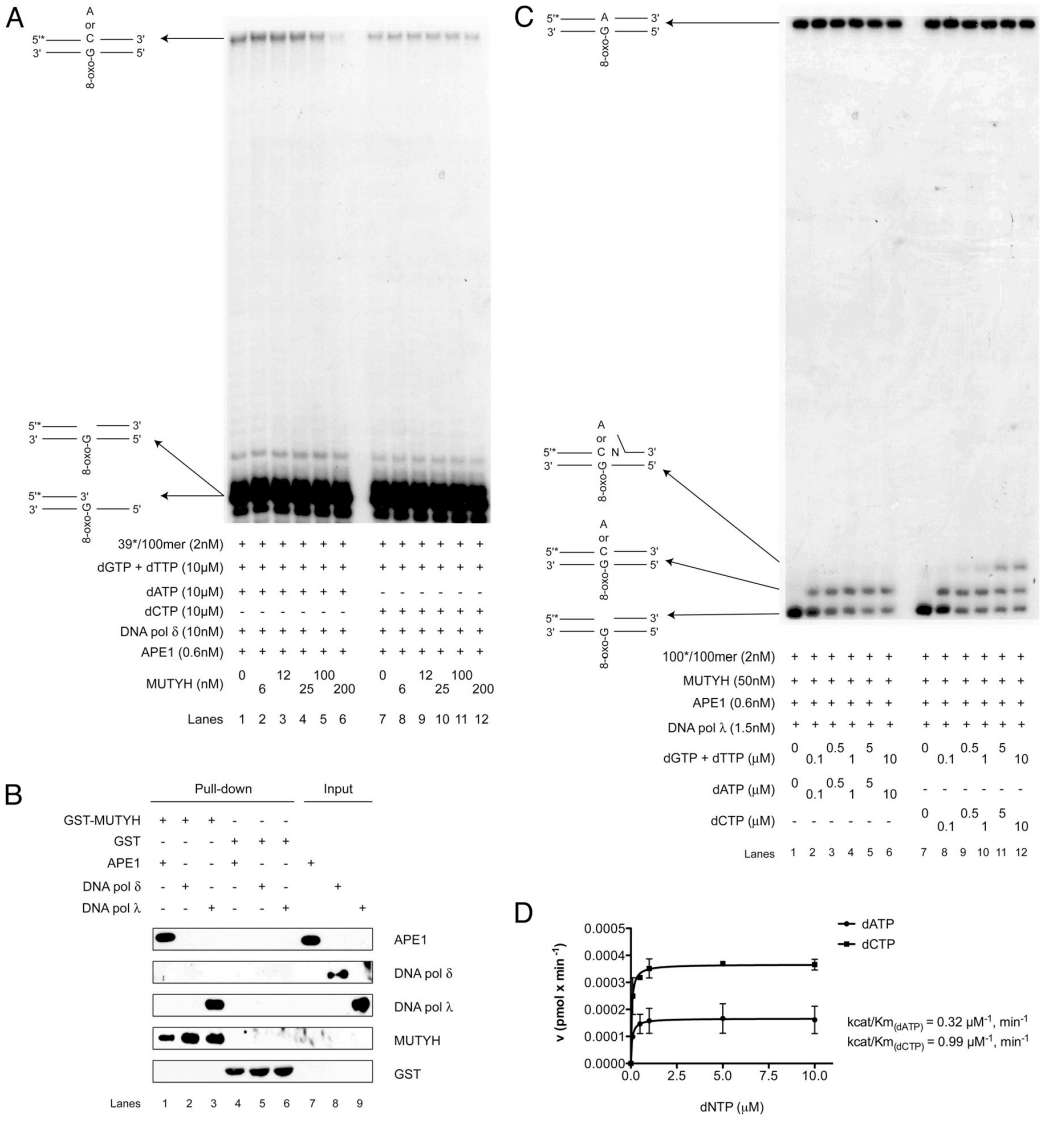

Fig. 2. DNA polymerase λ physically interacts with MUTYH and preferentially incorporates the correct dCTP opposite an 8-oxo-G after inaccurate replication by DNA polymerase δ. The experiments were done under the conditions as specified in *Materials and Methods*. (*A*) MUTYH titration in the presence of the indicated amounts of DNA pol δ, APE1, dGTP, dTTP and dATP (lanes 1–6) or dCTP (lanes 7–12). (*B*) Interaction of MUTYH and DNA pol λ using a GST pull-down assay. Incubation of APE1, DNA pols δ, and λ with GST-MUTYH (lanes 1–3) and GST (lanes 4–6). Lanes 7–9: input purified recombinant APE1, DNA pols δ, and λ, respectively. (*C*) dGTP, dTTP, and dATP (lanes 1–6) or dCTP (lanes 7–12) incorporation by DNA pol λ with MUTYH and APE1. (*D*) Summary of DNA pol λ activity in the presence of dATP (●) or dCTP (■) from three different experiments as the one documented in *C*; error bars, ± SD values.

RP-A, but does not interact with DNA pols δ and β (26). Therefore, we tested whether MUTYH interacts with DNA pol λ. GST pull-down experiments clearly showed that MUTYH specifically interacted with APE1 and DNA pol λ (Fig. 2*B*, lanes 1 and 3), but not DNA pol δ (Fig. 2*B*, lane 2). Based on this observation, we checked whether DNA pol λ could faithfully fill the gap opposite 8-oxo-G lesion, created by MUTYH and APE1. The double-stranded (ds) DNA template containing an A:8-oxo-G mispair was first incubated with MUTYH and APE1, followed by the addition of DNA pol λ into the reaction. DNA pol λ showed a 3-fold preference for dCTP versus dATP incorporation opposite 8-oxo-G lesion (Fig. 2 *C* and *D*).

PCNA and RP-A Promote the Accurate Incorporation Opposite 8-oxo-G by DNA Polymerase λ. We have shown that the auxiliary proteins RP-A and PCNA positively influence the accurate bypass of 8-oxo-G by DNA pol λ (18, 21). To test this effect in the 8-oxo-G specificity assay, RP-A or PCNA were titrated in the presence of MUTYH, APE1 and DNA pol λ. RP-A promoted accurate bypass of 8-oxo-G by DNA pol λ, by repressing the formation of A:8-oxo-G mispair and stimulating the formation of C:8-oxo-G base pair (Fig. 3*A*). As shown in Fig. 3*B*, PCNA inhibited the incorporation of dATP opposite 8-oxo-G by DNA pol λ thereby stimulating the accurate bypass. Thus, in a MUTYH and APE1 initiated reaction, the auxiliary proteins RP-A and PCNA can

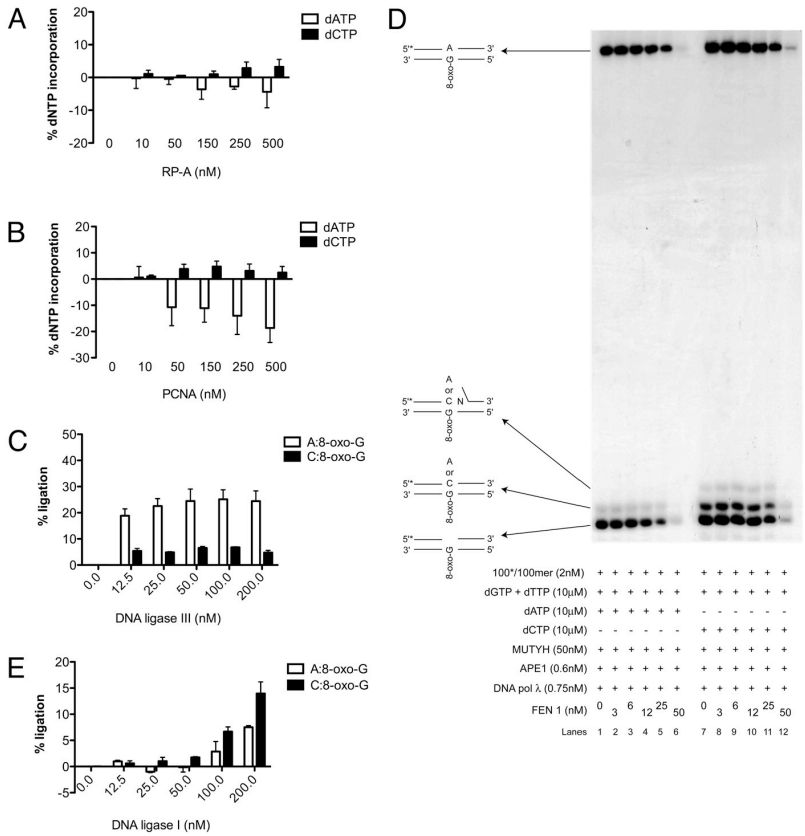

Fig. 3. RP-A and PCNA stimulate accurate incorporation by DNA polymerase λ and this product is specifically processed by FEN1 and DNA ligase I. The experiments were done under the conditions specified in *Materials and Methods*. (*A* and *B*) Incorporation of dGTP, dTTP, and dATP (white bars) or dCTP (black bars) by DNA pol λ in the presence of RP-A (*A*) or PCNA (*B*). Error bars, ± SD values of three independent experiments. (*C*) Products of the DNA pol λ repair synthesis containing A:8-oxo-G mispair (white bars) or C:8-oxo-G base pair (black bars) ligated by DNA ligase III in the presence of MUTYH and APE1. Error bars, ± SD values of three independent experiments. (*D*) dGTP, dTTP, and dATP (lanes 1–6) or dCTP (lanes 7–12) incorporation by DNA pol λ with MUTYH, APE1, and FEN1. (*E*) Products of the DNA pol λ repair synthesis containing A:8-oxo-G mispair (white bars) or C:8-oxo-G base pair (black bars) ligated by DNA ligase I in the presence of MUTYH, APE1, and FEN1. Error bars, ± SD values of three independent experiments.

additionally promote the accurate bypass of an 8-oxo-G lesion by DNA pol λ.

FEN1 and DNA Ligase I Are Required for Accurate Repair of A:8-oxo-G Mispairs. When DNA pol λ incorporated dCTP opposite an 8-oxo-G, addition of + 2nt was observed (Fig. 2*C*, lanes 11 and 12). However, this was not the case when dATP was incorporated, indicating that accurate repair could be mediated via the LP-BER (2–12-nt patch), and inaccurate (DNA containing A:8-oxo-G mispair) via the short patch (SP) BER (1-nt patch). To address this, we titrated the SP-BER protein, DNA ligase III, into the 8-oxo-G assay containing MUTYH, APE1, and DNA pol λ. DNA ligase III ligated 5-fold better products of repair synthesis containing A:8-oxo-G mispair, than C:8-oxo-G base pair (Fig. 3*C*). Next we tested the effect of the LP-BER protein, FEN1 on the repair fidelity. Addition of FEN1 in the presence of MUTYH and APE1 had no effect on DNA pol λ fidelity or polymerization activity (Fig. 3*D*). At higher amounts 5′->3′ exonuclease activity of FEN1 was observed (Fig. 3*D*, lanes 5, 6, 11, and 12). To test, whether another LP-BER protein, DNA ligase I, promotes inaccurate or accurate repair, we titrated it in the presence of constant amount of FEN1. Interestingly, DNA ligase I ligated 2-fold better a C:8-oxo-G than an A:8-oxo-G product of the DNA pol λ reaction (Fig. 3*E*), thereby mediating the accurate repair. In summary, the specific recruitment of MUTYH, DNA pol λ, PCNA, FEN1, and DNA ligases I and III from the WCE to the A:8-oxo-G lesion (Fig. 1 *D* and *E*) is in strong correlation with our in vitro observations that MUTYH initiated repair of 8-oxo-G can proceed either through an inaccurate SP-BER or an accurate LP-BER and that DNA pol λ acts as the key enzyme to promote the accurate pathway.

Discussion

The repair of A:8-oxo-G mispair is suggested to follow LP-BER involving DNA pols δ or ε (26–28). However, both of these DNA pols are significantly inaccurate during 8-oxo-G bypass, by incorporating dATP in 30–50% of the cases (18). In addition, both human DNA ligase III, acting in SP-BER and DNA ligase I, involved in LP-BER join 3′dA-terminated primer paired to 8-oxo-G much more efficiently than 3′dC-terminated primer (29). Thus, there is no available evidence suggesting a preferential role of either SP-BER or LP-BER in the repair of A:8-oxo-G mispairs. In this work we propose the accurate LP-BER pathway of A:8-oxo-G mispairs involving MUTYH, APE1, DNA pol λ, FEN1, and DNA ligase I. This repair pathway is in particular coordinated by the activities of MUTYH and DNA pol λ. MUTYH acts as a sensor for the A:8-oxo-G mispairs and initiates the repair by removing the A whereas DNA pol λ

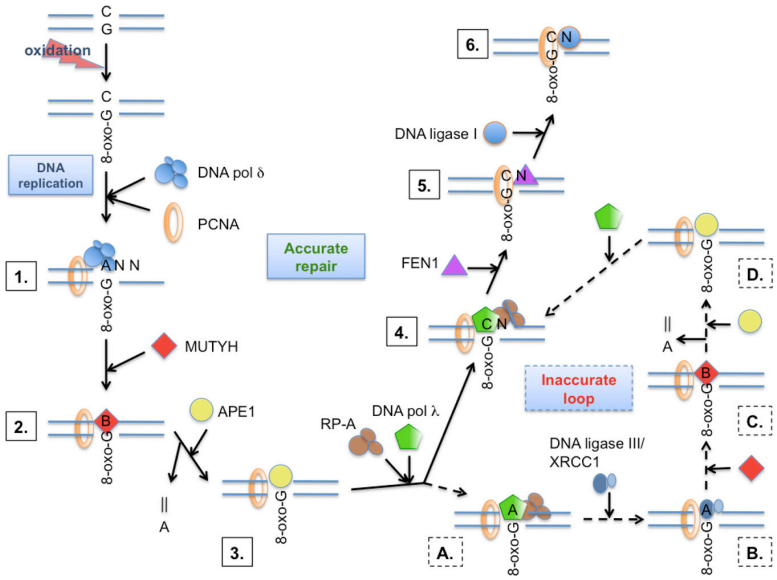

Fig. 4. Model for the MUTYH initiated long patch BER of 8-oxo-G, after misincorporation by the replication machinery. 1) DNA replication over an 8-oxo-G by DNA pol δ. 2) recognition of an A:8-oxo-G mispair by MUTYH, removal of the A and formation of an AP site (designated as *B*). 3) recruitment of APE1 mediated by MUTYH/PCNA and generation of 5′-P, 3′-OH gapped intermediate. 4) protection of the 1-nt gap by RP-A and PCNA mediated recruitment of DNA pol λ, with accurate gap filling (dCTP incorporation). 5) PCNA mediated recruitment of FEN1 and removal of 1-nt flap. 6) ligation of the nick by recruited DNA ligase I and further faithful OGG1 initiated DNA pol β mediated SP-BER of C:8-oxo-G product. Alternatively an inaccurate loop is initiated: (*A*) DNA pol λ catalyzes inaccurate gap filling; (*B*) recruitment of DNA ligase III/XRCC1-mediated by PCNA and ligation of the nick; (*C*) recognition of A:8-oxo-G mispair by MUTYH, removal of A and generation of AP site (designated as *B*); and (*D*) recruitment of APE1 mediated by MUTYH/PCNA, generation of 5′-P, 3′-OH gapped intermediate. This creates an opportunity for DNA pol λ to catalyze accurate LP-BER. For further details, see text.

preferential incorporates dCTP opposite 8-oxo-G and directly promotes the accurate repair. In addition we show that upon exposure of the cells to ROS protein level of MUTYH and DNA pol λ is increased and both proteins directly localize to the site of oxidative DNA damage. Role of DNA pol λ, in protection of the cells against ROS, is supported by the previous finding that DNA pol λ-null cells are highly hypersensitive to oxidative DNA damaging agents (30). In addition DNA pol λ-null cell extracts exhibit lower level of dCTP incorporation opposite 8-oxo-G lesion compared with wild-type cell extracts (18). MUTYH-null mouse embryonic stem (ES) cells, deficient in the repair of A:8-oxo-G mispairs, have a spontaneous mutation rate in Hprt locus 2-fold higher than the wild-type cells (31). The expression of wild-type mouse MUTYH restores the increased spontaneous mutation rate of the MUTYH-null (ES) cells to the wild-type level (31). Thus, the accurate A:8-oxo-G repair pathway is from a great importance in suppressing C:G to A:T transversion mutations and maintaining genomic stability.

Based on our data and known protein–protein interactions, we propose a model for the accurate MUTYH/DNA pol λ-coordinated repair of A:8-oxo-G mispairs (Fig. 4). Replicative DNA pols, such as DNA pol δ, during DNA replication, bypass 8-oxo-G in inaccurate manner. The MUTYH is through the interaction with PCNA recruited to the A:8-oxo-G mispair and removes the A. To restore a 3′-OH moiety and create gapped intermediate, APE1, another PCNA-interacting protein (32), is recruited. The created gapped substrate can be further recognized, by several factors, through competition for PCNA and RP-A binding. These auxiliary proteins will further promote the accurate bypass of 8-oxo-G and additional + 1-nt elongation reaction by DNA pol λ. After the lesion bypass, RP-A and DNA pol λ dissociate, allowing FEN1 to be recruited onto the resulting 1-nt flap intermediate through interaction with PCNA (33, 34). In the subsequent step DNA ligase I interacts with PCNA (35, 36), binds to the created nicked intermediate and ligates it. In this way accurate repair is ensured at the lesion bypass step, by the combined action of PCNA, RP-A, and DNA pol λ. Alternatively when DNA pol λ incorporates dATP opposite 8-oxo-G an inaccurate short patch loop will be initiated. After the lesion bypass, RP-A and DNA pol λ dissociate from the nicked intermediate enabling binding of DNA ligase III/XRCC1 (37) through interaction with PCNA, and subsequent ligation. Thus, the resulting product contains an A:8-oxo-G mispair that can be further recognized and processed by MUTYH and APE1, thereby creating another chance for an accurate repair to occur. Overall, our data suggest that the repair of A:8-oxo-G mispairs is an interplay between accurate long-patch BER and inaccurate short patch BER, in which DNA pol λ acts as the key enzyme to regulate the error rate.

Materials and Methods

Chemicals. Deoxynucleotides were purchased from Sigma. Labeled γ[^{32}P] ATP, α[^{32}P] dATP and α[^{32}P] dCTP were purchased from Hartmann Analytic. All of the other reagents were of analytic grade and purchased from Fluka, Sigma, or Merck. The 39-mer and 100-mer were purchased from Microsynth and the 100-mer containing 8-oxo-G and 3′-biotinylated 58-mer were from Purimex. Streptavidin-coupled magnetic beads were purchased from Invitrogen.

DNA Substrates. All oligonucleotides were purified from polyacrylamide denaturing gels (see *SI Text* for sequences, purification, and template preparation details). Annealing of 100-mer containing 8-oxo-G lesion with the unlabeled or 5′-labeled 39-mer primer or 100-mer created primer/template or ds substrate containing A:8-oxo-G mispair, respectively. Hairpin oligonucleotide substrates were created from 3′-biotinylated 58-mer.

Cells and Extracts. Human HeLa cells were purchased from American Type Culture Collection and grown according to standard protocols (see *SI Text* for details). HeLa cell pellets were purchased from Computer Cell Culture Center. WCEs were prepared as described in ref. 38 and stored at −80 °C.

Antibodies and Proteins. Antibodies against GST, DNA pols λ, and δ (polyclonal rabbit) were from our laboratory. Antibodies against APE1, MUTYH, and PCNA were purchased from Santa Cruz. Antibodies against 8-oxo-G were purchased from Millipore, against DNA ligase I from Genetex, and against DNA ligase III from Abcam. Recombinant human DNA pol λ, RP-A, PCNA, DNA pol δ, FEN1, DNA ligase I, and APE1 were expressed and purified as described (15, 18, 35, 39–44). The bacterial expression vector for human DNA ligase III was provided by G.L. Dianov. DNA ligase III was purified on Ni-NTA agarose (Invitrogen) as recommended by the manufacturer. The human *h*MUTYH gene was isolated from pGEV1-hMYH (gift from A.L. Lu) as a *Xho*I-*Nhe*I-digested fragment and transferred into pET41a (Novagene) to obtain the pET41a-MUTYH expression construct. GST-tagged MUTYH fusion protein was bound to the glutathione Sepharose (GE Healthcare) and purified as recommended by the manufacturer (see *SI Text* for details). The bacterial expression vector GST was expressed and purified as described in ref. 44.

Cell Treatment. Double thymidine block was achieved by seeding the HeLa cells in six-well plates 8 h before incubation in medium with 2 mM thymidine for 16 h. The cells were washed and incubated in fresh medium for 8 h. A second 16-h incubation in 2 mM thymidine was carried out before releasing the block. Upon synchronization at G1/S boundary, cells were treated with 5 mM H_2O_2 for 40 min at 37 °C and then recovered in fresh medium for 5 h. For analysis of the cell synchronization at G1/S boundary (Fig. S1*A*), the cells were fixed in 70% ethanol, washed and incubated with 200 μg/mL RNase A (Roche Diagnostics) in PBS for 30 min at 37 °C. Propidium iodide (20 μg/mL; Sigma) was added and the DNA content was analyzed by flow cytometric analysis using a Cytomics FC 500 (Beckman Coulter).

Microscopy and UVA Laser Microirradiation. HeLa cells were grown on glass coverslips, synchronized by double thymidine block, and laser microirradiated (Fig. 1) or treated with 5 mM H_2O_2 (Fig. S1 *B*–*E*) as described above. Upon fixation, cells were incubated with primary 8-oxo-G, MUTYH, or DNA pol λ antibody. Next, cells were washed three times with PBS and incubated with secondary FITC or Texas Red antibody (Jackson ImmunoResearch) for 30 min at room temperature. Images were captured with an Olympus BX51 fluorescent microscope and acquired with CCD camera (Orca AG) using CellR software (Olympus). At least 100 nuclei were analyzed in each experiment. For additional information see *SI Text*.

Cross-Linking Assay. The cross-linking assay with hairpin oligonucleotide substrates attached to streptavidin magnetic beads was performed as described in ref. 23. For direct comparison, cross-linked proteins from different substrates were analyzed in parallel on the two immunoblots treated simultaneously, under the same conditions and with the same exposure time.

GST Pull-Down Assay. Purified recombinant GST tagged MUTYH (3 μg) was coupled to glutathione Sepharose beads and used in a pull-down assay with 800 ng of purified recombinant human APE1, DNA pols δ, and λ. As an input control, 100 ng of purified recombinant human APE1, DNA pols δ, and λ was applied. Pull-down assay was performed as described in *SI Text*.

8-oxo-G Specificity Assays. ***Primer extension assay.*** For denaturing gel analysis of DNA synthesis products, the reaction mixture (10 μL) contained 50 mM Tris·HCl (pH 7.5), 20 mM KCl, 2 mM DTT, and 10 mM Mg^{2+}. Concentrations of DNA pol δ, MUTYH, APE1, PCNA, RP-A, dNTPs, the 5′ ^{32}P-labeled, and unlabelled primer/template were as indicated in the Figs. and Fig. Legends. Reaction products were analyzed on 7M urea/10% polyacrylamide gel (see *SI Text* for details).

Repair assay. For denaturing gel analysis of DNA repair products the reaction mixture (10 μL) contained 50 mM Tris·HCl (pH 7.5), 20 mM KCl, and 2 mM DTT. Concentrations of MUTYH, APE1, DNA pol λ, FEN1, DNA ligases I and III, PCNA, RP-A, dNTPs, and the 5′ ^{32}P-labeled double-stranded substrate containing A:8-oxo-G mispair were as indicated in the Figs. and Fig. Legends. Reaction products were separated on a 7 M urea/15% polyacrylamide gel. For reaction and assay details see *SI Text*.

Steady-State Kinetic Analysis. Reactions were performed as described above. Quantification was done by densitometry with a PhosphorImager (Typhoon Trio, GE Healthcare). The initial velocities of the reaction were calculated from the values of integrated gel band intensities with the programs ImageQuant and GraphPad Prism 5.0 (see *SI Text*).

ACKNOWLEDGMENTS. We thank G.L. Dianov, J.L. Parsons, I. Shevelev, and A.L. Lu for providing expression constructs; E. Ferrari and R. Imhof for purifying DNA pol λ, FEN1, and DNA ligase III; and G. Villani, G. Maga, K. Ramadan, and M. Stucki for critically reading of the manuscript and their suggestions. This work is supported by the Swiss National Science Foundation Grant 3100–109312/2 and the University of Zürich.

1. Collins AR (1999) Oxidative DNA damage, antioxidants, and cancer. *Bioessays* 21:238–246.
2. Avkin S, Livneh Z (2002) Efficiency, specificity and DNA polymerase-dependence of translesion replication across the oxidative DNA lesion 8-oxoguanine in human cells. *Mutat Res* 510:81–90.
3. Greenman C, et al. (2007) Patterns of somatic mutation in human cancer genomes. *Nature* 446:153–158.
4. Slupska MM, Luther WM, Chiang JH, Yang H, Miller JH (1999) Functional expression of hMYH, a human homolog of the *Escherichia coli* MutY protein. *J Bacteriol* 181:6210–6213.
5. Takao M, Zhang QM, Yonei S, Yasui A (1999) Differential subcellular localization of human MutY homolog (hMYH) and the functional activity of adenine:8-oxoguanine DNA glycosylase. *Nucleic Acids Res* 27:3638–3644.
6. Braithwaite EK, et al. (2005) DNA polymerase lambda mediates a back-up base excision repair activity in extracts of mouse embryonic fibroblasts. *J Biol Chem* 280:18469–18475.
7. Fortini P, et al. (1998) Different DNA polymerases are involved in the short- and long-patch base excision repair in mammalian cells. *Biochemistry* 37:3575–3580.
8. Stucki M, et al. (1998) Mammalian base excision repair by DNA polymerases delta and epsilon. *Oncogene* 17:835–843.
9. Allinson SL, Dianova II, Dianov GL (2001) DNA polymerase beta is the major dRP lyase involved in repair of oxidative base lesions in DNA by mammalian cell extracts. *EMBO J* 20:6919–6926.
10. Dianov GL, Prasad R, Wilson SH, Bohr VA (1999) Role of DNA polymerase beta in the excision step of long patch mammalian base excision repair. *J Biol Chem* 274:13741–13743.
11. Podlutsky AJ, Dianova II, Podust VN, Bohr VA, Dianov GL (2001) Human DNA polymerase beta initiates DNA synthesis during long-patch repair of reduced AP sites in DNA. *EMBO J* 20:1477–1482.
12. Sobol RW, et al. (1996) Requirement of mammalian DNA polymerase-beta in base-excision repair. *Nature* 379:183–186.
13. Sobol RW, et al. (2000) The lyase activity of the DNA repair protein beta-polymerase protects from DNA-damage-induced cytotoxicity. *Nature* 405:807–810.
14. Ramadan K, Shevelev I, Hubscher U (2004) The DNA-polymerase-X family: Controllers of DNA quality? *Nat Rev Mol Cell Biol* 5:1038–1043.
15. Garcia-Diaz M, Bebenek K, Kunkel TA, Blanco L (2001) Identification of an intrinsic 5′-deoxyribose-5-phosphate lyase activity in human DNA polymerase lambda: A possible role in base excision repair. *J Biol Chem* 276:34659–34663.
16. Lee JW, et al. (2004) Implication of DNA polymerase lambda in alignment-based gap filling for nonhomologous DNA end joining in human nuclear extracts. *J Biol Chem* 279:805–811.
17. Nick McElhinny SA, et al. (2005) A gradient of template dependence defines distinct biological roles for family X polymerases in nonhomologous end joining. *Mol Cell* 19:357–366.
18. Maga G, et al. (2007) 8-oxo-guanine bypass by human DNA polymerases in the presence of auxiliary proteins. *Nature* 447:606–608.
19. Maga G, et al. (2002) Human DNA polymerase lambda functionally and physically interacts with proliferating cell nuclear antigen in normal and translesion DNA synthesis. *J Biol Chem* 277:48434–48440.
20. Picher AJ, Blanco L (2007) Human DNA polymerase lambda is a proficient extender of primer ends paired to 7,8-dihydro-8-oxoguanine. *DNA Repair (Amst)* 6:1749–1756.
21. Maga G, et al. (2008) Replication protein A and proliferating cell nuclear antigen coordinate DNA polymerase selection in 8-oxo-guanine repair. *Proc Natl Acad Sci USA* 105:20689–20694.
22. Kong X, et al. (2009) Comparative analysis of different laser systems to study cellular responses to DNA damage in mammalian cells. *Nucleic Acids Res* 37:e68.
23. Parsons JL, Dianov GL (2004) Monitoring base excision repair proteins on damaged DNA using human cell extracts. *Biochem Soc Trans* 32:962–963.
24. Moldovan GL, Pfander B, Jentsch S (2007) PCNA, the maestro of the replication fork. *Cell* 129:665–679.
25. Maga G, Hubscher U (2003) Proliferating cell nuclear antigen (PCNA): A dancer with many partners. *J Cell Sci* 116:3051–3060.
26. Parker A, et al. (2001) Human homolog of the MutY repair protein (hMYH) physically interacts with proteins involved in long patch DNA base excision repair. *J Biol Chem* 276:5547–5555.
27. Fortini P, et al. (2003) 8-Oxoguanine DNA damage: At the crossroad of alternative repair pathways. *Mutat Res* 531:127–139.
28. Parlanti E, Fortini P, Macpherson P, Laval J, Dogliotti E (2002) Base excision repair of adenine/8-oxoguanine mispairs by an aphidicolin-sensitive DNA polymerase in human cell extracts. *Oncogene* 21:5204–5212.
29. Hashimoto K, Tominaga Y, Nakabeppu Y, Moriya M (2004) Futile short-patch DNA base excision repair of adenine:8-oxoguanine mispair. *Nucleic Acids Res* 32:5928–5934.
30. Braithwaite EK, et al. (2005) DNA polymerase lambda protects mouse fibroblasts against oxidative DNA damage and is recruited to sites of DNA damage/repair. *J Biol Chem* 280:31641–31647.
31. Hirano S, et al. (2003) Mutator phenotype of MUTYH-null mouse embryonic stem cells. *J Biol Chem* 278:38121–38124.
32. Dianova II, Bohr VA, Dianov GL (2001) Interaction of human AP endonuclease 1 with flap endonuclease 1 and proliferating cell nuclear antigen involved in long-patch base excision repair. *Biochemistry* 40:12639–12644.
33. Warbrick E, Lane DP, Glover DM, Cox LS (1997) Homologous regions of Fen1 and p21Cip1 compete for binding to the same site on PCNA: A potential mechanism to co-ordinate DNA replication and repair. *Oncogene* 14:2313–2321.
34. Li X, Li J, Harrington J, Lieber MR, Burgers PM (1995) Lagging strand DNA synthesis at the eukaryotic replication fork involves binding and stimulation of FEN-1 by proliferating cell nuclear antigen. *J Biol Chem* 270:22109–22112.
35. Jonsson ZO, Hindges R, Hubscher U (1998) Regulation of DNA replication and repair proteins through interaction with the front side of proliferating cell nuclear antigen. *EMBO J* 17:2412–2425.
36. Levin DS, Bai W, Yao N, O'Donnell M, Tomkinson AE (1997) An interaction between DNA ligase I and proliferating cell nuclear antigen: Implications for Okazaki fragment synthesis and joining. *Proc Natl Acad Sci USA* 94:12863–12868.
37. Fan J, Otterlei M, Wong HK, Tomkinson AE, Wilson DM, 3rd (2004) XRCC1 co-localizes and physically interacts with PCNA. *Nucleic Acids Res* 32:2193–2201.
38. Manley JL, Fire A, Samuels M, Sharp PA (1983) In vitro transcription: Whole-cell extract. *Methods Enzymol* 101:568–582.
39. Podust VN, Chang LS, Ott R, Dianov GL, Fanning E (2002) Reconstitution of human DNA polymerase delta using recombinant baculoviruses: The p12 subunit potentiates DNA polymerizing activity of the four-subunit enzyme. *J Biol Chem* 277:3894–3901.
40. van Loon B, Ferarri E, Hubscher U (2009) in *DNA Replication, Methods and Protocols*, eds Vengrova S, Dalgaard JZ (Humana Press – Springer, New York), pp 345–359.
41. Ramadan K, et al. (2003) Human DNA polymerase lambda possesses terminal deoxyribonucleotidyl transferase activity and can elongate RNA primers: Implications for novel functions. *J Mol Biol* 328:63–72.
42. Stucki M, Jonsson ZO, Hubscher U (2001) In eukaryotic flap endonuclease 1, the C terminus is essential for substrate binding. *J Biol Chem* 276:7843–7849.
43. Saparbaev M, et al. (2002) 1,N(2)-ethenoguanine, a mutagenic DNA adduct, is a primary substrate of *Escherichia coli* mismatch-specific uracil-DNA glycosylase and human alkylpurine-DNA-N-glycosylase. *J Biol Chem* 277:26987–26993.
44. Toueille M, et al. (2004) The human Rad9/Rad1/Hus1 damage sensor clamp interacts with DNA polymerase beta and increases its DNA substrate utilisation utilization efficiency: Implications for DNA repair. *Nucleic Acids Res* 32:3316–3324.

Supporting Information

van Loon and Hübscher 10.1073/pnas.0907280106

SI Text

DNA Substrates. The sequences of used oligonucleotides were:

100-mer template, 3′-ATGTTGGTTCTCGTATGCTGCCGGTCACGGCTTAAGTGTXCCACAACACACAACCAACACCACCACAACACACCAACAACCCACAACACACACAACCACAC-AC-5′;

39-mer primer, 5′-TACAACCAAGAGCATACGACGGCCAGTGCCGAATTCACA-3′; complementary 100-mer, 5′-TACAACCAAGAGCATACGACGGCCAGTGCCGAATTCACAAGGTGTTGTGTGTTGGTTGTGGTGGTGTTGTGTGGTTGTTGGTGTTGTGTGTTGGTGTG-3′;

58-mer hairpin containing the lesion, 5′-CGACGCTATTCACAGGTGCTCTGAGGGTTTTCCCTCAGAGCACCXGTGAATAGCGTCG - BIOTIN-3′

58-mer hairpin control, 5′-CGACGCTATTCACCGGTGCTCTGAGGGTTTTCCCTCAGAGCACCGGTGAATAGCGTCG - BIOTIN-3′.

The bold letter X corresponds to the position of 8-oxo-G lesion.

Annealing of 100-mer containing 8-oxo-G lesion with the unlabeled or 5′-labeled 39-mer primer or 100-mer created primer/template or double-stranded substrate containing A:8-oxo-G mispair, respectively. The 39-mer primer and complementary 100-mer oligonucleotides were labeled with T4 polynucleotide kinase (New England Biolabs) in the presence of γ[^{32}P] ATP. Each labeled oligonucleotide was mixed with the 100-mer template oligonucleotide at 1:1 (M/M) ratio in the presence of 20 mM Tris·HCl (pH 7.4) and 150 mM NaCl, heated at 95 °C for 10 min, and then slowly cooled down at room temperature.

The hairpin 58-mer oligos were prepared in 10 mM Tris·HCl (pH 8.0), 1 mM EDTA (pH 8.0), and 200 mM NaCl, heated at 95 °C for 3 min, and then fast-cooled on ice.

Cells and Extracts. Human HeLa cells were grown at 37 °C in 5% CO_2 incubator in DMEM containing GlutaMAX-I supplemented with 10% FBS and 100 U/mL penicillin-streptomycin (all obtained from Gibco, Invitrogen).

Antibodies and Proteins. The human *h*MUTYH gene was isolated from pGEV1-hMYH (gift from A. L. Lu, University of Maryland, Baltimore, MD) as a *Xho*I-*Nhe*I-digested fragment and transferred into pET41a (Novagene) to obtain the pET41a-MUTYH expression construct. The pET41a-MUTYH expression construct was transformed into *E. coli* BL21 cells containing pRARE2 vector (Novagene). The cells were grown at 37 °C in Luria–Bertani (LB) medium containing appropriate antibiotics. Protein expression was induced at an OD_{600} of 0.6 by adding isopropyl β-D-thiogalactoside (IPTG) to a final concentration of 1 mM and incubating at 20 °C for a further 20 h before harvesting the cells. Cell pellet was resolved in lysis buffer [PBS: 125 mM NaCl, 1.5 mM KH_2PO4, 2.5 mM KCl-HCl (pH 7.4), and 8 mM Na_2HPO_4 plus 0.1% Triton X-100, 1 mM phenylmethanesulphonylfluoride (PMSF), 1 μg/mL leupeptin, 1 μg/mL pepstatin, and 1 μg/mL bestatin] and cells lysed by two passages through a French press. The cell lysate was additionally sonicated at 4 °C for 2 min. GST-tagged MUTYH fusion protein was further bound to the glutathione Sepharose beads according to manufacturer's instructions (GE Healthcare). The cell lysate was incubated with the beads at 4 °C overnight. This was followed by six washing steps in 10 vol washing buffer (PBS, 0.2% Triton X-100, 1 μg/mL leupeptin, 1 μg/mL pepstatin, and 1 μg/mL bestatin) at 4 °C for 20 min. In the last washing step PBS only was used. Bound proteins were eluted by addition of elution buffer [30 mM Tris·HCl (pH 8.0), 50 mM gluthatione (pH 8.0), 10% glycerol, and 150 mM NaCl] and partially purified proteins were visualized by 10% SDS/PAGE. Fractions containing MUTYH were pooled, dialysed with dialysis buffer [30 mM Tris·HCl (pH 7.5), 1 mM EDTA (pH 8.0), 1 mM β-mercaptoethanol, 50 mM NaCl, and 10% glycerol], and divided into small aliquots and stored at −80 °C.

Microscopy and UVA Laser Microirradiation. HeLa cells were grown on glass coverslips, synchronized by double thymidine block, and laser microirradiated (Fig. 1) or treated with 5 mM H_2O_2 (Fig. S1 *B–E*). For laser microirradiation, MMI CELLCUT system containing a UVA laser of 355 nm (Molecular Machines & Industries) was used. Immediately after treatment, cells were placed back to incubator and incubated for 3 h. Treated cells were next fixed with 4% paraformaldehyde for 15 min and permeabilized at room temperature (23 °C) in PBS + 0.2% Triton for 10 min. After being blocked in PBS containing 10% FBS for 1 h at room temperature, cells were incubated with indicated primary antibody for an additional 1 h. Next cells were washed three times with PBS and incubated with secondary FITC or Texas Red antibody (Jackson ImmunoResearch) for 30 min at room temperature. Nuclear DNA was counterstained with DAPI (4′,6′-diamidino-2-phenylindole; Vector Laboratories). Images were captured with a Olympus BX51 fluorescent microscope and aquired with CCD camera (Orca AG) using CellR software (Olympus). At least 100 nuclei were analyzed in each experiment.

GST Pull-Down Assay. Glutathione Sepharose beads were equilibrated in pull-down buffer (PBS containing 1 μg/mL leupeptin, 1 μg/mL pepstatin, 1 μg/mL bestatin, and 1 mM PMSF) and precoated with BSA. To each of the tubes two proteins were added (i) 3 μg of either GST tagged MUTYH or GST and (ii) 800 ng one of the recombinant human proteins: APE1, DNA pol δ, or DNA pol λ. The samples were incubated for 2 h at 4 °C. After centrifugation the supernatant was removed and the beads were washed three times with 10 vol washing buffer (PBS containing 0.2% Triton X-100, 1 mM DTT, 1 μg/mL leupeptin, 1 μg/mL pepstatin, 1 μg/mL bestatin, and 1 mM PMSF) for 5 min at 4 °C. The beads were finally boiled in Laemmli sample loading buffer and subjected to 10% SDS PAGE. Proteins were transferred to a nitrocellulose membrane and detected by immunoblot analysis with the respective specific antibodies. As an input control, 100 ng of purified recombinant human APE1, DNA pol δ, and DNA pol λ was applied.

8-oxo-G Specificity Assays. *Primer Extension Assay.* For denaturing gel analysis of DNA synthesis products, the reaction mixture (10 μL) contained 50 mM Tris·HCl (pH 7.5), 20 mM KCl, 2 mM DTT, and 10 mM Mg^{2+}. Concentrations of DNA pol δ, MUTYH, APE1, PCNA, RP-A, dNTPs, the 5′ ^{32}P-labeled, and unlabelled primer/template were as indicated in the *Figures*. Reactions containing DNA pol δ, PCNA, RP-A, 5′ ^{32}P-labeled primer/template, dGTP, dTTP, and dATP or dCTP were incubated for 20 min at 37 °C. When the effect of MUTYH on the product of DNA pol δ synthesis was tested (Fig. 2*A*), reactions containing 5′ ^{32}P-labeled primer/template, dGTP, dTTP, and dATP or dCTP were treated in following steps: (i) incubation at 37 °C for 20 min in the presence of DNA pol δ, (ii) addition of MUTYH and APE1 and (iii) incubation for 20 min at 37 °C. Reactions containing DNA pol δ, PCNA, RP-A, unlabeled primer/template, dGTP, dTTP, and either α[^{32}P] dATP and dCTP or α[^{32}P] dCTP and dATP were incubated for 20 min at 37 °C. All reactions were stopped by addition of standard denaturing gel loading buffer (95% formamide, 10 mM

EDTA, xylene cyanol, and bromophenol blue), heated at 95 °C for 3 min and loaded on a 7 M urea/10% polyacrylamide gel.

Repair assay. For denaturing gel analysis of DNA repair products the reaction mixture (10 μL) contained 50 mM Tris·HCl (pH 7.5), 20 mM KCl, and 2 mM DTT. Concentrations of MUTYH, APE1, DNA pol λ, FEN1, DNA ligases I and III, PCNA, RP-A, dNTPs, and the 5′ ^{32}P-labeled ds substrate containing A:8-oxo-G mispair were as indicated in the *Figures*. Reactions containing MUTYH and 5′ ^{32}P-labeled ds substrate containing A:8-oxo-G mispair were treated in following steps: (i) incubation 5 min at 30 °C, (ii) addition of APE1 and 1 mM Mg^{2+}, (iii) incubation for 10 min at 30 °C, (iv) addition of dGTP, dTTP, dATP, or dCTP and DNA pol λ (in Fig. 3 *A*, *B*, and *D*; at this step additionally RP-A, PCNA, or FEN1 were added), and (v) incubation 15 min at 37 °C. Ligation experiments (Fig. 3 *C* and *E*) involved two additional steps: (vi) supplementation of the reactions with 14 mM $MgCl^{++}$ and DNA ligase I or III, and (vii) incubation 20 min at 37 °C. All reactions were stopped by addition of standard denaturing gel loading buffer (95% formamide, 10 mM EDTA, xylene cyanol, and bromophenol blue), heated at 95 °C for 3 min and loaded on a 7 M urea/15% polyacrylamide gel.

Steady-State Kinetic Analysis. Reactions were performed as described above. Quantification was done by densitometry with a PhosphorImager (Typhoon Trio, GE Healthcare). The initial velocities of the reaction were calculated from the values of integrated gel band intensities with the programs ImageQuant and GraphPad Prism 5.0:

$$I^*_T/I_{T-1},$$

where T is the target site, the template position of interest; I^*_T is the sum of the integrated intensities at positions T, $T + 1$,…, $T + n$.

All of the intensity values were normalized to the total intensity of the corresponding lane to correct for differences in gel loading. The apparent K_m and k_{cat} values were calculated by plotting the initial velocities in dependence of the nucleotide [dNTP] or primer [3′-OH] substrate concentrations and fitting the data according to Michaelis-Menten equation:

$$k_{cat}[E]_0/(1 + K_m/[S]),$$

where $[E]_0$, was the input enzyme concentration and $[S]$ was the variable substrate. Substrate incorporation efficiencies were defined as the k_{cat}/K_m ratio. Substrate concentrations used for dNTPs were 0.1–10 μM.

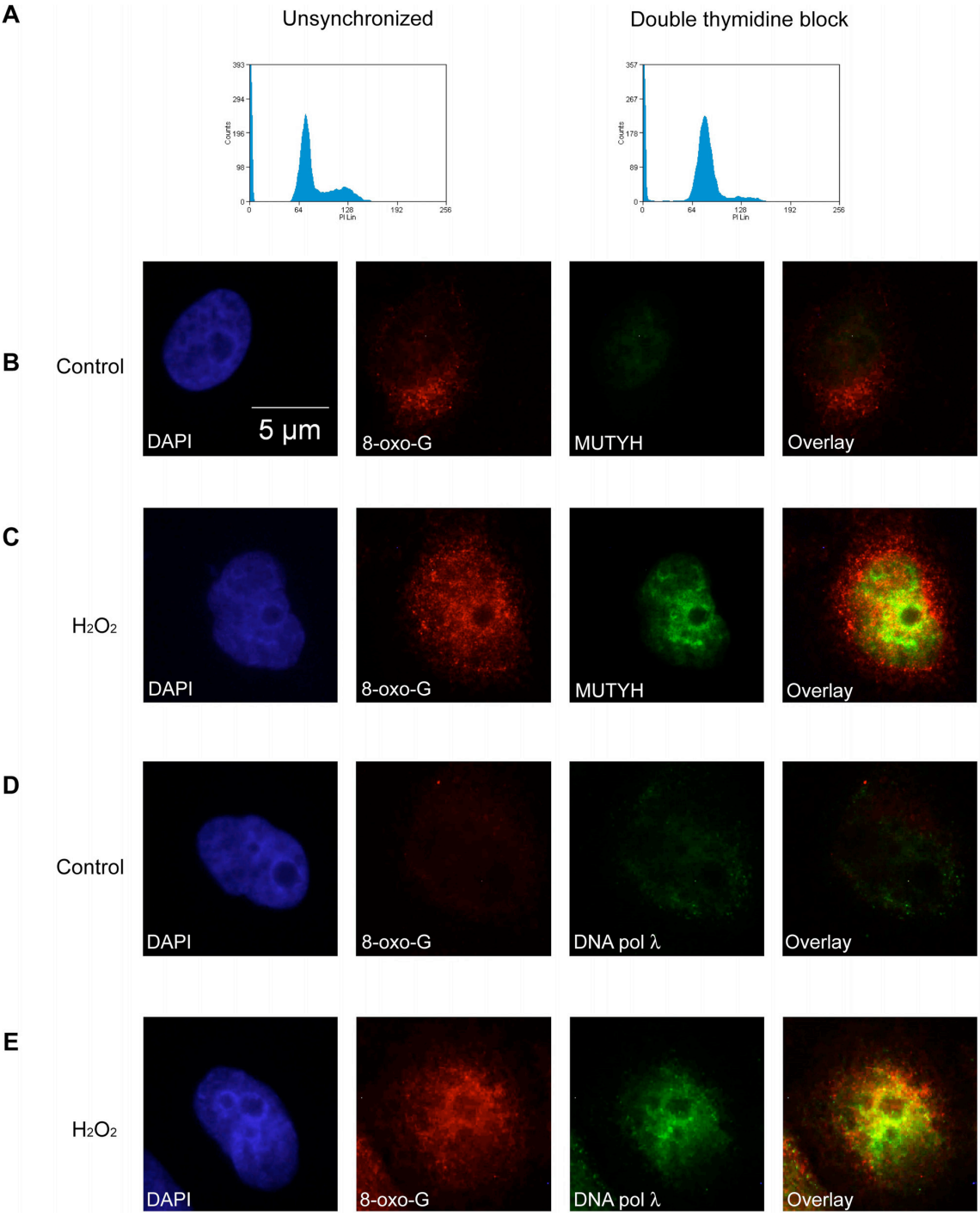

Fig. S1. MUTYH and DNA polymerase λ colocalize with the sites of oxidative DNA damage. The experiments were done as described in *Materials and Methods*. (*A*) Flow cytometric analysis of the unsynchronized (*Left*) and HeLa cells synchronized (*Right*) by the double thymidine block. Synchronized cells were collected immediately after the release. (*B–E*) HeLa cells were synchronised in S-phase by Double Thymidine block and were released (*B* and *D*) or treated with 5 mM H_2O_2 (*C* and *E*) for 40 min. Upon 5-h recovery, cells were stained with antibodies against 8-oxo-G and MUTYH (*B* and *C*) or DNA pol λ (*D* and *E*).

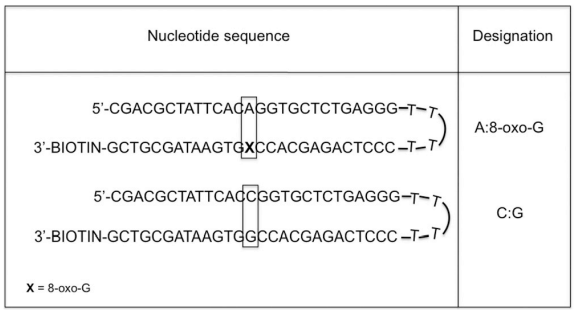

Fig. S2. Structure of oligonucleotides used in the cross-linking experiments. To construct 3′-biotinylated hairpin substrates for cross-linking, oligonucleotides were designed to contain the complementary sequence with a TTTT hairpin loop and a 3′-biotynylated moiety. A:8-oxo-G substrate contains A:8-oxo-G mispair, whereas the control substrate contains C:G base pair at the same position.

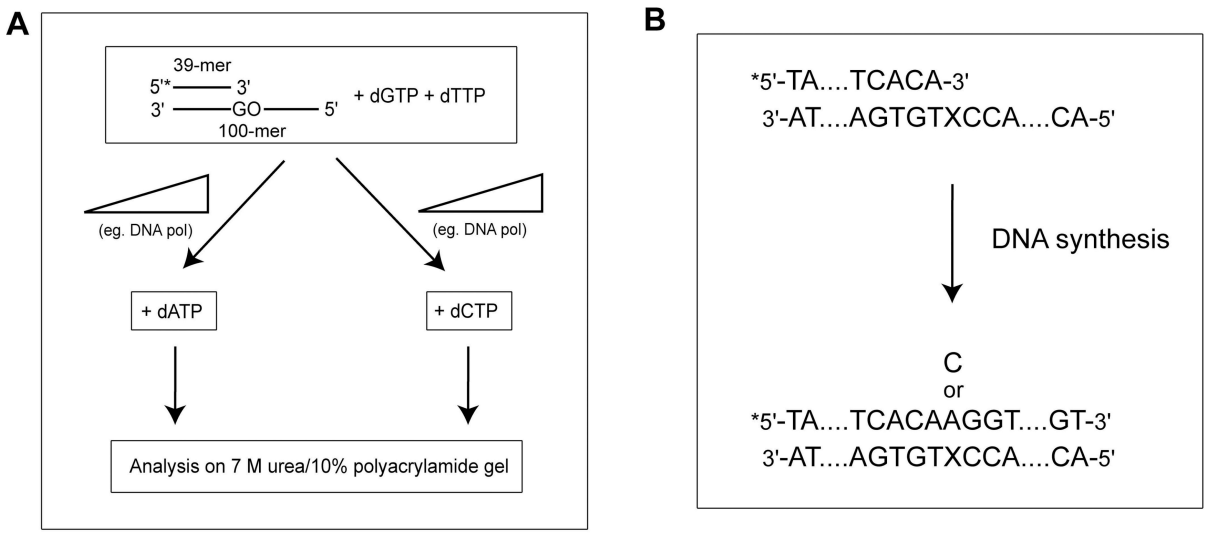

Fig. S3. An 8-oxo-G specificity assay enables the direct detection of the DNA polymerase fidelity during replication. (*A*) Schematic representation of the 8-oxo-G specificity assay. The master mix of 8-oxo-G specificity assay contained dGTP, dTTP and 5′-labeled primer/template with an 8-oxo-G lesion at + 1 position. The mix was next divided in two equal halves. To one, dATP was added and to the other, dCTP. Mix containing dATP or dCTP was equally distributed to the reaction tubes and proteins of interest titrated. The reaction products were separated on a polyacrylamide gel and quantified. (*B*) Schematic representation of the primer/template used in 8-oxo-G specificity assay. The only position where dATP or dCTP can be incorporated during DNA synthesis, on such template, is opposite the 8-oxo-G lesion (designated as X) itself. Upon bypass of the lesion for the elongation, only dGTP and dTTP are required.

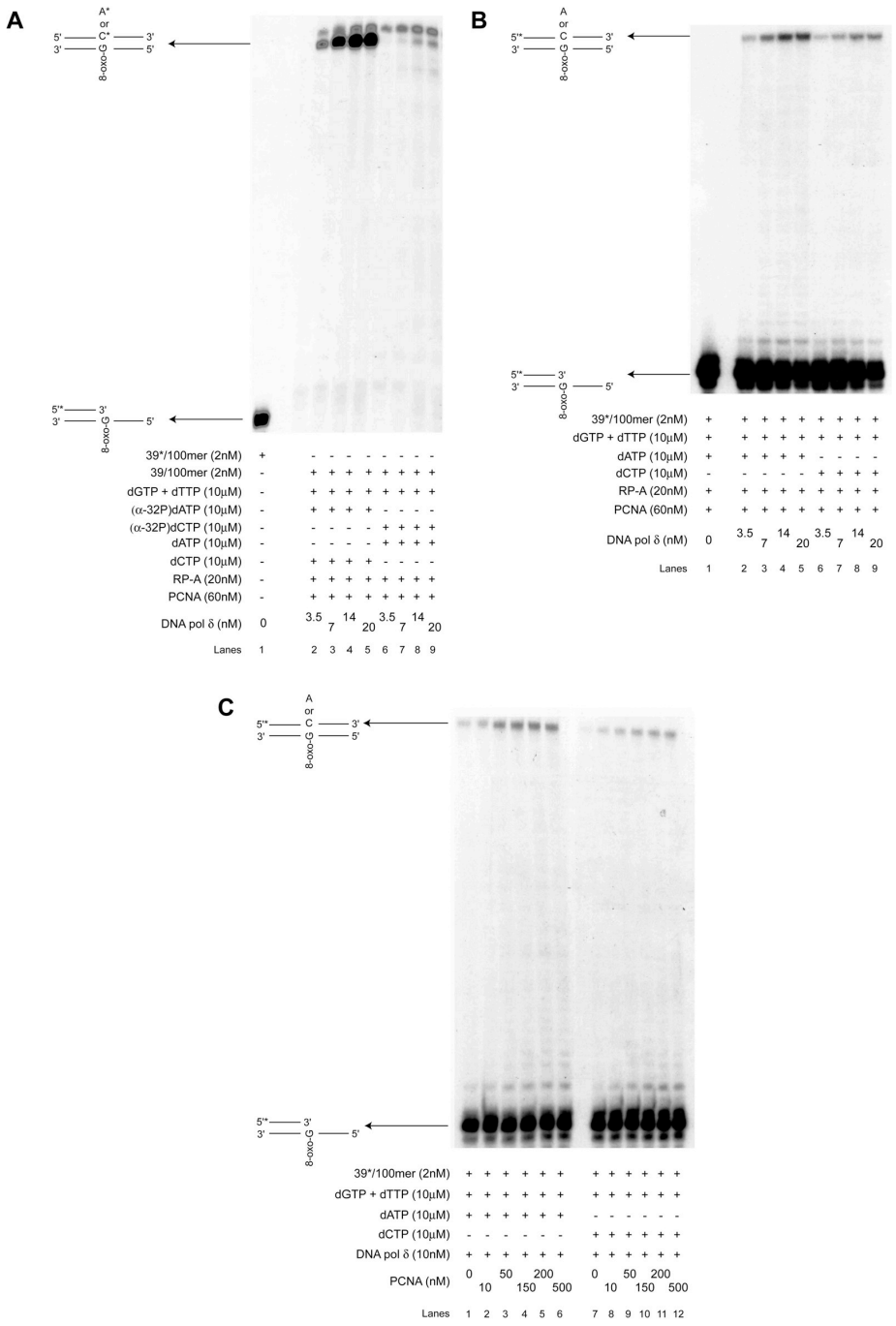

Fig. S4. The replicative DNA polymerase δ preferentially incorporates dATP opposite an 8-oxo-G even in the presence of PCNA. The experiments were done as described in *Materials and Methods*. (*A*) Replication over an unlabeled primer/template by DNA pol δ in the presence of PCNA, RP-A, dGTP, dTTP, and α[^{32}P] dATP + dCTP (lanes 2–5) or α[^{32}P] dCTP + dATP (lanes 6–9). The structure of the templates and reaction products are shown next to the panel. Lane 1: control reaction containing labeled primer/template in the absence of DNA pol δ. (*B*) Replication over a radioactively labeled primer/template by DNA pol δ in the presence of PCNA, RP-A, dGTP, dTTP, and dATP (lanes 2–5) and dCTP (lanes 6–9). The structure of the templates and reaction products are shown next to the panel. Lane 1: control reaction containing labeled primer in the absence of DNA pol δ. (*C*) Effect of PCNA on the replication over primer/template by DNA pol δ in the presence of dGTP, dTTP and dATP (lanes 2–6) or dCTP (lanes 8–12). The structure of the templates and reaction products is shown next to the panel. Lanes: 1 and 7 control reactions in the absence of PCNA.

6.2. Replication Protein A and Proliferating Cell Nuclear Antigen Coordinate DNA Polymerase Selection in 8-oxo-guanine Repair

Reprinted from *Proceedings of National Academy of Sciences USA* (2008) **105**, 20689-94.

My contribution to this paper was to show the physical interaction between replication protein A and DNA polymerases λ and β.

Replication protein A and proliferating cell nuclear antigen coordinate DNA polymerase selection in 8-oxo-guanine repair

Giovanni Maga[a,1], Emmanuele Crespan[a], Ursula Wimmer[b], Barbara van Loon[b], Alessandra Amoroso[a], Chiara Mondello[a], Cristina Belgiovine[a], Elena Ferrari[b], Giada Locatelli[c], Giuseppe Villani[c], and Ulrich Hübscher[b]

[a]Institute of Molecular Genetics, Consiglio Nazionale delle Ricerche, Via Abbiategrasso 207, I-27100 Pavia, Italy; [b]Institute for Veterinary Biochemistry and Molecular Biology, University of Zurich-Irchel, Winterthurerstrasse 190, CH-8057 Zurich, Switzerland; and [c]Institut de Pharmacologie et de Biologie Structurale, Centre National de la Recherche Scientifique, Unité Mixte de Recherche 5089, Université Paul Sabatier Toulouse III, 205 Route de Narbonne, 31077 Toulouse Cedex, France

Communicated by I. Robert Lehman, Stanford University School of Medicine, Stanford, CA, November 6, 2008 (received for review June 24, 2008)

The adenine misincorporated by replicative DNA polymerases (pols) opposite 7,8-dihydro-8-oxoguanine (8-oxo-G) is removed by a specific glycosylase, leaving the lesion on the DNA. Subsequent incorporation of C opposite 8-oxo-G on the resulting 1-nt gapped DNA is essential for the removal of the 8-oxo-G to prevent G–C to T–A transversion mutations. By using model DNA templates, purified DNA pols β and λ and knockout cell extracts, we show here that the auxiliary proteins replication protein A and proliferating cell nuclear antigen act as molecular switches to activate the DNA pol λ- dependent highly efficient and faithful repair of A:8-oxo-G mismatches in human cells and to repress DNA pol β activity. By using an immortalized human fibroblast cell line that has the potential to induce cancer in mice, we show that the development of a tumoral phenotype in these cells correlated with a differential expression of DNA pols λ and β.

Reactive oxygen species (ROS) are produced during normal cell metabolism and through the action of exogenous agents (1). When ROS react with DNA, the most frequently generated lesion (10^3 to 10^4 per cell per day) is 7,8-dihydro-8-oxoguanine (8-oxo-G) (2), whose mutagenic potential in aging, tumor transformation, and neurodegenerative diseases is well established. The presence of 8-oxo-G in the replicating strand can lead to frequent misincorporation of A opposite the lesion by the human replicative DNA polymerases (pols) α, δ, and ε (3). Full repair of 8-oxo-G lesion is guaranteed by 2 different base excision repair (BER) systems: (*i*) an OGG1-dependent, which targets C:8-oxo-G mispairs, removes the lesion and leaves an intact DNA strand to act as template for the resynthesis step (4); and (*ii*) a MUTYH-dependent pathway, which targets the A:8-oxo-G base pair and removes the adenine (5–7). Subsequent error-free bypass of the lesion requires a specialized DNA pol that can catalyze the correct incorporation of C opposite 8-oxo-G during the resynthesis step, reconstituting a C:8-oxo-G base pair that could subsequently be repaired by the OGG1-dependent BER. However, the majority of human DNA pols insert an adenine opposite 8-oxo-G on the template strand with high frequencies (10–75% of the time). Thus, the molecular mechanism ensuring correct and efficient repair of A:8-oxo-G mismatches in human cells is currently undetermined.

We have recently shown (8) that the BER enzyme DNA pol λ, which belongs to DNA pol family X (9), is very efficient in performing error-free translesion synthesis past the 2 major oxidative lesions 8-oxo-G (8) and 2-hydroxy-adenine (2-OH-A) (10). Moreover, its fidelity and efficiency is enhanced 2 orders of magnitude by the auxiliary proteins proliferating cell nuclear antigen (PCNA) and replication protein A (RP-A), both for normal and translesion synthesis, resulting in dATP incorporation frequencies opposite 8-oxo-G as low as 10^{-3}. On the other hand, the other major BER enzyme DNA pol β shows a relaxed nucleotide insertion specificity opposite 8-oxo-G, with erroneous (i.e., dATP) incorporation occurring in 20–30% of the cases.

Because of the apparently overlapping roles in BER of DNA pol β and λ, a discriminatory mechanism is required for the repair machinery to properly select DNA pol λ vs. DNA pol β in the MUTYH-dependent BER pathway. The DNA glycosylase MUTYH has been shown to interact with both PCNA and RP-A, suggesting its involvement in replication-coupled BER of A:8-oxo-G mismatches. DNA pol λ also interacts with PCNA and its activity is modulated by RP-A (11–14). In the present work, we show a role of PCNA and RP-A in selecting the most appropriate DNA pol for 8-oxo-G repair. In addition, we investigated the variation of the relative levels of DNA pol λ and β in a model cell line, cen3tel (15). Cen3tel cells acquired the ability to replicate indefinitely, but also showed neoplastic transformation driven by successive stepwise mutations in tumor suppressor genes and oncogenes such as *p16INK4a*, *p14ARF p53*, and *c-myc*, ultimately becoming able to induce tumors when injected in immunocompromised mice (16). Our results suggest that the misregulated expression of DNA pols β and λ might play an important role in cancer development.

Results

8-Oxo-G Bypass Efficiency and Selectivity of DNA Pol λ Are Independent from Gap Size. As shown in Fig. 1 *A* and *B* and Table S1, DNA pol λ incorporated dCTP better than dATP opposite an 8-oxo-G lesion on DNA substrates with gaps of increasing size (1, 2, and 8 nt), irrespective of the size of the gap. A 1-nt strand displacement event, corresponding to a +2-nt product, was observed on the 1-nt gap substrate (Fig. S1*A*, lanes 11–14 and 21), whereas no strand displacement was observed on the 2- or 8-nt gapped substrates (Fig. S1*A*, lane 22 and *B*, lanes 11–16). This 1-nt strand displacement depended on both the nucleotide and the enzyme concentration (Fig. S1*C*, compare lanes 1 and 5 with lanes 9 and 13) and was likely caused by transient "breathing" of the 5′ end, which allowed insertion of 1 additional nucleotide, as already described for DNA pol β (17). Under these conditions, PCNA showed no enhancement of strand displacement (Fig. S1*C*).

RP-A Increases the Error-Free Bypass of 8-Oxo-G by DNA Pol λ on a 1-nt Gapped Substrate. When RP-A was included in the reaction, it reduced the rate of dATP, but not dCTP, incorporation opposite

Author contributions: G.M., G.V., and U.H. designed research; G.M., E.C., U.W., B.v.L., A.A., C.B., E.F., and G.L. performed research; C.M., G.V., and U.H. contributed new reagents/analytic tools; G.M., C.M., G.V., and U.H. analyzed data; and G.M., C.M., G.V., and U.H. wrote the paper.

The authors declare no conflict of interest.

[1]To whom correspondence should be addressed. E-mail: maga@igm.cnr.it.

This article contains supporting information online at www.pnas.org/cgi/content/full/0811241106/DCSupplemental.

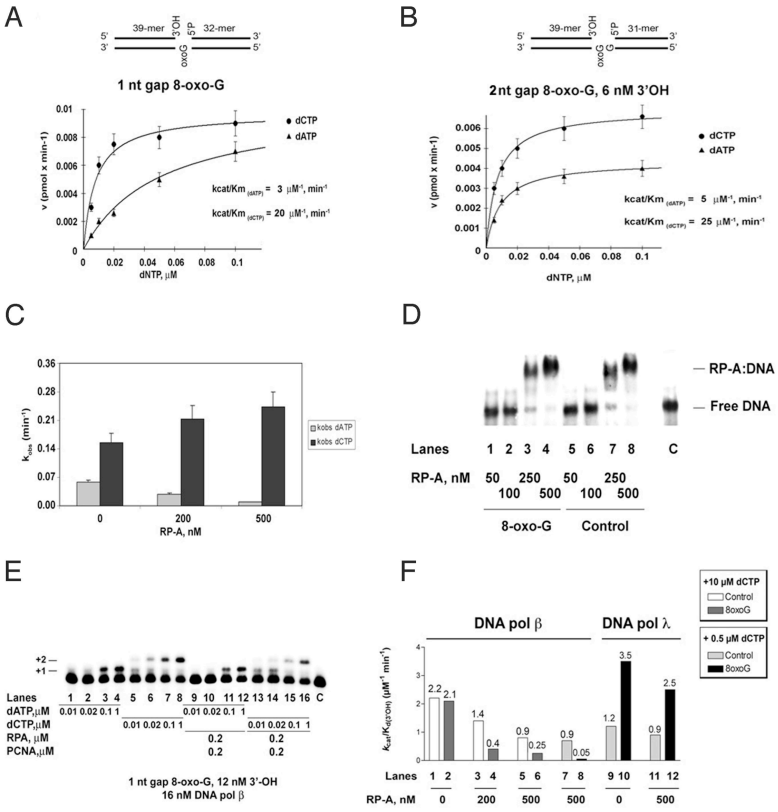

Fig. 1. PCNA and RP-A promoted error-free bypass of 8-oxo-G by DNA pol λ and inhibited DNA pol β incorporation opposite an 8-oxoG on gapped DNA templates. Reactions were performed with recombinant DNA pols under the conditions specified in *Materials and Methods*. (*A*) Variation of the initial velocities of the reaction catalyzed by 6 nM DNA pol λ on the 1-nt gapped 8-oxo-G template (6 nM) in the presence of dCTP (○) or dATP (△), as a function of the nucleotide substrate concentration. Values are the mean of 3 independent experiments. Error bars are ± SD. (*B*) Variation of the initial velocities of the reaction catalyzed by 6 nM DNA pol λ on the 8-nt gapped 8-oxo-G template (6 nM) in the presence of dCTP (○) or dATP (△), as a function of the nucleotide substrate concentration. Values are the mean of 3 independent experiments. Error bars are ± SD. (*C*) Effects of increasing amounts of RP-A on the apparent incorporation rates for dATP (light gray bars) or dCTP (dark gray bars) on a 1-nt gapped 8-oxo-G template by DNA pol λ. Values are the mean of 3 independent replicates. Error bars represent ± SD values. (*D*) RP-A was incubated in the presence of 200 nM 5′-labeled 8-oxo-G or undamaged 1-nt gapped DNA substrates. Samples were run on a native PAGE. The positions of the free probe and the RP-A/DNA complex are shown on the right. (*E*) DNA pol β was incubated in the presence of the 1-nt gapped 8-oxo-G template and dATP (lanes 1–4 and 9–12) or dCTP (lanes 5–8 and 13–16), in the absence (lanes 1–8) or the presence (lanes 9–16) of PCNA and RP-A. Lane C, control reaction in the absence of nucleotides. (*F*) Effects of RP-A on the efficiency of primer binding (k_{cat}/K_d) by DNA pols λ and β on control and 8-oxo-G 1-nt gapped DNA templates. The k_{cat} and K_d values were obtained from 3 independent experiments as described in *Materials and Methods*. Mean values were used to calculate the k_{cat}/K_d ratios.

the lesion in a dose-dependent manner (Fig. 1*C* and Fig. S1 *D–F*). The selectivity of DNA pol λ for correct dCTP vs. the incorrect dATP increased >100-fold in the presence of RP-A (Table S1). Band-shift experiments (Fig. 1*D*) performed with either the 8-oxo-G (Fig. 1*D*, lanes 1–4) or the undamaged (Fig. 1*D*, lanes 5–8) 1-nt gapped templates clearly demonstrated that RP-A was able to bind both DNA substrates with similar affinities. Comparison of the bound vs. free signals showed that 500 nM RP-A was enough to fully saturate 200 nM of the DNA substrate (Fig. 1*D*, lanes 4 and 8). This molar excess reflected the change in the affinity of RP-A from 10^{-9} M for ssDNA to 10^{-7} M for dsDNA (18).

DNA Pol λ Is More Efficient than DNA Pol β in Error-Free Gap Filling Opposite an 8-Oxo-G Lesion in the Presence of RP-A and PCNA. As shown in Fig. 1*E* (lanes 1–8), DNA pol β showed similar incorporation efficiencies for dATP and dCTP opposite the lesion, with a selectivity index of ≈3 (Table S1), whereas, unlike DNA pol λ (8), it showed a greatly reduced efficiency of dCTP incorporation opposite an 8-oxo-G lesion with respect to the undamaged template (Fig. S1*G*, compare lanes 1–4 with lanes 5–8). Interestingly, PCNA and RP-A inhibited both dCTP and dATP incorporation by DNA pol β opposite the lesion (Fig. 1*E*, lanes 9–16 and Fig. S1*H*, lanes 5–8 and 13–16). As a result, in the presence of PCNA and RP-A DNA pol λ displays a 32-fold higher probability than DNA pol β to fill the gap opposite the lesion (Table S1). PCNA reduced dCTP incorporation opposite the lesion by DNA pol β by 30%, whereas RP-A inhibited the same reaction by 70% (Fig. S2*A*). PCNA or RP-A had no effect on dCTP incorporation opposite an undamaged G (Fig. S2*A*). DNA pol λ proved to be more efficient in inserting dCTP opposite 8-oxo-G than DNA pol β also in the presence of all 4 dNTPs (Fig. S3). In addition, RP-A selectively inhibited dCTP incorporation by DNA pol β but not by DNA λ opposite 8-oxo-G on a different sequence context (Fig. S4). Thus, RP-A appeared to be the major determinant for the decreased ability of DNA pol β to incorporate dCTP opposite the 8-oxo-G lesion.

RP-A Modulates the DNA Primer Binding Affinity of DNA Pols λ and β, Depending on the Presence of an 8-Oxo-G Lesion on the Template Strand. We next measured the DNA primer utilization efficiency ($k_{cat}/K_{d3'OH}$) of DNA pol λ and β by determining the amount of elongated primer as a function of the gapped DNA substrate concentration, in the presence of a fixed dCTP concentration. The calculated k_{cat}/K_d values are shown in Fig. 1*F*. In the absence of RP-A, DNA pol β was able to bind a 3′-OH primer end with the same efficiency in the absence (Fig. 1*F*, lane 1) or in the presence (Fig. 1*F*, lane 2) of the lesion, whereas DNA pol λ showed 3-fold preference for the damaged template (Fig. 1*F*, compare lanes 10 and 9). In the presence of 500 nM RP-A and 10 μM dCTP, DNA pol β interacted with the primer in the presence of an 8-oxo-G lesion 4-fold less efficiently than with the undamaged template (Fig. 1*F*, lanes 5 and 6). When dCTP was used at 0.5 μM in the presence of 500 nM RP-A, the loss of efficiency by DNA pol β for the damaged vs. undamage template was 18-fold (Fig. 1*F*, lanes 7 and 8). Conversely, when tested under the same conditions (0.5 μM dCTP, 500 nM RP-A), DNA pol λ showed a 2.7-fold preference for the damaged template (Fig. 1*F*, compare lanes 12 and 11). Under these conditions, DNA pol λ was 50-fold more efficient than DNA pol β in the presence of an 8-oxo-G lesion (Fig. 1*F*, compare lanes 8 and 12). These data clearly suggest that under low dCTP concentration (and this might be the case in vivo under oxidative stress and other emergency situations) the correct dCTP incorporation is better guaranteed by DNA pol λ in the presence of RP-A.

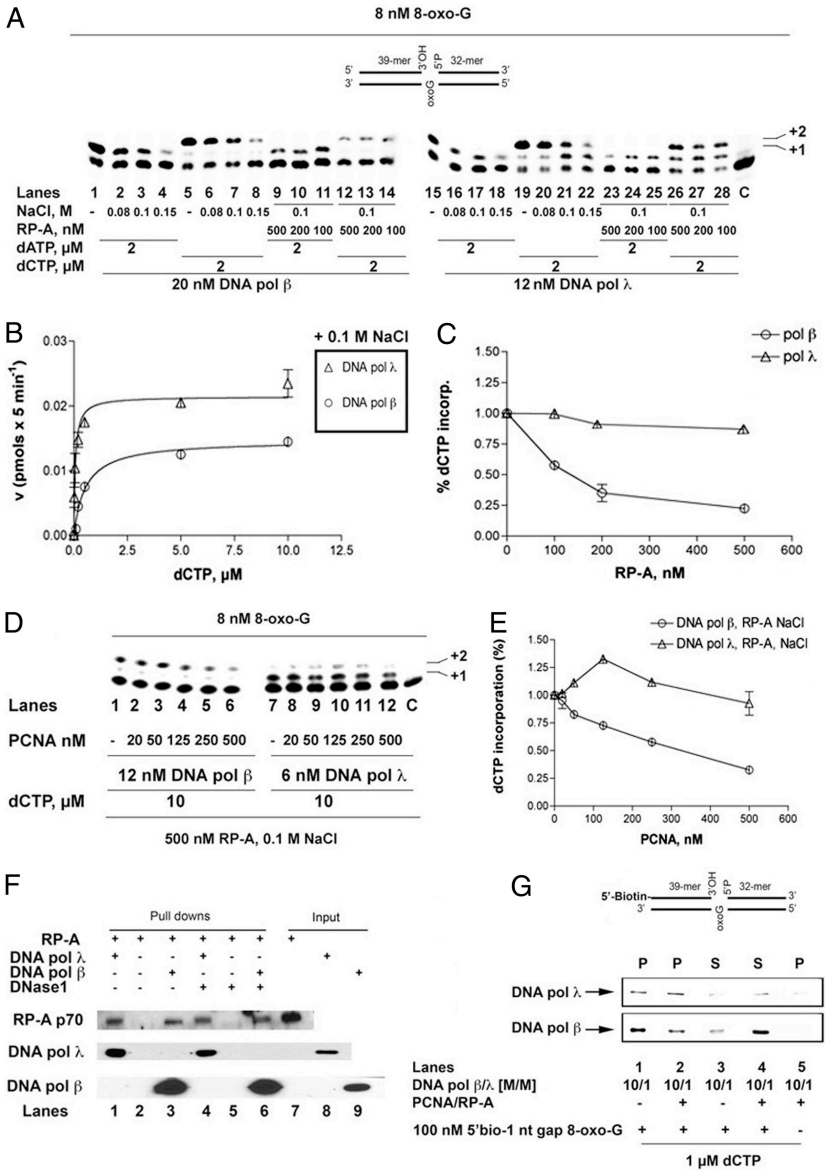

Fig. 2. PCNA and RP-A favor DNA pol λ gap filling and recruitment over DNA pol β at the 8-oxo-G lesion under physiological salt conditons. Reactions were performed with recombinant DNA pols under the conditions specified in *Materials and Methods*. (*A*) DNA pol β (lanes 1–14) or DNA pol λ (lanes 15–28) were incubated in the presence of the 1-nt gapped 8-oxo-G DNA template, 2 μM dATP (lanes 1–4, 9–11, 15–18, and 23–25) or 2 μM dCTP (lanes 5–8, 12–14, 19–22, and 26–28) and in the absence (lanes 1, 5, 15, and 19) or the presence of the indicated amounts of NaCl, either alone (lanes 1–8 and 15–22) or in combination with RP-A (lanes 9–14 and 23–28). Lane C, control reaction in the absence of nucleotides. The structure of the template used is shown at the top. (*B*) Variation of the apparent reaction velocities for dCTP incorporation opposite 8-oxo-G by DNA pol λ (△) or DNA pol β (○), as a function of the nucleotide substrate concentration, in the presence of 0.1 M NaCl. Values are the mean of 3 independent replicates. Error bars represent ± SD values. Template and enzyme concentrations were as in *A*. (*C*) Effects of increasing amounts of RP-A on the incorporation of dCTP opposite 8-oxo-G by DNA pol β (○) or DNA pol λ (△). Values are the mean of 3 independent replicates. Error bars represent ± SD values. Reactions conditions were as in *A*. (*D*) DNA pol β (lanes 1–6) or DNA pol λ (lanes 7–12) were incubated in the presence of the 1-nt gapped 8-oxo-G DNA template, 10 μM dCTP, RP-A and in the absence (lanes 1 and 7) or presence (lanes 2–6 and 8–12) of increasing amounts of PCNA. Lane C, control reaction in the absence of nucleotides. (*E*) Effect of increasing amounts of PCNA on the dCTP incorporation opposite 8-oxo-G by DNA pol λ (△) or DNA pol β (○), in the presence of 0.1 M NaCl, 500 nM RP-A. Values are the mean of 3 independent replicates. Error bars represent ± SD values. Template and enzymes were as in *D*. (*F*) Pull-down was performed as outlined in *Materials and Methods*. Lane 1: DNA pol λ bound to Ni-beads pulls down RP-A; lane 2: Ni-beads incubated with RP-A; lane 3: DNA pol β bound to Ni-beads pulls down RP-A; lanes 4–6: as lanes 1–3, but in the presence of DNase 1 (6 units); lane 7: input RP-A (100 ng); lane 8: input DNA pol λ (100 ng); lane 9: input DNA pol β (100 ng). (*G*) For pull-down experiments, DNA pols β and λ were incubated at a 10:1 molar ratio, in the presence of the 5′ biotinylated 1-nt gapped 8-oxo-G DNA template, 1 μM dCTP and in the absence (lanes 1 and 3) or presence (lanes 2 and 4) of 200 nM PCNA and 500 nM RP-A. Bound (pellet, P) and unbound (supernatant, S) proteins were detected by immunoblot. One-half of the supernatant was loaded on the gel. The structure of the template is shown on the right. Lane 5, control reaction in the absence of DNA template.

Physiological Salt Concentrations, PCNA, and RP-A Favor DNA Pol λ Over DNA Pol β on 1-nt Gapped Intermediates Bearing an 8-Oxo-G Lesion. Increasing salt concentrations (80–150 mM NaCl) reduced the incorporation of dATP and dCTP opposite 8-oxo-G by both DNA pol λ and β (Fig. 2*A*, lanes 1–8 and 15–22). However, DNA pol λ was significantly more efficient than DNA pol β in dCTP incorporation opposite 8-oxo-G in the presence of 0.1 M NaCl (Fig. 2*B*). By comparing the respective k_{cat}/K_m values (Table S1), DNA pol λ was 23.5-fold more efficient than DNA pol β in dCTP incorporation opposite 8-oxo-G in the presence of 0.1 M NaCl. Overall, dCTP incorporation by DNA pol β was reduced by RP-A by 75%, whereas under the same conditions DNA pol λ was affected <10% (Fig. 2*C*). At low dCTP concentrations (0.2–1 μM), the activity of DNA pol β was almost completely suppressed, whereas DNA pol λ was able to catalyze efficient error-free incorporation (Fig. S2*B*, compare lanes 1 and 2 with lanes 5 and 6). Comparison of the relative k_{cat}/K_m values, showed that DNA pol λ was 145-fold more efficient than DNA pol β for dCTP incorporation opposite 8-oxo-G in the presence of both RP-A and salt (Table S1). On the control template (i.e., in the absence of the 8-oxo-G lesion) DNA pol β and λ showed similar efficiencies of dCTP incorporation in the presence of both salt and RP-A, suggesting that the observed effect depended on the presence of the lesion (Fig. S2*C*). In the presence of RP-A and salt, PCNA was able to further reduce the ability to incorporate dCTP opposite 8-oxo-G of DNA pol β (Fig. 2*D*, lanes 1–6), but not of DNA pol λ (Fig. 2*D*, lanes 7–12). Quantification of the results showed that PCNA inhibited dCTP incorporation of DNA pol β by 70%, whereas DNA pol λ was

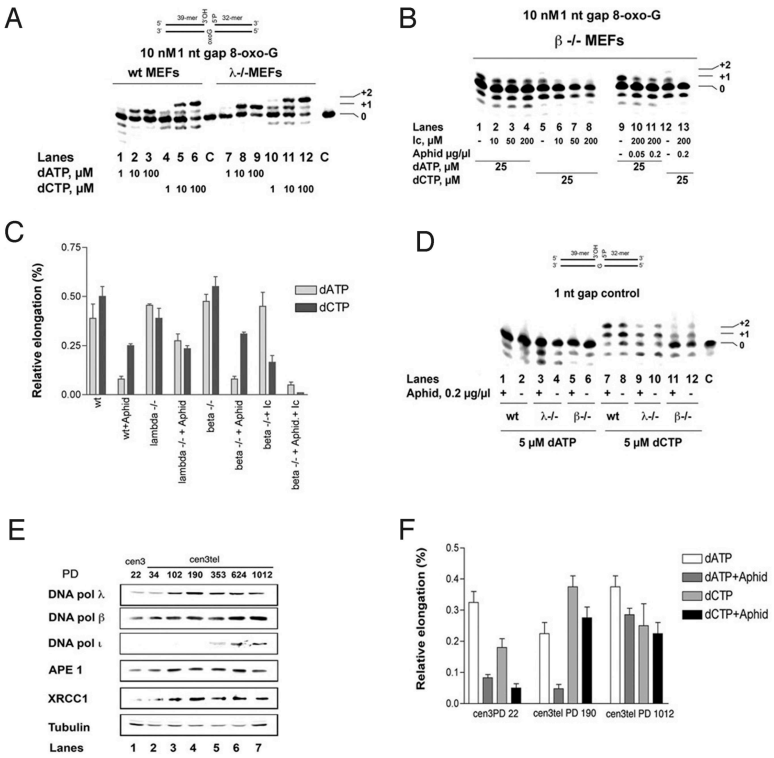

Fig. 3. The fidelity of 8-oxo-G bypass correlates with the relative levels of DNA pols λ and β in normal and tumor cells. Reactions were performed with cell extracts under the conditions specified in *Materials and Methods*. (*A*) WT (lanes 1–6) or $\lambda^{-/-}$ (lanes 8–12) MEF extracts (2 μg of total proteins) were incubated in the presence of dATP (lanes 1–3 and 7–9) or dCTP (lanes 4–6 and 10–12). Lanes C, control reactions in the absence of extracts. The structure of the template used is shown at the top. (*B*) $\beta^{-/-}$ MEF extracts (2 μg of total proteins) were incubated in the presence of the 1-nt gapped 8-oxo-G DNA template, dATP (lanes 1–4 and 9–11), dCTP (lanes 5–8, 12, and 13), and absence (lanes 1, 5, 9, and 12) or presence of compound Ic (lanes 2–4 and 6–8) or Aphidicolin (lanes 10, 11, and 13). (*C*) Relative activity, expressed as percentage of elongated primer ends, for dATP (light gray bars) or dCTP (dark gray bars) incorporation with the 1-nt gapped 8-oxo-G DNA template (50 nM) by different combinations of MEF extracts (2 μg of total proteins) and Aphidicolin (0.2 μg/μl) or Ic (200 μM). Values are the mean of 3 independent replicates. Error bars represent ± SD values. (*D*) Two micrograms of total proteins of WT MEFs (lanes 1, 2, 7, and 8), $\lambda^{-/-}$ MEFs (lanes 3, 4, 9, and 10), or $\beta^{-/-}$ MEFs (lanes 5, 6, 11, and 12) were incubated in the presence of 10 nM of the 1-nt gapped undamaged template, dATP (lanes 1–6), or dCTP (lanes 7–12), and in the presence (odd lanes) or absence (evens) of Aphidicolin. The structure of the template used is shown at the top. (*E*) Western blot analysis was performed by using extracts (20 μg of total proteins) from cen3 or cen3tel cells at different PDs, as indicated at the top. (*F*) Relative incorporation activity, expressed as percentage of elongated primer ends, of extracts (2 μg) from cen3 and cen3tel cells at different PDs, in the presence of 5 μM dATP (white bars), 5 μM dATP + 0.2 μg/μL Aphidicolin (dark gray bars), 5 μM dCTP (light gray bars) and 5 μM dCTP + 0.2 μg/μL Aphidicolin (black bars), on the 1-nt gapped 8-oxo-G DNA template (50 nM).

not affected (Fig. 2*E*). Taken together, these data suggest that PCNA and RP-A may favor the recruitment of DNA pol λ over DNA pol β on a 1-nt gap containing an 8-oxo-G lesion. Indeed, we found that either DNA pol λ (Fig. 2*F*, lane 1) or DNA pol β (Fig. 2*F*, lane 3) were able to pull down RP-A (visualized with anti-p70 Abs). No unspecific binding of RP-A to the beads (Fig. 2*F*, lanes 2), nor effect of DNase1 treatment was noted (Fig. 2*F*, lanes 4–6), ruling out unspecific DNA-mediated interactions. Next, we incubated the 1-nt gapped 8-oxo-G substrate carrying a 5′ biotinylated primer in the presence of 1 μM dCTP, DNA pols β and λ at a 10:1 molar ratio and in the absence or presence of PCNA and RP-A. Bound DNA pols pulled down by streptavidin-coupled agarose beads were visualized by Western blot analysis with specific antibodies. As shown in Fig. 2*G*, both DNA pols β and λ were recovered in the pellet in the absence of PCNA and RP-A (Fig. 2*G*, lane 1). Addition of auxiliary proteins, however, caused a marked reduction of bound DNA pol β (Fig. 2*G*, lane 2) and its correspondent increase in the supernatant (Fig. 2*G*, lane 4). Association of RP-A to the biotinylated DNA substrate under these conditions did not affect DNA pol λ binding (Fig. S2*D*). Overall, these data suggested that PCNA and RP-A strongly restrict association of DNA pol β to a 1-nt gapped substrate during dCTP incorporation opposite 8-oxo-G.

DNA Pol λ Is Responsible for the Majority of Error-Free Gap Filling in the Presence of an 8-Oxo-G Lesion. Extracts from WT or DNA pol λ knockout ($\lambda^{-/-}$) mouse embryonic fibroblasts (MEFs) were compared for their ability to incorporate either dATP or dCTP opposite 8-oxo-G on a 1-nt gapped substrate. Compared with WT MEFs, $\lambda^{-/-}$ cells showed an increased dATP incorporation (Fig. 3*A* and Fig. S5*A*). The dCTP vs. dATP bias of $\lambda^{-/-}$ MEFs dropped from 2.5 to 0.8. Next, the effect of Aphidicolin, a specific inhibitor of the family B DNA pols α, δ, ε, and ζ, was evaluated on WT, $\lambda^{-/-}$, and DNA pol β knockout ($\beta^{-/-}$) MEFs, in the absence (Fig. S5 *B* and *C*) or the presence (Fig. 3*B*) of compound Ic (*N*-9-fluorenylmethoxycarbonyl-aminoalkyl-triphosphate), a specific inhibitor of DNA pol λ (19). The results are quantified in Fig. 3*C*. In the absence of DNA pol β error-prone bypass of 8-oxo-G was almost exclusively caused by Aphidicolin-sensitive pols, whereas the majority of error-free bypass (75%) depended on DNA pol λ, as indicated by the effects of the inhibitor Ic. In $\lambda^{-/-}$ cell extracts there was a significant increase in Aphidicolin-resistant error-prone (i.e., dATP) incorporation, likely caused by a more prominent role of DNA pol β. Similar experiments were repeated in the presence of an undamaged 1-nt gapped template (Fig. 3*D*). No dATP incorporation was observed opposite a normal G on the template (Fig. 3*D*, lanes 1–6). The dCTP incorporation was substantially Aphidicolin-resistant in all 3 extracts (Fig. 3*D*, compare lanes 7, 9, and 11 with lanes 8, 10, and 12). Moreover, $\lambda^{-/-}$ MEFs showed only a marginal decrease in dCTP incorporation activity (Fig. 3*D*, compare lanes 7 and 8 with lanes 9 and 10), whereas $\beta^{-/-}$ cells showed a substantially reduced activity (Fig. 3*D*, compare lanes 7 and 8 with lanes 11 and 12), suggesting that DNA pol β is the major enzyme acting in normal BER. In summary, our results suggest that, in the cellular milieu, DNA pol λ is preferentially used over DNA pol β in gap-filling reactions in the presence of an 8-oxo-G lesion.

Relative Levels of DNA Pol λ and β Correlate with the Fidelity of 8-Oxo-G Bypass During Neoplastic Transformation. The levels of DNA pol β, DNA pol λ, and the BER enzymes AP-endonuclease (APE1) and XRCC1 were evaluated by Western blot analysis in extracts of cen3tel cells at different population doublings (PDs), ranging from nontumorigenic cen3tel cells (PD34) to highly tumorigenic cen3tel cells (PD1012), together with primary cells (cen3

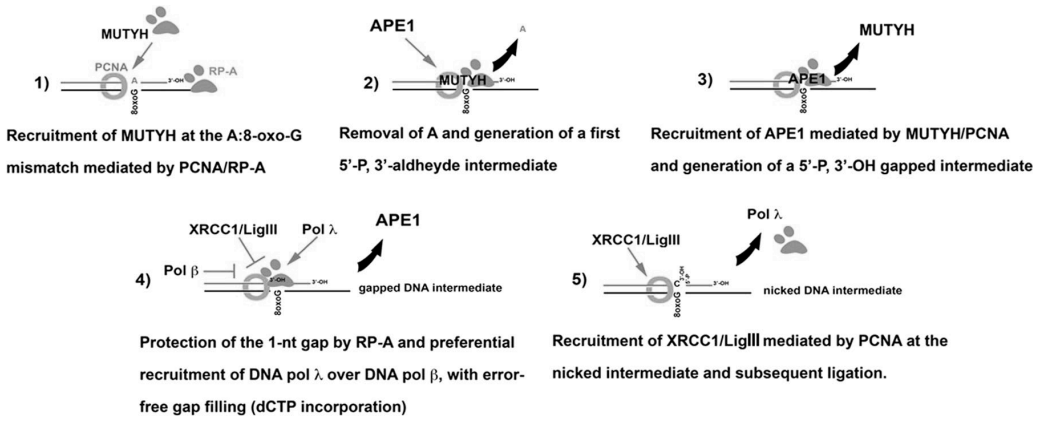

Fig. 4. A model for the coordinated action of PCNA, RP-A, and DNA pol λ during A:8-oxo-G mismatch repair. For details see *Discussion*.

cells, PD22) (Fig. 3*E*). Quantification of the bands, normalized toward the tubulin marker, is shown in Fig. S5*D*. DNA pol λ levels raised rapidly, reaching a peak ≈PD190, whereas DNA pol β showed a slower, but steady, increase, reaching a plateau ≈PD600. Thus, at PD190 DNA pol λ levels were ≈3-fold higher than those of DNA pol β, whereas at PD1012 the situation was reversed, with DNA pol β being 2.5-fold higher than DNA pol λ. Next, we analyzed the ability of extracts from cen3 primary fibroblast, cen3tel cells at PD190 and PD1012 to incorporate dATP or dCTP opposite 8-oxo-G, in the absence or presence of Aphidicolin (Fig. S5*E* and Fig. 3*F*). As can be seen, the correct dCTP vs. incorrect dATP incorporation ratio opposite 8-oxo-G decreased from 6 at PD190 to <1 at PD1012 and correlated with the correspondent changes in the relative levels of DNA pol λ to DNA pol β from 3:1 to 1:2.5. The levels of another translesion enzyme, DNA pol ι, which were undetectable before PD190, started to raise at later stages (PD >300) of transformation (Fig. 3*E*). The increase of this highly error-prone enzyme further suggests that deregulation of specialized DNA pols can play a role in tumor development.

Discussion

Earlier investigations suggested that long-patch (LP) BER involving DNA pols δ/ε was the major mechanism for the repair of A:8-oxo-G mismatches (20); however, in vitro reconstituted LP- and short-patch (SP) BER reactions were rather error-prone (21). In this work, we compared the activities of DNA pol λ and DNA pol β, the 2 major SP-BER pols (22–23), and showed that both DNA pol λ and DNA pol β physically interact with RP-A (Fig. 2*F*), which, together with PCNA, reduced the efficiency of gap-filling by DNA pol β in the presence of an 8-oxo-G lesion (Fig. 1*F*), by preventing its binding to the 1-nt gapped DNA (Fig. 2*G*). As a result, PCNA and RP-A ensure that dCTP is incorporated 750-fold better than dATP opposite 8-oxo-G on 1-nt gapped DNA, rendering DNA pol λ 145-fold more efficient than DNA pol β in processing 1-nt gap DNA intermediates containing an 8-oxo-G lesion. RP-A and PCNA increased the thermodynamic barrier for dCTP incorporation opposite 8-oxo-G by DNA pol β from 2 kcal × mol^{-1} (24) to ≈4 kcal × mol^{-1}, making this event thermodynamically equivalent to a misincorporation (25). Thus, PCNA and RP-A did not provide DNA pols with novel properties, but rather rendered the DNA substrate containing an 8-oxo-G optimal for DNA pol λ but very inefficient for DNA pol β. Two pathways may then act in the cell to remove A:8-oxo-G mispairs: 1 very error-prone and dependent on DNA pols δ/ε and LP-BER and important for immediate, replication-coupled repair of 8-oxo-G (20), and another more accurate one dependent on DNA pol λ and SP BER that might act to "clean up" the newly replicated DNA in the G_2 phase before mitosis.

In Fig. 4, we show a model for the MUTYH-dependent efficient and faithful repair of DNA containing A:8-oxo-G mismatches, resulting from error-prone lesion bypass by replicative DNA pols. This model is based on known protein–protein interactions among BER proteins and on the interactions of the DNA pols λ and β with RP-A. The bifunctional DNA glycosylase MUTYH is recruited to the A:8-oxo-G mismatch through interaction with RP-A and PCNA and removes the A. The action of APE1, another PCNA-interacting protein, which restores a 3′-OH moiety, the resulting gapped intermediate, can be recognized by several factors through competition for PCNA binding. In particular, the PCNA-interacting protein XRCC1 binds in vitro both gapped and nicked DNA intermediates with similar affinity. Binding to the gap by XRCC1 could potentially interfere with the filling step by the DNA pol. RP-A might prevent binding of the XRCC1/LigIII complex to the gap by covering it. PCNA and RP-A will also restrict DNA pol β action while favoring error-free gap filling of the 8-oxo-G-containing gap by DNA pol λ. Importantly, DNA pol β will not be inhibited by PCNA and RP-A on a gapped intermediate bearing a normal G, thus ensuring DNA pol β action during OGG1-dependent BER. After gap filling, RP-A and DNA pol λ dissociate, allowing XRCC1/LigIII binding to the resulting nicked intermediate through interaction with PCNA and subsequent ligation. In this way, the error-free processing is ensured at the gap-filling step by the combined action of PCNA and RP-A, so that only C-terminated 3′ ends are presented for ligation to the XRCC1/LigIII complex.

DNA pol λ is highly expressed in germinal tissues, particularly testis (26). Highly proliferating cells, particularly those that store the genetic information to be passed to the offspring, might be advantaged in having a very efficient and faithful mechanism for removing the dangerous promutagenic mispair A:8-oxo-G. Both DNA pol λ and DNA pol β are also overexpressed in many tumor types, along with the error-prone enzyme DNA pol ι (27). High levels of DNA pol β and ι have been shown to correlate with genomic instability, high frequency of mutations, and tumor progression (28–32). We found that DNA pol λ and β levels rise with different kinetics in cen3tel cells. We also found a close correlation between the relative levels of DNA pols λ and β, the fidelity of 8-oxo-G lesion bypass in these cells, and the different stages of neoplastic transformation. In summary, our data indicated that the auxiliary proteins PCNA and RP-A act as molecular switches to activate the DNA pol λ-dependent highly efficient and faithful repair of A:8-oxo-G mismatches in human cells, and that this pathway might be relevant during the development of cancer. In support of this hypothesis, we have previously provided preliminary evidence that targeting DNA pol

λ by specific inhibitors can reduce the proliferation of specific types of tumor cells (33).

Materials and Methods

Chemicals. Deoxynucleotides were purchased from GeneSpin. Labeled γ[^{32}P]ATP was purchased from GE Healthcare. Aphidicolin was purchased from Sigma. All other reagents were of analytical grade and purchased from Merck or Fluka. The 39-, 32-, 31-, and 25-mer oligonucleotides, either unlabeled or 5′-biotinylated, were purchased from MWG. Streptavidine-coupled magnetic beads were from Promega.

DNA Substrates. All oligonucleotides were purified from polyacrylamide denaturing gels (see *SI Text* for sequences, purification and template preparation details). Annealing of the 72-mer, either undamaged or containing the 8-oxo G lesion (8-oxo-dG-CEPhosphoramidite; Glen Research), with the 5′-labeled 39-mer primer and the 32-, 31-, or 25-mer terminator oligonucleotides generated the 1-, 2-, and 8-nt gapped templates, respectively.

Cells and Extracts. Immortalized Polλ$^{+/+}$, Polλ$^{-/-}$, Polβ$^{+/+}$, and Polβ$^{-/-}$ MEFs were grown and lysed according to standard protocols (see *SI Text* for details).

Telomerase immortalized cen3tel cells were obtained from primary cen3 fibroblasts by infection with an *hTERT*-containing retrovirus as described (15). Primary and immortalized cells were grown and extracts prepared as described (see *SI Text*).

Antibodies and Proteins. Antibodies against Tubulin, APE1, and XRCC1 were purchased from Santa Cruz. Antibodies against DNA pol ι were purchased from Abcam. Recombinant human DNA pols β and λ, RP-A, and PCNA were expressed and purified as described (8). Antibodies against DNA pol β and λ (polyclonal rabbit) and polyclonal chicken antibodies against RP-A p70 were from U.H. and G.M. laboratories.

Pull-Down Assays.

Ni-NTA agarose beads. Purified recombinant DNA pol λ (3 μg) and purified recombinant DNA pol β (3 μg) were coupled to Ni-NTA beads and used in pull-down experiments with 800 ng of purified recombinant RP-A, as described in *SI Text*.

Biotinylated substrate. For details see *SI Text*.

EMSAs. Purified recombinant RP-A was incubated 5 min at 37 °C in the presence of 5′-labeled 1-nt gapped substrate, either undamaged or containing the 8-oxo-G lesion, in 10 μL of reaction buffer [50 mM Tris·HCl (pH 7.0), 0.25 mg/ml BSA, 1 mM DTT, and 1 mM Mg^{2+}]. Samples were mixed with nondenaturing gel loading buffer [40% (wt/vol) sucrose, 0.25% bromophenol blue] and subjected to PAGE on a 5% native gel at 4 °C for 2 h at 5 V/cm. Position of the free probe and the protein–DNA complexes on the gel was visualized by laser scanning densitometry.

In Vitro Translesion Assays. For denaturing gel analysis of DNA synthesis products, the reaction mixtures (10 μL) contained 50 mM Tris·HCl (pH 7.0), 0.25 mg/mL BSA, 1 mM DTT, and 1 mM Mg^{2+}. Concentrations of crude extracts or purified DNA pols λ and β, PCNA, RP-A, dNTPs, and the 5′ ^{32}P-labeled primer/template were as indicated in the figure legends. Reactions were incubated for 5 min at 37 °C (unless otherwise stated) and then stopped by addition of standard denaturing gel loading buffer (95% formamide, 10 mM EDTA, xylene cyanol, and bromophenol blue), heated at 95 °C for 3 min and loaded on a 7 M urea/10% polyacrylamide gel.

Steady-State Kinetic Analysis. See *SI Text* for details.

ACKNOWLEDGMENTS. This work was supported partly by the Centre National de la Recherche Scientifique and a grant from the Association pour la Recherche sur le Cancer (to G.V.). U.H., B.v.L., E.F., and U.W. are supported by Oncosuisse, Union Bank of Switzerland ''im Auftrag eines Kunden,'' the Swiss National Science Foundation, and the University of Zurich. G.M. was supported by a grant from Vetsuisse Dean FR Althaus and by an Investigator Grant from Associazione Italiana Ricerca sul Cancro. G.V. is a scientist of Institut National de la Santé et de la Recherche Médicale. Work in C.M.'s laboratory is supported by Fondazione Cariplo Grant 2006-0734. E.C. is supported by a Fondazione Italiana per la Ricerca sul Cancro Fellowship.

1. Valko M, Izakovic M, Mazur M, Rhodes CJ, Telser J (2004). Role of oxygen radicals in DNA damage and cancer incidence. *Mol Cell Biochem* 266:37–56.
2. Collins AR (1999) Oxidative DNA damage, antioxidants, and cancer. *BioEssays* 21:238–246.
3. Avkin S, Livneh Z (2002) Efficiency, specificity, and DNA polymerase dependence of translesion replication across the oxidative DNA lesion 8-oxoguanine in human cells. *Mutat Res* 510:81–90.
4. van der Kemp PA, Thomas D, Barbey R, de Oliveira R, Boiteux S (1996) Cloning and expression in *Escherichia coli* of the OGG1 gene of *Saccharomyces cerevisiae*, which codes for a DNA glycosylase that excises 7,8-dihydro-8-oxoguanine and 2,6-diamino-4-hydroxy-5-*N*-methylformamidopyrimidine. *Proc Natl Acad Sci USA* 93:5197–5202.
5. McCann JA, Berti PJ (2003) Adenine release is fast in MutY-catalyzed hydrolysis of G:A and 8-Oxo-G:A DNA mismatches. *J Biol Chem* 278:29587–29592.
6. Ohtsubo T, *et al.* (2000) Identification of human MutY homolog (hMUTYH) as a repair enzyme for 2-hydroxyadenine in DNA and detection of multiple forms of hMUTYH located in nuclei and mitochondria. *Nucleic Acids Res* 28:1355–1364.
7. Russo MT, De Luca G, Degan P, Bignami M (2007) Different DNA repair strategies to combat the threat from 8-oxoguanine. *Mutat Res* 614:69–76.
8. Maga G, *et al.* (2007) 8-oxo-guanine bypass by human DNA polymerases in the presence of auxiliary proteins. *Nature* 447:606–608.
9. Ramadan K, Shevelev I, Hubscher U (2004) The DNA-polymerase-X family: Controllers of DNA quality? *Nat Rev Mol Cell Biol* 5:1038–1043.
10. Crespan E, Hubscher U, Maga G (2007) Error-free bypass of 2-hydroxyadenine by human DNA polymerase λ with proliferating cell nuclear antigen and replication protein A in different sequence contexts. *Nucleic Acids Res* 35:5173–5181.
11. Maga G, *et al.* (2004) The human DNA polymerase lambda interacts with PCNA through a domain important for DNA primer binding and the interaction is inhibited by p21/WAF1/CIP1. *FASEB J* 18:1743–1745.
12. Maga G, *et al.* (2005) DNA elongation by the human DNA polymerase λ polymerase and terminal transferase activities are differentially coordinated by proliferating cell nuclear antigen and replication protein A. *J Biol Chem* 280:1971–1981.
13. Maga G, Shevelev I, Villani G, Spadari S, Hubscher U (2006) Human replication protein A can suppress the intrinsic in vitro mutator phenotype of human DNA polymerase lambda. *Nucleic Acids Res* 34:1405–1415.
14. Maga G, *et al.* (2002) Human DNA polymerase λ functionally and physically interacts with proliferating cell nuclear antigen in normal and translesion DNA synthesis. *J Biol Chem* 277:48434–48440.
15. Mondello C, *et al.* (2003) Karyotype instability and anchorage-independent growth in telomerase-immortalized fibroblasts from two centenarian individuals. *Biochem Biophys Res Commun* 308:914–921.
16. Zongaro S, *et al.* (2005) Stepwise neoplastic transformation of a telomerase-immortalized fibroblast cell line. *Cancer Res* 65:11411–11418.
17. Singhal RK, Wilson SH (1993) Short gap-filling synthesis by DNA polymerase β is processive. *J Biol Chem* 268:15906–15911.
18. Lao Y, Lee CG, Wold MS (1999) Replication protein A interactions with DNA. 2. Characterization of double-stranded DNA-binding/helix-destabilization activities and the role of the zinc-finger domain in DNA interactions. *Biochemistry* 38:3974–3984.
19. Crespan E, *et al.* (2005) Incorporation of non-nucleoside triphosphate analogues opposite to an abasic site by human DNA polymerases β and λ. *Nucleic Acids Res* 33:4117–4127.
20. Parlanti E, Fortini P, Macpherson P, Laval J, Dogliotti E (2002) Base excision repair of adenine/8-oxoguanine mispairs by an aphidicolin-sensitive DNA polymerase in human cell extracts. *Oncogene* 21:5204–5212.
21. Hashimoto K, Tominaga Y, Nakabeppu Y, Moriya M (2004) Futile short-patch DNA base excision repair of adenine:8-oxoguanine mispair. *Nucleic Acids Res* 32:5928–5934.
22. Braithwaite EK, *et al.* (2005) DNA polymerase λ mediates a back-up base excision repair activity in extracts of mouse embryonic fibroblasts. *J Biol Chem* 280:18469–18475.
23. Tano K, *et al.* (2007) Interplay between DNA polymerases β and λ in repair of oxidation DNA damage in chicken DT40 cells. *DNA Repair (Amst)* 6:869–875.
24. Plum GE, Grollman AP, Johnson F, Breslauer KJ (1995) Influence of the oxidatively damaged adduct 8-oxodeoxyguanosine on the conformation, energetics, and thermodynamic stability of a DNA duplex. *Biochemistry* 34:16148–16160.
25. Florian J, Goodman MF, Warshel A (2003) Computer simulation studies of the fidelity of DNA polymerases. *Biopolymers* 68:286–299.
26. Aoufouchi S, *et al.* (2000) Two novel human and mouse DNA polymerases of the polX family. *Nucleic Acids Res* 28:3684–3693.
27. Albertella MR, Lau A, O'Connor MJ (2005) The overexpression of specialized DNA polymerases in cancer. *DNA Repair (Amst)* 4:583–593.
28. Frechet M, Canitrot Y, Cazaux C, Hoffmann JS (2001) DNA polymerase β imbalance increases apoptosis and mutagenesis induced by oxidative stress. *FEBS Lett* 505:229–232.
29. Frechet M, *et al.* (2002) Deregulated DNA polymerase β strengthens ionizing radiation-induced nucleotidic and chromosomal instabilities. *Oncogene* 21:2320–2327.
30. Yang J, Chen Z, Liu Y, Hickey RJ, Malkas LH (2004) Altered DNA polymerase ι expression in breast cancer cells leads to a reduction in DNA replication fidelity and a higher rate of mutagenesis. *Cancer Res* 64:5597–5607.
31. Zhang Y, Yuan F, Wu X, Taylor J-S, Wang Z (2001) Response of human DNA polymerase ι to DNA lesions. *Nucleic Acids Res* 29:928–935.
32. Kauffmann A, *et al.* (2008) High expression of DNA repair pathways is associated with metastasis in melanoma patients. *Oncogene* 27:565–573.
33. Locatelli GA, *et al.* (2005) Diketo hexenoic acid derivatives are novel selective non-nucleoside inhibitors of mammalian terminal deoxynucleotidyl transferases, with potent cytotoxic effect against leukemic cells. *Mol Pharmacol* 68:538–550.

7. FURTHER UNPUBLISHED DATA

7.1. Selected Unpublished Results

7.1.1. DNA Polymerase β Repair Activity in MUTYH and APE1 Initiated Repair

The action of MUTYH and APE1 on a ds DNA template containing A:8-oxo-G mispair results in the formation of 1nt gap opposite 8-oxo-G. The fidelity of DNA pol β to bypass 8-oxo-G on such a template was tested by using the 8-oxo-G specificity assay (for assay details see section 6.1). The ds DNA template containing an A:8-oxo-G mispair was first incubated with MUTYH and APE1, followed by the addition of DNA pol β into the reaction. DNA pol β showed a preference to incorporate dCTP opposite an 8-oxo-G (Figure 9A and 9B). Interestingly, when DNA pol β incorporated dCTP opposite an 8-oxo-G an additional strand displacement and extension by 1nt was observed, thereby creating a short 1nt flap (Figure 9A, lane 12). However, this was not the case when dATP was incorporated (Figure 9A, lane 6). This suggests that the accurate repair (formation of C:8-oxo-G base pair) could be mediated via the LP-BER (2-12nt patch) and the inaccurate via the SP-BER.

7.1.2. PCNA and RP-A Inhibit the Incorporation of the Correct dCTP Opposite 8-oxo-G by DNA Polymerase β

In previous work from our laboratory it was shown that the auxiliary proteins RP-A and PCNA increase the inaccurate bypass of 8-oxo-G by DNA pol β (72,73). In order to test whether a similar effect can be observed in the 8-oxo-G specificity assay when MUTYH, APE1 and DNA pol β are present, RP-A or PCNA were titrated. RP-A inhibited the incorporation of both dATP and dCTP by DNA pol β opposite 8-oxo-G (Figure 9D). In addition, as shown in Figures 9C, PCNA inhibited the incorporation of dCTP and promoted error-prone gap filling by DNA pol β. Thus, in a reaction initiated by MUTYH and APE1, the auxiliary proteins RP-A and PCNA can promote the incorporation of wrong dATP opposite an 8-oxo-G lesion by DNA pol β.

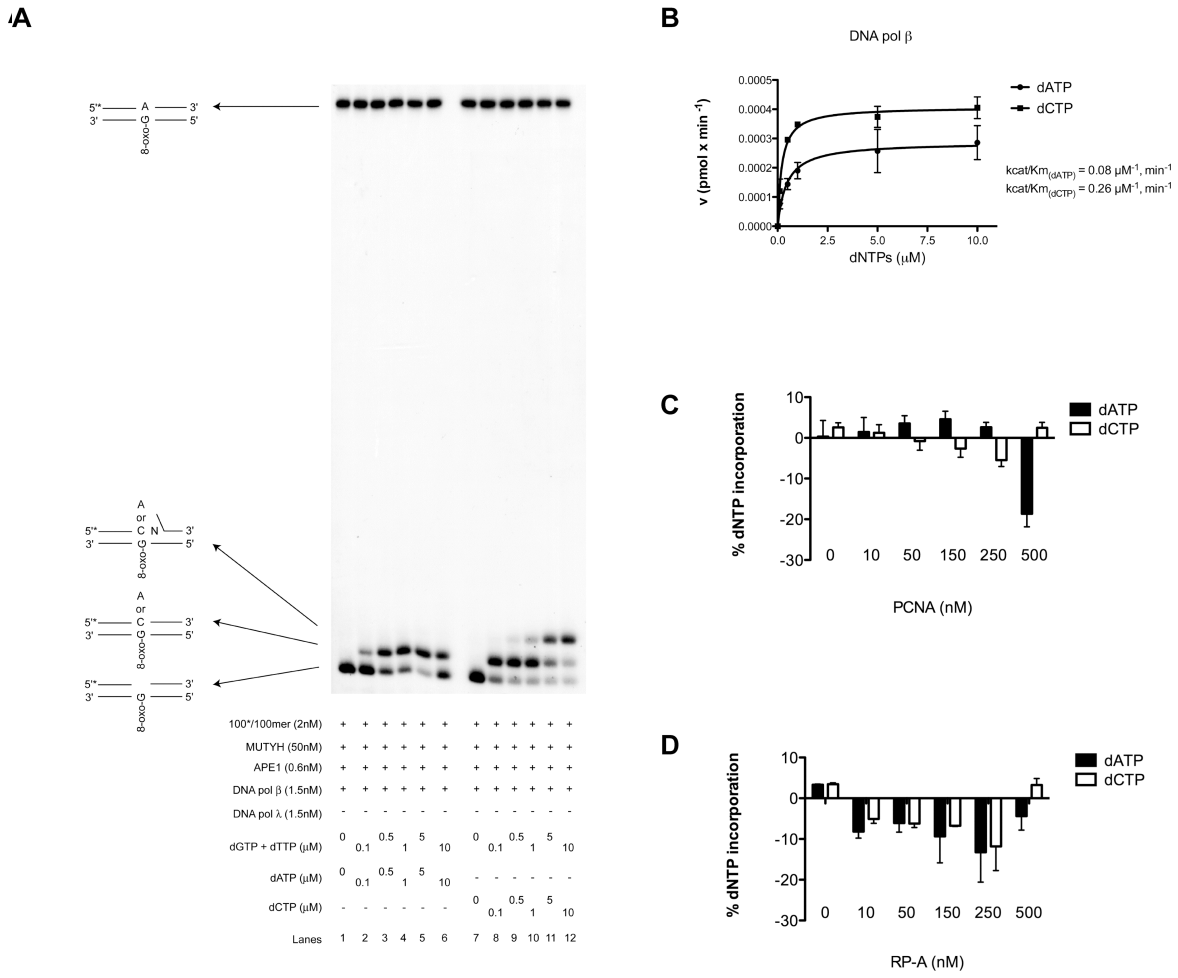

Figure 9. PCNA and RP-A inhibit the incorporation of the correct dCTP opposite 8-oxo-G by DNA polymerase β. The reactions were done under the conditions described in section 6.1. **A**) Variation of the initial velocities of the reaction (initiated by 50nM MUTYH and 0.6nM APE1) catalyzed by 0.75nM DNA pol β on the double stranded template containing A/8-oxo-G mispair (2nM) in the presence of dGTP, dTTP and dATP (lanes 1-6) or dCTP (lanes 7-12), as a function of nucleotide substrate concentration. **B**) Summary of DNA pol β activity in the presence of dATP (●) or dCTP (■) from three different experiments as the one documented in (A), error-bars represent ± SD values. **C**) Effect of increasing amounts of PCNA, in the presence of 50nM MUTYH and 0.6nM APE1, on the incorporation of 0.5μM dATP (dark bars) or 0.5μM dCTP (light bars) opposite 8-oxo-G lesion (2nM) by 0.75nM DNA pol β. Values are the mean of 3 independent experiments. Error bars are ± SD values. **D**) Effect of increasing amounts of RP-A, in the presence of 50nM MUTYH and 0.6nM APE1, on the incorporation of 0.5μM dATP (dark bars) or 0.5μM dCTP (light bars) opposite the 8-oxo-G lesion (2nM) by 0.75nM DNA pol β. Values are the mean of 3 independent experiments. Error bars represent ± SD values.

7.1.3. DNA Ligases III and I Preferentially Ligate the Inaccurate Product of DNA Polymerase β Repair Synthesis

The finding that DNA pol β was only able after incorporation of the correct dCTP opposite an 8-oxo-G to additionally elongate by 1nt (Figure 9A, lane 12), suggested that a MUTYH initiated repair of DNA containing A:8-oxo-G mispair could be an interplay of the two BER sub pathways. Therefore the effect of the SP-BER protein, DNA ligase III, on the MUTYH initiated repair of A:8-oxo-G mispair was first tested. A ds A:8-oxo-G template was incubated with MUTYH and APE1, followed by the addition of DNA pol β and finally DNA ligase III was titrated into the reactions. After the repair synthesis was catalyzed by DNA pol β, DNA ligase III was able to ligate exclusively an A:8-oxo-G product (Figure 10A). Thus, the A:8-oxo-G product of DNA repair synthesis is processed by the error-prone SP-BER. Next, the effect of the LP-BER protein FEN1, on DNA pol β repair synthesis was tested. The ds A:8-oxo-G template was incubated with MUTYH and APE1, followed by filling of the 1nt gap by DNA pol β and finally FEN1 was titrated. FEN1 stimulated strand displacement activity of DNA pol β, both when dATP or dCTP were incorporated opposite an 8-oxo-G (Figure 10B, lanes 1-12). At higher concentrations the 5'→3' exonuclease activity of FEN1 was observed (Figure 10B, lanes 5,6,11 and12). Next the LP-BER ligase, DNA ligase I, was tested for its ability to ligate efficiently an A:8-oxo-G or a C:8-oxo-G product of DNA repair synthesis. DNA ligase I was tested similarly as DNA ligase III, just this time an additional constant amount of FEN1 was present in the reactions. As shown in Figure 10C, DNA ligase I ligated two fold better an incorrect A:8-oxo-G than a correct C:8-oxo-G product of the DNA pol β reaction. Thus, when DNA repair synthesis is mediated by DNA pol β, both SP-BER and LP-BER have an inaccurate outcome and lead to the final formation of an A:8-oxo-G mispair.

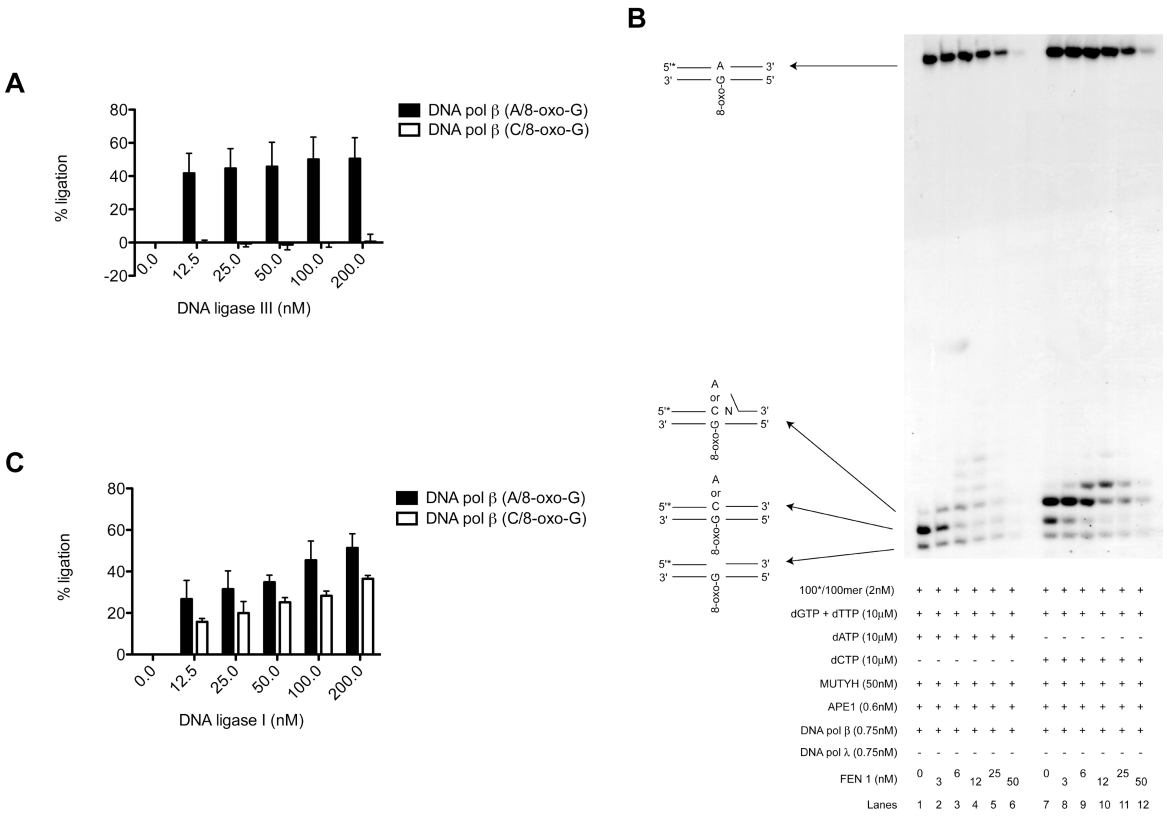

Figure 10. DNA ligases III and I preferentially ligate the incorrect product of DNA polymerase β reaction. The reactions were done under the conditions described in section 6.1. **A**) Ligation activity of the increasing amounts of DNA ligase III on the products of DNA pol β (0.75nM) repair synthesis, containing A/8-oxo-G mispair (dark bars) or C/8-oxo-G base pair (light bars) in the presence of 50nM MUTYH and 0.6nM APE1. Values are the mean of 3 independent experiments. Error bars represent ± SD values. **B**) Effect of the increasing amounts of FEN1 on DNA repair synthesis catalyzed by DNA pol β in the presence of MUTYH and APE1. **C**) Ligation activity of the increasing amounts of DNA ligase I on the products of DNA pol β (0.75nM) repair synthesis, containing A/8-oxo-G mispair (dark bars) or C/8-oxo-G base pair (light bars) in the presence of 50nM MUTYH, 0.6nM APE1 and 10nM FEN1. Values are the mean of 3 independent experiments. Error bars represent ± SD values.

7.2. Discussion of the Unpublished Results

In this thesis a key role of MUTYH and DNA pol λ in the repair of 8-oxo-G was demonstrated (own reference on page 31 and ref. 156). The critical repair components, MUTYH, DNA pol λ, PCNA, FEN1 and DNA ligases I and III were specifically recruited from the human whole cell extracts (WCEs) to A:8-oxo-G DNA, but not to the control DNA containing C:G base pair. By using purified human proteins and a novel 8-oxo-G specificity assay, the whole accurate BER pathway for the repair of A:8-oxo-G mispairs formed during DNA replication was reconstituted. On the 1nt gapped template formed by activity of MUTYH and APE1, DNA pol λ preferentially incorporated dCTP opposite 8-oxo-G and additionally elongated by adding 1nt (156). This is in correlation with the just presented data in section 7.1., where DNA pol β bypassed 8-oxo-G in accurate manner (Figure 9A and 9B). The presence of the auxiliary proteins RP-A and PCNA, in MUTYH and APE1 initiated reaction, further stimulated the accurate bypass of 8-oxo-G by DNA pol λ (156). In contrary when repair synthesis is mediated by DNA pol β, PCNA and RP-A stimulated the inaccurate bypass (Figure 9C and 9D). Finally, DNA ligase I in the presence of FEN1 ligated two fold better a correct C:8-oxo-G product of DNA pol λ repair synthesis than an incorrect A:8-oxo-G product (156). However, when the repair synthesis was mediated by DNA pol β neither DNA ligase III nor DNA ligase I was able to ligate the correct C:8-oxo-G product (Figure 10A and 10C). This discriminatory activity of DNA ligase I for the products of DNA pol λ versus DNA pol β repair synthesis could be directly connected with the FEN1 effect that preceded the ligation step. In MUTYH and APE1 initiated reactions FEN1 had no effect on DNA pol λ polymerization or strand displacement activities (156), therefore the ligatable nick stayed in direct proximity of the lesion. However, the presence of FEN1 (Figure 10B) stimulated strand displacement and extension activity of DNA pol β, both when dATP or dCTP were incorporated opposite 8-oxo-G, directly resulting in a shift of the created ligatable nick downstream of the lesion. This DNA pol β dependent and FEN1 mediated redistribution of the nick away from the lesion, might have a direct effect on activity of DNA ligase I, since the ligation of the nick is no more occurring nearby the lesion.

8. CONCLUSIONS AND PERSPECTIVES

In this thesis the mechanism responsible for the faithful repair of A:8-oxo-G mispairs formed during DNA replication has been addressed. So far it was not completely clear (i) which DNA pol enables error-free MUTYH initiated repair to occur, and (ii) whether this repair proceeds via SP-BER or LP-BER pathway. Earlier investigations suggested that the LP-BER pathway, involving aphidicolin-sensitive DNA pols, such as DNA pols δ and ε, is responsible for the repair of A:8-oxo-G mispairs (44,157). However it is unknown whether the aphidicolin-sensitive DNA pols catalyze both nucleotide insertion opposite 8-oxo-G and extension, or the extension only; since both DNA pol δ and ε are significantly error-prone during 8-oxo-G bypass (72).

In the present thesis work, a key role of MUTYH and DNA pol λ in the repair of 8-oxo-G, upon exposure of the cells to ROS, has been shown. In addition, a dramatic increase in the protein levels of both MUTYH and DNA pol λ is observed, when cells are treated with H_2O_2. Very recently it was shown that DNA pol λ is phosphorylated in S phase and thereby protected from degradation (77). However, nothing is known about the possible mechanism of regulation of the protein levels upon H_2O_2 treatment. Thus, it would be interesting to test, if the observed changes are the result of an increase on mRNA or stabilization at the protein level. In addition the role of ubiquitylation in such a process could be addressed.

Next, the critical repair components have been identified, by specific recruitment of MUTYH, DNA pol λ, PCNA, FEN1 and DNA ligases I and III from the human WCEs to A:8-oxo-G DNA. It would be interesting to test, if there are other possible proteins involved in repair of A:8-oxo-G mispairs. This could be assessed, by incubation of the DNA containing A:8-oxo-G mispair or C:G base pair with the WCE, followed by the mass spectrometry analysis.

By using purified human proteins and a novel 8-oxo-G specificity assay it is found that DNA pol δ preferentially forms A:8-oxo-G mispair during replication and that MUTYH recognizes this mispair thereby generating an AP site, subsequently processed by APE1. On the newly formed 1nt gapped template DNA pol λ preferentially incorporates dCTP opposite 8-oxo-G and additionally

elongates by adding 1nt, thereby creating a short 1nt flap. The presence of auxiliary proteins RP-A and PCNA, further promotes the accurate DNA repair synthesis by DNA pol λ. Interestingly, no elongation occurs when in the rare cases DNA pol λ synthesizes an A:8-oxo-G mispair. Finally, DNA ligase I in the presence of FEN1 ligates two fold better a correct C:8-oxo-G product of DNA pol λ repair synthesis than an incorrect A:8-oxo-G product. Since the preference of DNA ligase I for product of DNA pol λ repair synthesis containing C:8-oxo-G base pair is only two fold, it would be interesting to check if some other co-factor could additionally promote an even more accurate ligation. In addition, it is not clear how DNA ligase I is able to distinguish between a DNA substrate containing an A:8-oxo-G mispair or a C:8-oxo-G base pair. In order to address this question, a crystal structure of DNA ligase I bound to each of these substrates, would be necessary.

All *in vitro* experiments, presented in this study were performed by using recombinant proteins and relatively short DNA oligomers. It would be therefore, interesting to construct a plasmid containing an 8-oxo-G lesion, to transfect it into the human cells and measure the repair rate as well as cell sensitivity, under the different conditions. In this way, repair mechanism presented here, could be additionally be verified *in vivo*.

9. REFERENCES (in addition to the citations in the reprints)

1. Lindahl, T. (1993). Instability and decay of the primary structure of DNA. *Nature* **362**, 709-15.
2. Friedberg EC, Walker GC, Wolfram S, Wood RD, Schultz AD, Ellenberger T. (2006). DNA repair and Mutagenesis. (ASM Press, Washington DC).
3. Duncan, B. K. & Miller, J. H. (1980). Mutagenic deamination of cytosine residues in DNA. *Nature* **287**, 560-1.
4. Mosbaugh, D. W. & Bennett, S. E. (1994). Uracil-excision DNA repair. *Prog Nucleic Acid Res Mol Biol* **48**, 315-70.
5. Sung, J. S. & Demple, B. (2006). Roles of base excision repair subpathways in correcting oxidized abasic sites in DNA. *Febs J* **273**, 1620-9.
6. Dalhus, B., Laerdahl, J. K., Backe, P. H. & Bjoras, M. (2009). DNA base repair - recognition and initiation of catalysis. *FEMS Microbiol Rev*. (ahead of print).
7. Fry, R. C., Begley, T. J. & Samson, L. D. (2005). Genome-wide responses to DNA-damaging agents. *Annu Rev Microbiol* **59**, 357-77.
8. Hirano, T. (2008). Repair system of 7, 8-dihydro-8-oxoguanine as a defense line against carcinogenesis. *J Radiat Res (Tokyo)* **49**, 329-40.
9. Ercal, N., Gurer-Orhan, H. & Aykin-Burns, N. (2001). Toxic metals and oxidative stress part I: mechanisms involved in metal-induced oxidative damage. *Curr Top Med Chem* **1**, 529-39.
10. Klaunig, J. E. & Kamendulis, L. M. (2004). The role of oxidative stress in carcinogenesis. *Annu Rev Pharmacol Toxicol* **44**, 239-67.
11. Bohr, V. A., Stevnsner, T. & de Souza-Pinto, N. C. (2002). Mitochondrial DNA repair of oxidative damage in mammalian cells. *Gene* **286**, 127-34.
12. Maynard, S., Schurman, S. H., Harboe, C., de Souza-Pinto, N. C. & Bohr, V. A. (2009). Base excision repair of oxidative DNA damage and association with cancer and aging. *Carcinogenesis* **30**, 2-10.
13. Batista, L. F., Kaina, B., Meneghini, R. & Menck, C. F. (2009). How DNA lesions are turned into powerful killing structures: insights from UV-induced apoptosis. *Mutat Res* **681**, 197-208.
14. Berti, P. J. & McCann, J. A. (2006). Toward a detailed understanding of base excision repair enzymes: transition state and mechanistic analyses of N-glycoside hydrolysis and N-glycoside transfer. *Chem Rev* **106**, 506-55.
15. Fortini, P. & Dogliotti, E. (2007). Base damage and single-strand break repair: mechanisms and functional significance of short- and long-patch repair subpathways. *DNA Repair (Amst)* **6**, 398-409.
16. Demple, B., Herman, T. & Chen, D. S. (1991). Cloning and expression of APE, the cDNA encoding the major human apurinic endonuclease: definition of a family of DNA repair enzymes. *Proc Natl Acad Sci U S A* **88**, 11450-4.
17. Dianov, G., Price, A. & Lindahl, T. (1992). Generation of single-nucleotide repair patches following excision of uracil residues from DNA. *Mol Cell Biol* **12**, 1605-12.

18. Frosina, G., Fortini, P., Rossi, O., Carrozzino, F., Raspaglio, G., Cox, L. S., Lane, D. P., Abbondandolo, A. & Dogliotti, E. (1996). Two pathways for base excision repair in mammalian cells. *J Biol Chem* **271**, 9573-8.
19. Klungland, A. & Lindahl, T. (1997). Second pathway for completion of human DNA base excision-repair: reconstitution with purified proteins and requirement for DNase IV (FEN1). *Embo J* **16**, 3341-8.
20. Podlutsky, A. J., Dianova, II, Podust, V. N., Bohr, V. A. & Dianov, G. L. (2001). Human DNA polymerase beta initiates DNA synthesis during long-patch repair of reduced AP sites in DNA. *Embo J* **20**, 1477-82.
21. Pascucci, B., Stucki, M., Jonsson, Z. O., Dogliotti, E. & Hubscher, U. (1999). Long patch base excision repair with purified human proteins. DNA ligase I as patch size mediator for DNA polymerases delta and epsilon. *J Biol Chem* **274**, 33696-702.
22. Cappelli, E., Taylor, R., Cevasco, M., Abbondandolo, A., Caldecott, K. & Frosina, G. (1997). Involvement of XRCC1 and DNA ligase III gene products in DNA base excision repair. *J Biol Chem* **272**, 23970-5.
23. Sleeth, K. M., Robson, R. L. & Dianov, G. L. (2004). Exchangeability of mammalian DNA ligases between base excision repair pathways. *Biochemistry* **43**, 12924-30.
24. Wiederhold, L., Leppard, J. B., Kedar, P., Karimi-Busheri, F., Rasouli-Nia, A., Weinfeld, M., Tomkinson, A. E., Izumi, T., Prasad, R., Wilson, S. H., Mitra, S. & Hazra, T. K. (2004). AP endonuclease-independent DNA base excision repair in human cells. *Mol Cell* **15**, 209-20.
25. Xanthoudakis, S., Smeyne, R. J., Wallace, J. D. & Curran, T. (1996). The redox/DNA repair protein, Ref-1, is essential for early embryonic development in mice. *Proc Natl Acad Sci U S A* **93**, 8919-23.
26. Sobol, R. W., Horton, J. K., Kuhn, R., Gu, H., Singhal, R. K., Prasad, R., Rajewsky, K. & Wilson, S. H. (1996). Requirement of mammalian DNA polymerase-beta in base-excision repair. *Nature* **379**, 183-6.
27. Tebbs, R. S., Flannery, M. L., Meneses, J. J., Hartmann, A., Tucker, J. D., Thompson, L. H., Cleaver, J. E. & Pedersen, R. A. (1999). Requirement for the Xrcc1 DNA base excision repair gene during early mouse development. *Dev Biol* **208**, 513-29.
28. Larsen, E., Gran, C., Saether, B. E., Seeberg, E. & Klungland, A. (2003). Proliferation failure and gamma radiation sensitivity of Fen1 null mutant mice at the blastocyst stage. *Mol Cell Biol* **23**, 5346-53.
29. Bentley, D., Selfridge, J., Millar, J. K., Samuel, K., Hole, N., Ansell, J. D. & Melton, D. W. (1996). DNA ligase I is required for fetal liver erythropoiesis but is not essential for mammalian cell viability. *Nat Genet* **13**, 489-91.
30. Starcevic, D., Dalal, S. & Sweasy, J. B. (2004). Is there a link between DNA polymerase beta and cancer? *Cell Cycle* **3**, 998-1001.
31. Albertella, M. R., Lau, A. & O'Connor, M. J. (2005). The overexpression of specialized DNA polymerases in cancer. *DNA Repair (Amst)* **4**, 583-93.
32. David, S. S., O'Shea, V. L. & Kundu, S. (2007). Base-excision repair of oxidative DNA damage. *Nature* **447**, 941-50.
33. Collins, A. R. (1999). Oxidative DNA damage, antioxidants, and cancer. *Bioessays* **21**, 238-46.
34. Klaunig, J. E. & Kamendulis, L. M. (2004). The role of oxidative stress in carcinogenesis. *Annu Rev Pharmacol Toxicol* **44**, 239-67.

35. Shibutani, S., Takeshita, M. & Grollman, A. P. (1991). Insertion of specific bases during DNA synthesis past the oxidation-damaged base 8-oxodG. *Nature* **349**, 431-4.
36. Barnes, D. E. & Lindahl, T. (2004). Repair and genetic consequences of endogenous DNA base damage in mammalian cells. *Annu Rev Genet* **38**, 445-76.
37. Manuel, R. C., Hitomi, K., Arvai, A. S., House, P. G., Kurtz, A. J., Dodson, M. L., McCullough, A. K., Tainer, J. A. & Lloyd, R. S. (2004). Reaction intermediates in the catalytic mechanism of Escherichia coli MutY DNA glycosylase. *J Biol Chem* **279**, 46930-9.
38. Guan, Y., Manuel, R. C., Arvai, A. S., Parikh, S. S., Mol, C. D., Miller, J. H., Lloyd, S. & Tainer, J. A. (1998). MutY catalytic core, mutant and bound adenine structures define specificity for DNA repair enzyme superfamily. *Nat Struct Biol* **5**, 1058-64.
39. Hitomi, K., Iwai, S. & Tainer, J. A. (2007). The intricate structural chemistry of base excision repair machinery: implications for DNA damage recognition, removal, and repair. *DNA Repair (Amst)* **6**, 410-28.
40. Fromme, J. C., Banerjee, A., Huang, S. J. & Verdine, G. L. (2004). Structural basis for removal of adenine mispaired with 8-oxoguanine by MutY adenine DNA glycosylase. *Nature* **427**, 652-6.
41. Ohtsubo, T., Nishioka, K., Imaiso, Y., Iwai, S., Shimokawa, H., Oda, H., Fujiwara, T. & Nakabeppu, Y. (2000). Identification of human MutY homolog (hMYH) as a repair enzyme for 2-hydroxyadenine in DNA and detection of multiple forms of hMYH located in nuclei and mitochondria. *Nucleic Acids Res* **28**, 1355-64.
42. Takao, M., Zhang, Q. M., Yonei, S. & Yasui, A. (1999). Differential subcellular localization of human MutY homolog (hMYH) and the functional activity of adenine:8-oxoguanine DNA glycosylase. *Nucleic Acids Res* **27**, 3638-44.
43. Tsai-Wu, J. J., Su, H. T., Wu, Y. L., Hsu, S. M. & Wu, C. H. (2000). Nuclear localization of the human mutY homologue hMYH. *J Cell Biochem* **77**, 666-77.
44. Parker, A., Gu, Y., Mahoney, W., Lee, S. H., Singh, K. K. & Lu, A. L. (2001). Human homolog of the MutY repair protein (hMYH) physically interacts with proteins involved in long patch DNA base excision repair. *J Biol Chem* **276**, 5547-55.
45. Takao, M., Aburatani, H., Kobayashi, K. & Yasui, A. (1998). Mitochondrial targeting of human DNA glycosylases for repair of oxidative DNA damage. *Nucleic Acids Res* **26**, 2917-22.
46. Lu, A. L., Bai, H., Shi, G. & Chang, D. Y. (2006). MutY and MutY homologs (MYH) in genome maintenance. *Front Biosci* **11**, 3062-80.
47. Yang, H., Clendenin, W. M., Wong, D., Demple, B., Slupska, M. M., Chiang, J. H. & Miller, J. H. (2001). Enhanced activity of adenine-DNA glycosylase (Myh) by apurinic/apyrimidinic endonuclease (Ape1) in mammalian base excision repair of an A/GO mismatch. *Nucleic Acids Res* **29**, 743-52.
48. Hayashi, H., Tominaga, Y., Hirano, S., McKenna, A. E., Nakabeppu, Y. & Matsumoto, Y. (2002). Replication-associated repair of adenine:8-oxoguanine mispairs by MYH. *Curr Biol* **12**, 335-9.

49. Boldogh, I., Milligan, D., Lee, M. S., Bassett, H., Lloyd, R. S. & McCullough, A. K. (2001). hMYH cell cycle-dependent expression, subcellular localization and association with replication foci: evidence suggesting replication-coupled repair of adenine:8-oxoguanine mispairs. *Nucleic Acids Res* **29**, 2802-9.
50. Al-Tassan, N., Chmiel, N. H., Maynard, J., Fleming, N., Livingston, A. L., Williams, G. T., Hodges, A. K., Davies, D. R., David, S. S., Sampson, J. R. & Cheadle, J. P. (2002). Inherited variants of MYH associated with somatic G:C→T:A mutations in colorectal tumors. *Nat Genet* **30**, 227-32.
51. Halford, S. E., Rowan, A. J., Lipton, L., Sieber, O. M., Pack, K., Thomas, H. J., Hodgson, S. V., Bodmer, W. F. & Tomlinson, I. P. (2003). Germline mutations but not somatic changes at the MYH locus contribute to the pathogenesis of unselected colorectal cancers. *Am J Pathol* **162**, 1545-8.
52. Jones, S., Emmerson, P., Maynard, J., Best, J. M., Jordan, S., Williams, G. T., Sampson, J. R. & Cheadle, J. P. (2002). Biallelic germline mutations in MYH predispose to multiple colorectal adenoma and somatic G:C→T:A mutations. *Hum Mol Genet* **11**, 2961-7.
53. Sieber, O. M., Lipton, L., Crabtree, M., Heinimann, K., Fidalgo, P., Phillips, R. K., Bisgaard, M. L., Orntoft, T. F., Aaltonen, L. A., Hodgson, S. V., Thomas, H. J. & Tomlinson, I. P. (2003). Multiple colorectal adenomas, classic adenomatous polyposis, and germ-line mutations in MYH. *N Engl J Med* **348**, 791-9.
54. Sampson, J. R., Dolwani, S., Jones, S., Eccles, D., Ellis, A., Evans, D. G., Frayling, I., Jordan, S., Maher, E. R., Mak, T., Maynard, J., Pigatto, F., Shaw, J. & Cheadle, J. P. (2003). Autosomal recessive colorectal adenomatous polyposis due to inherited mutations of MYH. *Lancet* **362**, 39-41.
55. Ramadan, K., Shevelev, I. & Hubscher, U. (2004). The DNA-polymerase-X family: controllers of DNA quality? *Nat Rev Mol Cell Biol* **5**, 1038-43.
56. Hubscher, U., Maga, G. & Spadari, S. (2002). Eukaryotic DNA polymerases. *Annu Rev Biochem* **71**, 133-63.
57. Garcia-Diaz, M., Bebenek, K., Gao, G., Pedersen, L. C., London, R. E. & Kunkel, T. A. (2005). Structure-function studies of DNA polymerase lambda. *DNA Repair (Amst)* **4**, 1358-67.
58. Banos, B., Lazaro, J. M., Villar, L., Salas, M. & de Vega, M. (2008). Characterization of a Bacillus subtilis 64-kDa DNA polymerase X potentially involved in DNA repair. *J Mol Biol* **384**, 1019-28.
59. Uchiyama, Y., Takeuchi, R., Kodera, H. & Sakaguchi, K. (2009). Distribution and roles of X-family DNA polymerases in eukaryotes. *Biochimie* **91**, 165-70.
60. Garcia-Escudero, R., Garcia-Diaz, M., Salas, M. L., Blanco, L. & Salas, J. (2003). DNA polymerase X of African swine fever virus: insertion fidelity on gapped DNA substrates and AP lyase activity support a role in base excision repair of viral DNA. *J Mol Biol* **326**, 1403-12.
61. Garcia-Diaz, M., Dominguez, O., Lopez-Fernandez, L. A., de Lera, L. T., Saniger, M. L., Ruiz, J. F., Parraga, M., Garcia-Ortiz, M. J., Kirchhoff, T., del Mazo, J., Bernad, A. & Blanco, L. (2000). DNA polymerase lambda (Pol lambda), a novel eukaryotic DNA polymerase with a potential role in meiosis. *J Mol Biol* **301**, 851-67.

62. Aoufouchi, S., Flatter, E., Dahan, A., Faili, A., Bertocci, B., Storck, S., Delbos, F., Cocea, L., Gupta, N., Weill, J. C. & Reynaud, C. A. (2000). Two novel human and mouse DNA polymerases of the polX family. *Nucleic Acids Res* **28**, 3684-93.
63. Garcia-Diaz, M., Bebenek, K., Krahn, J. M., Blanco, L., Kunkel, T. A. & Pedersen, L. C. (2004). A structural solution for the DNA polymerase lambda-dependent repair of DNA gaps with minimal homology. *Mol Cell* **13**, 561-72.
64. Garcia-Diaz, M., Bebenek, K., Larrea, A. A., Havener, J. M., Perera, L., Krahn, J. M., Pedersen, L. C., Ramsden, D. A. & Kunkel, T. A. (2009). Template strand scrunching during DNA gap repair synthesis by human polymerase lambda. *Nat Struct Mol Biol* **16**, 967-72.
65. Garcia-Diaz, M., Bebenek, K., Kunkel, T. A. & Blanco, L. (2001). Identification of an intrinsic 5'-deoxyribose-5-phosphate lyase activity in human DNA polymerase lambda: a possible role in base excision repair. *J Biol Chem* **276**, 34659-63.
66. Ramadan, K., Shevelev, I. V., Maga, G. & Hubscher, U. (2002). DNA polymerase lambda from calf thymus preferentially replicates damaged DNA. *J Biol Chem* **277**, 18454-8.
67. Shimazaki, N., Yoshida, K., Kobayashi, T., Toji, S., Tamai, K. & Koiwai, O. (2002). Over-expression of human DNA polymerase lambda in E. coli and characterization of the recombinant enzyme. *Genes Cells* **7**, 639-51.
68. Garcia-Diaz, M., Bebenek, K., Sabariegos, R., Dominguez, O., Rodriguez, J., Kirchhoff, T., Garcia-Palomero, E., Picher, A. J., Juarez, R., Ruiz, J. F., Kunkel, T. A. & Blanco, L. (2002). DNA polymerase lambda, a novel DNA repair enzyme in human cells. *J Biol Chem* **277**, 13184-91.
69. Ramadan, K., Maga, G., Shevelev, I. V., Villani, G., Blanco, L. & Hubscher, U. (2003). Human DNA polymerase lambda possesses terminal deoxyribonucleotidyl transferase activity and can elongate RNA primers: implications for novel functions. *J Mol Biol* **328**, 63-72.
70. Lee, J. W., Blanco, L., Zhou, T., Garcia-Diaz, M., Bebenek, K., Kunkel, T. A., Wang, Z. & Povirk, L. F. (2004). Implication of DNA polymerase lambda in alignment-based gap filling for nonhomologous DNA end joining in human nuclear extracts. *J Biol Chem* **279**, 805-11.
71. Bertocci, B., De Smet, A., Flatter, E., Dahan, A., Bories, J. C., Landreau, C., Weill, J. C. & Reynaud, C. A. (2002). Cutting edge: DNA polymerases mu and lambda are dispensable for Ig gene hypermutation. *J Immunol* **168**, 3702-6.
72. Maga, G., Villani, G., Crespan, E., Wimmer, U., Ferrari, E., Bertocci, B. & Hubscher, U. (2007). 8-oxo-guanine bypass by human DNA polymerases in the presence of auxiliary proteins. *Nature* **447**, 606-8.
73. Maga, G., Crespan, E., Wimmer, U., van Loon, B., Amoroso, A., Mondello, C., Belgiovine, C., Ferrari, E., Locatelli, G., Villani, G. & Hubscher, U. (2008). Replication protein A and proliferating cell nuclear antigen coordinate DNA polymerase selection in 8-oxo-guanine repair. *Proc Natl Acad Sci U S A* **105**, 20689-94.
74. Braithwaite, E. K., Kedar, P. S., Lan, L., Polosina, Y. Y., Asagoshi, K., Poltoratsky, V. P., Horton, J. K., Miller, H., Teebor, G. W., Yasui, A. & Wilson, S. H. (2005). DNA polymerase lambda protects mouse fibroblasts

against oxidative DNA damage and is recruited to sites of DNA damage/repair. *J Biol Chem* **280**, 31641-7.

75. Maga, G., Villani, G., Ramadan, K., Shevelev, I., Tanguy Le Gac, N., Blanco, L., Blanca, G., Spadari, S. & Hubscher, U. (2002). Human DNA polymerase lambda functionally and physically interacts with proliferating cell nuclear antigen in normal and translesion DNA synthesis. *J Biol Chem* **277**, 48434-40.
76. Frouin, I., Toueille, M., Ferrari, E., Shevelev, I. & Hubscher, U. (2005). Phosphorylation of human DNA polymerase lambda by the cyclin-dependent kinase Cdk2/cyclin A complex is modulated by its association with proliferating cell nuclear antigen. *Nucleic Acids Res* **33**, 5354-61.
77. Wimmer, U., Ferrari, E., Hunziker, P. & Hubscher, U. (2008). Control of DNA polymerase lambda stability by phosphorylation and ubiquitination during the cell cycle. *EMBO Rep* **9**, 1027-33.
78. Fritz, G. (2000). Human APE/Ref-1 protein. *Int J Biochem Cell Biol* **32**, 925-9.
79. Krokan, H. E., Standal, R. & Slupphaug, G. (1997). DNA glycosylases in the base excision repair of DNA. *Biochem J* **325 (Pt 1)**, 1-16.
80. Yoshida, A., Urasaki, Y., Waltham, M., Bergman, A. C., Pourquier, P., Rothwell, D. G., Inuzuka, M., Weinstein, J. N., Ueda, T., Appella, E., Hickson, I. D. & Pommier, Y. (2003). Human apurinic/apyrimidinic endonuclease (Ape1) and its N-terminal truncated form (AN34) are involved in DNA fragmentation during apoptosis. *J Biol Chem* **278**, 37768-76.
81. Wilson, D. M., 3rd & Barsky, D. (2001). The major human abasic endonuclease: formation, consequences and repair of abasic lesions in DNA. *Mutat Res* **485**, 283-307.
82. Dyrkheeva, N. S., Khodyreva, S. N. & Lavrik, O. I. (2007). [Multifunctional human apurinic/apyrimidinic endonuclease 1: the role of additional functions]. *Mol Biol (Mosk)* **41**, 450-66.
83. Evans, A. R., Limp-Foster, M. & Kelley, M. R. (2000). Going APE over ref-1. *Mutat Res* **461**, 83-108.
84. Xanthoudakis, S. & Curran, T. (1992). Identification and characterization of Ref-1, a nuclear protein that facilitates AP-1 DNA-binding activity. *Embo J* **11**, 653-65.
85. Xanthoudakis, S., Miao, G., Wang, F., Pan, Y. C. & Curran, T. (1992). Redox activation of Fos-Jun DNA binding activity is mediated by a DNA repair enzyme. *Embo J* **11**, 3323-35.
86. Bennett, R. A., Wilson, D. M., 3rd, Wong, D. & Demple, B. (1997). Interaction of human apurinic endonuclease and DNA polymerase beta in the base excision repair pathway. *Proc Natl Acad Sci U S A* **94**, 7166-9.
87. Ranalli, T. A., Tom, S. & Bambara, R. A. (2002). AP endonuclease 1 coordinates flap endonuclease 1 and DNA ligase I activity in long patch base excision repair. *J Biol Chem* **277**, 41715-24.
88. Krishna, T. S., Fenyo, D., Kong, X. P., Gary, S., Chait, B. T., Burgers, P. & Kuriyan, J. (1994). Crystallization of proliferating cell nuclear antigen (PCNA) from Saccharomyces cerevisiae. *J Mol Biol* **241**, 265-8.
89. Moldovan, G. L., Pfander, B. & Jentsch, S. (2007). PCNA, the maestro of the replication fork. *Cell* **129**, 665-79.

90. Hubscher, U., Maga, G. & Spadari, S. (2002). Eukaryotic DNA polymerases. *Annu Rev Biochem* **71**, 133-63.
91. Majka, J. & Burgers, P. M. (2004). The PCNA-RFC families of DNA clamps and clamp loaders. *Prog Nucleic Acid Res Mol Biol* **78**, 227-60.
92. Gulbis, J. M., Kelman, Z., Hurwitz, J., O'Donnell, M. & Kuriyan, J. (1996). Structure of the C-terminal region of p21(WAF1/CIP1) complexed with human PCNA. *Cell* **87**, 297-306.
93. Zou, Y., Liu, Y., Wu, X. & Shell, S. M. (2006). Functions of human replication protein A (RPA): from DNA replication to DNA damage and stress responses. *J Cell Physiol* **208**, 267-73.
94. Maga, G., Ramadan, K., Locatelli, G. A., Shevelev, I., Spadari, S. & Hubscher, U. (2005). DNA elongation by the human DNA polymerase lambda polymerase and terminal transferase activities are differentially coordinated by proliferating cell nuclear antigen and replication protein A. *J Biol Chem* **280**, 1971-81.
95. Haracska, L., Unk, I., Johnson, R. E., Phillips, B. B., Hurwitz, J., Prakash, L. & Prakash, S. (2002). Stimulation of DNA synthesis activity of human DNA polymerase kappa by PCNA. *Mol Cell Biol* **22**, 784-91.
96. Fortune, J. M., Stith, C. M., Kissling, G. E., Burgers, P. M. & Kunkel, T. A. (2006). RPA and PCNA suppress formation of large deletion errors by yeast DNA polymerase delta. *Nucleic Acids Res* **34**, 4335-41.
97. Morland, I., Rolseth, V., Luna, L., Rognes, T., Bjoras, M. & Seeberg, E. (2002). Human DNA glycosylases of the bacterial Fpg/MutM superfamily: an alternative pathway for the repair of 8-oxoguanine and other oxidation products in DNA. *Nucleic Acids Res* **30**, 4926-36.
98. Nagelhus, T. A., Haug, T., Singh, K. K., Keshav, K. F., Skorpen, F., Otterlei, M., Bharati, S., Lindmo, T., Benichou, S., Benarous, R. & Krokan, H. E. (1997). A sequence in the N-terminal region of human uracil-DNA glycosylase with homology to XPA interacts with the C-terminal part of the 34-kDa subunit of replication protein A. *J Biol Chem* **272**, 6561-6.
99. Ranalli, T. A., DeMott, M. S. & Bambara, R. A. (2002). Mechanism underlying replication protein a stimulation of DNA ligase I. *J Biol Chem* **277**, 1719-27.
100. Lieber, M. R. (1997). The FEN-1 family of structure-specific nucleases in eukaryotic DNA replication, recombination and repair. *Bioessays* **19**, 233-40.
101. Nazarkina Zh, K., Lavrik, O. I. & Khodyreva, S. N. (2008). [Flap endonuclease-1 and its role in the processes of DNA metabolism in eucaryotic cells]. *Mol Biol (Mosk)* **42**, 405-21.
102. Zheng, L., Zhou, M., Chai, Q., Parrish, J., Xue, D., Patrick, S. M., Turchi, J. J., Yannone, S. M., Chen, D. & Shen, B. (2005). Novel function of the flap endonuclease 1 complex in processing stalled DNA replication forks. *EMBO Rep* **6**, 83-9.
103. Liu, R., Qiu, J., Finger, L. D., Zheng, L. & Shen, B. (2006). The DNA-protein interaction modes of FEN-1 with gap substrates and their implication in preventing duplication mutations. *Nucleic Acids Res* **34**, 1772-84.

104. Tom, S., Henricksen, L. A. & Bambara, R. A. (2000). Mechanism whereby proliferating cell nuclear antigen stimulates flap endonuclease 1. *J Biol Chem* **275**, 10498-505.
105. Li, X., Li, J., Harrington, J., Lieber, M. R. & Burgers, P. M. (1995). Lagging strand DNA synthesis at the eukaryotic replication fork involves binding and stimulation of FEN-1 by proliferating cell nuclear antigen. *J Biol Chem* **270**, 22109-12.
106. Nazarkina, J. K., Petrousseva, I. O., Safronov, I. V., Lavrik, O. I. & Khodyreva, S. N. (2003). Interaction of flap endonuclease-1 and replication protein A with photoreactive intermediates of DNA repair. *Biochemistry (Mosc)* **68**, 934-42.
107. Bae, S. H., Bae, K. H., Kim, J. A. & Seo, Y. S. (2001). RPA governs endonuclease switching during processing of Okazaki fragments in eukaryotes. *Nature* **412**, 456-61.
108. Prasad, R., Dianov, G. L., Bohr, V. A. & Wilson, S. H. (2000). FEN1 stimulation of DNA polymerase beta mediates an excision step in mammalian long patch base excision repair. *J Biol Chem* **275**, 4460-6.
109. Maga, G., van Loon, B., Crespan, E., Villani, G. & Hubscher, U. (2009). The block of DNA polymerase delta strand displacement activity by an abasic site can be rescued by the concerted action of DNA polymerase beta and Flap endonuclease 1. *J Biol Chem* **284**, 14267-75.
110. Lehman, I. R. (1974). DNA ligase: structure, mechanism, and function. *Science* **186**, 790-7.
111. Ellenberger, T. & Tomkinson, A. E. (2008). Eukaryotic DNA ligases: structural and functional insights. *Annu Rev Biochem* **77**, 313-38.
112. Soderhall, S. & Lindahl, T. (1976). DNA ligases of eukaryotes. *FEBS Lett* **67**, 1-8.
113. Teraoka, H. & Tsukada, K. (1982). Eukaryotic DNA ligase. Purification and properties of the enzyme from bovine thymus, and immunochemical studies of the enzyme from animal tissues. *J Biol Chem* **257**, 4758-63.
114. Chan, J. Y. & Becker, F. F. (1985). DNA ligase activities during hepatocarcinogenesis induced by N-2-acetylaminofluorene. *Carcinogenesis* **6**, 1275-7.
115. Henderson, L. M., Arlett, C. F., Harcourt, S. A., Lehmann, A. R. & Broughton, B. C. (1985). Cells from an immunodeficient patient (46BR) with a defect in DNA ligation are hypomutable but hypersensitive to the induction of sister chromatid exchanges. *Proc Natl Acad Sci U S A* **82**, 2044-8.
116. Lonn, U., Lonn, S., Nylen, U. & Winblad, G. (1989). Altered formation of DNA replication intermediates in human 46 BR fibroblast cells hypersensitive to 3-aminobenzamide. *Carcinogenesis* **10**, 981-5.
117. Prigent, C., Satoh, M. S., Daly, G., Barnes, D. E. & Lindahl, T. (1994). Aberrant DNA repair and DNA replication due to an inherited enzymatic defect in human DNA ligase I. *Mol Cell Biol* **14**, 310-7.
118. Araujo, S. J., Tirode, F., Coin, F., Pospiech, H., Syvaoja, J. E., Stucki, M., Hubscher, U., Egly, J. M. & Wood, R. D. (2000). Nucleotide excision repair of DNA with recombinant human proteins: definition of the minimal set of factors, active forms of TFIIH, and modulation by CAK. *Genes Dev* **14**, 349-59.

119. Bentley, D., Selfridge, J., Millar, J. K., Samuel, K., Hole, N., Ansell, J. D. & Melton, D. W. (1996). DNA ligase I is required for fetal liver erythropoiesis but is not essential for mammalian cell viability. *Nat Genet* **13**, 489-91.
120. Barnes, D. E., Tomkinson, A. E., Lehmann, A. R., Webster, A. D. & Lindahl, T. (1992). Mutations in the DNA ligase I gene of an individual with immunodeficiencies and cellular hypersensitivity to DNA-damaging agents. *Cell* **69**, 495-503.
121. Webster, A. D., Barnes, D. E., Arlett, C. F., Lehmann, A. R. & Lindahl, T. (1992). Growth retardation and immunodeficiency in a patient with mutations in the DNA ligase I gene. *Lancet* **339**, 1508-9.
122. Levin, D. S., Bai, W., Yao, N., O'Donnell, M. & Tomkinson, A. E. (1997). An interaction between DNA ligase I and proliferating cell nuclear antigen: implications for Okazaki fragment synthesis and joining. *Proc Natl Acad Sci U S A* **94**, 12863-8.
123. Song, W., Levin, D. S., Varkey, J., Post, S., Bermudez, V. P., Hurwitz, J. & Tomkinson, A. E. (2007). A conserved physical and functional interaction between the cell cycle checkpoint clamp loader and DNA ligase I of eukaryotes. *J Biol Chem* **282**, 22721-30.
124. Montecucco, A., Rossi, R., Levin, D. S., Gary, R., Park, M. S., Motycka, T. A., Ciarrocchi, G., Villa, A., Biamonti, G. & Tomkinson, A. E. (1998). DNA ligase I is recruited to sites of DNA replication by an interaction with proliferating cell nuclear antigen: identification of a common targeting mechanism for the assembly of replication factories. *Embo J* **17**, 3786-95.
125. Smirnova, E., Toueille, M., Markkanen, E. & Hubscher, U. (2005). The human checkpoint sensor and alternative DNA clamp Rad9-Rad1-Hus1 modulates the activity of DNA ligase I, a component of the long-patch base excision repair machinery. *Biochem J* **389**, 13-7.
126. Wang, W., Lindsey-Boltz, L. A., Sancar, A. & Bambara, R. A. (2006). Mechanism of stimulation of human DNA ligase I by the Rad9-rad1-Hus1 checkpoint complex. *J Biol Chem* **281**, 20865-72.
127. Caldecott, K. W., McKeown, C. K., Tucker, J. D., Ljungquist, S. & Thompson, L. H. (1994). An interaction between the mammalian DNA repair protein XRCC1 and DNA ligase III. *Mol Cell Biol* **14**, 68-76.
128. Dulic, A., Bates, P. A., Zhang, X., Martin, S. R., Freemont, P. S., Lindahl, T. & Barnes, D. E. (2001). BRCT domain interactions in the heterodimeric DNA repair protein XRCC1-DNA ligase III. *Biochemistry* **40**, 5906-13.
129. Nash, R. A., Caldecott, K. W., Barnes, D. E. & Lindahl, T. (1997). XRCC1 protein interacts with one of two distinct forms of DNA ligase III. *Biochemistry* **36**, 5207-11.
130. Okano, S., Lan, L., Caldecott, K. W., Mori, T. & Yasui, A. (2003). Spatial and temporal cellular responses to single-strand breaks in human cells. *Mol Cell Biol* **23**, 3974-81.
131. Okano, S., Lan, L., Tomkinson, A. E. & Yasui, A. (2005). Translocation of XRCC1 and DNA ligase IIIalpha from centrosomes to chromosomes in response to DNA damage in mitotic human cells. *Nucleic Acids Res* **33**, 422-9.
132. Moser, J., Kool, H., Giakzidis, I., Caldecott, K., Mullenders, L. H. & Fousteri, M. I. (2007). Sealing of chromosomal DNA nicks during

nucleotide excision repair requires XRCC1 and DNA ligase III alpha in a cell-cycle-specific manner. *Mol Cell* **27**, 311-23.
133. Tebbs, R. S., Flannery, M. L., Meneses, J. J., Hartmann, A., Tucker, J. D., Thompson, L. H., Cleaver, J. E. & Pedersen, R. A. (1999). Requirement for the Xrcc1 DNA base excision repair gene during early mouse development. *Dev Biol* **208**, 513-29.
134. Puebla-Osorio, N., Lacey, D. B., Alt, F. W. & Zhu, C. (2006). Early embryonic lethality due to targeted inactivation of DNA ligase III. *Mol Cell Biol* **26**, 3935-41.
135. Marsin, S., Vidal, A. E., Sossou, M., Menissier-de Murcia, J., Le Page, F., Boiteux, S., de Murcia, G. & Radicella, J. P. (2003). Role of XRCC1 in the coordination and stimulation of oxidative DNA damage repair initiated by the DNA glycosylase hOGG1. *J Biol Chem* **278**, 44068-74.
136. Vidal, A. E., Boiteux, S., Hickson, I. D. & Radicella, J. P. (2001). XRCC1 coordinates the initial and late stages of DNA abasic site repair through protein-protein interactions. *Embo J* **20**, 6530-9.
137. Kubota, Y., Nash, R. A., Klungland, A., Schar, P., Barnes, D. E. & Lindahl, T. (1996). Reconstitution of DNA base excision-repair with purified human proteins: interaction between DNA polymerase beta and the XRCC1 protein. *Embo J* **15**, 6662-70.
138. Hubscher, U. DNA replication fork proteins. In *DNA Replication*, Methods and Protocols. (2009). eds Vengrova S, Dalgaard JZ (Hum. Press – Springer, New York), pp 19-33.
139. Garg, P. & Burgers, P. M. (2005). DNA polymerases that propagate the eukaryotic DNA replication fork. *Crit Rev Biochem Mol Biol* **40**, 115-28.
140. McCulloch, S. D. & Kunkel, T. A. (2008). The fidelity of DNA synthesis by eukaryotic replicative and translesion synthesis polymerases. *Cell Res* **18**, 148-61.
141. Johnson, A. & O'Donnell, M. (2005). Cellular DNA replicases: components and dynamics at the replication fork. *Annu Rev Biochem* **74**, 283-315.
142. Swan, M. K., Johnson, R. E., Prakash, L., Prakash, S. & Aggarwal, A. K. (2009). Structural basis of high-fidelity DNA synthesis by yeast DNA polymerase delta. *Nat Struct Mol Biol* **16**, 979-86.
143. Yang, G., Franklin, M., Li, J., Lin, T. C. & Konigsberg, W. (2002). Correlation of the kinetics of finger domain mutants in RB69 DNA polymerase with its structure. *Biochemistry* **41**, 2526-34.
144. Hunter, W. N., Brown, T., Anand, N. N. & Kennard, O. (1986). Structure of an adenine-cytosine base pair in DNA and its implications for mismatch repair. *Nature* **320**, 552-5.
145. Hunter, W. N., Brown, T., Kneale, G., Anand, N. N., Rabinovich, D. & Kennard, O. (1987). The structure of guanosine-thymidine mismatches in B-DNA at 2.5-A resolution. *J Biol Chem* **262**, 9962-70.
146. Kennard, O. & Salisbury, S. A. (1993). Oligonucleotide X-ray structures in the study of conformation and interactions of nucleic acids. *J Biol Chem* **268**, 10701-4.
147. Leontis, N. B., Stombaugh, J. & Westhof, E. (2002). The non-Watson-Crick base pairs and their associated isostericity matrices. *Nucleic Acids Res* **30**, 3497-531.

148. Prive, G. G., Heinemann, U., Chandrasegaran, S., Kan, L. S., Kopka, M. L. & Dickerson, R. E. (1987). Helix geometry, hydration, and G.A mismatch in a B-DNA decamer. *Science* **238**, 498-504.
149. Flohr, T., Dai, J. C., Buttner, J., Popanda, O., Hagmuller, E. & Thielmann, H. W. (1999). Detection of mutations in the DNA polymerase delta gene of human sporadic colorectal cancers and colon cancer cell lines. *Int J Cancer* **80**, 919-29.
150. da Costa, L. T., Liu, B., el-Deiry, W., Hamilton, S. R., Kinzler, K. W., Vogelstein, B., Markowitz, S., Willson, J. K., de la Chapelle, A., Downey, K. M. & et al. (1995). Polymerase delta variants in RER colorectal tumours. *Nat Genet* **9**, 10-1.
151. Maga, G. & Hubscher, U. (2008). Repair and translesion DNA polymerases as anticancer drug targets. *Anticancer Agents Med Chem* **8**, 431-47.
152. Vaisman, A. & Chaney, S. G. (2000). The efficiency and fidelity of translesion synthesis past cisplatin and oxaliplatin GpG adducts by human DNA polymerase beta. *J Biol Chem* **275**, 13017-25.
153. Efrati, E., Tocco, G., Eritja, R., Wilson, S. H. & Goodman, M. F. (1997). Abasic translesion synthesis by DNA polymerase beta violates the "A-rule". Novel types of nucleotide incorporation by human DNA polymerase beta at an abasic lesion in different sequence contexts. *J Biol Chem* **272**, 2559-69.
154. Hirose, F., Hotta, Y., Yamaguchi, M. & Matsukage, A. (1989). Difference in the expression level of DNA polymerase beta among mouse tissues: high expression in the pachytene spermatocyte. *Exp Cell Res* **181**, 169-80.
155. Louat, T., Servant, L., Rols, M. P., Bieth, A., Teissie, J., Hoffmann, J. S. & Cazaux, C. (2001). Antitumor activity of 2',3'-dideoxycytidine nucleotide analog against tumors up-regulating DNA polymerase beta. *Mol Pharmacol* **60**, 553-8.
156. van Loon, B. & Hubscher, U. (2009). An 8-oxo-guanine repair pathway coordinated by MUTYH glycosylase and DNA polymerase λ. *Proc Natl Acad Sci U S A* **106**, 18201-6.
157. Parlanti, E., Fortini, P., Macpherson, P., Laval, J. & Dogliotti, E. (2002). Base excision repair of adenine/8-oxoguanine mispairs by an aphidicoline-sensitive DNA polymerase in human cell extracts. *Oncogene* **21**, 5204-12.

10. ACKNOWLEDGEMENTS

The work presented in this thesis is not just a result of ideas, experiments and years spent as a graduate student in the lab. It also reflects the relationship with many warm and inspiring people that I have met since the beginning of my graduate work. My deepest gratitude goes:

To my advisor, Professor Ulrich Hübscher, whose encouraging attitude, constant support, thoughtful criticism and generosity made the years of my PhD a pleasant and valuable experience.

To my thesis committee members Professor Eugenia Dogliotti and Professor Michael Hengartner for encouraging words, fruitful discussions and support on many occasions.

To Dr. Kristijan Ramadan, for sharing his enthusiasm and bringing up new ideas during numerous discussions.

To all past and present members of a Ueli's group, especially: Elena Ferrari, who introduced me to laboratory techniques; Prasanna Parasuraman, for being my lab mate from very beginning; and Enni Markkanen for discussions and translation of the "Zusammenfassung". I thank also to all other institute colleges for help, assistance and friendly environment.

To the organisers of the Cancer Biology PhD program for stimulating retreats, meetings and courses. The Swiss National Science Foundation and UBS for financial support.

To my parents, Nevenka and Eugen, brothers Ivan and Pavao, and to Ana; for their love and support during many years of my education.

And finally, to Alex, my supportive, understanding, caring, generous and loving husband. With you everything is possible!

11. CURRICULUM VITAE

PERSONAL INFORMATION

Name: Barbara van Loon
Maiden name: Bohacek
Date of birth: 02.08.1982
Place of birth: Vinkovci, Croatia

EDUCATION

1988-1990 Primary School, Lipovac, Croatia
1990-1996 Primary School, Zagreb, Croatia
1996-2000 General qualification for university entrance, "Girls High School of Sisters of Charity", Zagreb, Croatia
2000-2006 Diploma in Molecular Biology, Faculty of Science, University of Zagreb, Croatia
Thesis title: "Detection of retrotransposone Tto1 region responsible for recombination instability in Bacterium *Agrobacterium tumefaciens*"
2006-2009 PhD student, Institute of Veterinary Biochemistry and Molecular biology, University of Zürich, Switzerland
Cancer biology PhD program of the Life Science Graduate School, Zürich, Switzerland

EMPLOYMENT

2003, 2004 Student assistant, Department of Molecular Biology, Faculty of Science, University of Zagreb, Croatia
Topic: Cell Biology
2005, 2006 Trainee, Novartis Institute for BioMedical Research, Basel Switzerland
Assessing the potency, duration of action and potential for side effects of muscarinic receptor antagonists

PUBLICATIONS

1. van Loon, B. & Hubscher, U. (2009). An 8-oxo-guanine repair pathway coordinated by MUTYH glycosylase and DNA polymerase λ. *Proc Natl Acad Sci U S A* **106**, 18201-6.
2. van Loon, B., Ferrari, E. & Hubscher, U. DNA replication fork proteins. In *DNA Replication*, Methods and Protocols. (2009). eds.

Vengrova, S. & Dalgaard, J.Z. (Hum. Press – Springer, New York), pp 19-33.

3. Maga, G., van Loon, B., Crespan, E., Villani, G. & Hubscher, U. (2009). The block of DNA polymerase delta strand displacement activity by an abasic site can be rescued by the concerted action of DNA polymerase beta and Flap endonuclease 1. *J Biol Chem* **284**, 14267-75.
4. Maga, G., Crespan, E., Wimmer, U., van Loon, B., Amoroso, A., Mondello, C., Belgiovine, C., Ferrari, E., Locatelli, G., Villani, G. & Hubscher, U. (2008). Replication protein A and proliferating cell nuclear antigen coordinate DNA polymerase selection in 8-oxo-guanine repair. *Proc Natl Acad Sci U S A* **105**, 20689-94.
5. Selak, N., Bachrati, C.Z., Shevelev, I., Dietschy, T., van Loon, B., Jakob, A., Hubscher, U., Hoheisel, J.D., Hickson, J. & Stagljar, I. (2008). The Bloom's syndrome helicase (BLM) interacts physically and functionally with p12, the smallest subunit of human DNA polymerase delta. *Nucl Acids Res* **36**, 5166-79.

APPENDIX

A. Isolation of Recombinant DNA Elongation Proteins

(Book Chapter)

Reprinted from *DNA Replication*, Methods and Protocols. (2009). eds. Vengrova, S. & Dalgaard J.Z. (Humana Press – Springer, New York), pp 345-359.

Chapter 19

Isolation of Recombinant DNA Elongation Proteins

Barbara van Loon, Elena Ferrari, and Ulrich Hübscher

Summary

This chapter summarizes isolation procedures of four recombinant human proteins crucial for DNA replication: (a) the replicative DNA polymerase (pol) δ, (b) proliferating cell nuclear antigen (PCNA), (c) replication protein A (RP-A), and (d) replication factor C (RF-C). Pol δ is a four-subunit enzyme essential for replication of the lagging strand and possibly of the leading strand. PCNA is a central player important for coordination of the complex network of proteins interacting at the replication fork. RP-A is single-strand DNA-binding protein involved in DNA replication, DNA repair, DNA recombination, and checkpoint control. RF-C as a clamp loader is required for loading of PCNA onto double-stranded DNA and therefore enables PCNA-dependent elongation by pol δ and pol ε. To reconstitute the intact pol δ and RF-C, a baculovirus expression system is used, where insect cells are infected with baculoviruses, each coding for one of the four or five subunits of pol δ or RF-C, respectively. We also present two easy methods to isolate the homotrimeric human PCNA and the heterotrimeric human RP-A from an *Escherichia coli* expression system.

Key words: DNA polymerase (pol)δ, Proliferating cell nuclear antigen, Replication protein A, Replication factor C, Baculovirus, *Escherichia coli*, Affinity chromatography.

1. Introduction

DNA carries all the information that is necessary for a normal cell growth and development. It is of a major importance that this information is faithfully replicated before cell division, in order to be transferred to the daughter cells. DNA replication is a complex mechanism that requires coordinated interplay of dozens of different proteins. The large protein complex responsible for DNA replication is called the replisome (*(1)*; *see* chapter "DNA Replication Fork Proteins" in this volume as an overview). The replisomal proteins can be divided into two main categories: the

Sonya Vengrova and Jacob Z. Dalgaard (eds.), *Methods in Molecular Biology, DNA Replication, vol. 521*

DOI: 10.1007/978-1-60327-817-5_19

DNA polymerases (pols) and the accessory proteins. The pols catalyze DNA polymerization, whereas the accessory proteins are necessary for assembly and functioning of the replisome. Three major pols responsible for DNA synthesis during the progression of the DNA replication fork are pols α, δ, and ε. DNA accessory proteins that are best explored are the proliferating cell nuclear antigen (PCNA), replication factor C (RF-C), and replication protein A (RP-A).

Pol δ is essential for elongation of primers at the lagging strand and possibly at the leading strand. Human pol δ is a four-subunit enzyme of which the catalytic subunit possesses an intrinsic 3′ → 5′ exonuclease proofreading activity. In this chapter we will present purification protocols of human pol δ from insect cells infected with four recombinant baculoviruses encoding the p125, p50, p66, and p12 subunits *(2)*. To test the activity of isolated pol δ two assays are being used: the poly(dA)/oligo(dT) assay (*(2)*; *see* **Subheading 3.2**) and the pol δ holoenzyme assay (also known as RF-C-dependent DNA replication assay) (*(3)*; *see* **Subheading 3.8**).

PCNA appears to be a key player among the many accessory proteins. It not only acts as a processivity factor or as a clamp for pol δ, but it also plays a role in coordinating the complex network of proteins interacting at the replication fork *(4,5)*. The PCNA genes of various organisms have been cloned and used for expression in *E. coli* using several different expression systems *(6–9)*. In general PCNA can be expressed at a high level, as a soluble and biologically active protein from bacteria. In addition, heterologous expression allows an easy way of constructing various fusion derivates of PCNA as well as amino acid-specific mutants. Fusing shorter sequences to either the N or C termini does not significantly alter the properties of PCNA as seen in in vitro DNA replication assays *(10)*. Since PCNA is in most cases obtained from expression strains, we will describe in this section the behavior of PCNA during isolation from over expressing *E. coli* strains. Human PCNA (hPCNA) is a highly acidic protein with a pI of 4.5 *(11)* and a calculated molecular weight of 28.8 kDa. However due to its charge hPCNA runs as an approximately 36-kDa protein on SDS–PAGE. The chromatographic behavior of PCNA from different organisms is very similar. In aqueous solution PCNA forms a stable homotrimer *(10,12,13)* and will therefore behave as a trimer in native PAGE, glycerol gradient centrifugation, and gel filtration.

RP-A is an essential protein that participates in DNA replication, DNA repair, and homologous DNA recombination *(14,15)*. It is a heterotrimeric structure with polypeptides of molecular weight of 70 kDa (called RP-A1), 32–34 kDa (called RP-A2), and 11–14 kDa (called RP-A3). All three subunits of RP-A are of crucial importance for cell viability. While several procedures

are described in the literature to obtain an essential homogenous three-subunit RP-A preparation *(16–18)*, the most commonly used method is the *E. coli* expression clone p11d-tRPA that coexpresses all three subunits together *(19)*. The composition and activity of isolated RPA can be determined by three different approaches: (a) by testing individual fractions with monoclonal *(20)* or polyclonal *(21)* antibodies, (b) by complementation of an RF-C-dependent DNA replication assay, or (c) by an unwinding assay (*(16,19–21)*; *see* **Subheading 3.6**).

RF-C is a heteropentameric protein essential for DNA replication and DNA repair *(14,15)*. It is a molecular matchmaker required for loading of PCNA onto double-stranded DNA and therefore for PCNA-dependent DNA elongation by pol δ and ε. RF-C can be isolated by conventional techniques over several chromatographic steps from cells and tissues *(22–24)*. Due to the duality of its matchmaker functions, namely to binding to DNA and to PCNA, it was found that the RF-C complex has peculiar physiological properties that lead to many problems during isolation, such as stability, solubility in low salt, sensitivity to freezing, thawing, and heterogeneity in its behavior on various chromatographic steps. RF-C can now be isolated from expression vectors in a procedure that involves simultaneous expression of its five subunits in recombinant baculovirus infected insect cells *(25)*. Purified RF-C is usually assayed (a) by testing its stimulatory effects on pol δ under certain assay conditions or (b) by RF-C-dependent loading of radioactively labeled PCNA onto DNA *(26)*.

2. Materials

2.1. Isolation of Human Pol δ

1. Grace's Insect Medium (Invitrogen) containing 1% penicillin–streptomycin (10,000 units/mL) and 10% Fetal Calf Serum (Invitrogen).
2. Cell line IPLB-Sf21-AE (*Spodoptera frugiperda* pupal ovarian tissue).
3. Transfer vectors pVL1393-p125, pBacHisA-p66, pBac-p50, pVL1393-p12 *(2)*.
4. ÄKTA purifier (Amersham Biosciences).
5. HiTrap Q HP column (GE Healthcare).
6. HisTrap HP column (GE Healthcare).
7. Dounce homogenizer (B. Braun Melsungen).
8. PBS: 125 mM NaCl, 1.5 mM KH_2PO_4, 8 mM Na_2HPO_4, 2.5 mM KCl (use HCl to adjust pH to 7.4).

9. Buffer A: 20 mM Tris–HCl, pH 7.5, 100 mM NaCl, 0.2% NP-40, 1 mM phenylmethanesulfonyl fluoride (PMSF), 5 mM imidazole–HCl, pH 7.5, 1 µg/mL leupeptin, 1 µg/mL pepstatin, 1 µg/mL bestatin.
10. Buffer B: 20 mM Tris–HCl, pH 7.5, 100 mM NaCl, 0.02% NP-40, 0.5 M imidazole–HCl, pH 7.5, 1 mM PMSF, 10% glycerol.
11. Dilution buffer: 20 mM Tris–HCl, pH 7.5, 0.02% NP-40, 1 mM PMSF, 1 mM dithiothreitol (DTT), 10% glycerol.
12. Buffer C: 20 mM Tris–HCl, pH 7.5, 20 mM NaCl, 0.02% NP-40, 1 mM DTT, 10% glycerol.
13. Buffer D: 20 mM Tris–HCl, pH 7.5, 500 mM NaCl, 0.02% NP-40, 1 mM DTT, 10% glycerol.
14. Storage buffer: 25 mM Tris–HCl, pH 7.5, 75 mM NaCl, 0.01% NP-40, 1 mM DTT, 50% glycerol.

2.2. Poly(dA)/Oligo(dT) Assay

1. Automatic liquid scintillation counter MR 300 (Kontron).
2. 5× Reaction buffer: 250 mM bis-Tris, pH 6.5, 1.25 mg/mL bovine serum albumin (BSA), 5 mM DTT, 30 mM $MgCl_2$, 50 mM KCl.
3. Poly(dA)/oligo(dT) (base ratio of 10:1).
4. [α-^{3}H]dTTP (e.g., 1.1 Ci/mmol).
5. PCNA.
6. 10% Trichloroacetic acid.
7. 0.1 M Sodium pyrophosphate.
8. 1 M HCl.
9. 95% Ethanol.
10. Toluene-based scintillation fluid.

2.3. Expression and Purification of Recombinant hPCNA from E. coli

1. Sonicator.
2. French pressure cell press (Sim-Aminco).
3. 10-mL Phosphocellulose column (Whatman).
4. 4 mL Q-Sepharose (Pharmacia).
5. Econo-Pac CHT-II Cartridge (Bio Rad).
6. *E. coli* expression strain BL21(DE3)pLysS carrying plasmid pT7/hPCNA.
7. Isopropyl-beta-d-thiogalactopyranosid (IPTG) (Biosynth).
8. LB medium containing 50 µg/mL ampicillin (LA medium).
9. Gel-loading buffer: 60 mM Tris–HCl, pH 6.8, 2% (w/v) SDS, 2% glycerol, 0.005% (w/v) bromophenol blue, 2% 2-mercaptoethanol.

10. Lysis buffer: 20 mM Tris–HCl, pH 6.8, 1 mM EDTA, 10 mM $NaHSO_3$, 0.01% NP-40, 1 mM DTT, 1 mM PMSF.
11. Buffer A: 20 mM Tris–HCl, pH 6.8, 1 mM EDTA, 10 mM $NaHSO_3$, 0.01% NP40, 10% glycerol.
12. Buffer B: 10 mM Tris–HCl, pH 6.8, 5% glycerol.
13. Storage buffer: 25 mM Tris–HCl, pH 7.5, 50% glycerol, 50 mM NaCl, 1 mM EDTA, 1 mM DTT.

2.4. Expression and Purification of Recombinant his-hPCNA

1. French pressure cell press (Sim-Aminco).
2. CAT RM5 rotator (Zipper GmbH, D-79219 Stauffen, Germany).
3. Ni-NTA resin (Qiagen).
4. *E. coli* expression strain BL21(DE3)pLysS carrying plasmid pT7/his-hPCNA.
5. Isopropyl-beta-D-thiogalactopyranosid (IPTG) (Biosynth).
6. LB medium containing 50 µg/mL ampicillin (LA medium).
7. Lysis buffer: *see* **Subheading 2.3.**
8. Buffer A: 20 mM KPO_4, pH 7.8, 300 mM NaCl, 10% glycerol.
9. 1 M imidazole–HCl, pH 7.2.
10. Storage buffer: *see* **Subheading 2.3.**
11. Gel-loading buffer: *see* **Subheading 2.3.**

2.5. Isolation of Recombinant Human RP-A

1. French pressure cell press (Sim-Aminco).
2. Conductometer MR 300 (Kontron).
3. Econo-Pac Blue Cartridge (Bio Rad).
4. 1-mL HI Trap Q HP column (GE Healthcare).
5. HAP (hydroxylapatite) column.
6. *E. coli* expression strain BL21(DE3) carrying plasmid p11dtRPA.
7. Isopropyl-beta-d-thiogalactopyranosid (IPTG) (Biosynth).
8. LB medium containing 100 µg/mL ampicillin (LA medium).
9. HI buffer: 30 mM HEPES–NaOH, pH 7.8, 1 mM DTT, 0.25 mM EDTA, 0.25% (w/v) inositol, 0.01% NP-40, 1 mM PMSF.
10. 1.5 M NaSCN.

2.6. Unwinding Assay for RP-A

1. Kodak X-Omat AR film.
2. Single-stranded M13 circle onto which a short (e.g., 24mer) radioactively labeled oligonucleotide has been hybridized (3,000 cpm/pmol) *(27)*.

3. 5× Reaction buffer: 100 mM Tris–HCl, pH 7.5, 20% (w/v) sucrose, 40 mM DTT, 400 mg/mL BSA.
4. Stop buffer: 50 mM EDTA, 20% (w/v) sucrose, 1% (w/v) SDS, 0.03% (w/v) xylene cyanol, and 0.03% (w/v) bromophenol blue.
5. 10% (w/v) Trichloroacetic acid.
6. 12% Native polyacrylamide gel in Tris borate/EDTA buffer, pH 8.3.

2.7. Isolation of Recombinant Human RF-C

1. Grace's Insect Medium (Invitrogen) containing 1% penicillin–Streptomycin (10,000 units/mL) and 10% Fetal Calf Serum (Invitrogen).
2. Cell line IPLB-Sf21-AE (*Spodoptera frugiperda* pupal ovarian tissue).
3. Recombinant baculoviruses: v36, v37, v38-his, v40, v140-N-his *(28)*.
4. ÄKTA purifier (Amersham Biosciences).
5. HiTrap Q HP column (GE Healthcare).
6. HisTrap HP column (GE Healthcare).
7. Dounce homogenizer (B. Braun Melsungen).
8. PBS: 125 mM NaCl, 1.5 mM KH_2PO4, 8 mM Na_2HPO_4, 2.5 mM KCl (use HCl to adjust pH to 7.4).
9. Bovine serum albumin (BSA): 20 mg/mL (DNase free).
10. Buffer A: 20 mM Tris–HCl, pH 7.5, 0.2% NP-40, 1 mM PMSF, 1 µg/mL leupeptin, 1 µg/mL pepstatin, 1 µg/mL bestatin.
11. Buffer B: 20 mM Tris–HCl, pH 7.5, 0.3 M NaCl, 0.02% NP-40, 2 mM imidazole–HCl, pH 7.5.
12. Buffer C: 0.3 M NaCl, 0.3 M imidazole–HCl, pH 7.5, 20% glycerol.
13. Buffer Q: 20 mM Tris–HCl, pH 8, 0.01% NP-40, 1 mM DTT, 0.5 mM EDTA, 20% glycerol.
14. Buffer Q_A: 20 mM Tris–HCl, pH 8, 0.1 M NaCl, 0.01% NP-40, 1 mM DTT, 0.5 mM EDTA, 20% glycerol.
15. Buffer Q_B: 20 mM Tris–HCl, pH 8, 0.5 M NaCl, 0.01% NP-40, 1 mM DTT, 0.5 mM EDTA, 20% glycerol.
16. 87% Glycerol.

2.8. RF-C-Dependent DNA Replication Assay

1. Automatic liquid scintillation counter MR 300 (Kontron).
2. Heating lamp.
3. 5× Reaction buffer: 200 mM Tris–HCl, pH 7.5, 1 mg/mL BSA, 5 mM DTT, 50 mM $MgCl_2$.

4. 10 mM ATP.
5. All four dNTPs at 500 µM each.
6. [α-^{3}H]dTTP (50 Ci/µmol).
7. Primed M13 single-stranded DNA (must be circular DNA).
8. *E. coli* SSB (or RP-A).
9. pol δ.
10. 10% Trichloroacetic acid.
11. 0.1 M Sodium pyrophosphate.
12. 1 M HCl.
13. 95% Ethanol.
14. Toluene-based scintillation fluid.

3. Methods

3.1. Isolation of Human Pol δ

This method requires basic training in handling the baculovirus expression system.

1. Infect 2 × 10^8 Sf21 insect cells with the four baculoviruses that correspond to four subunits of pol δ (p125, p 66, p50, and p12) at multiplicity of infection (MOI) 5 for 48 h.
2. Upon protein expression, harvest the cells by centrifugation at 250 × *g*, wash pellet gently three times with ice-cold sterile PBS–HCl, and store it at –80°C (*see* **Note 1**).
3. Thaw the pellet slowly on ice and resuspend it in 20 mL of ice-cold Buffer A. Break the swollen cells with ten strokes of a tightly fitting Dounce homogenizer (*see* **Note 2**).
4. To remove the cell debris spin at 18,000 × *g* for 30 min at 4°C.
5. Load the supernatant slowly (0.2 mL/min) on a 1-mL HisTrap HP column using an ÄKTA purifier. One-milliliter HisTrap HP column is previously equilibrated with Buffer A. While loading collect the flow-through.
6. Wash the column first with 5 column volumes of Buffer A and then additionally with 10 column volumes of Buffer A containing 10% glycerol. Collect the washes.
7. Use an ÄKTA purifier to elute pol δ at a speed of 0.25 mL/min with a 10-mL linear gradient from 0.005 to 0.5 M imidazole–HCl in Buffer B and collect fractions of 0.2 mL (*see* **Note 3**). In a second elution step add 3 mL of Buffer B to the column and collect fractions of 0.2 mL.

8. Analyze pol δ activity of every second fraction by testing stimulatory effect of PCNA in a poly(dA)/oligo (dT) assay (*see* **Subheading 3.2**).
9. Fractions where PCNA stimulation is the strongest pool together and dilute with Dilution buffer to a final NaCl concentration of 20 mM. This fraction slowly loads (0.25 mL/min) on a 1-mL HiTrap Q HP column, previously equilibrated with Buffer C.
10. Wash the column with 5 column volumes of Buffer C.
11. Elute the bound proteins first with a 15-mL linear NaCl gradient in Buffer D from 20 to 500 mM. In a second step elute with 3 mL of Buffer D containing 500 mM NaCl. In both cases collect fractions of 0.25 mL.
12. Analyze the pol δ activity of every second fraction by testing stimulatory effect of PCNA in a poly(dA)/oligo(dT) assay. Pool together fractions with the strongest PCNA stimulation.
13. Dialyze the purified pol δ pools against Storage buffer (*see* **Subheading 2.1**) and store pol δ in sml aliquots at −80°C. Pol δ is stabile under these conditions for at least 6 months (*see* **Note 4**).

3.2. Poly(dA)/Oligo(dT) Assay

1. Prepare the 25-µL reaction containing 1× Reaction buffer, 25 µM [α-^{3}H]dTTP, 500 ng poly(dA)/oligo(dT) and titrate purified pol δ (*see* **Note 5**). Test purified pol δ under two reaction conditions: without PCNA and with 150 ng of PCNA.
2. Incubate reactions for 30 min at 37°C.
3. Terminate reactions by adding 100 µL of 0.1 M sodium pyrophosphate and 1 mL of ice-cold 10% (w/v) trichloroacetic acid. Leave reactions for 5 min on ice.
4. Collect the precipitate on a Whatman GF/C filter, wash three times with 1 M HCl containing 0.1 M sodium pyrophosphate, rinse with 95% ethanol, and dry for 5 min under heating lamp.
5. Transfer dry Whatman GF/C filter with attached precipitate in a tube and add 5 mL of toluene-based scintillation fluid.
6. Measure radioactivity in a liquid scintillation counter.

3.3. Expression and Purification of Recombinant hPCNA from E. coli

1. Start an overnight preculture of BL21(DE3)pLysS:pT7/hPCNA in 25 mL LA medium (either from freshly grown colonies from a plate or from a glycerol stock). Grow at 37°C with shaking *(29)*.
2. Next morning dilute the preculture into 1 L of LA medium and continue to shake at 37°C (*see* **Note 6**).

3. When the OD_{600} of the culture has reached 0.6, IPTG is added to 0.5 mM and shaking continued for 4–5 h. Take a 1-mL sample before induction and store at 4°C for SDS–PAGE analysis of the induction.
4. After induction remove again a 1-mL sample for SDS–PAGE analysis and harvest the rest of the culture by spinning at 5,000 × *g*. Store the harvested cells at –70°C until use (*see* **Note 7**).
5. To monitor the induction, spin down cells from 100 µL of the uninduced and induced cultures (**steps 3** and **4**) and resuspend them in SDS–PAGE Gel-loading buffer. Boil for 2 min and load 40 µL of each onto a 12% SDS–PAGE gel. The overexpressed PCNA should be clearly visible at around 36 kDa.
6. Add 50 mL of Lysis buffer and lyse the whole bacterial pellet by three times freezing–thawing (freeze pellet in liquid N_2 and then thaw it at 37°C) followed by sonication at 4°C, 20 pulse, microtip output 6. Sonication is done in order to reduce viscosity (*see* **Note 8**).
7. Spin the lysate for 15 min at 20,000 × *g* at 4°C and discard the pellet.
8. Assemble a 10-mL phosphocellulose column and a 4-mL Q-Sepharose column so that the outlet of the phosphocellulose column is connected directly to the outlet of the Q-Sepharose column. Equilibrate both columns in Buffer A containing 0.1 M NaCl and load the supernatant from **step 7** onto the columns at a flow rate 0.2 mL/min by using an Akta purifier. Under these conditions PCNA will pass through phosphocellulose column and will bind to the Q-Sepharose.
9. Finish loading by washing both columns with 10 mL Buffer A containing 0.1 M NaCl with the columns still connected. Remove the phosphocellulose column and wash the Q-Sepharose column with 10 mL Buffer A containing 0.1 M NaCl.
10. Elute PCNA with a 60-mL NaCl gradient in Buffer A, from 0.1 to 0.7 M NaCl, collecting fractions of 0.8 mL. Identify PCNA-containing fractions by loading 10 µL of each (or every second) fraction onto an SDS–PAGE and pool the peak fractions containing the 36-kDa band.
11. Equilibrate a 1-mL CHT II Cartridge column with 5 mL Buffer B containing 300 mM NaCl.
12. Load directly the pool from the Q-Sepharose step at a flow rate 0.2 mL/min.
13. Wash with 10 mL Buffer B containing 1 M $MgCl_2$ followed by 6 mL Buffer B containing 100 mM NaCl.

14. Elute PCNA with a gradient from 0 to 250 mM $NaPO_4$, pH 6.8, in Buffer B and monitor PCNA-containing fractions as indicated in **step 10**.
15. The purified PCNA can be stored at 4°C for several weeks or brought to 50% glycerol by dilution or dialyzed against Storage buffer. In the latter two cases store PCNA at –20°C (*see* **Note 9**). PCNA is stable under these conditions for more than 1 year.
16. Finally, the activity of purified PCNA can be quantified by determining the stimulation of pol δ in a poly(dA)/oligo(dT) assay (*see* **Subheading 3.2**).

3.4. Expression and Purification of Recombinant his-hPCNA

1. Induce and harvest cells as outlined in **Subheading 3.3, steps 1–5** *(29)*.
2. Add 50 mL of Buffer A and lyse the bacteria by freezing–thawing, followed by brief sonication to reduce viscosity.
3. Spin the lysate for 15 min at 25,000 × *g* at 4°C and discard the pellet.
4. Mix the supernatant with 8 mL Ni-NTA resin and put it on a CAT RM5 rotator for 1 h at 4°C.
5. Wash the resin once with 40 mL Buffer A containing 10% glycerol and pack it into a column. Load the supernatant from **step 3** onto the column at a flow rate of 0.2 mL/min.
6. Wash the column with 80 mL Buffer A containing 10% glycerol.
7. Elute his-PCNA with a 100-mL gradient from 0.01 to 0.5 M imidazol–HCl, pH 7.2, in 10% glycerol.
8. Monitor his-PCNA-containing fractions by SDS–PAGE. $(His)_{10}$-PCNA elutes between 0.25 and 0.3 M imidazole–HCl, pH 7.2.
9. Remove imidazole by dialysis against Storage buffer and store as outlined in **Subheading 3.3, step 15**. his-PCNA is stabile under these conditions for more than 1 year.
10. Test the activity of isolated his-PCNA as described in **Subheading 3.2, step 1-6**.

3.5. Isolation of Recombinant Human RP-A

1. Inoculate each of two 1-L flasks containing LA medium with one colony of BL21:p11dtRPA and let them grow overnight at 30°C without shaking *(29)*.
2. Next morning shake until the cells reach an OD_{600} of 0.6 and induce them with 0.4 mM IPTG for 2 h.
3. Collect the cells by centrifugation at 1,500 × *g* for 20 min, freeze the pellet at –80°C, thaw and resuspend the pellet in 60 mL of cold HI buffer.
4. Lyse the cells by two passages through a French press.

5. Spin at 18,000 × *g* for 30 min at 4°C.
6. Load the cell lysate immediately (without freezing) on 5 mL Econo-Pac Blue Cartridge column previously equilibrated with 5 column volumes of HI buffer containing 50 mM KCl.
7. Wash the column sequentially with 5 column volumes of HI buffer containing 50 mM KCl, followed by 4 column volumes of HI buffer containing 0.8 M KCl and 3 column volumes of HI buffer containing 0.5 M NaSCN.
8. Elute RP-A with 5 column volumes HI buffer containing 1.5 M NaSCN.
9. Load the eluted RP-A directly on a 20-mL HAP column, previously equilibrated in HI buffer (*see* **Note 10**).
10. Wash the HAP column with 2 column volumes of HI buffer.
11. Elute RP-A with 5 column volumes of HI buffer containing 80 mM potassium phosphate; collect fractions of 5 mL.
12. Analyze the fractions by SDS–PAGE and pool the RP-A containing fractions; avoid the *E. coli* single-strand binding protein SBB (band at 18 kDa). Three RP-A subunits should be clearly visible at around 70, 34, and 11 kDa. Check the conductivity of the pool with conductometer and adjust it to the same conductivity (by diluting with HI buffer) as the subsequent HI Trap Q HP Equilibration buffer.
13. Load the HAP eluate onto a 1-mL HI Trap Q HP column equilibrated in HI buffer containing 100 mL KCl.
14. Wash the column with HI buffer containing 200 mM KCl and elute with a linear gradient of 200–1,000 mM KCl (50 fractions of 200 µL). RP-A elutes at about 400 mM KCl.
15. Test the activity of the final RP-A preparation in an unwinding assay (*see* **Subheading 3.6**) or in complementation of an RF-C-dependent DNA replication assay (*see* **Subheading 3.8**) (*see* **Note 11**).
16. Store the purified RP-A in small aliquots at –80°C. RP-A is stabile under these conditions for more the 1 year.

3.6. Unwinding Assay for RP-A

1. Set up a 25-µL reaction containing 1× Reaction buffer, 10 ng ^{32}P-labeled DNA substrate and the protein fractions to be tested.
2. Incubate reactions for 60 min at 37°C.
3. Stop the reactions by addition of the Stop buffer and separate the reaction products by electrophoresis through a 12% native polyacrylamide gel in Tris borate/EDTA buffer, pH 8.3 at 80 V. Under these conditions the substrate stays at the

top of the gel, while the unwound oligonucleotide migrates in the gel.

4. After electrophoresis fix DNA in 10% (w/v) trichloroacetic acid, dry the gel, and expose it for an autoradiogram to a Kodak X-Omat AR film.

3.7. Isolation of Recombinant Human RF-C

1. Infect 2 × 10^8 Sf21 insect cells with the five corresponding viruses: v36, v37, v38-his, v40, and v140-N-his at MOI 5 for 64 h (*see* **Note 12**).
2. Harvest the cells and wash the pellet gently three times with ice-cold sterile PBS.
3. Resuspend the cell pellet in 12 mL of ice-cold Buffer A containing 0.35 M NaCl. Break the swollen cells with ten strokes of a tightly fitting Dounce homogenizer (*see* **Note 13**).
4. Spin at 18,000 × *g* for 30 min at 4°C.
5. Load the supernatant very slowly (0.2 mL/min) on a 1-mL HisTrap HP column, using ÄKTA purifier. Column previously equilibrated with Buffer A containing 0.35 M NaCl. Collect the flow-through and wash the column subsequently with 5 column volumes of Buffer B.
6. Elute bound proteins at a speed of 0.2 mL/min with 5 column volumes of Buffer C.
7. Dilute the RF-C eluate with Buffer Q, to a final NaCl concentration of 0.1 M and load it very slowly (0.15 mL/min) on 1-mL HiTrap Q HP column, equilibrated with Buffer Q_A (*see* **Note 14**).
8. Before the elution of the protein bound to the HiTrap Q column is started, preload the elution tubes with 20 µL of BSA (20 mg/mL) and add 20 µL of 87% glycerol.
9. Using an ÄKTA purifier elute RF-C slowly, at a speed 0.15 mL/min, with a 20-mL linear NaCl gradient from 0.1 to 0.5 M NaCl in Buffer Q_B and collect fractions of 0.4 mL (*see* **Note 3**).
10. Analyze the eluted fractions in an RF-C-dependent DNA replication assay (also known as pol δ holoenzyme assay) (*see* **Subheading 3.8**).
11. Pool the active fractions and freeze them by dripping small aliquots of 20 µL directly into liquid nitrogen, poured in a small nitrogen vessel. Store purified RF-C protein in a liquid nitrogen (*see* **Note 15**). RF-C is stabile under those conditions for at least 3 months.

3.8. RF-C-Dependent DNA Replication Assay

1. Set up a reaction mixture of 25 µL containing 1× reaction buffer, 1 mM ATP, 40 µM each of dATP, dGTP, dCTP, 15 µM [α-^{3}H]dTTP, 100 ng primed M13 single-stranded DNA,

100 ng PCNA, 350 ng *E. coli* SBB (or 500 ng RP-A), 0.2 units of pol δ, and RF-C fractions to be tested. About 100 ng purified RF-C saturates the reaction under these conditions.

2. Incubate the reactions for 30 min 37°C.
3. Assay the trichloroacetic acid insoluble material as described in **Subheading 3.2.**

4. Notes

1. If not necessary, do not store the cell pellet at −80°C for longer than 24 h. It is, however, advisable to directly proceed with protein purification. This can result in higher yields.
2. All protease inhibitors (leupeptin, pepstatin, bestatin) as well as PMSF are unstable and should be added to the solutions just prior to use.
3. The ÄKTA purifier machine has a program for automatic linear gradient formation in defined period of time. The gradient of choice is achieved by mixing in right ratios buffer containing 0% component B (B can be, e.g., imidazole–HCl or NaCl) with buffer containing 100% component B.
4. From 2×10^8 infected Sf21 insect cells about 7 mg of purified pol δ can be expected.
5. A unit is defined as the incorporation of 1 pmol of total deoxyribonucleoside monophosphate per 1 min at 37°C.
6. Increased yields are obtained if the culture is well aerated; it is therefore recommended to split the culture into several culture flasks.
7. The harvested cells can be stored at −70°C for several months without a loss of PCNA activity.
8. Alternatively, the cells can be lysed by passage through a French press.
9. From 1 L of culture 50 mg of purified PCNA can be obtained.
10. It is better not to couple the two columns together because of their differences in size.
11. A yield of 0.3 mg homogenous active RP-A can be expected from a 1-L culture.
12. From our experience the p38 subunit is the limiting polypeptide to form the correct formation of the RF-C heteropentameric complex. We therefore recommend infecting insect cells with virus encoding for p38 subunit at MOI 8.

13. During isolation of human RF-C it is of a great importance that every step is performed at 4°C and that all materials and solutions are kept ice-cold. One should furthermore try to work as fast as possible.
14. The RF-C complex is very unstable and sensitive to low salt concentration. Dilution process should therefore be preformed carefully slowly by adding the Dilution buffer. Note that you must not go below a salt concentration of 100 mM.
15. Due to the high instability of RF-C complex, it is recommended to test the activity of purified RF-C protein every few weeks.

Acknowledgments

We thank G. Villani for comments on the manuscript. B.V.L. is supported by Swiss National Science Foundation and University of Zürich. E.F. and U.H. are supported by University of Zürich.

References

1. Waga, S., and Stillman, B. (1998) The DNA replication fork in eukaryotic cells, *Annu Rev Biochem* 67, 721–751.
2. Podust, V.N., Chang, L.S., Ott, R., Dianov, G.L., and Fanning, E. (2002) Reconstitution of human DNA polymerase delta using recombinant baculoviruses: the p12 subunit potentiates DNA polymerizing activity of the four-subunit enzyme, *J Biol Chem* 277, 3894–3901.
3. Maga, G., and Hubscher, U. (1996) DNA replication machinery: functional characterization of a complex containing DNA polymerase alpha, DNA polymerase delta, and replication factor C suggests an asymmetric DNA polymerase dimer, *Biochemistry* 35, 5764–5777.
4. Maga, G., Stucki, M., Spadari, S., and Hubscher, U. (2000) DNA polymerase switching: I. Replication factor C displaces DNA polymerase alpha prior to PCNA loading, *J Mol Biol* 295, 791–801.
5. Yuzhakov, A., Kelman, Z., Hurwitz, J., and O'Donnell, M. (1999) Multiple competition reactions for RPA order the assembly of the DNA polymerase delta holoenzyme, *EMBO J* 18, 6189–6199.
6. Biswas, E.E., Chen, P.H., and Biswas, S.B. (1995) Overexpression and rapid purification of biologically active yeast proliferating cell nuclear antigen, *Protein Expr Purif* 6, 763–770.
7. Fien, K., and Stillman, B. (1992) Identification of replication factor C from *Saccharomyces cerevisiae*: a component of the leading-strand DNA replication complex, *Mol Cell Biol* 12, 155–163.
8. Matsumoto, T., Hata, S., Suzuka, I., and Hashimoto, J. (1994) Expression of functional proliferating-cell nuclear antigen from rice (Oryza sativa) in Escherichia coli. Activity in association with human DNA polymerase delta, *Eur J Biochem* 223, 179–187.
9. Zhang, P., Zhang, S. J., Zhang, Z., Woessner, J. F., Jr., and Lee, M. Y. (1995) Expression and physicochemical characterization of human proliferating cell nuclear antigen, *Biochemistry* 34, 10703–10712.
10. Jonsson, Z. O., Podust, V. N., Podust, L. M., and Hubscher, U. (1995) Tyrosine 114 is essential for the trimeric structure and the functional activities of human proliferating cell nuclear antigen, *EMBO J* 14, 5745–5751.
11. Tan, C. K., Castillo, C., So, A. G., and Downey, K. M. (1986) An auxiliary protein for DNA polymerase-delta from fetal calf thymus, *J Biol Chem* 261, 12310–12316.

12. Bauer, G. A., and Burgers, P. M. (1988) The yeast analog of mammalian cyclin/proliferating-cell nuclear antigen interacts with mammalian DNA polymerase delta, *Proc Natl Acad Sci U S A* 85, 7506–7510.
13. Brand, S. R., Bernstein, R. M., and Mathews, M. B. (1994) Trimeric structure of human proliferating cell nuclear antigen. Implications for enzymatic function and autoantibody recognition, *J Immunol* 153, 3070–3078.
14. Toueille, M., and Hubscher, U. (2004) Regulation of the DNA replication fork: a way to fight genomic instability, *Chromosoma* 113, 113–125.
15. Hübscher, U., Maga, G., and Podust, V. N. (1996) DNA replication accessory proteins, in *DNA Replication in Eukaryotic Cells*, (De Pamphilis, M. L.,), Cold Spring Harbor, NY, pp. 525–543.
16. Georgaki, A., Strack, B., Podust, V., and Hubscher, U. (1992) DNA unwinding activity of replication protein A, *FEBS Lett* 308, 240–244.
17. Wobbe, C. R., Weissbach, L., Borowiec, J. A., Dean, F. B., Murakami, Y., Bullock, P., and Hurwitz, J. (1987) Replication of simian virus 40 origin-containing DNA in vitro with purified proteins, *Proc Natl Acad Sci U S A* 84, 1834–1838.
18. Wold, M. S., Weinberg, D. H., Virshup, D. M., Li, J. J., and Kelly, T. J. (1989) Identification of cellular proteins required for simian virus 40 DNA replication, *J Biol Chem* 264, 2801–2809.
19. Henricksen, L. A., Umbricht, C. B., and Wold, M. S. (1994) Recombinant replication protein A: expression, complex formation, and functional characterization, *J Biol Chem* 269, 11121–11132.
20. Kenny, M. K., Schlegel, U., Furneaux, H., and Hurwitz, J. (1990) The role of human single-stranded DNA binding protein and its individual subunits in simian virus 40 DNA replication, *J Biol Chem* 265, 7693–7700.
21. Georgaki, A., and Hubscher, U. (1993) DNA unwinding by replication protein A is a property of the 70 kDa subunit and is facilitated by phosphorylation of the 32 kDa subunit, *Nucleic Acids Res* 21, 3659–3665.
22. Podust, V. N., Georgaki, A., Strack, B., and Hubscher, U. (1992) Calf thymus RF-C as an essential component for DNA polymerase delta and epsilon holoenzymes function, *Nucleic Acids Res* 20, 4159–4165.
23. Tsurimoto, T., and Stillman, B. (1989) Purification of a cellular replication factor, RF-C, that is required for coordinated synthesis of leading and lagging strands during simian virus 40 DNA replication in vitro, *Mol Cell Biol* 9, 609–619.
24. Yoder, B. L., and Burgers, P. M. (1991) Saccharomyces cerevisiae replication factor C. I. Purification and characterization of its ATPase activity, *J Biol Chem* 266, 22689–22697.
25. Cai, J., Uhlmann, F., Gibbs, E., Flores-Rozas, H., Lee, C. G., Phillips, B., Finkelstein, J., Yao, N., O'Donnell, M., and Hurwitz, J. (1996) Reconstitution of human replication factor C from its five subunits in baculovirus-infected insect cells, *Proc Natl Acad Sci U S A* 93, 12896–12901.
26. Podust, L. M., Podust, V. N., Sogo, J. M., and Hubscher, U. (1995) Mammalian DNA polymerase auxiliary proteins: analysis of replication factor C-catalyzed proliferating cell nuclear antigen loading onto circular double-stranded DNA, *Mol Cell Biol* 15, 3072–3081.
27. Thömmes, P., Ferrari E., Jessberger, R. and Hübscher, U. (1992) Four different DNA helicases from Calf Thymus, *J Biol Chem* 267, 6063–6073.
28. Podust, V. N., Tiwari, N., Stephan, S., and Fanning, E. (1998) Replication factor C disengages from proliferating cell nuclear antigen (PCNA) upon sliding clamp formation, and PCNA itself tethers DNA polymerase delta to DNA, *J Biol Chem* 273, 31992–31999.
29. Hübscher, U., Mossi, R., Ferrari, E., Stucki, M., and Jónsson, Z. O. (1999) Functional analysis of DNA replication accessory proteins, in ***Eukaryotic DNA Replication***, (Cotterill, S., eds), Oxford University Press, Qxford, pp. 119–137.

B. The Block of DNA Polymerase δ Strand Displacement Activity by an Abasic Site Can Be Rescued by the Concerted Action of DNA Polymerase β and Flap Endonuclease 1

Reprinted from *Journal of Biological Chemistry* (2009) **284**, 14267-75.

My contribution to this paper was to purify recombinant four subunit DNA polymerase δ from baculovirus and to show the interaction of DNA polymerase β and flap endonuclease 1.

Supplemental Material can be found at:
http://www.jbc.org/content/suppl/2009/03/31/M900759200.DC1.html

THE JOURNAL OF BIOLOGICAL CHEMISTRY VOL. 284, NO. 21, pp. 14267–14275, May 22, 2009

The Block of DNA Polymerase δ Strand Displacement Activity by an Abasic Site Can Be Rescued by the Concerted Action of DNA Polymerase β and Flap Endonuclease 1 [S]

Received for publication, February 2, 2009, and in revised form, March 23, 2009 Published, JBC Papers in Press, March 27, 2009, DOI 10.1074/jbc.M900759200

Giovanni Maga[‡1], **Barbara van Loon**[§2], **Emmanuele Crespan**[‡3], **Giuseppe Villani**[¶4], **and Ulrich Hübscher**[§2]

From the [‡]*Institute of Molecular Genetics National Research Council, via Abbiategrasso 207, I-27100 Pavia, Italy, the* [§]*Institute for Veterinary Biochemistry and Molecular Biology, University of Zürich-Irchel, Winterthurerstrasse 190, CH-8057 Zürich, Switzerland, and the* [¶]*Institute de Pharmacologie et de Biologie Structurale, CNRS-Université Paul Sabatier Toulouse III, UMR 5089, 205 Route de Narbonne, 31077 Toulouse Cedex, France*

Abasic (AP) sites are very frequent and dangerous DNA lesions. Their ability to block the advancement of a replication fork has been always viewed as a consequence of their inhibitory effect on the DNA synthetic activity of replicative DNA polymerases (DNA pols). Here we show that AP sites can also affect the strand displacement activity of the lagging strand DNA pol δ, thus preventing proper Okazaki fragment maturation. This block can be overcome through a polymerase switch, involving the combined physical and functional interaction of DNA pol β and Flap endonuclease 1. Our data identify a previously unnoticed deleterious effect of the AP site lesion on normal cell metabolism and suggest the existence of a novel repair pathway that might be important in preventing replication fork stalling.

Loss of purine and pyrimidine bases is a significant source of DNA damage in prokaryotic and eukaryotic organisms. Abasic (apurinic and apyrimidinic) lesions occur spontaneously in DNA; in eukaryotes it has been estimated that about 10^4 depurination and 10^2 depyrimidation events occur per genome per day. An equally important source of abasic DNA lesions results from the action of DNA glycosylases, such as uracil glycosylase, which excises uracil arising primarily from spontaneous deamination of cytosines (1). Although most AP sites are removed by the base excision repair (BER)[5] pathway, a small fraction of lesions persists, and DNA with AP lesions presents a strong block to DNA synthesis by replicative DNA polymerases (DNA pols) (2, 3). Several studies have been performed to address the effects of AP sites on the template DNA strand on the synthetic activity of a variety of DNA pols. The major replicative enzyme of eukaryotic cells, DNA pol δ, was shown to be able to bypass an AP lesion, but only in the presence of the auxiliary factor proliferating cell nuclear antigen (PCNA) and at a very reduced catalytic efficiency if compared with an undamaged DNA template (4). On the other hand, the family X DNA pols β and λ were shown to bypass an AP site but in a very mutagenic way (5). Recent genetic evidence in *Saccharomyces cerevisiae* cells showed that DNA pol δ is the enzyme replicating the lagging strand (6). According to the current model for Okazaki fragment synthesis (7–9), the action of DNA pol δ is not only critical for the extension of the newly synthesized Okazaki fragment but also for the displacement of an RNA/DNA segment of about 30 nucleotides on the pre-existing downstream Okazaki fragment to create an intermediate Flap structure that is the target for the subsequent action of the Dna2 endonuclease and the Flap endonuclease 1 (Fen-1). This process has the advantage of removing the entire RNA/DNA hybrid fragment synthesized by the DNA pol α/primase, potentially containing nucleotide misincorporations caused by the lack of a proofreading exonuclease activity of DNA pol α/primase. This results in a more accurate copy synthesized by DNA pol δ. The intrinsic strand displacement activity of DNA pol δ, in conjunction with Fen-1, PCNA, and replication protein A (RP-A), has been also proposed to be essential for the S phase-specific long patch BER pathway (10, 11). Although it is clear that an AP site on the template strand is a strong block for DNA pol δ-dependent synthesis on single-stranded DNA, the functional consequences of such a lesion on the ability of DNA pol δ to carry on strand displacement synthesis have never been investigated so far. Given the high frequency of spontaneous hydrolysis and/or cytidine deamination events, any detrimental effect of an AP site on the strand displacement activity of DNA pol δ might have important consequences both for lagging strand DNA synthesis and for long patch BER. In this work, we addressed this issue by constructing a series of synthetic gapped DNA templates with a single AP site at different positions with respect to the downstream primer to be displaced by DNA pol δ (see Fig. 1*A*). We show that an AP site immediately upstream of a single- to double-strand DNA junction constitutes a strong block to the strand displacement activity of DNA pol δ, even in the presence of RP-A and PCNA. Such a block could be resolved only through a "polymerase switch" involving the concerted physical and functional interaction of DNA pol β and

[S] The on-line version of this article (available at http://www.jbc.org) contains supplemental "Experimental Procedures" and Figs. S1 and S2.

[1] Supported by an Associazione Italiana per la Ricerca sul Cancro-AIRC Investigator Grant. To whom correspondence should be addressed: Institute of Molecular Genetics IGM-CNR, via Abbiategrasso 207, I-27100 Pavia, Italy. Tel.: 39-0382546354; Fax: 39-0382422286; E-mail: maga@igm.cnr.it.

[2] Supported by the Swiss National Science Foundation, by the Union Bank of Switzerland Im Auftrag eines Kunden and by the University of Zürich.

[3] Recipient of a Fondazione Italiana per la Ricerca sul Cancro-FIRC Fellowship.

[4] Researcher of Institut National de la Santé et de la Recherche Médicale. Supported by CNRS and Association pour la Recherche sur le Cancer Grant 4969.

[5] The abbreviations used are: BER, base excision repair; AP, abasic; pol, polymerase; PCNA, proliferating cell nuclear antigen; Fen-1, Flap endonuclease 1; RP-A, replication protein A; BSA, bovine serum albumin; nt, nucleotide(s); ss, single-stranded; ds, double-stranded.

Fen-1. The closely related DNA pol λ could only partially substitute for DNA pol β. Based on our data, we propose that stalling of a replication fork by an AP site not only is a consequence of its ability to inhibit nucleotide incorporation by the replicative DNA pols but can also stem from its effects on strand displacement during Okazaki fragment maturation. In summary, our data suggest the existence of a novel repair pathway that might be important in preventing replication fork stalling and identify a previously unnoticed deleterious effect of the AP site lesion on normal cell metabolism.

EXPERIMENTAL PROCEDURES

Oligonucleotide DNA Substrates—All of the oligonucleotides both undamaged and containing a single synthetic AP site (tetrahydrofurane moiety) were from Eurogentec (Angers, France) and PAGE-purified according to the manufacturer's protocol. For detailed sequence description see supplemental "Experimental Procedures." Primers were 5′-labeled with 3000 Ci/mmol [γ-^{32}P]ATP with T4 polynucleotide kinase, according to the manufacturer's protocol.

Proteins—Recombinant human DNA pol β was from Trevigen Inc. (Gaithersburg, MD). Recombinant human DNA pols δ and λ, PCNA, RP-A, and Fen-1 were isolated as described (12–16).

Antibodies—Antibodies against DNA pol β were from our laboratory (13). Antibodies against Fen-1 were purchased form GeneTex, Inc. (San Antonio, TX).

Primer Elongation Assays—For denaturing gel analysis of DNA synthesis products, the reaction mixtures (10 μl) contained 50 mM Tris-HCl, pH 7.0, 0.25 mg/ml BSA, 1 mM dithiothreitol, 50 μM dNTPs, 1 mM $MgCl_2$, and 10–20 nM (3′-OH ends) of the 5′ ^{32}P-labeled primer/templates. Concentrations of DNA pols λ and β, PCNA, RP-A, and Fen-1 were as indicated in the figures and figure legends. The reactions were incubated for 5 min at 37 °C (unless otherwise stated) and then stopped by the addition of standard denaturing gel loading buffer (95% formamide, 10 mM EDTA, xylene cyanol, and bromphenol blue), heated at 95 °C for 3 min, and loaded on a 7 M urea, 10% polyacrylamide gel.

Far Western Blot Analysis—Purified recombinant human Fen-1 (500 ng) and BSA (500 ng) were mixed with Laemmli buffer and subjected to SDS-PAGE, and the proteins were transferred to a nitrocellulose membrane. All of the subsequent steps were preformed at 4 °C. The membrane was first incubated two times for 10 min in denaturing buffer (6 M guanidine hydrochloride in phosphate-buffered saline). To renature proteins the membrane was incubated in serial dilutions (1:1) of denaturing buffer and phosphate-buffered saline supplemented with 1 mM dithiothreitol, up to final concentration of 93.75 mM guanidine hydrochloride. The membrane was then blocked for 1 h in 10 mM Tris-HCl, pH 7.5, 150 mM NaCl, 0.3% Tween, and 10% milk powder, followed by washing for 10 min in wash buffer (10 mM Tris-HCl, pH 7.5, 150 mM NaCl, 0.3% Tween, 0.25% milk powder, 1 mM dithiothreitol, 1 mM phenylmethylsulfonyl fluoride). Additionally the membrane was cut in half, followed by incubation for 2 h 30 min at 4 °C and then 30 min at room temperature, with one half in 1 μg/ml dilution of purified recombinant DNA pol β in wash buffer and the other half in wash buffer alone. The membranes were then washed four times for 10 min in wash buffer, with an exception that a second wash contained 0.0001% glutaraldehyde. From this point a conventional immunoblot analysis was performed, and the proteins were detected with the respective specific antibodies.

RESULTS

An Abasic Site Immediately Upstream of a Double-stranded DNA Region Inhibits the Strand Displacement Activity of DNA Polymerase δ—Human DNA pol δ was tested on linear or gapped DNA templates, either undamaged or bearing a single AP site (tetrahydrofuran) at position +38 from the 3′-OH of the primer (Fig. 1*A*). The gapped DNA substrate was constructed so that the size of the gap was 38 nt, and the abasic site was placed at the last single-stranded (ss) template position, immediately upstream the double-stranded (ds) region. In all cases, the downstream terminator oligonucleotide was 5′-phosphorylated with cold ATP, whereas the 5′-end of the primer was radioactively labeled. As shown in Fig. 1*B*, with the undamaged templates, DNA pol δ was expected to be able to synthesize full-length products in a strictly PCNA-dependent manner both on the linear (*lanes 1–8*) and on the gapped (*lanes 9–16*) DNA substrates. However, on gapped DNA, pol δ was effectively slowed down by the presence of a downstream dsDNA, as shown by the accumulation of products >38 residues long (*lanes 10–12* and *14–16*) and by the requirement of an higher DNA pol δ concentration than with the linear template to reach full-length products (compare *lanes 2–4* with *lanes 10–12* and *14–16*). When DNA pol δ was tested on the same templates but in the presence of an AP site, a strong accumulation of products was noted at the position corresponding to the lesion both on the linear and on the gapped DNA templates (Fig. 1*C*, *lanes 2–4* and *6–9*). However, whereas on the linear template DNA pol δ was eventually able to overcome the lesion, reaching full-length products on the gapped DNA the synthesis was abortive, with accumulation of products between +38 and +45, and no full-length synthesis, even in the presence of high PCNA concentrations (*lanes 6–9*), was observed. Thus, the presence of an additional block, such as an AP site, immediately upstream of a dsDNA region was able to prevent strand displacement by DNA pol δ.

PCNA Promotes Efficient Bypass of an Abasic Site by DNA Polymerase β on Linear but Not on Gapped DNA Templates—Next, human DNA pol β was tested on the same templates. As shown in Fig. 2*A*, the ability of DNA pol β to synthesize full-length products on the linear (*lanes 1–3*) or gapped (*lanes 7–9*) undamaged templates increased as a function of enzyme concentration, according to the well known distributive mode of DNA synthesis by DNA pol β. DNA pol β was able to bypass an AP site both on linear (*lanes 4–6*) or gapped (*lanes 10–12*) DNA templates but with abortive synthesis of products slightly longer than +38, even at the highest concentration tested, suggesting that the lesion significantly increased the distributive DNA synthesis. DNA pol β has been reported to physically interact with PCNA, even though no functional role for this interaction has been shown so far. Thus, increasing amounts of PCNA were titrated in the reaction in the presence of low amounts of DNA pol β on both the linear and gapped DNA

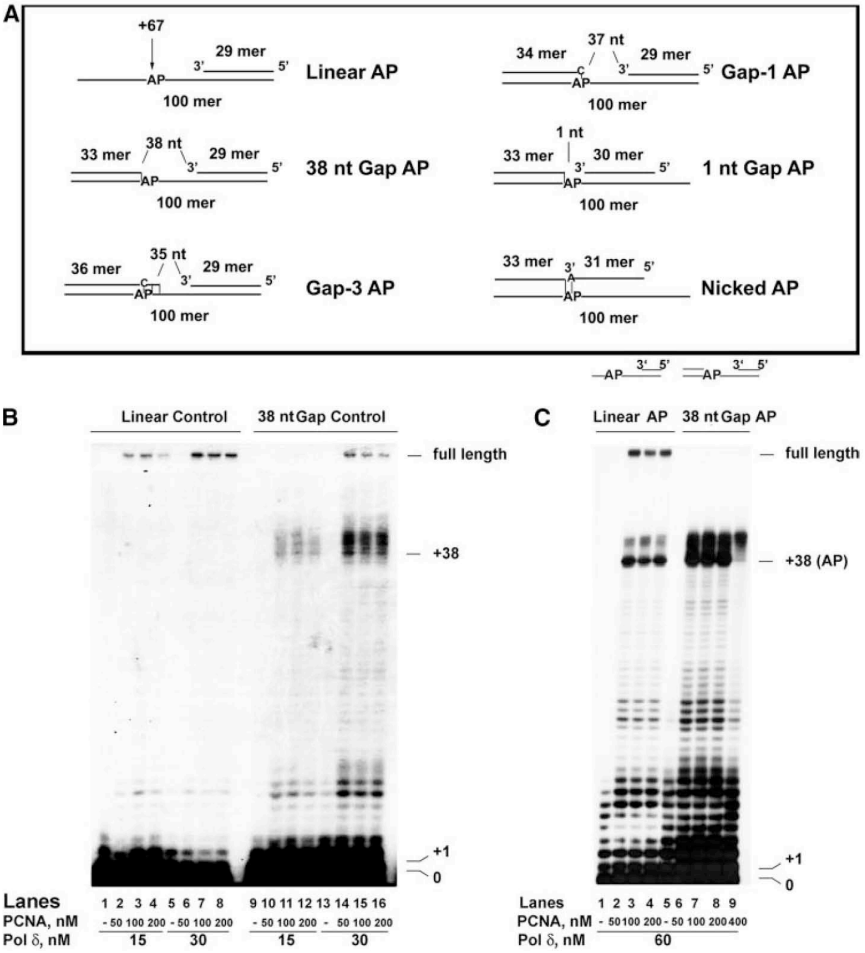

FIGURE 1. **An abasic site immediately upstream of a double-stranded DNA region inhibits the strand displacement activity of DNA polymerase δ.** The reactions were performed as described under "Experimental Procedures." *A*, schematic representation of the various DNA templates used. The size of the resulting gaps is indicated in nt. The position of the AP site on the 100-mer template strand is indicated relative to the 3′ end. Base pairs in the vicinity of the lesion are indicated by *dashes*. The size of the gaps (35–38 nt) is consistent with the size of ssDNA covered by a single RP-A molecule, which has to be released during Okazaki fragment synthesis when the DNA pol is approaching the 5′-end of the downstream fragment. When the AP site is covered by the downstream terminator oligonucleotide (Gap-3 and Gap-1 templates) the nucleotide placed on the opposite strand is C to mimic the situation generated by spontaneous loss of a guanine or excision of an oxidized guanine, whereas when the AP site is covered by the primer (nicked AP template), the nucleotide placed on the opposite strand is A to mimic the most frequent incorporation event occurring opposite an AP site. *B*, human PCNA was titrated in the presence of 15 nM (*lanes 2–4* and *10–12*) or 30 nM (*lanes 6–8* and *14–16*) recombinant human four subunit DNA pol δ, on a linear control (*lanes 1–8*) or a 38-nt gap control (*lanes 9–16*) template. *Lanes 1*, *5*, *9*, and *13*, control reactions in the absence of PCNA. *C*, human PCNA was titrated in the presence of 60 nM DNA pol δ, on a linear AP (*lanes 2–4*) or 38-nt gap AP (*lanes 6–9*) template. *Lanes 1* and *5*, control reactions in the absence of PCNA.

templates bearing an AP site. As shown in Fig. 2*B*, PCNA promoted the synthesis of full-length products past the lesion, but only on the linear template (*lanes 1-5*). If the mechanism of termination at the AP site was an increased dissociation rate of the enzyme from the DNA template, the bypass efficiency should be also influenced by the incubation time. To test this, a time course experiment was performed in the presence of fixed amounts of DNA pol β and PCNA, starting from 10 min (the same incubation time of the experiments shown in Fig. 2*B*) and up to 40 min. As shown in Fig. 2*C*, the amount of full-length products synthesized by DNA pol β increased with time (*lanes 2–5*). PCNA was essential for the stimulation of DNA synthesis, because in its absence no full-length products accumulated, even after 40 min (*lanes 6* and *7*). Thus, PCNA appears to be a stimulatory factor for DNA pol β bypass of an AP site. This is the first report of a functional interaction between these two proteins. However, no full-length synthesis could be detected on gapped DNA even with long incubation times (data not shown), suggesting that, similar to what has been observed with DNA pol δ (Fig. 1*B*), the presence of an AP site immediately upstream of a dsDNA region constitutes a strong block also to DNA pol β activity.

The Presence of a Double-stranded DNA Region Upstream of an Abasic Site Facilitates Bypass by DNA Polymerase δ but Not β—Next, we investigated whether the position of the AP site relative to the dsDNA region might influence the ability of DNA pol δ to overcome the lesion. To this aim, a gapped substrate was constructed, where the AP site was placed 3 nt within the dsDNA, resulting in a ssDNA gap of 35 nt. As shown in Fig. 3*A*, DNA pol δ was able to fully displace the downstream terminator oligonucleotide, synthesizing full-length products (*lanes 2–5*). The addition of the ssDNA-binding protein RP-A further promoted full-length DNA synthesis (*lanes 6–9*). When DNA pol β was tested under the same conditions (Fig. 3*B*), however, no full-length synthesis was detected, irrespective of the presence or RP-A alone (*lanes 9–12*) or in combination with PCNA (*lanes 17–20*). Thus, the position of the AP lesion on gapped DNA substrates relative to the 5′-dsDNA region is important for DNA pol δ but not for DNA pol β. It has been suggested that DNA pol β interacts with a gapped DNA differently from DNA pol δ, by contacting first the 5′- downstream end of the gap (17). This different binding mode between DNA pols β and δ might explain the observed differences.

Fen-1 Inhibits the Synthesis of Products beyond the Abasic Site by DNA Polymerase δ but Is Essential for Efficient Strand Displacement-dependent Bypass of the Abasic Site by DNA Polymerase β—When the AP site is placed 3 nt within the dsDNA, both DNA pol δ and β would generate a short (3-nt)

Block of DNA Polymerase δ Strand Displacement Activity

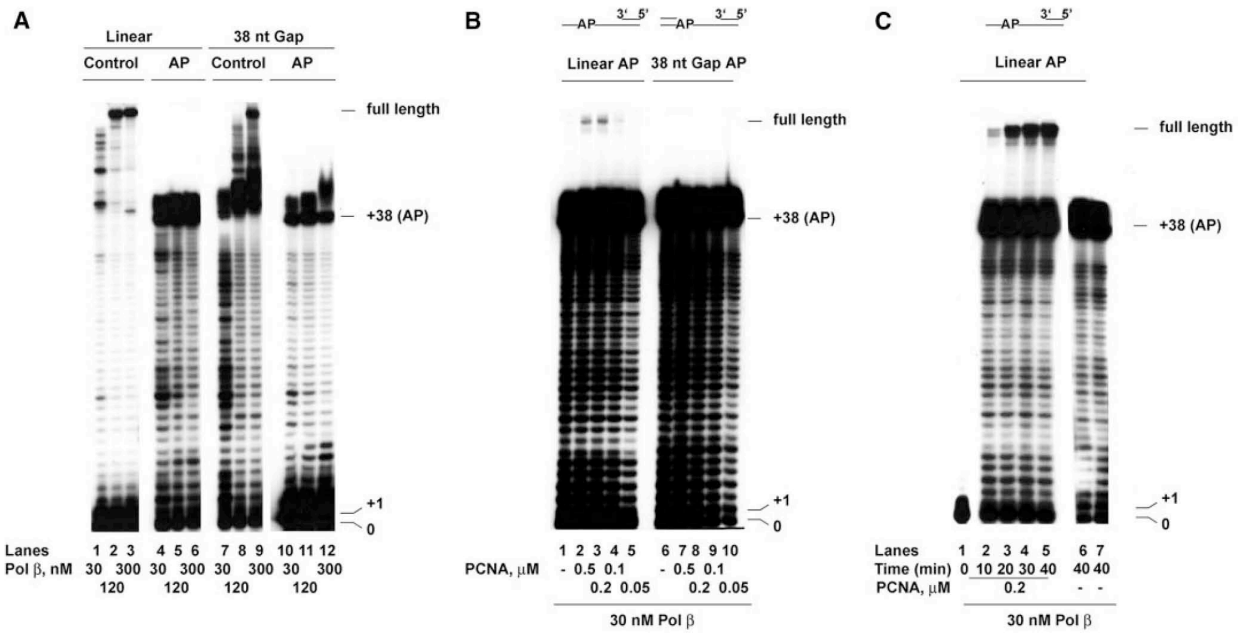

FIGURE 2. **PCNA promotes efficient bypass of an abasic site by DNA polymerase β on linear but not on gapped DNA templates.** The reactions were performed as described under "Experimental Procedures." *A*, recombinant human DNA pol β was incubated 10 min in the presence of linear control (*lanes 1–3*), linear AP (*lanes 4–6*), 38-nt gap control (*lanes 7–9*), or 38-nt gap AP (*lanes 10–12*) templates. *B*, 30 nM of DNA pol β were incubated 10 min in the absence (*lanes 1* and *6*) or in the presence (*lanes 2–5* and *7–10*) of increasing amounts of PCNA on a linear AP (*lanes 1–5*) or a 38 nt gap AP (*lanes 6–10*) template. *C*, 30 nM of DNA pol β were incubated for the indicated times on a linear AP substrate in the presence (*lanes 1–5*) or in the absence (*lanes 6* and *7*) of 200 nM PCNA.

DNA Flap before encountering the AP site. In eukaryotic cells the endonuclease Fen-1 can specifically bind and cut Flap DNA structures. When Fen-1 was added in the reaction together with DNA pol δ, a strong reduction of DNA synthesis was observed (Fig. 3*A*), irrespective of the absence (*lanes 10–13*) or presence (*lanes 14–17*) of a fixed amount of RP-A. Because RP-A was able to promote full-length synthesis by DNA pol δ on this template (Fig. 3*A*, *lanes 6–9*), increasing amounts of RP-A were titrated into the reaction. As shown in Fig. 3*B*, in the absence of Fen-1, RP-A effectively promoted synthesis by DNA pol δ in a dose-dependent manner (*lanes 1–4*). However, the addition of Fen-1 (*lanes 5–8*) resulted in strong inhibition of DNA synthesis. Inhibition of DNA pol δ synthetic activity by Fen-1 on linear templates has been reported. However, on this gapped template, at the highest RP-A concentration, Fen-1 addition caused a strong reduction of bypass products (*i.e.* those of >38 residues, arising from strand displacement synthesis), whereas the amount of shorter products (*i.e.* those of <38 residues, synthesized during the gap filling step) was almost unaffected (compare *lane 1* with *lane 5*), suggesting a mechanistic relationship between strand displacement by DNA pol δ and Fen-1 inhibition.

DNA pol β was unable to overcome the block imposed by an AP site on gapped DNA, resulting in abortive synthesis of short bypass products even in the presence of PCNA and RP-A (Figs. 2*B* and 3*B*). However, when Fen-1 was added into the reaction, efficient bypass of the AP site was achieved and resulted in the accumulation of full-length products, irrespective of whether PCNA and RP-A were absent (Fig. 3*B*, *lanes 13–16*) or present (*lanes 21–24*). When similar experiments were repeated in the presence of increasing salt concentrations, a stimulatory effect of PCNA on the strand displacement activity of DNA pol β on the 38-nt Gap AP template could be observed even in the presence of Fen-1, suggesting that both proteins were required for lesion bypass under physiological salt conditions (supplemental Fig. S1). Thus, Fen-1 and PCNA appear to be necessary to promote efficient strand displacement-dependent AP site bypass by DNA pol β.

The Effect of Fen-1 on the Abasic Site Bypass by DNA Polymerases δ and β Is Not Dependent on the Position of the Lesion—Next, the influence of Fen-1 on the ability of DNA pol δ or β to bypass an AP site was tested on a gapped substrate where the AP site was placed 1 nt within the 5′-ds region, resulting in a ssDNA gap of 37 nt. On this template, an incoming DNA pol has to displace only 1 nt to face the AP site on the template. As shown in Fig. 4*A*, DNA pol δ was able to bypass the lesion by extending the products up to the full length (*lanes 2* and *3*). However, the addition of Fen-1 caused a strong reduction of the bypass products (*lanes 4* and *5*), suggesting that a 1-nt Flap was already sufficient to activate the inhibitory mechanism by Fen-1. RP-A did not show any effect on this reaction (compare *lanes 2* and *4* with *lanes 3* and *5*). When these experiments were repeated with DNA pol β, extension of products beyond the lesion was observed again only in the presence of Fen-1 (compare *lanes 7* and *8* with *lanes 9* and *10*) and RP-A stimulated the reaction (compare *lane 9* with *lane 10*). However, the overall efficiency of Fen-1 stimulation was lower than with the 35-nt gapped DNA template (compare Fig. 4*A* with Fig. 3*B*). The experiments shown in Fig. 4*A* were incubated for 10 min. Increasing the incubation time up to 20 min (Fig. 4*B*) resulted in

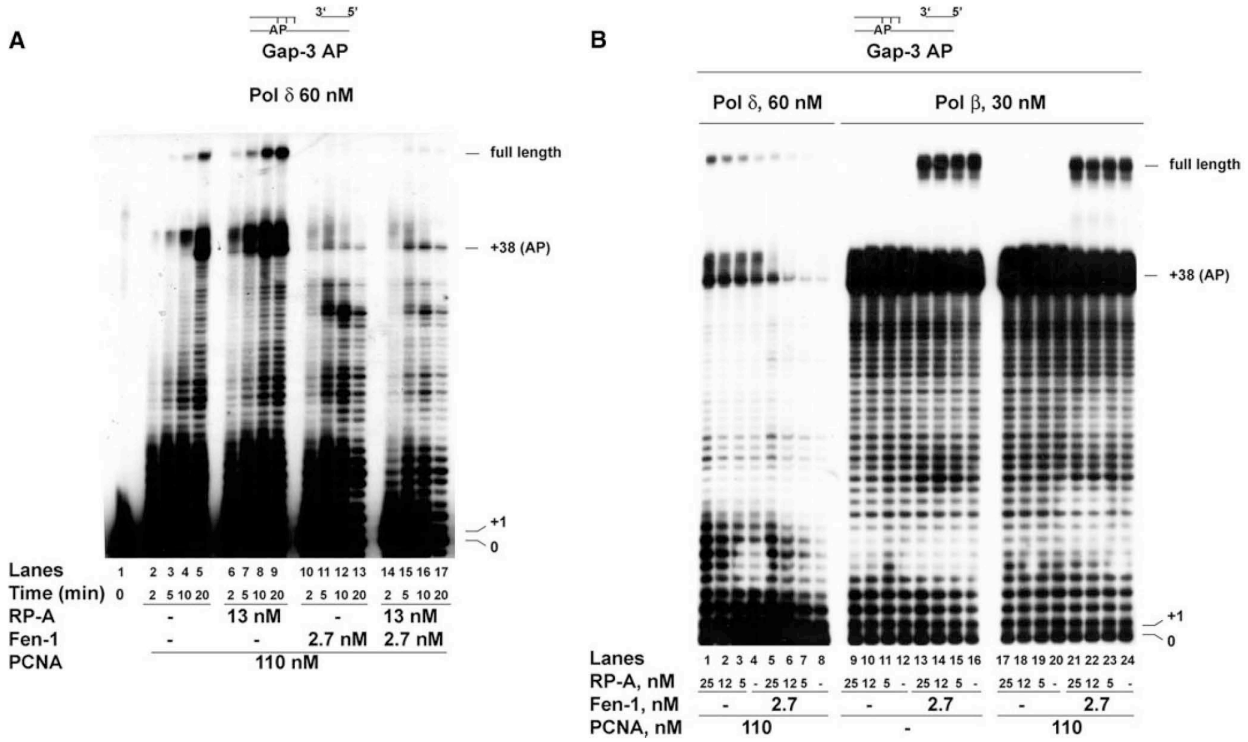

FIGURE 3. **Fen-1 inhibits the synthesis of products beyond the abasic site by DNA polymerase δ but is essential for efficient strand displacement-dependent bypass of the abasic site by DNA polymerase β.** The reactions were performed as described under "Experimental Procedures." *A*, 60 nM DNA pol δ were incubated for the indicated times on the Gap-3 AP template in the presence of 110 nM PCNA alone (*lanes 2–5*) or in combination with 13 nM (as trimer) RP-A (*lanes 6–9*) or 2.7 nM recombinant human Fen-1 (*lanes 10–13*) or both (*lanes 14–17*). *B*, 60 nM DNA pol δ (*lanes 1–8*) or 30 nM DNA pol β (*lanes 9–24*), were incubated with 110 nM PCNA alone (*lanes 1–8* and *17–24*) or in combination with 2.7 nM Fen-1 (*lanes 5–8* and *21–24*), in the absence (*lanes 4*, *8*, *20*, and *24*) or in the presence (*lanes 1–3*, *17–19*, and *21–23*) of increasing amounts of RP-A. *Lanes 9–16*, RP-A titration in the presence of 30 nM DNA pol β in the absence of PCNA and in the absence (*lanes 9–12*) or in the presence (*lanes 13–16*) of 2.7 nM Fen-1.

higher accumulation of full-length products by DNA pol β but always in a strictly Fen-1-dependent manner (compare *lanes 1–4* with *lanes 5–8*). Thus, the effects of Fen-1 on either DNA pol δ or β were not influenced by the length of the Flap generated during strand displacement-dependent bypass of the AP site.

Fen-1 Can Promote Strand Displacement-dependent Bypass of an Abasic Site Immediately Upstream of a Double-stranded DNA Region by DNA Polymerase β but Not by δ—As shown in Figs. 1 and 2, the presence of an AP site immediately upstream of the 5′-dsDNA tract on a gapped template (38-nt Gap) constituted a strong block to strand displacement by both DNA pol δ and β. When increasing amounts of Fen-1 were titrated on this template in the presence of DNA pol δ, PCNA, and RP-A, (Fig. 4*C*), inhibition rather than stimulation of synthesis past the lesion was observed (*lanes 5–8*). In contrast, in the presence of DNA pol β, Fen-1 promoted efficient strand displacement beyond the lesion, with generation of full-length products (*lanes 13–16*). The effects of Fen-1 were also dependent on the presence of the lesion. In fact, on the undamaged 38-nt gapped template, no inhibition by Fen-1 of DNA pol δ was observed (Fig. 4*C*, *lanes 1–4*). On the contrary, Fen-1 facilitated strand displacement by both DNA pol δ and β, as shown by the reduction in the pausing sites corresponding to the first strand displacement events (Fig. 4*C*, compare *lane 1* with *lane 4* and *lane 9* with *lane 12*; pausing sites are marked with *asterisks* at positions 38–42).

Fen-1 Can Act on Abasic Site Bypass by DNA Polymerases δ and β Either at the Incorporation or Elongation Steps—The data presented above show that Fen-1 can differentially influence the activities of DNA pol δ and β while they attempt to bypass an AP site during strand displacement DNA synthesis. However, a question still remains as to whether this action occurs at the level of incorporation or elongation. To verify this, Fen-1 was tested in the presence of either DNA pol δ or β on two different templates, mimicking the reaction intermediates generated during gap filling before and after incorporation opposite the lesion. To this aim, in a first construct a 30-mer primer was annealed to the template strand, which terminates immediately upstream of the lesion, together with a 5′-phosphorylated terminator oligonucleotide that was annealed immediately downstream the AP site. This generated a 1-nt gapped DNA, with the AP site as the only ssDNA template residue, mimicking the reaction intermediate at the pre-incorporation step. In a second construct, a 31-mer primer was used that annealed opposite the lesion. This, together with the downstream terminator oligonucleotide, generated a nicked DNA, with an A residue base-paired to the AP site, thus mimicking the most frequent post-incorporation product generated by AP site bypass. As shown in Fig. 5*A*, the nicked DNA was a poor substrate for

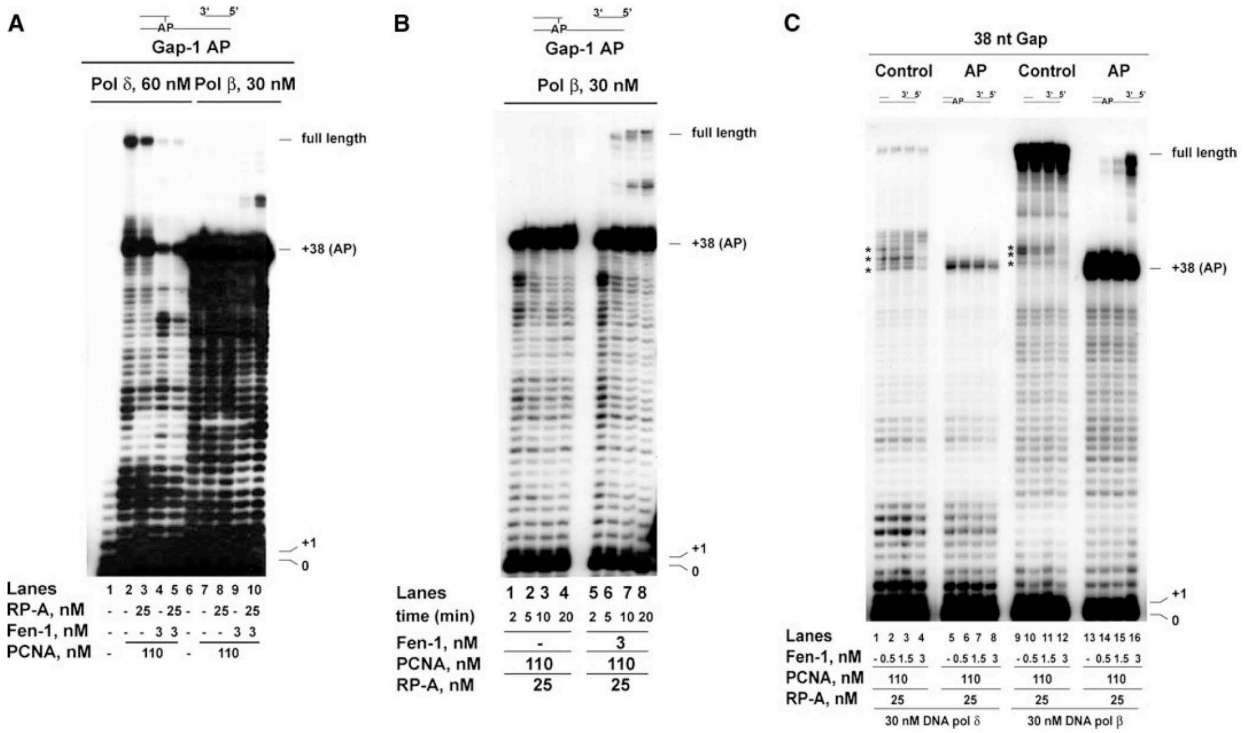

FIGURE 4. **The effect of Fen-1 on the abasic site bypasses by DNA polymerases δ and β are not dependent on the position of the lesion.** The reactions were performed as described under "Experimental Procedures." *A*, 60 nM DNA pol δ (*lanes 1–5*) or 30 nM DNA pol β (*lanes 6–10*) were incubated on the Gap-1 AP template, in the absence (*lanes 1* and *6*) or in the presence of 110 nM PCNA, either alone (*lanes 2* and *7*) or in combination with 25 nM RP-A (*lanes 3* and *8*) or 3 nM Fen-1 (*lanes 4* and *9*) or both (*lanes 5* and *10*). *B*, 30 nM DNA pol β were incubated for the indicated times on the Gap-1 AP template in the presence of PCNA and RP-A and in the absence (*lanes 1–4*) or in the presence (*lanes 5–8*) of 3 nM Fen-1. *C*, 30 nM DNA pol δ (*lanes 1–8*) or DNA pol β (*lanes 9–16*) were incubated on the 38 nt Gap control (*lanes 1–4* and *9–12*) or AP (*lanes 5–8* and *13–16*) template in the presence of PCNA and RP-A and in the absence (*lanes 1*, *5*, *9*, and *13*) or in the presence (*lanes 2–4*, *6–8*, *10–12*, and *14–16*) of increasing amounts of Fen-1. *Asterisks* mark the position of pausing sites during strand displacement DNA synthesis.

DNA pol δ, which incorporated one nucleotide only when PCNA and RP-A were present (*lanes 2* and *3*) but not in their absence (*lane 1*). The addition of Fen-1, however, completely abolished nucleotide incorporation by DNA pol δ even in the presence of PCNA and RP-A (*lane 4*). On the opposite, DNA pol β efficiently incorporated one nucleotide on this substrate, either in the absence (*lane 5*) or in the presence of PCNA and RP-A (*lanes 6* and *7*). The addition of Fen-1 greatly stimulated strand displacement-coupled DNA synthesis by DNA pol β, allowing the incorporation of several nucleotides (*lane 8*). With the 1-nt gapped DNA substrate (Fig. 5*B*), DNA pol δ could efficiently fill the gap opposite the AP site even in the absence of PCNA and RP-A (*lane 1*). The addition of PCNA and RP-A allowed limited strand displacement activity, resulting in the incorporation of additional two nucleotides (*lanes 2* and *3*). Again, the addition of Fen-1 completely abolished strand displacement by DNA pol δ, resulting in the accumulation of +1 product only, even in the presence of PCNA and RP-A (*lane 4*). DNA pol β, as expected, was able to efficiently fill the gap and also to perform limited strand displacement, generating +2 products (*lane 5*). PCNA and RP-A further stimulated its activity, allowing +3 products to be synthesized (*lanes 6* and *7*). However, the addition of Fen-1 dramatically increased the strand displacement-dependent DNA synthesis by DNA pol β, with the generation of long elongation products (*lane 8*). Next, higher amounts of DNA pol δ (Fig. 5*C*) or β (Fig. 5*D*) were incubated on both substrates, in the presence of PCNA and RP-A, and in the absence or presence of increasing amounts of Fen-1. Under these conditions, in the absence of Fen-1, DNA pol δ showed limited strand displacement activity on both the nicked (*lane 1*) or the 1-nt gapped (Fig. 5*C*, *lane 5*) templates. The addition of Fen-1 caused a clear reduction of the strand displacement products (*lanes 2–4* and *5–8*). DNA pol β in the absence of Fen-1 also showed on both substrates limited strand displacement activity (Fig. 5*D*, *lanes 1* and *6*), which was, however, dramatically stimulated by Fen-1 in a dose-dependent manner (*lanes 2–5* and *7–10*). Thus, Fen-1 was able to inhibit DNA pol δ and to stimulate DNA pol β, during AP site bypass, both at the incorporation and elongation steps.

DNA Polymerase β Physically Interacts with Fen-1—It has been shown that both DNA pol β and Fen-1 interact with PCNA. To verify whether they also interact with each other, a Far Western blot analysis was performed. Fen-1 was immobilized on a nitrocellulose membrane, and after *in situ* renaturation, the membrane was incubated with a solution of 1 μg/ml DNA pol β. Development of the membrane with anti-DNA pol β antibodies revealed the presence of DNA pol β on the membrane in correspondence of the signal of Fen-1 (*lane 1*). Replacement of Fen-1 with the same amount of BSA (*lane 2*) or omission of DNA pol β from the incubation buffer (*lane 3*)

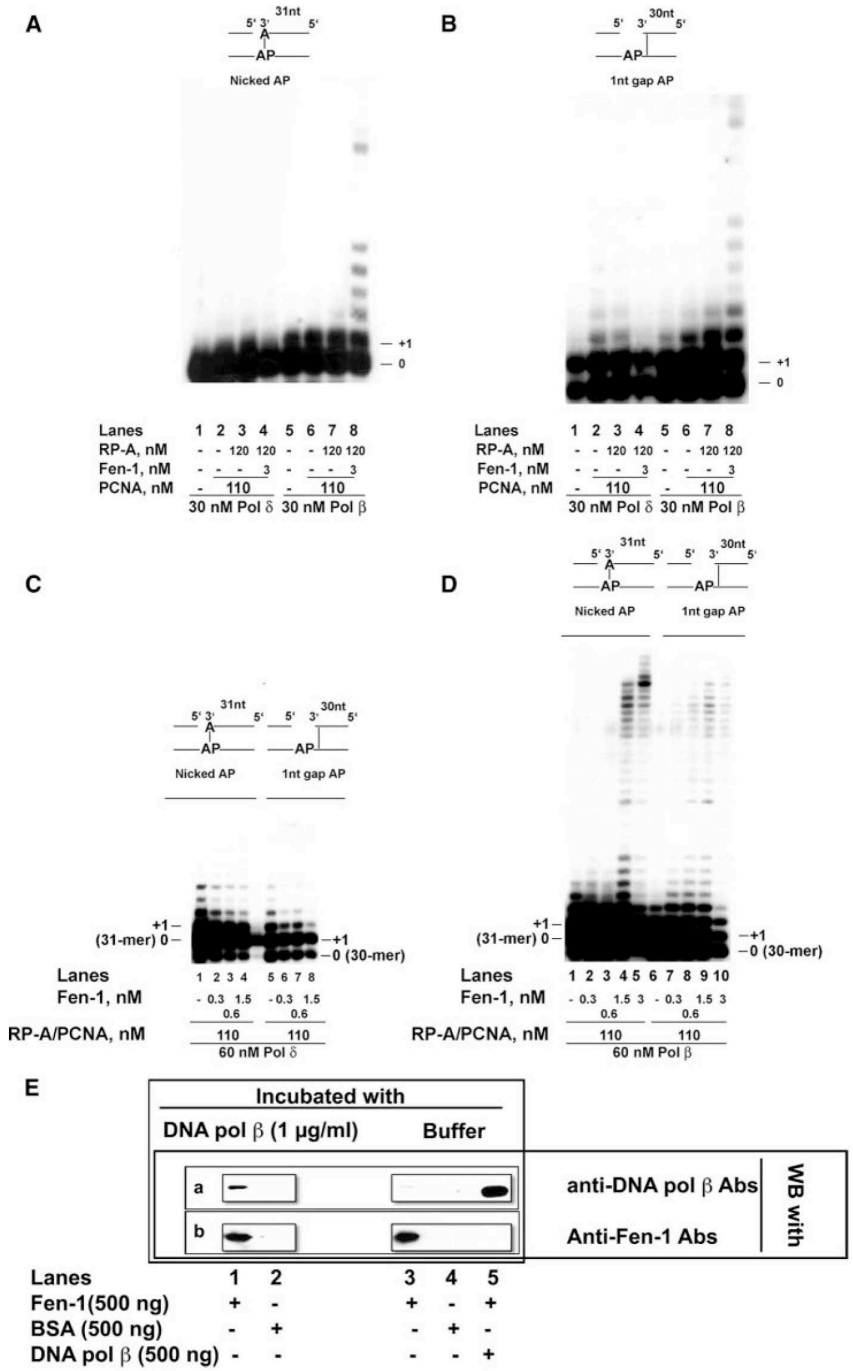

FIGURE 5. **Fen-1 influences both the incorporation and elongation steps by DNA polymerases δ and β during abasic site bypass and can physically interact with DNA polymerase β.** The reactions were performed as described under "Experimental Procedures." *A*, 30 nM DNA pol δ (*lanes 1–4*) or DNA pol β (*lanes 5–8*) were incubated on the nicked AP template in the absence (*lanes 1* and *5*) or in the presence of PCNA either alone (*lanes 2* and *6*) or in combination with RP-A (*lanes 3* and *7*) or 120 nM RP-A together with 3 nM Fen-1 (*lanes 4–8*). *B*, as in *A* but on the 1-nt gap AP template. *C*, 60 nM DNA pol δ were incubated on the nicked AP (*lanes 1–4*) or on the 1-nt Gap AP (*lanes 5–8*) templates, in the presence of a combination of equimolar amounts of PCNA and RP-A (110 nM), and in the absence (*lanes 1* and *5*) or in the presence (*lanes 2–4* and *6–8*) of increasing amounts of Fen-1. *D*, as in *C* but in the presence of 60 nM DNA pol β. *E*, 500 ng of Fen-1 (*lanes 1*, *3*, and *5*), BSA (*lanes 2* and *4*) or DNA pol β (*lane 5*) were incubated either in the presence (*lanes 1* and *2*) or in the absence (*lanes 3–5*) of DNA pol β. The membranes were developed either with anti-Fen-1 (*membrane* ***a***) or anti-DNA pol β (*membrane* ***b***) antibodies, and the signals were detected by chemiluminescence.

abolished the signal of DNA pol β, suggesting that Fen-1 and DNA pol β can physically interact.

DNA Polymerase λ Cooperates Less Efficiently with Fen-1 in Abasic Site Bypass than DNA Polymerase β—DNA pol λ is another family X enzyme closely related to DNA pol β. As shown in supplemental Fig. S2 A, on both linear and gapped DNA substrates, DNA pol λ was able to synthesize full-length products in the absence (*lanes 1–3* and *7–9*) but not in the presence (*lanes 4–6* and *10–12*) of an AP site. Comparison with DNA pol β (Fig. 2*A*) also showed that DNA pol λ was generally less efficient on all the substrates tested (supplemental Fig. S2). Next, DNA pol λ was tested on undamaged or AP-containing 38-nt gapped DNA substrates in the absence or in the presence of Fen-1 and PCNA. As shown in supplemental Fig. S2, Fen-1 promoted strand displacement-coupled DNA synthesis on undamaged DNA (compare *lane 1* with *lanes 2–4*). The addition of PCNA (*lanes 8–11*) further promoted strand displacement, leading to full-length products synthesis (compare *lane 8* with *lanes 9–11*). In the presence of an AP site, however, DNA pol λ was stalled at the lesion (*lanes 5* and *12*), and Fen-1 could only promote very limited strand displacement synthesis beyond the AP site (*lanes 6* and *7*). The addition of PCNA enhanced the effect of Fen-1 (*lanes 12–15*) but did not increase the size of the elongation products made by strand displacement. Thus, DNA pol λ could cooperate with Fen-1 and PCNA in AP site bypass on gapped DNA substrates but with lower efficiency than DNA pol β (compare supplemental Fig. S2 with Fig. 4*C*).

DISCUSSION

In eukaryotes, little is known on how DNA lesions differentially affect leading *versus* lagging strand replication and whether and how they are differentially handled during the lesion bypass (3, 18, 19). The effects of blocking lesions such as AP sites have been always viewed as

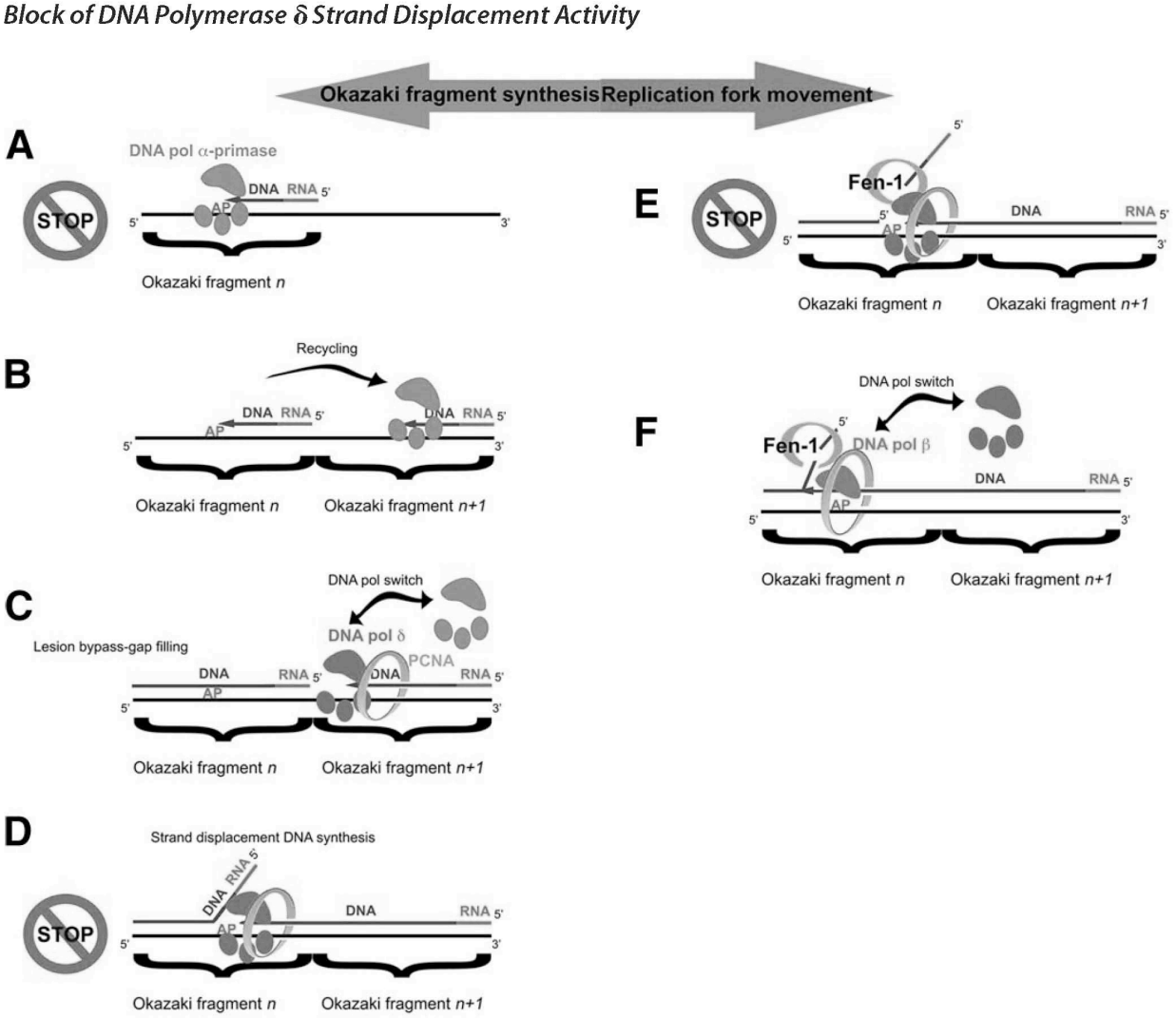

FIGURE 6. **Model for the bypass of the replication block imposed by an abasic site on the lagging strand of the replication fork.** Because of the antiparallel nature of the DNA double helix, the apparent direction of lagging strand synthesis (*green arrow*) is opposite to the direction of replication fork advancement (*orange arrow*). For simplicity only the relevant proteins are shown. For details see text.

the consequence of the inability of replicative DNA pols to perform translesion synthesis because of a dramatic drop of either the incorporation or the elongation rates when attempting to copy AP sites. This is certainly true in the case of leading strand replication. However, in the case of lagging strand synthesis, where about 2.5×10^7 Okazaki fragments have to be correctly replicated, the situation is much more complex (Fig. 6). The current model predicts that, after the synthesis of an RNA/DNA hybrid fragment of about 30 nt by DNA pol α/primase, DNA pol δ gets in and proceeds to synthesize the remaining 100–120 nt of a typical Okazaki fragment. When the 5′-end of the downstream fragment is reached, DNA pol δ initiates strand displacement DNA synthesis, removing the RNA/DNA hybrid synthesized by DNA pol α/primase. If an AP site is encountered by DNA pol α/primase, Okazaki fragment synthesis is impaired (Fig. 6*A*). Studies based on the analysis of replication products using SV40-origin containing DNA plasmids in UV-irradiated mammalian cells suggested that a blocking lesion on the lagging strand template inhibits the completion of the nascent Okazaki fragment, leaving a small gap in the lagging strand (20, 21). Synthesis of a new Okazaki fragment (fragment *n+1* in Fig. 6*B*) is then initiated by DNA pol α/primase, whereas the gap on the damaged strand of the previous fragment (fragment *n* in Fig. 6*C*) is being filled presumably by DNA pol δ and/or β. After the polymerase switch between DNA pol α/primase and DNA pol δ has occurred, and DNA pol δ has reached the 5′-end of the downstream Okazaki fragment (fragment *n* in Fig. 6*C*), strand displacement synthesis is initiated. During this step, however, DNA pol δ will encounter the AP site still present on the template strand (Fig. 6*D*). Biochemical data have shown that DNA pol δ is considerably slowed down by the presence of an AP site on the template strand (4, 22). Thus, it is conceivable that strand displacement synthesis will be paused at the site of the lesion, enabling Fen-1 to process the generated Flap (Fig. 6*E*). The data presented in this work suggest that the resulting intermediate, where the AP site is placed at the

ss/dsDNA junction, constitutes an impassable block for DNA pol δ, even in the presence of PCNA and RP-A. This potentially very dangerous situation can be resolved through a special polymerase switch, whereby the repair enzyme DNA pol β can replace DNA pol δ and, in coordination with Fen-1, continues the strand displacement synthesis, thus bypassing the lesion (Fig. 6*F*). Fen-1 appears to be absolutely required for this reaction, and the fact that Fen-1 and DNA pol β physically interact strengthen this. A stimulatory effect of Fen-1 on the activity of DNA pol β has been already shown to take place in the context of BER reactions (23). Because both of these enzymes also interact with PCNA (24), it is possible to envisage a coordinated trade-off mechanism, where pausing of DNA pol δ allows the recruitment of Fen-1 to the Flap through interaction with PCNA. Then DNA pol β is recruited by physical interaction with Fen-1 and PCNA, thus replacing DNA pol δ. As shown in Fig. 2 (*B* and *C*), PCNA promoted AP site bypass by DNA pol β. This is the first time that a functional effect for the physical interaction between DNA pol β and PCNA is reported (25, 26). In summary, our data suggest that, because the first 30 nt of each Okazaki fragment have to be copied twice, first by DNA pol α/primase and subsequently by DNA pol δ in the context of strand displacement synthesis, the presence of an AP site in this tract will cause a double block that must be resolved by two distinct mechanisms. Thus, our data identify a previously unnoticed deleterious effect of the AP site lesion on normal cell metabolism and suggest the existence of a novel repair pathway that might be important in preventing replication fork stalling.

REFERENCES

1. Lindahl, T. (1993) *Nature* **362,** 709–715
2. Shibutani, S., Takeshita, M., and Grollman, A. P. (1997) *J. Biol. Chem.* **272,** 13916–13922
3. Higuchi, K., Katayama, T., Iwai, S., Hidaka, M., Horiuchi, T., and Maki, H. (2003) *Genes Cells* **8,** 437–449
4. Mozzherin, D. J., Shibutani, S., Tan, C. K., Downey, K. M., and Fisher, P. A. (1997) *Proc. Natl. Acad. Sci. U. S. A.* **94,** 6126–6131
5. Blanca, G., Villani, G., Shevelev, I., Ramadan, K., Spadari, S., Hubscher, U., and Maga, G. (2004) *Biochemistry* **43,** 11605–11615
6. Nick McElhinny, S. A., Gordenin, D. A., Stith, C. M., Burgers, P. M., and Kunkel, T. A. (2008) *Mol. Cell* **30,** 137–144
7. Bae, S. H., and Seo, Y. S. (2000) *J. Biol. Chem.* **275,** 38022–38031
8. Maga, G., Villani, G., Tillement, V., Stucki, M., Locatelli, G. A., Frouin, I., Spadari, S., and Hubscher, U. (2001) *Proc. Natl. Acad. Sci. U. S. A.* **98,** 14298–14303
9. Rossi, M. L., and Bambara, R. A. (2006) *J. Biol. Chem.* **281,** 26051–26061
10. Stucki, M., Pascucci, B., Parlanti, E., Fortini, P., Wilson, S. H., Hubscher, U., and Dogliotti, E. (1998) *Oncogene* **17,** 835–843
11. Pascucci, B., Stucki, M., Jónsson, Z. O., Dogliotti, E., and Hübscher, U. (1999) *J. Biol. Chem.* **274,** 3040–3046
12. Podust, V. N., Chang, L. S., Ott, R., Dianov, G. L., and Fanning, E. (2002) *J. Biol. Chem.* **277,** 3894–3901
13. Maga, G., Crespan E., Wimmer, U., van Loon, B., Amoroso, A., Mondello, C., Belgiovine, C., Ferrari, E., Locatelli, G., Villani, G., and Hübscher, U. (2008) *Proc. Natl. Acad. Sci. U. S. A.* **105,** 20689–20694
14. Jonsson, Z. O., Hindges, R., and Hubscher, U. (1998) *EMBO J.* **17,** 2412–2425
15. Henricksen, L. A., Umbricht, C. B., and Wold, M. S. (1994) *J. Biol. Chem.* **269,** 11121–11132
16. Stucki, M., Jonsson, Z. O., and Hübscher, U. (2001) *J. Biol. Chem.* **276,** 7843–7849
17. Beard, W. A., Prasad, R., and Wilson, S. H. (2006) *Methods Enzymol.* **408,** 91–107
18. Nikolaishvili-Feinberg, N., and Cordeiro-Stone, M. (2001) *Biochemistry* **40,** 15215–15223
19. Cordeiro-Stone, M., and Nikolaishvili-Feinberg, N. (2002) *Mutat. Res.* **510,** 91–106
20. Cordeiro-Stone, M., Zaritskaya, L. S., Price, L. K., and Kaufmann, W. K. (1997) *J. Biol. Chem.* **272,** 13945–13954
21. Mezzina, M., Menck, C. F., Courtin, P., and Sarasin, A. (1988) *J. Virol.* **62,** 4249–4258
22. Maga, G., Villani, G., Ramadan, K., Shevelev, I., Tanguy Le Gac, N., Blanco, L., Blanca, G., Spadari, S., and Hubscher, U. (2002) *J. Biol. Chem.* **277,** 48434–48440
23. Liu, Y., Beard, W. A., Shock, D. D., Prasad, R., Hou, E. W., and Wilson, S. H. (2005) *J. Biol. Chem.* **280,** 3665–3674
24. Maga, G., and Hubscher, U. (2003) *J. Cell Sci.* **116,** 3051–3060
25. Kedar, P. S., Kim, S. J., Robertson, A., Hou, E., Prasad, R., Horton, J. K., and Wilson, S. H. (2002) *J. Biol. Chem.* **277,** 31115–31123
26. Maga, G., Villani, G., Crespan, E., Wimmer, U., Ferrari, E., Bertocci, B., and Hübscher, U. (2007) *Nature* **447,** 606–608

C. The Bloom's Syndrome Helicase (BLM) Interacts Physically and Functionally with p12, the Smallest Subunit of Human DNA Polymerase δ

Reprinted from *Nucleic Acids Research* (2008) **36**, 5166-79.

My contribution to this paper was to show the effect of Bloom's syndrome helicase on the polymerisation activity of DNA polymerase δ.

5166–5179 *Nucleic Acids Research, 2008, Vol. 36, No. 16* *Published online 5 August 2008*
doi:10.1093/nar/gkn498

The Bloom's syndrome helicase (BLM) interacts physically and functionally with p12, the smallest subunit of human DNA polymerase δ

Nives Selak[1], Csanád Z. Bachrati[2], Igor Shevelev[3,4], Tobias Dietschy[3,4], Barbara van Loon[1], Anette Jacob[5], Ulrich Hübscher[1], Joerg D. Hoheisel[5], Ian D. Hickson[2] and Igor Stagljar[3,4,*]

[1]Institute of Veterinary Biochemistry and Molecular Biology, University of Zürich, Winterthurerstr. 190, CH-8057 Zürich, Switzerland, [2]Cancer Research UK, Weatherall Institute of Molecular Medicine, University of Oxford, John Radcliffe Hospital, Oxford OX3 9DS, UK, [3]Department of Biochemistry, [4]Department of Molecular Genetics, Faculty of Medicine, Terrence Donnelly Centre for Cellular and Biomolecular Research (dCCBR), University of Toronto, 160 College Street, Toronto ON, Canada, M5S 3E1 and [5]Functional Genome Analysis, Deutsches Krebsforschungszentrum, Im Neuenheimer Feld 580, D-69120 Heidelberg, Germany

Received April 22, 2008; Revised July 18, 2008; Accepted July 20, 2008

ABSTRACT

Bloom's syndrome (BS) is a cancer predisposition disorder caused by mutation of the *BLM* gene, encoding a member of the RecQ helicase family. Although the phenotype of BS cells is suggestive of a role for BLM in repair of stalled or damaged replication forks, thus far there has been no direct evidence that BLM associates with any of the three human replicative DNA polymerases. Here, we show that BLM interacts specifically *in vitro* and *in vivo* with p12, the smallest subunit of human POL δ (hPOL δ). The hPOL δ enzyme, as well as the isolated p12 subunit, stimulates the DNA helicase activity of BLM. Conversely, BLM stimulates hPOL δ strand displacement activity. Our results provide the first functional link between BLM and the replicative machinery in human cells, and suggest that BLM might be recruited to sites of disrupted replication through an interaction with hPOL δ. Finally, our data also define a novel role for the poorly characterized p12 subunit of hPOL δ.

INTRODUCTION

The faithful completion of chromosomal DNA replication is of crucial importance in determining the fidelity with which genetic information is passed from mother to daughter cells. Incomplete replication or the erroneous copying of a damaged DNA template can give rise to genome instability, accumulation of mutations and, in multicellular organisms, to neoplastic transformation (1). Chromosomal DNA replication in eukaryotic cells requires three distinct DNA polymerases named DNA polymerase α (POL α), ε (POL ε) and δ (POL δ). POL δ and POL ε are required for replication of the leading strand and for completion of lagging strand DNA synthesis. Their respective roles in the replication of leading and lagging strands are still uncertain, though it has been proposed that POL δ and POL ε function specifically at the lagging and leading strands of the replication fork, respectively. POL δ is also involved in different DNA repair pathways as a gap filling enzyme (2). The mammalian POL δ has been studied extensively as a core enzyme consisting of four subunits named p125, p66, p50 and p12 (3). Two of the subunits form a tightly-associated catalytic heterodimer consisting of the catalytic p125 subunit, which has both 5′ to 3′ DNA polymerase and 3′ to 5′ exonuclease activities, and p50. The role of the p66 subunit is to bind PCNA, the homotrimeric sliding clamp that functions as a processivity factor for POL δ during DNA replication (4). A specific role for the p12 subunit has not been identified thus far, although it has been shown to interact with the p125 and p50 subunits of POL δ and Proliferating Cell Antigen (PCNA) (5), and data from *in vitro* DNA replication assays indicate that addition of p12 enhances the DNA polymerizing activity of the enzyme (6). The levels of p12 are regulated by the

*To whom correspondence should be addressed. Tel: +1 416 946 78 28; Fax: +1 416 978 82 87; Email: igor.stagljar@utoronto.ca
Present address:
Nives Selak, Friedrich Miescher Institute, Maulbeerstrasse 66, CH-4058 Basel, Switzerland

The authors wish it to be known that, in their opinion, the first three authors should be regarded as joint First Authors

proteasome through the mechanism that is not dependent upon p12 ubiquitination (7). Apart from PCNA, no other interacting protein has been characterized that specifically associates with p12.

The RecQ family of DNA helicases represents a group of evolutionarily conserved enzymes that are involved in the maintenance of genome stability (8,9). There are five members of this family known in humans called RECQL1, BLM, WRN, RECQL4 and RECQL5. Defects in three of these give rise to defined clinical disorders associated with cancer predisposition and various aspects of premature aging: mutations in the *WRN* and *RECQL4* genes result in Werner's syndrome (WS) and Rothmund Thomson syndrome (RTS), respectively, both of which feature genome instability, predisposition to some types of cancer and the early onset of several aging features. Mutations in the *BLM* gene cause Bloom's syndrome (BS), which is also associated with excessive chromosomal instability and a high incidence of cancers of all types. In contrast to WS and RTS, no obvious premature aging has been observed in BS patients (10). Cells derived from BS patients show a 10-fold higher frequency of reciprocal exchanges between sister chromatids (SCEs), as well as excessive chromosome breakage (11). The BLM protein is a DNA structure-specific helicase that unwinds DNA in 3′ to 5′ direction (12), and shows an apparent preference for unwinding of synthetic Holliday junctions, G-quadruplex (G4) DNA and D-loop DNA substrates (13,14). These substrates represent different DNA structures that can be formed *in vivo* during DNA replication and homologous recombination (HR) processes. Cell biological studies have shown that BLM is localized in the nucleus of human cells within discrete foci termed promyelocytic leukemia (PML) nuclear bodies (15). BLM also localizes to nucleoli in S-phase cells (16), and to telomeres in cells lacking telomerase (17). On the basis of the aforementioned reports, it has been proposed that BLM functions at the interface of DNA replication and recombination, and facilitates the repair of damaged DNA replication forks (9,18).

A large body of evidence implicates BLM in DNA replication. First, DNA replication defects, such as a retarded rate of nascent DNA chain elongation (19) and accumulation of abnormal replication intermediates (20), have been described in BS cells. Second, BLM interacts physically and functionally with several proteins that play important roles during DNA replication, such as replication protein A (RPA) (21), FEN-1 (22) and chromatin assembly factor 1 (CAF-1) (23). Third, BLM is localized to replication foci, particularly during late S phase, and this co-localization increases in the presence of agents that inhibit DNA replication (23). Fourth, BLM expression is activated at the G1/S boundary and peaks in late S-phase/G2 (15,16,24,25). Fifth, BS cells are hypersensitive to agents that perturb DNA replication, such as hydroxyurea (HU) (26).

In this work, we report the physical and functional interaction of BLM with p12, the smallest subunit of human POL δ (hPOL δ). Consistent with this interaction playing an important biological function, we show that the presence of the hPOL δ enzyme, as well as the p12 subunit alone, can specifically stimulate the DNA helicase activity of BLM. We also find that BLM specifically promotes hPOL δ strand displacement activity. Furthermore, we show that the co-localization of BLM and hPOL δ in nuclear foci is activated during replicative stress. Our data are consistent with a role for hPOL δ in the recruitment of BLM to sites of arrested or disrupted DNA replication forks, in order for it to effect its role in fork repair and/or stabilization.

MATERIALS AND METHODS

Purification of the hPOL δ enzyme

Four-subunit hPOL δ was expressed by infection of insect cells with four recombinant baculoviruses, each encoding a subunit of hPOL δ. Recombinant baculoviruses encoding the hPOL δ subunits were a kind gift from Dr Valdimir Podust. In order to produce an exonuclease deficient hPOL δ mutant, a D402A substitution mutation was introduced into the p125/wt cDNA by PCR-based site-directed mutagenesis of the transfer vector pVL1393/p125. Primer sequences are available upon request. Baculovirus-mediated expression of p125 D402A in insect cells using the BacPAK6 system was conducted in accordance with the manufacturer's instructions (Clontech Laboratories, Mountain View, California, USA). hPOL δ enzymes, wt and the exonuclease deficient mutant, as well as a three-subunit exonuclease-deficient mutant lacking the p12 subunit, were purified from insect cells as described previously (6).

Purification of 6xHis-p12 protein

The p12 cDNA was cloned into the pRSETb vector. The resulting pRSETb-p12 construct was verified by DNA sequencing. p12 was expressed in *Escherichia coli* BL21(DE3) (Novagen, Merck KGaA, Darmstadt, Germany). Expression of p12 was induced by addition of 1 mM IPTG to cultures grown at 37°C to an A_{600} of 0.4. After incubation at 37°C for 3 h, the cells were harvested by centrifugation. The *E. coli* pellet was resuspended in 30 ml of buffer A (30 mM phosphate buffer, 10 mM Tris HCl, pH 8.0, 500 mM NaCl, 10 mM imidazole, 1 mM PMSF, 1 μM benzamidine, 5 μg/ml leupeptin and 2 μg/ml pepstatin A). The cells were disrupted with a French Press (twice) and the lysate was sonicated on ice for 1 min. After centrifugation (20 000 r.p.m. for 30 min at 4°C in a SS-34 rotor), the soluble fraction was loaded onto a 1 ml HiTrap Chelating (Ni^+) column pre-equilibrated with buffer A. The column was washed with 50 ml buffer A, and then with 20 ml buffer A containing 50 mM imidazole. The bound protein was eluted with 300 mM imidazole in buffer A. After desalting to buffer B (40 mM Tris HCl pH 7.5, 50 mM NaCl, 1 mM EDTA, 1 mM 2-mercaptoethanol, 15% (v/v) glycerol, 1 mM PMSF, 1 μM benzamidine, 5 μg/ml leupeptin and 2 μg/ml pepstatin A) using a HiTrap Desalting column, the eluate was loaded onto a 1 ml HiTrap Heparin column pre-equilibrated with buffer B. The column was washed with 20 ml buffer B, and the p12 protein was eluted with a 20 ml linear NaCl gradient (50 1000 mM). p12 was eluted at 300 mM NaCl as tested by SDS PAGE and western blotting using an antibody against p12.

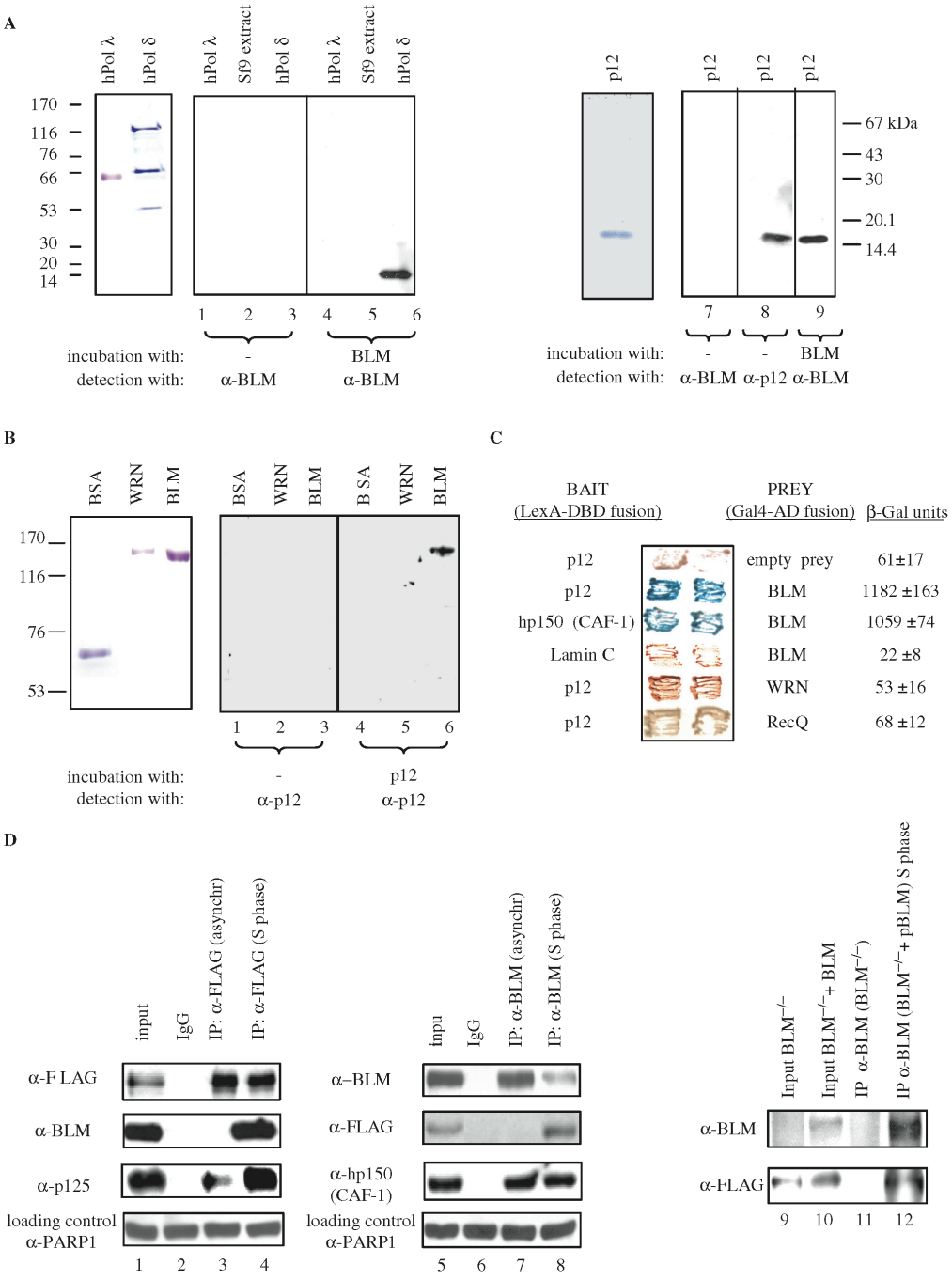

Figure 1. BLM and p12 of hPOL δ interact *in vitro* and *in vivo*. (**A**) Left panel, far-western analysis. hPOL λ, total protein extract from Sf9 insect cells, and hPOL δ enzyme were subjected to SDS–PAGE, transferred to a nitrocellulose membrane, and were incubated with purified recombinant BLM. Anti-BLM antibodies were used to permit the detection of p12 as a novel BLM-interacting protein (lane 6). Molecular weight markers are also indicated on the left. Right panel, purified p12 subunit of hPOL δ was subjected to SDS–PAGE, transferred to nitrocellulose membrane, incubated with BLM, and subsequently probed with the anti-BLM antibody (lane 9). (**B**) Reciprocal far-western analysis. BSA, WRN and BLM (left panel) were hybridized with the purified p12 and probed with the anti-p12 antibody (right panel). Anti-p12 antibodies were used to confirm that p12 specifically binds to BLM (lane 6). (**C**) BLM and p12 of hPOL δ interact in the YTH assay. The L40 yeast reporter strain was co-transformed with plasmids encoding the indicated full-length 'bait' (LexA-DBD) and 'prey' (Gal4-AD) fusions. Two independent colonies were grown on SD agar plates lacking tryptophan and leucine, but containing X-gal, prior to assessment of β-galactosidase activity. Also shown are two negative controls, p12 co-transformed with an empty prey vector and BLM co-transformed with lamin C protein. The previously described BLM/hp150 (CAF-1)

The pool of p12 protein was diluted to 50 mM NaCl and finally loaded onto a Mono S column pre-equilibrated with buffer B. Chromatography was performed as for the HiTrap Heparin column. The yield from a 1 l culture was ~0.3 mg of p12 protein with a purity of over 99.5%, as judged by Coomassie Blue staining. Protein concentrations were determined by the Bradford method (27) by using Bovine Serum Albumin (BSA) as a calibration standard.

Production and purification of the p12 antibody

To produce the p12 antibody, the 6xHis-p12 protein was expressed in *E. coli* from the pRSETb-p12 plasmid, and purified from *E. coli* using conventional chromatography (see above). Rabbits were immunized three times with 300 μg of 6xHis-p12 protein being used for each immunization. After the third immunization, the rabbit was sacrificed to obtain the serum. The p12 serum was first purified over a Protein G sepharose column, to isolate total IgG, and then purified over a column coupled to the p12 protein, to obtain the IgG_{p12}. For all subsequent studies, the anti-IgG p12 was used at concentration of 0.2 μg/ml in dilution 1:100 in TBS, 0.05% Tween-20. Control IgG was purified from preimune serum using Protein G sepharose column.

Far-western analysis

Far-western assays were performed as described previously (28). Human WRN was a kind gift from Dr Pavel Janscak, University of Zürich. Briefly, total extracts of Sf21 insect cells (0.825 μg), 0.8 μg of hPOL δ, 0.3 μg of hPOL λ and 0.2 μg of p12 were subjected to 12% SDS PAGE and transferred to a nitrocellulose filter. After blocking in 10% milk, 0.3% Tween-20 in TBS, for 1 h at RT, the filter was incubated for 2 h at 4°C with BLM (0.5 μg/ml) in TBS supplemented with 0.25% milk, 0.3% Tween-20, 1 mM DTT and 1 mM PMSF (hybridization solution). After the washing step (4 × 15 min, 0.25% milk, 0.3% Tween-20 in TBS), western blot was performed using the anti-BLM IHIC33 antibody (29) to detect the presence of BLM. For the experiment presented in Figure 1, BLM (1.2 μg), WRN (0.8 μg) and BSA (0.4 μg) were separated on a 7.5% SDS gel and transferred to a nitrocellulose membrane. The membrane was incubated with 6xHis-p12 in hybridization solution, with a final concentration 6xHis-p12 of 0.1 μg/ml. After washing, the membrane was probed with an anti-p12 antibody (this study) to detect the presence of p12. The input samples were visualized with antibodies against BLM [IHIC33, (29)] and WRN (ab-200, Abcam, Cambridge, UK). The membrane was incubated with the BLM protein in hybridization solution, with a final concentration of BLM of 0.5 μg/ml. After washing, western blot using an anti-BLM IHIC33 antibody was performed to detect the presence of BLM. The input samples were visualized with antibodies against hPOL λ (ab5954, Abcam) and p12 (this study).

Yeast two-hybrid assay

Yeast two-hybrid (YTH) assays were performed as described previously (23). The activity of the reporter gene (β-galactosidase) was assessed using a liquid culture assay with *O*-nitrophenyl-D-galactopyranoside as a substrate. The constructs used to map the region of BLM that interacts with p12 have been described previously (30). The different p12 constructs were generated by PCR using pMALc2e-p12 as a template, and were cloned into the pBTM116 + 2 (MBN) vector. Sequences of all plasmids, primers used and construction schemes are available upon request.

Transfections and immunoprecipitation assay

The p12 cDNA was cloned into the p3xFLAG-myc-CMV-23 (Sigma-Aldrich, Buchs, SG, Switzerland) vector using plasmid pRSETb-p12 as a template and primers 5′-gga agatctcataggggatagagatgccag -3′ (BglII) and 5′- cccaagctt atgggccggaagcggctc - 3′ (HindIII). The resulting construct was sequenced. 293T cells were transiently transfected with p3xFLAG-myc-CMV-23-p12 by the calcium phosphate precipitation method. Thirty-six hours after transfection, cells were treated with 1 mM HU for 24 h, and were then harvested. Nuclear extracts were prepared from 293T cells as described previously (31). Aliquots (500 μg) of the nuclear extracts were incubated with 3 μg of anti-FLAG antibody coupled to magnetic, tosyl-activated Dynabeads (Dynal Biotech, Invitrogen, Paisley, UK, M-280) according to manufacturer's instructions in immunoprecipitation (IP) buffer (20 mM HEPES pH 7.5, 150 mM NaCl, 5 mM $MgCl_2$, 0.1% Nonidet P 40, protease inhibitor) at 4°C for 3 h. As a control, nuclear extracts were incubated with a control rabbit IgG. The beads were washed three times in IP buffer, before any protein complexes bound to beads were eluted and analysed by SDS PAGE. A 50 μg portion of nuclear extract was used as input control. Subsequently, western blot analysis was performed using the anti-FLAG (Sigma M2) and anti-BLM ab 476 antibody (Abcam). C-18 (anti-BLM, Santa Cruz) was used for the reciproical co-IP in the above-mentioned IP buffer containing 150 mM KCl.

interaction (23) was used as a positive control. (**D**) BLM and hPOL δ form a complex in human cells. 293T cells were transiently transfected with FLAG-p12, and were synchronized in S phase using 1 mM HU. Nuclear extracts derived from either unsynchronized (lane 3) or S-phase synchronized cells (lane 4) were immunoprecipitated with the anti-FLAG antibody or control IgG, and were analysed by SDS–PAGE. One-tenth (50 μg) of the same nuclear extract was used as input control (lane 1). Immunoprecipitated FLAG-p12 and BLM were detected by western blotting using the anti-FLAG and anti-BLM antibody, respectively (lane 4). p125, the largest subunit of hPOL δ, was also efficiently co-immunoprecipitated using the same anti-FLAG antibody (lanes 3 and 4). Reciprocal co-IP is shown in the middle panel: lane 5, input; lane 6, IP with the control IgG; lane 7, IP with an anti-BLM antibody (C-18) from nuclear extracts derived from unsynchronized 293T cells; lane 8, IP with an anti-BLM antibody (C-18) from nuclear extracts derived from the S-phase synchronized 293T cells. The known BLM interacting protein, hp150 (CAF-1) was also efficiently co-immunoprecipitated using the same anti-BLM antibody (lanes 7 and 8). As a loading control for lanes 1–8, 50 μg of the corresponding nuclear extract was probed with an anti-PARP1 antibody. Right panel shows co-IP with anti-BLM antibody (C-18) from BS cell nuclear extracts (BS) and BS cells containing the *BLM* cDNA (BS + pBLM). p12 could be co-immunoprecipitated in the presence of BLM from the S-phase synchronized nuclear extracts (lane 12) but not in the absence of BLM (lane 11). Lanes 9 and 10 are the inputs of the two different nuclear extracts.

Nuclear extracts from BS cells were used as a negative control for the C-18 reciprocal co-IP.

DNA polymerase primer extension assay

A 18-nt primer was 5′-end labeled with ^{32}P using T4 polynucleotidekinase and purified on a Sephadex G25 microcolumn. The X-poly template was generated by annealing an 18-nt primer to four complementary oligonucleotides. Three of these oligonucleotides are 50-nt long; the fourth oligonucleotide has an extended arm that is complementary to the 18-mer primer at its 3′ end. Twenty-five nucleotides of each four oligonucleotides are fully complementary to two out of three other oligonucleotides, so that the result of annealing is a cruciform structure. Annealing and purification of the X-poly substrate was carried out as described previously (32). Sequences of the primers used are available upon request. Reactions (10 μl final volume) were carried out in buffer containing 40 mM Tris HCl buffer (pH 8.0), 3 Mm $MgCl_2$, 1 mM ATP, 50 mM NaCl, 2 mM DTT, 0.1 mg/ml BSA, 10% glycerol, 0.15 pmol of ^{32}P-18-nt-X-poly template, 100 μM each of dATP, dGTP, dCTP and dTTP, 10 ng of hPOL δ exo, and the indicated amounts of BLM, human PCNA or *E. coli* RecQ. Reactions were incubated at 37°C for 30 min, and were terminated by rapid cooling on ice and addition of an equal volume of denaturing loading buffer. The samples were boiled, and 10 μl of sample were electrophoresed through 12.5% polyacrylamide 8 M urea gel in 0.5 × TBE buffer, and the extension products were visualized by autoradiography.

DNA helicase assays. Recombinant BLM protein was purified from yeast cells as described previously (12). The splayed arm DNA substrate that mimics a replication fork was generated by annealing two partially complementary oligonucleotides, consisting of 25 nt of fully complementary and 25 nt of non-complementary sequences, and was purified as described previously (13,32). The helicase reactions were carried out under presumed single-turnover conditions; that is with helicase concentration in excess over substrate concentration. The 10 μl reactions contained 1 × helicase buffer [33 mM Tris acetate (pH 7.8); 1 mM $MgCl_2$; 66 mM sodium acetate; 0.1 mg/ml BSA; 1 mM DTT; 1 mM ATP], 100 pM substrate, various concentrations of BLM and other proteins as stated in figure legends. The reaction was allowed to progress for 15 min at 37°C unless otherwise stated. Analysis of reaction products was carried out as described previously (32).

Indirect immunofluorescence analysis

GM00637 transformed normal human fibroblasts were grown on coverslips and were either treated with 2.5 mM HU for 18 h or cultured untreated, and were then pulse labeled with 25 μM BrdU for 5 min. The coverslips were then rinsed with ice-cold PBS. Soluble proteins were removed by incubating the slides in pre-extraction buffer [10 mM PIPES, 300 mM sucrose, 3 mM $MgCl_2$, 20 mM NaCl, 0.5% Triton X-100 (pH 6.8)] for 5 min on ice. The cells were then fixed in 4% paraformaldehyde for 20 min on ice. The immunostaining was performed as described earlier (33) using the IHIC34 rabbit polyclonal antibody (29) and the AlexaFluor 488 conjugated donkey anti-rabbit secondary antibody (Molecular Probes, Invitrogen, Paisley, UK) to detect BLM, at 1 : 200 and 1 : 800 dilutions, respectively. The A-9 mouse monoclonal antibody (Santa Cruz Biotechnology Inc., Santa Cruz, California, USA) against the catalytic subunit of hPOL δ and the CY3 conjugated sheep anti-mouse secondary antibody (Sigma-Aldrich, Gillingham, UK) were used to detect hPOL δ, at 1 : 400 and 1 : 1000 dilutions, respectively. BrdU incorporation was detected after repeated paraformaldehyde fixation and HCl denaturation with rat anti-BrdU primary antibody (Abcam) and AlexaFluor 350 conjugated goat anti-rat secondary antibody (Molecular Probes), each at 1 : 300 dilution. Epifluorescence microscopy, image acquisition and analysis were carried out on a Nikon Eclipse 80i microscope with the Lucia G software (Laboratory Imaging s.r.o., Prague, Czech Republic). Grabbed images were scored manually using the Adobe Photoshop program. Foci obtained following staining with either antibody (green or red) were marked and counted. Foci were counted as co-localizing if more than 50% of the green and red signal was overlapping. Co-localization was expressed as percentage of the total number of BLM (green) or POL δ (red) foci. The total number of cells scored in each treatment was 100. Two independent experiments were conducted with nearly identical results, of which only one is presented.

RESULTS

BLM and hPOL δ interact *in vitro* and *in vivo*

To analyse the possible functional interaction of BLM and hPOL δ, we first purified both BLM and the four subunit hPOL δ enzyme (Supplementary Figure. 1). A far-western assay was then used to test for a specific interaction between BLM and one or more of the hPOL δ subunits. As shown in Figure 1A, the BLM protein specifically interacted with a protein of apparent molecular mass of 14 kDa (lane 6), which corresponds to p12, the smallest subunit of hPOL δ. In contrast, BLM did not interact with any of the other three hPOL δ subunits, with an unrelated human DNA polymerase, hPOL λ (lane 4), or with any protein from the extract of Sf9 insect cells from which the recombinant hPOL δ enzyme was purified (lane 5). In order to confirm that BLM specifically binds to p12, the far-western analysis was repeated using full-length BLM and purified recombinant p12 immobilized on nitrocellulose. Clear evidence of binding was obtained (Figure 1A, lane 9). Moreover, in a reverse far-western, purified p12 specifically bound to full-length BLM (Figure 1B, lane 6), but not to BSA (Figure 1B, lane 4) or to another human RecQ helicase, WRN (Figure 1B, lane 5). No cross-reactivity of either the anti-BLM antibody with p12, or the anti-p12 antibody with BLM was detected (Figure 1A, lanes 1 3 and 7 and Figure 1B, lanes 1 3). Taken together, these data indicate that BLM and p12 interact specifically *in vitro*.

To validate the results obtained from far-western assays, we next performed YTH analysis. As shown in Figure 1C, p12 interacted with full-length BLM, but not with full-length WRN or *E. coli* RecQ, indicating that the physical interaction between p12 and BLM is specific. Furthermore, no YTH interaction could be detected between the full-length BLM fused to Gal4-AD and any of the other three hPOL δ subunits (p125, p66 and p50) fused to LexA-DBD (data not shown).

To gain insight into the possible association of BLM and p12 in human cells, we performed co-IP assays (Figure 1D). Because the endogenous levels of p12 are very low and our newly generated anti-p12 antisera did not work in IP assays, we were forced to use ectopically expressed p12. For this, FLAG-p12 was transiently transfected into 293T cells and the cells were subsequently synchronized in S phase by treatment with 1 mM HU for 24 h. Synchronization of the 293T cells was confirmed by fluorescence activated cell sorter (FACS) analysis (data not shown). Using an anti-FLAG antibody, we were able to specifically co-immunoprecipitate BLM from HU-treated cells (Figure 1D, lane 4), but not from unsynchronized cells (Figure 1D, lane 3). As expected, the anti-FLAG antibody efficiently precipitated p125, the largest subunit of hPOL δ, from both HU-treated and unsynchronized cells (Figure 1D, lanes 3 and 4, lower panel). No BLM was present in the precipitate when a control antibody was used (Figure 1D, lane 2). A reciprocal co-IP experiment was also carried out, in which an anti-BLM polyclonal antibody was used to immunoprecipitate FLAG-p12 from 293T nuclear extracts. As shown in Figure 1D, p12 could be specifically co-immunoprecipitated with endogenous BLM from the S phase-synchronized cells (lane 8), but not from unsynchronized 293T cells (lane 7). Furthermore, in addition to p12, the anti-BLM antibody efficiently co-immunoprecipitated hp150, the largest subunit of CAF-1 (Figure 1D, lanes 7 and 8, lower panel), a protein shown previously to interact with BLM (23). Similar co-IP results were obtained when 293T-derived nuclear cell extracts were incubated with ethidium bromide, indicating that the *in vivo* interaction of p12 and BLM is unlikely to be mediated by DNA (data not shown). Finally, the specificity of co-IPs with the anti-BLM antibody was demonstrated in a control experiment using nuclear extracts from BS ($BLM^{-/-}$) cells: in this case, the anti-BLM antibody could not co-immunoprecipitate p12 from these cells (Figure 1D, lane 11, lower panel), whereas it could efficiently co-immunoprecipitate p12 from S phase-synchronized BS cells containing the *BLM* cDNA ($BLM^{-/-}$ + pBLM) (Figure 1D, lane 12, lower panel). Collectively, these data indicate that BLM directly associates with the p12 subunit of hPOL δ *in vitro* and *in vivo*, and that the BLM/p12 interaction in human cells is exclusively or predominantly seen in cells in which DNA replication is arrested.

Mapping of the interacting regions on BLM and p12

BLM contains several important domains; a conserved helicase domain (aa 649 1006), an RecQ familiy C-terminal (RQC) domain (aa 1006 1077) and an Helicase, RNAse D C terminal (HRDC) domain (aa 1212 1292), all of which are involved in mediating protein DNA interactions, and possibly also protein protein interactions (Figure 2A). To identify the region of BLM that mediates the interaction with p12, we generated a series of BLM deletion mutants and tested them for their ability to interact with full-length p12 in the YTH assay (Figure 2A). The results indicated that p12 binds BLM in the region between amino acids 447 and 770. This fragment of BLM comprises the helicase-proximal region of the N-terminal domain and part of the helicase domain. A similar YTH approach was used to map the region of p12 that interacts with BLM. A single short region of p12, comprising amino acids 31 60, was found to be necessary and sufficient for interaction with BLM (Figure 2B).

The hPOL δ enzyme stimulates the BLM-mediated unwinding of a model replication fork substrate

The physical interaction between BLM and hPOL δ suggested the possibility that the two proteins might functionally regulate each other's activities during DNA replication, recombination or repair. To test this hypothesis, we first determined whether the hPOL δ enzyme influences BLM helicase activity. In order to see a potential effect of hPOL δ, either positive or negative, the BLM concentration used in the helicase assays was sufficient only for partial unwinding of the substrate during a 15-min reaction period. To prevent the potential degradation of the helicase substrate or product by the exonuclease activity of hPOL δ, the hPOL δ enzyme used carried a mutation in the exonuclease domain of p125 (D402A) and was, therefore, exonuclease defective. When hPOL δ was added to the reaction in concentrations giving molar ratios of 25 to 0.4 times that of the BLM concentration, we saw a significant, concentration-dependent stimulation of helicase activity (Figure 3A, lanes 6 12). BLM alone (Figure 3A, lane 3) and BLM incubated with heat-denatured hPOL δ (Figure 3A, lane 5) showed the expected low level of helicase activity, and hPOL δ alone displayed no DNA helicase activity (Figure 3A, lane 4). We were also able to demonstrate the stimulation of BLM helicase activity by hPOL δ in time-course experiments; hPOL δ reproducibly increased the initial velocity of the unwinding reaction (Figure 4C center panel and D; and data not shown).

Next, we analysed the specificity of this apparent functional interaction. We found that this stimulatory effect was specific to the BLM/hPOL δ complex, as hPOL δ had no effect on another RecQ helicase, *E. coli* RecQ, in the same concentration range (Supplementary Figure 2A, lanes 7 17, and B). Moreover, we showed that another human DNA polymerase, hPOL λ, which we had shown did not bind to BLM in far-western analysis (Figure 1A), did not influence BLM helicase activity (Supplementary Figure 2C, lanes 6 17, and D). Taken together, these data indicate that hPOL δ shows a specific, functional interaction with BLM.

The far-western and YTH analyses localized the BLM/hPOL δ interaction to the smallest p12 subunit of hPOL δ between residues 31 and 60 (Figures 1 and 2). We tested,

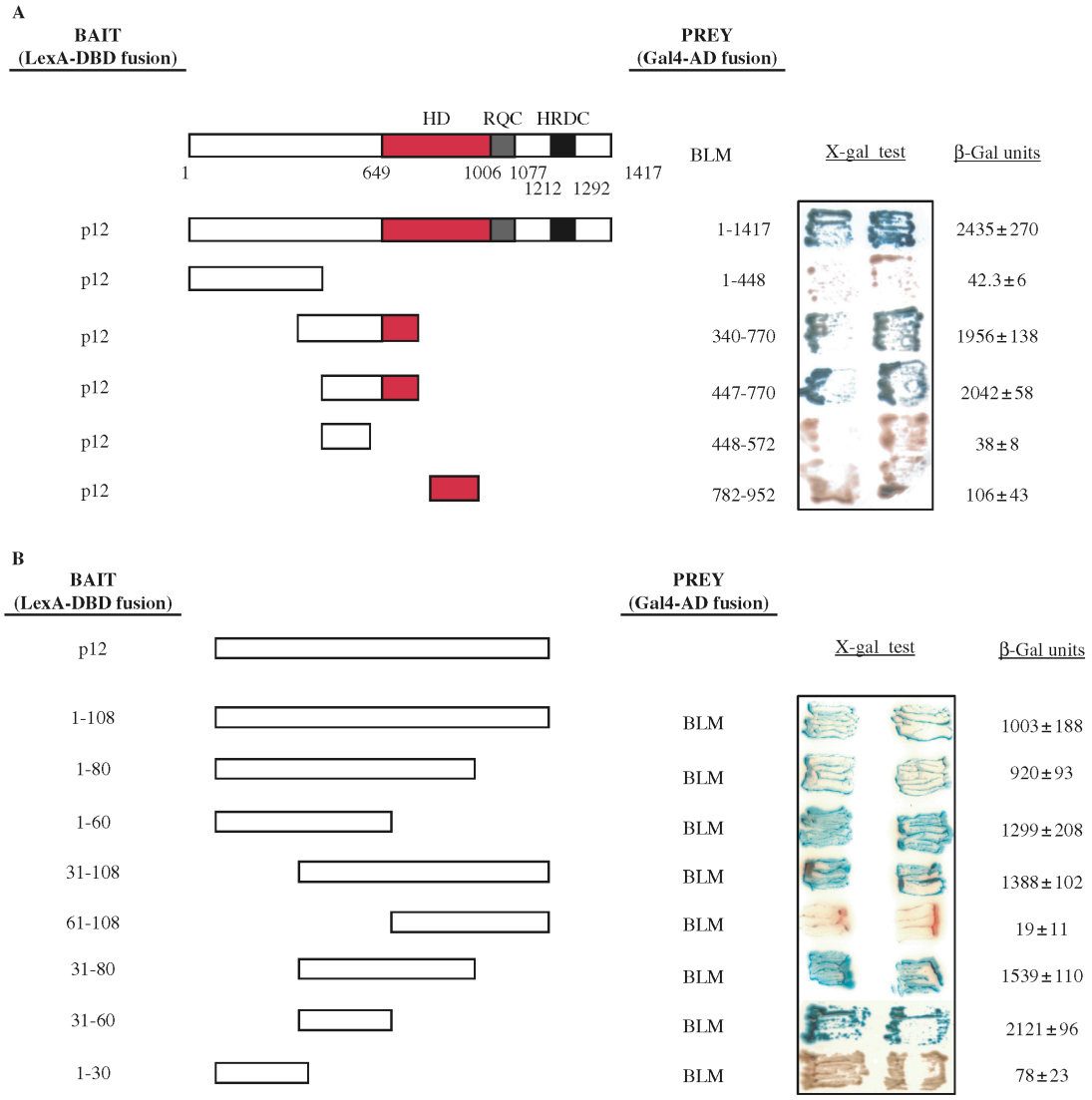

Figure 2. Interaction region mapping of BLM and p12. (**A**) Mapping of the BLM interaction region. The L40 yeast strain was co-transformed with plasmids encoding the indicated BLM fragments fused to Gal4-AD and the full-length p12 fused to LexA-DBD. Two independent colonies were grown on SD agar plates lacking tryptophan and leucine, but containing X-gal, prior to assessment of β-galactosidase activity. Blue coloration of colonies is a marker of interaction. Full length BLM is also shown, with a red bar indicating its conserved helicase domain, a blue bar indicating RQC and a black bar indicating the HRDC domain. Interactions between a given bait/prey pair were quantified by measurements of β-galactosidase activity. Values represent means ± SD of three independent experiments. (**B**) Mapping of the p12 interaction region. The L40 yeast strain was co-transformed with plasmids encoding the indicated p12 fragments fused to LexA-DBD and full length BLM fused to Gal4-AD. In both (**A**) and (**B**) the sequence boundaries of deletion mutants tested are shown with the corresponding amino acid positions indicated on the right. Values obtained from liquid β-galactosidase assay are shown on the right and represent means ± SD of three independent experiments.

therefore, the effect of recombinant p12 subunit on the helicase activity of BLM. p12 showed a concentration-dependent stimulatory effect on BLM similar to that of the hPOL δ enzyme; however, the effective concentration range was such that there was a large molar excess of p12 over BLM (Figure 4A, lanes 6–15). Interestingly, heat-denatured p12 was also able to stimulate BLM helicase activity at this high concentration (1.609 μM; Figure 4A, lane 5), which, in the light of the results showing that a small peptide is also able to stimulate the helicase activity of BLM, is not inexplicable (see below). As described earlier, we saw concentration-dependent stimulation of BLM helicase activity by p12 only at high p12 concentration. Therefore, we designed a different system to study this effect and monitored the progress of the unwinding reaction over time in the presence or absence of p12. This revealed that p12 and the hPOL δ enzyme increased the kinetics of the BLM unwinding reaction to a similar extent (Figure 4C and D).

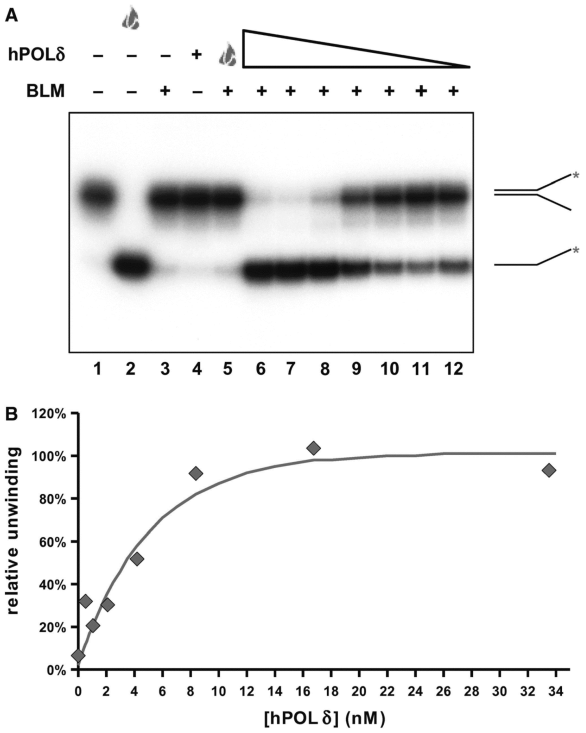

Figure 3. The hPOL δ enzyme specifically stimulates the BLM-mediated unwinding of the replication fork substrate in a concentration-dependent manner. (**A**) A total of 1.3 nM BLM was pre-incubated with the exonuclease-defective hPOL δ enzyme in various concentrations (33.5, 16.8, 8.4, 4.2, 2.1, 1 and 0.5 nM; lanes 6–12, respectively) on ice for 3 min, and the samples were then warmed to 37°C. The unwinding reaction was initiated immediately by the addition of substrate and ATP. Flame symbol depicts heat-denatured substrate (lane 2), or BLM incubated with heat-denatured hPOL δ enzyme at the highest concentration of the titration range (33.5 nM; lane 5), as described earlier. (**B**) Quantification of data presented in (A). Data were normalized to the non-treated (lane 1, taken as 0%) and boiled (lane 2, taken as 100%) samples. Maximal stimulation (at 6 times above BLM basal helicase activity) was achieved with a 13 × molar excess of hPOL δ.

The effect was concentration-dependent and reproducible using various molar ratios of BLM and hPOLδ or p12 (1 : 0.8–1 : 3.9, Supplementary Figure 3 and data not shown; 1 : 23.5, Figures 4C, D and 5). The initial linear part of the progress curves permitted us to approximate the initial velocity of the reaction. Depending on the molar ratio of hPOL δ or hp12 and BLM, we saw a 2–15 times increase in the initial velocity of unwinding (Supplementary Figure 3, and data not shown).

This result prompted us to test the effect on BLM activity of the tightly-defined interacting region of p12. For this, two peptides were chemically synthesized: $p12^{30–60}$ covers the BLM-binding region, while $p12^{71–100}$ maps to a region of p12 that shows no BLM-binding, as revealed in the YTH mapping studies (Figure 2B). Full-length p12 and $p12^{30–60}$ showed a similar degree of stimulation of BLM activity in a time-course experiment. In contrast, $p12^{71–100}$ had no effect on BLM helicase activity (Figure 5A and B). Taken together, these results confirm that the helicase activity of BLM is stimulated by hPOL δ, and that this stimulation is dependent on the binding between the two proteins through amino acid residues 30–60 in the p12 subunit of hPOL δ.

BLM increases the strand displacement activity of hPOL δ

Given the data described earlier indicating that hPOL δ has a significant stimulatory effect on BLM helicase activity, it was important to examine whether BLM affects the polymerase activity of hPOL δ. To that end, we performed primer extension assays (Figure 6). hPOL δ-specific polymerization activity was monitored by visualizing extension of a 5′-end labeled 18-mer primer on an 85-mer DNA template, which contains an X-junction at the 3′end. This template was chosen because we wanted to examine whether BLM can help hPOL δ to traverse X-junction at the end of template. We observed that hPOL δ alone was able to incorporate dNTPs up to the start of the X-junction structure (Figure 6, lane 2). The inability of hPOL δ to extend the primer beyond the pause site indicates that the X-junction structure effectively blocked progression of hPOL δ along the template strand.

When BLM was added to the reaction in concentrations giving molar ratios of 1.5–7.5 times that of the hPOL δ concentration, we observed an increase in both the amount of primer extended and the maximal length of product (Figure 6, lanes 3–5) such that the longest products represented polymerization extending 5 nt beyond the position of the X-junction. This effect was similar to that produced by PCNA, although the degree of stimulation of hPOL δ by PCNA was more pronounced (Figure 6, lanes 7–9). Importantly, BLM alone showed no polymerase activity (Figure 6, lane 6). The stimulatory effect of BLM on hPOL δ was found to be specific, as another member of the RecQ helicase family, *E. coli* RecQ, had no effect on hPOL δ (Figure 6, lane 10). In order to test whether BLM had a stimulatory effect on hPOL δ polymerase activity *per se* we performed primer extension assay using a more conventional DNA substrate comprising a 72-nt long template and a 17-nt primer. As shown in Supplementary Figure 4, we found that BLM does not stimulate hPOL δ polymerase activity on such a DNA template.

Altogether, these results indicate that BLM does not stimulate hPOL δ polymerase activity but, similar to PCNA, BLM promotes strand displacement by hPOL δ.

BLM and hPOL δ partially co-localize *in vivo* in response to perturbation of DNA replication

The *in vitro* studies described earlier prompted us to analyse whether hPOL δ and BLM might interact *in vivo*. As indicated earlier (Figure 1D), BLM and hPOL δ could be co-immunoprecipitated from 293T cells only after HU treatment, which suggested that the interaction is either S-phase specific or induced specifically in response to perturbation of replication. To differentiate between these possibilities, we addressed whether BLM and hPOL δ co-localize either in unperturbed, cycling cells or in cells blocked with HU. For this, GM00637 (BLM proficient)

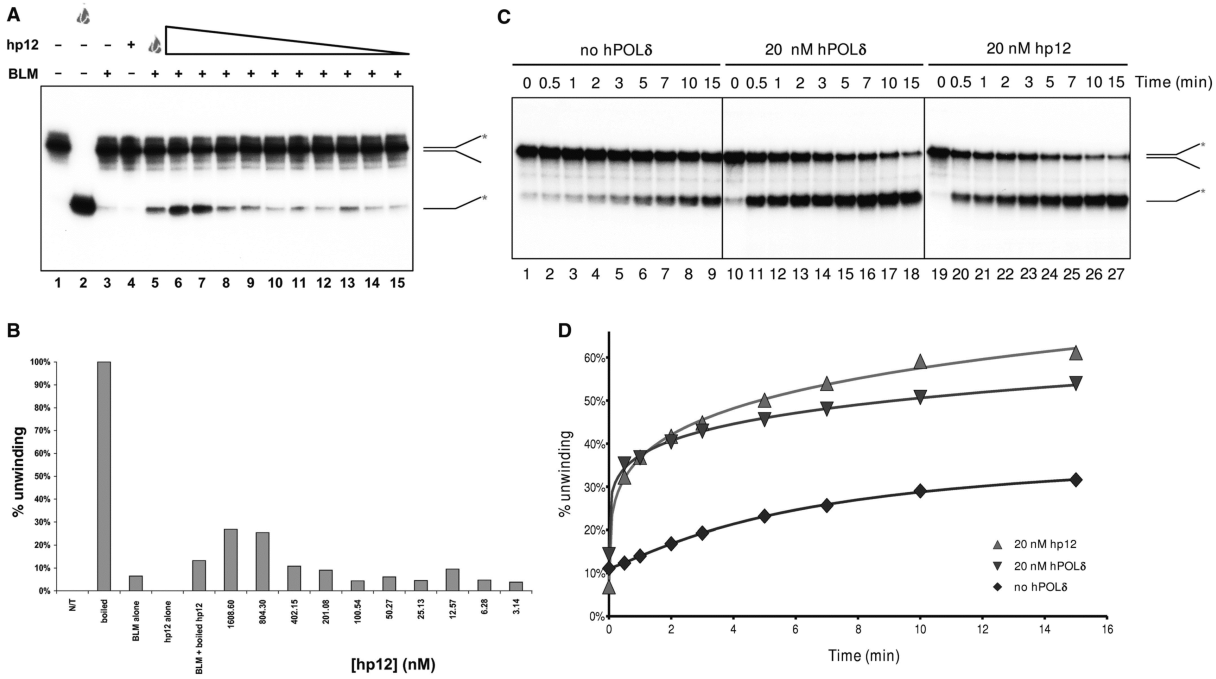

Figure 4. The small subunit of the hPOL δ enzyme, p12, is sufficient to stimulate BLM helicase activity. (**A**) A total of 1.3 nM BLM was pre-incubated with various concentrations of p12 (1609, 804.5, 402.25, 201.13, 100.56, 50.28, 25.14, 12.57, 6.29 and 3.14 nM; lanes 6–15, respectively) on ice for 3 min, and the samples were then warmed to 37°C. The unwinding reaction was initiated immediately by the addition of substrate and ATP. Controls and symbols are as in Figure 3. (**B**) Quantification of data from (A). (**C**) A total of 0.85 nM BLM was incubated at 37°C for 5 min alone (lanes 1–9), or with 20 nM hPOL δ (lanes 10–18), or 20 nM p12 (lanes 19–27). The unwinding reaction was then initiated by the addition of ATP and substrate. Samples were withdrawn at the time points indicated above the lanes. (**D**) Quantification of data from (C).

human fibroblast cells were plated on coverslips and treated with 2.5 mM HU for 18 h, sufficient to block replication, as evidenced by the depression of BrdU incorporation into the nuclei (not shown). A control culture was incubated in parallel without HU treatment. In both sets of cells, BrdU was added to a final concentration of 25 μM 5 min before the cells were fixed. The fixed samples were stained for the presence of hPOL δ, BLM and BrdU, as described in Materials and methods section. To detect hPOL δ were restricted in our use of antibodies, because our antibody to p12 did not work in immunofluorescence analysis. Hence, we chose an antibody against the catalytic subunit p125, which directly interacts with p12 (Figure 1D, lanes 3 and 4). As expected from previous analyses, BLM and hPOL δ showed a punctate nuclear pattern of localization (15,25,34). Representative images of the staining patterns are depicted in Figure 7A and B. The degree of co-localization of nuclear foci was then scored. This analysis indicated a low degree of co-localization in an untreated asynchronous cell population, which increased in response to HU treatment (Supplementary Figure 5). This increase in the extent of co-localization might be restricted to S phase or might be an effect of the HU-induced replication perturbation. To address this, we took advantage of the BrdU labeling of the actively replicating cells. When only the BrdU-positive subpopulation was scored in the untreated cultures, the degree of co-localization was similar to that of the whole asynchronous population. These results suggest that BLM and hPOL δ co-localize only to a limited extent *in vivo*, even during an unperturbed S phase, but that perturbation of DNA replication causes an increase in their co-localization. Nevertheless, even after treatment of cells with HU, most BLM and hPOL δ foci still did not co-localize, indicating that a significant fraction of BLM remains distant from sites of stalled replication forks.

DISCUSSION

We have shown that the BS helicase, BLM and the major replicative DNA polymerase, hPOL δ, interact specifically *in vitro* and *in vivo*. This interaction is direct and is mediated via the thus far poorly characterized p12 subunit of hPOL δ. We mapped the site of interaction of BLM with p12 to a region representing amino acids 447–770. This fragment includes the N-terminal part of the BLM helicase domain and it has been shown previously that this is involved in interaction with the WRN helicase (35). In addition, we mapped the region of p12 that interacts with BLM to a short fragment comprising amino acids 30–60. Database searches revealed that this p12 fragment does not represent any known conserved protein domain and

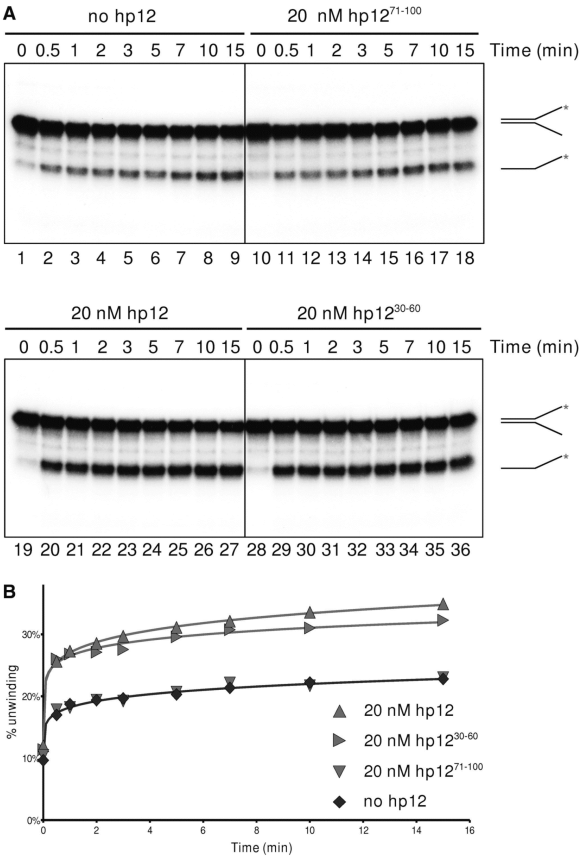

Figure 5. The stimulatory effect of p12 can be localized to a small peptide, spanning the region that binds BLM. (**A**) A total of 0.85 nM BLM was incubated at 37°C for 5 min alone (lanes 1–9), or with 20 nM $p12^{71–100}$ (a peptide that shows no binding to BLM; lanes 10–18), full length p12 (lanes 19–27) or $p12^{30–60}$ (a peptide that spans the binding region to BLM; lanes 28–36). Reactions were run as in Figure 4B. (**B**) Quantification of data from (A).

that it shows no sequence homology to any known BLM interacting partner. Of most importance, we have also shown that BLM and hPOL δ can functionally associate in that their interaction leads to stimulation of the BLM helicase activity and hPOL δ strand displacement activity.

There are a number of possible scenarios in DNA replication/repair where the productive co-operation of BLM and hPOL δ might be advantageous. Perhaps the most plausible is during the process of fork regression under circumstances where a replication fork is arrested by a DNA adduct or another blockade, particularly those that block leading strand synthesis. We have shown recently that BLM can promote the regression of a model replication fork *in vitro* (36). This may be a reaction that is beneficial for DNA repair simply because, through promoting fork back-tracking, it allows access to the blocking 'lesion'. However, there is also potential for fork regression to be important in a lesion bypass pathway of DNA damage tolerance. If the lesion blocks leading strand synthesis, it appears that the synthesis of the

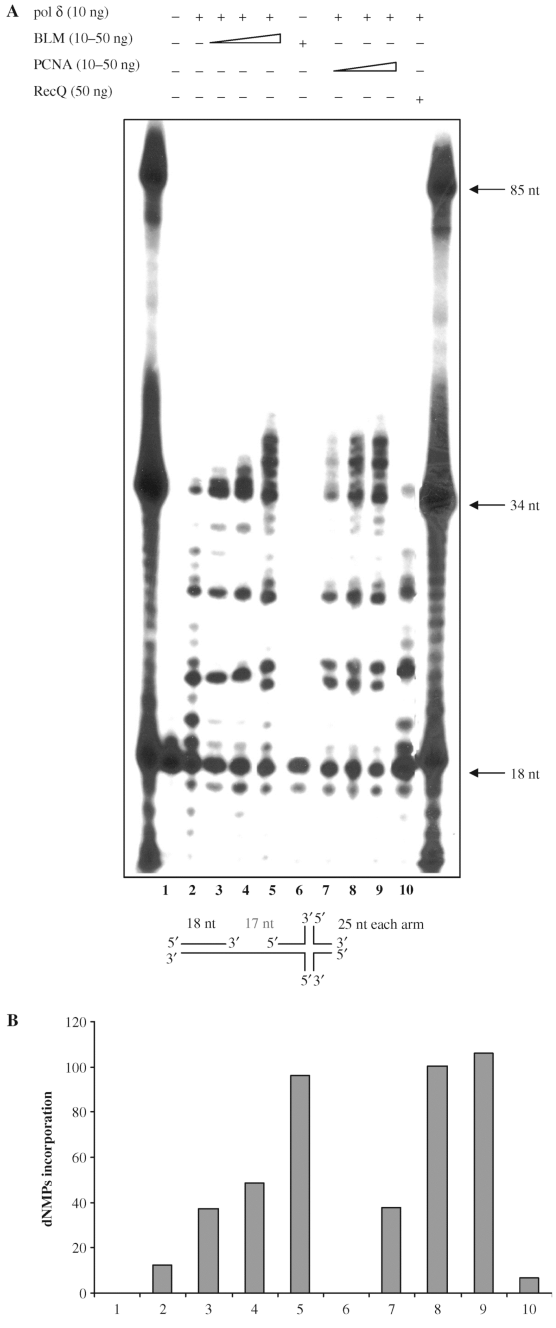

Figure 6. BLM stimulates hPOL δ strand displacement activity. (**A**) Ten nanogram of hPOL δ alone (lane 2) or in the presence of an increasing amount (10, 20 or 50 ng) of BLM (lanes 3–5), PCNA (lanes 7–9) or 50 ng of *E. coli* RecQ (lane 10) were tested in primer extension assays using the X-poly DNA template as described in Materials and methods section. Eighteen-nucleotide primer was 5′ end labeled. Lane 6 contains 50 ng of BLM alone and shows that BLM does not have DNA polymerase activity. Lane 1: substrate alone; positions of oligonucleotide size-markers are indicated. Schematic representation of the X-poly DNA template is shown. The limit of extension is indicated with the arrow. (**B**) Quantification of products longer than 34 nt from (A).

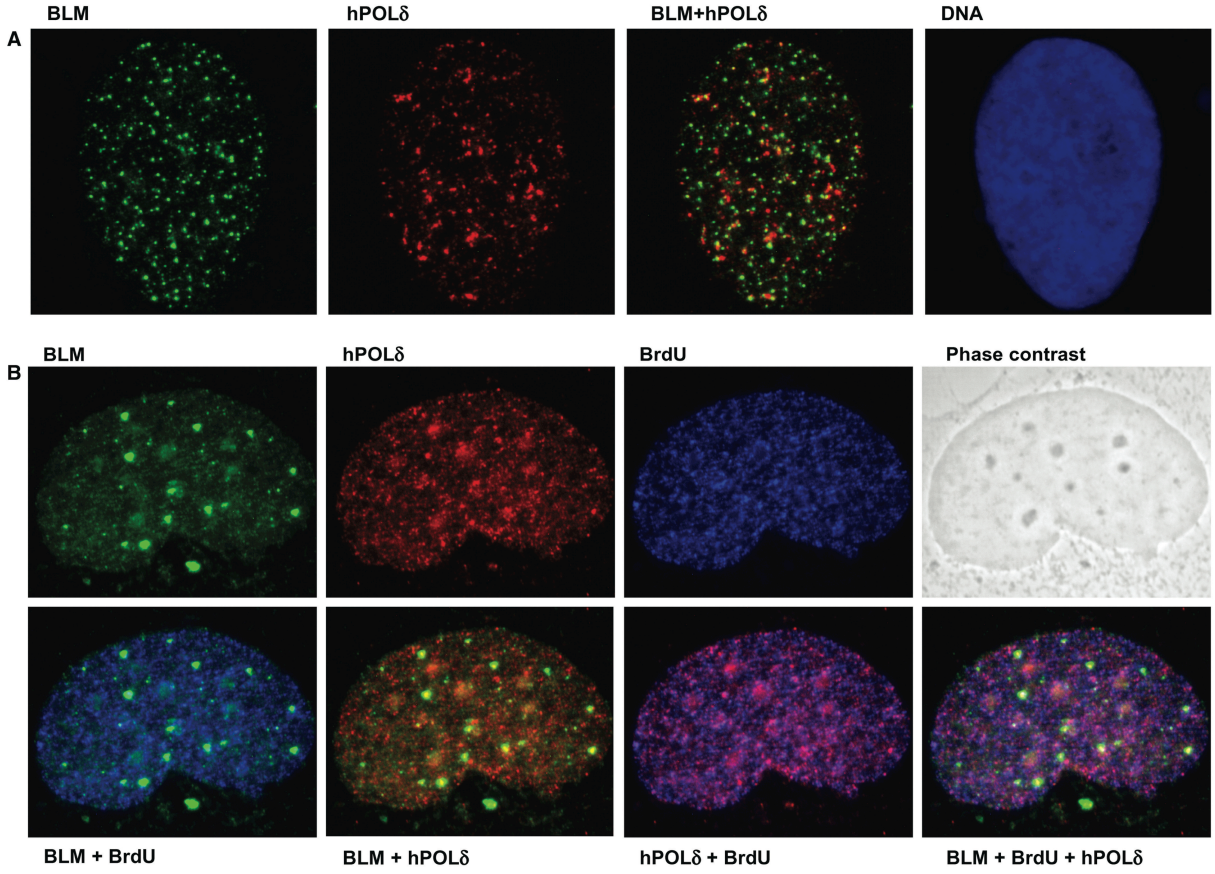

Figure 7. Dual staining for BLM and hPOL δ suggests co-localization *in vivo*, which is stimulated during replicative stress. (**A**) GM00637 cells were arrested with 2.5 mM HU, and were stained as described in Materials and methods section. A representative image showing punctate BLM (green, left) and hPOL δ (red, second from left) staining. Coincidence of the green and red signals (yellow signal) suggests co-localization of the two proteins. The right panel shows the nucleus of the same cell stained with the DNA dye Hoechst 33258. (**B**) GM00637 cells grown on coverslips without HU treatment and were pulse-labeled with 25 μM BrdU for 5 min, and then stained as described in Materials and methods section. Representative images show staining of the same nucleus for BLM in green (top left), for hPOL δ in red (top, second from left), for BrdU in blue (top, second from right). Phase contrast image of the same nucleus is depicted on the top right. In the bottom row, combined images of the individual stainings from the top row are shown. As expected, the BrdU signal correlates well with the signal for hPOLδ (magenta-color pattern second panel from bottom right). The coincidence of BLM signal with either BrdU (cyan signal in bottom left) or hPOLδ (yellow signal in second panel from bottom left) is less pronounced.

lagging strand may continue for some distance ahead of the site of the blocked leading strand. This apparently futile uncoupling of leading and lagging strand synthesis has the potential, after fork regression, to permit template switching with the shorter leading strand being extended by copying of the longer lagging strand template. In this way, once the regressed fork is reset, the leading strand would be extended beyond the site of the lesion and normal DNA replication could commence. hPOL δ might both recruit BLM to stalled forks and then stimulate its catalytic activity once there. Conversely, BLM might play a role in assisting hPOL δ to access the regressed '4th arm' and catalyse extension of the leading strand.

It has been suggested that RecQ helicases together with the type 1A topoisomerase, Top3, act at damaged replication forks to resolve recombination structures likely resulting from template switching (37). We suggest that BLM plays a dual role in rescuing arrested replication forks. One function is in assisting POL δ to bypass DNA lesions via fork regression and template switching, and the second function of BLM is to resolve the resulting pseudo double Holliday junction with a help of Top3. These two functions of BLM may be independent of each other.

A striking feature of the ability of hPOL δ to stimulate the helicase activity of BLM was our finding that a short peptide (aa 30–60) representing the minimal binding region of p12 is as efficient in this stimulatory role as is the hPOL δ enzyme. This would seem to rule out many possible mechanisms for the stimulation, including recruitment of BLM to the DNA substrate. Instead, these results argue for hPOL δ acting to alter the conformation of BLM in such a way as to enhance its helicase function.

Such a mechanism is further supported by the unusual reaction progress curves: after an initial burst of activity the reaction very quickly reaches its maximum without attaining 100% unwinding. Unwinding by helicases is believed to be a multi-step process: (i) changes of the quaternary structure of the enzyme alter its binding specificity; (ii) the enzyme binds to the substrate with an increased affinity; (iii) DNA binding initiates ATP hydrolysis; and (iv) unwinding commences. Under our single turnover unwinding conditions, we postulate that the rate-limiting step is the activation of the helicase. We postulate that hPOL δ facilitates these structural changes, and when the enzyme is mixed with its substrates (DNA and ATP) it is already in its active conformation ready to initiate unwinding immediately upon binding. Furthermore, hPOL δ also increases the extent of unwinding by BLM. This increase might be a consequence of increased processivity of the helicase, which in turn might also be the result of conformational changes initiated by hPOL δ. A major goal for the future will be to characterize in molecular detail how exactly this stimulation occurs, and how this short peptide can have such a marked effect on the BLM helicase.

Our data indicate that BLM and hPOL δ do not significantly co-localize in the nucleus of human cells under normal growth conditions, including within an unperturbed S phase. This is consistent with the known localization of BLM to PML bodies and not to sites of ongoing replication. However, we were able to detect a consistent increase in the percentage of nuclear BLM foci that co-localize with hPOL δ when cells were treated with HU. Taken together, these data indicate that this association at replication foci is driven by replication perturbation and not by cell-cycle phase *per se*. To support these results, we could show direct association of BLM with the p12 subunit of hPOL δ *in vivo* in cells which were synchronized in S phase by HU treatment. No interaction between BLM and p12 could be observed in unsynchronized cells. Our data showing that BLM and p12 co-immunoprecipitate from the nuclear extracts of the 293T cells after treatment with 1 mM HU seemingly contrast with the recent data of Zhang and colleagues (38), who reported that, in HeLa and 293T cells, p12 undergoes ubiquitination and degradation 20 h after the treatment with 2 mM HU. These differences are possibly the result of the different HU concentrations that have been employed in these two studies. Alternatively, it may well be that binding of BLM to p12 prevents p12 ubiquitination and degradation, which is the reason why we did not observe degradation of p12 in our experiments.

We have also shown that BLM, similar to PCNA (39,40), promotes the strand displacement activity of hPOL δ. BLM might help hPOL δ to traverse short regions of DNA secondary structure during the process of DNA replication, but we have no direct evidence for this and such a possibility still needs to be investigated. However, we could not observe any effect of BLM on hPOL δ polymerase activity on a simple primer/template substrate. It has been shown previously that WRN has a stimulatory effect on the polymerization activity of *Saccharomyces cerevisiae* POL δ in the absence of PCNA (41). However, WRN does not apparently have an effect on DNA synthesis catalysed by the POL δ-PCNA complex. These results suggest that WRN may not function in processive DNA synthesis reactions during normal DNA replication; instead, WRN may function in replication restart of stalled or collapsed replication forks from which the replication machinery has dissociated (41).

Our current hypothesis is that BLM may, in a similar manner to WRN, be involved in replication restart of stalled replication forks blocked by DNA damage or unusual secondary structures in DNA template (42). One such scenario is during the replication of ribosomal DNA in the nucleolus. Similar to telomeres, ribosomal DNA is GC rich and can adopt alternative DNA structures such as hairpins and G-quadruplexes. These structures are efficiently resolved *in vitro* by BLM and WRN (13,43 45). When overexpressed in HeLa cells, WRN can recruit the p50 and p125 subunit of hPOL δ from nucleoplasm to the nucleolus (46). In an unperturbed cell cycle, BLM is found primarily in PML nuclear bodies, except during late S phase when it co-localizes with WRN in the nucleolus (16). Additionally, BLM binds to ribosomal DNA and primarily at the non-transcribed spacer region where replication forks initiate (47). These findings suggest that BLM may be directly coupled to replication fork initiation and/or progression at particular sites of DNA synthesis. The fact that BLM and hPOL δ co-localize more prominently after blockade of replication, but that not all replication foci contain BLM under these conditions, suggests that BLM may be recruited to sites of DNA synthesis only in response to the formation of a particular DNA structure that needs BLM helicase function for its resolution. It will be interesting to address in the future whether BLM is recruited to hPOL δ foci only following posttranslational modification of one or both of these factors, or whether the association is mediated by other replication factors to which BLM binds, such as RPA (21).

SUPPLEMENTARY DATA

Supplementary Data are available at NAR Online.

ACKNOWLEDGEMENTS

We thank Pavel Janscak for the gift of purified recombinant WRN, Vladimir Podust for the gift of recombinant baculoviruses encoding the hPOL δ subunits, and Grant Brown for critical reading of the article and helpful discussions. C.Z.B. and I.D.H. are supported by Cancer Research UK. N.S. was supported by a Swiss National Foundation Grant (Nr. 3100A0-100256/1) to I.S. The Stagljar lab is supported by grants from the Canadian Foundation for Innovation (CFI), the Canadian Institute for Health Research (CIHR), the National Cancer Institute of Canada (NCIC), Gebert Rüf Foundation, Genentech, and Novartis. Funding to pay the Open Access publication charges for this article was provided by the National Cancer Institute of Canada (NCIC).

Conflict of interest statement. None declared.

REFERENCES

1. Bell,S.P. and Dutta,A. (2002) DNA replication in eukaryotic cells. *Annu. Rev. Biochem.*, **71**, 333–374.
2. Hubscher,U., Maga,G. and Spadari,S. (2002) Eukaryotic DNA polymerases. *Annu. Rev. Biochem.*, **71**, 133–163.
3. Liu,L., Mo,J., Rodriguez-Belmonte,E.M. and Lee,M.Y. (2000) Identification of a fourth subunit of mammalian DNA polymerase delta. *J. Biol. Chem.*, **275**, 18739–18744.
4. Maga,G. and Hubscher,U. (2003) Proliferating cell nuclear antigen (PCNA): a dancer with many partners. *J. Cell Sci.*, **116**, 3051–3060.
5. Li,H., Xie,B., Zhou,Y., Rahmeh,A., Trusa,S., Zhang,S., Gao,Y., Lee,E.Y. and Lee,M.Y. (2006) Functional roles of p12, the fourth subunit of human DNA polymerase delta. *J. Biol. Chem.*, **281**, 14748–14755.
6. Podust,V.N., Chang,L.S., Ott,R., Dianov,G.L. and Fanning,E. (2002) Reconstitution of human DNA polymerase delta using recombinant baculoviruses: the p12 subunit potentiates DNA polymerizing activity of the four-subunit enzyme. *J. Biol. Chem.*, **277**, 3894–3901.
7. Liu,G. and Warbrick,E. (2006) The p66 and p12 subunits of DNA polymerase delta are modified by ubiquitin and ubiquitin-like proteins. *Biochem. Biophys. Res. Commun.*, **349**, 360–366.
8. Bachrati,C.Z. and Hickson,I.D. (2003) RecQ helicases: suppressors of tumorigenesis and premature aging. *Biochem. J.*, **374**, 577–606.
9. Opresko,P.L., Cheng,W.H. and Bohr,V.A. (2004) At the junction of RecQ Helicase biochemistry and human disease. *J. Biol. Chem.*, **279**, 18099–18102.
10. Hickson,I.D. (2003) RecQ helicases: caretakers of the genome. *Nat. Rev. Cancer*, **3**, 169–178.
11. Ray,J.H. and German,J. (1983) The cytogenetics of the chromosome-breakage syndromes. In German,J. (ed.), *Chromosome Mutation and Neoplasia*, Alan R. Liss, Inc, New York, pp. 135–168.
12. Karow,J.K., Chakraverty,R.K. and Hickson,I.D. (1997) The Bloom's syndrome gene product is a 3′-5′ DNA helicase. *J. Biol. Chem.*, **272**, 30611–30614.
13. Mohaghegh,P., Karow,J.K., Brosh,R.M. Jr, Bohr,V.A. and Hickson,I.D. (2001) The Bloom's and Werner's syndrome proteins are DNA structure-specific helicases. *Nucleic Acids Res.*, **29**, 2843–2849.
14. Bachrati,C.Z., Borts,R.H. and Hickson,I.D. (2006) Mobile D-loops are a preferred substrate for the Bloom's syndrome helicase. *Nucleic Acids Res.*, **34**, 2269–2279.
15. Bischof,O., Kim,S.H., Irving,J., Beresten,S., Ellis,N.A. and Campisi,J. (2001) Regulation and localization of the Bloom syndrome protein in response to DNA damage. *J. Cell Biol.*, **153**, 367–380.
16. Yankiwski,V., Marciniak,R.A., Guarente,L. and Neff,N.F. (2000) Nuclear structure in normal and Bloom syndrome cells. *Proc. Natl Acad. Sci. USA*, **97**, 5214–5219.
17. Lillard-Wetherell,K., Machwe,A., Langland,G.T., Combs,K.A., Behbehani,G.K., Schonberg,S.A., German,J., Turchi,J.J., Orren,D.K. and Groden,J. (2004) Association and regulation of the BLM helicase by the telomere proteins TRF1 and TRF2. *Hum. Mol. Genet.*, **13**, 1919–1932.
18. Wu,L. and Hickson,I.D. (2006) DNA helicases required for homologous recombination and repair of damaged replication forks. *Annu. Rev. Genet.*, **40**, 279–306.
19. Hand,R. and German,J. (1975) A retarded rate of DNA chain growth in Bloom's syndrome. *Proc. Natl Acad. Sci. USA*, **72**, 758–762.
20. Lönn,U., Lönn,S., Nylen,U., Winblad,G. and German,J. (1990) An abnormal profile of DNA replication intermediates in Bloom's syndrome. *Cancer Res.*, **50**, 3141–3145.
21. Brosh,R.M. Jr, Li,J.L., Kenny,M.K., Karow,J.K., Cooper,M.P., Kureekattil,R.P., Hickson,I.D. and Bohr,V.A. (2000) Replication protein A physically interacts with the Bloom's syndrome protein and stimulates its helicase activity. *J. Biol. Chem.*, **275**, 23500–23508.
22. Sharma,S., Sommers,J.A., Wu,L., Bohr,V.A., Hickson,I.D. and Brosh,R.M. Jr. (2004) Stimulation of flap endonuclease-1 by the Bloom's syndrome protein. *J. Biol. Chem.*, **279**, 9847–9856.
23. Jiao,R., Bachrati,C.Z., Pedrazzi,G., Kuster,P., Petkovic,M., Li,J.L., Egli,D., Hickson,I.D. and Stagljar,I. (2004) Physical and functional interaction between the Bloom's syndrome gene product and the largest subunit of chromatin assembly factor 1. *Mol. Cell Biol.*, **24**, 4710–4719.
24. Sanz,M.M., Proytcheva,M., Ellis,N.A., Holloman,W.K. and German,J. (2000) BLM, the Bloom's syndrome protein, varies during the cell cycle in its amount, distribution, and co-localization with other nuclear proteins. *Cytogenet. Cell Genet.*, **91**, 217–223.
25. Dutertre,S., Ababou,M., Onclercq,R., Delic,J., Chatton,B., Jaulin,C. and Amor-Gueret,M. (2000) Cell cycle regulation of the endogenous wild type Bloom's syndrome DNA helicase. *Oncogene*, **19**, 2731–2738.
26. Davies,S.L., North,P.S., Dart,A., Lakin,N.D. and Hickson,I.D. (2004) Phosphorylation of the Bloom's syndrome helicase and its role in recovery from S-phase arrest. *Mol. Cell Biol.*, **24**, 1279–1291.
27. Bradford,M.M. (1976) A rapid and sensitive method for the quantitation of microgram quantities of protein utilizing the principle of protein-dye binding. *Anal. Biochem.*, **72**, 248–254.
28. Jiao,R., Harrigan,J.A., Shevelev,I., Dietschy,T., Selak,N., Indig,F.E., Piotrowski,J., Janscak,P., Bohr,V.A. and Stagljar,I. (2007) The Werner syndrome protein is required for recruitment of chromatin assembly factor 1 following DNA damage. *Oncogene*, **26**, 3811–3822.
29. Wu,L., Davies,S.L., North,P.S., Goulaouic,H., Riou,J.F., Turley,H., Gatter,K.C. and Hickson,I.D. (2000) The Bloom's syndrome gene product interacts with topoisomerase III. *J. Biol. Chem.*, **275**, 9636–9644.
30. Pedrazzi,G., Perrera,C., Blaser,H., Kuster,P., Marra,G., Davies,S.L., Ryu,G.H., Freire,R., Hickson,I.D., Jiricny,J. *et al.* (2001) Direct association of Bloom's syndrome gene product with the human mismatch repair protein MLH1. *Nucleic Acids Res.*, **29**, 4378–4386.
31. Petkovic,M., Dietschy,T., Freire,R., Jiao,R. and Stagljar,I. (2005) The human Rothmund-Thomson syndrome gene product, RECQL4, localizes to distinct nuclear foci that coincide with proteins involved in the maintenance of genome stability. *J. Cell Sci.*, **118**, 4261–4269.
32. Bachrati,C.Z. and Hickson,I.D. (2006) Analysis of the DNA unwinding activity of RecQ family helicases. *Methods Enzymol.*, **409**, 86–100.
33. Pedrazzi,G., Bachrati,C.Z., Selak,N., Studer,I., Petkovic,M., Hickson,I.D. and Stagljar,I. (2003) The Bloom's syndrome helicase directly interacts with the human mismatch repair protein MSH6. *Biol. Chem.*, **384**, 1155–1164.
34. Ababou,M., Dutertre,S., Lecluse,Y., Onclercq,R., Chatton,B. and Amor-Gueret,M. (2000) ATM-dependent phosphorylation and accumulation of endogenous BLM protein in response to ionizing radiation. *Oncogene*, **19**, 5955–5963.
35. von Kobbe,C., Karmakar,P., Dawut,L., Opresko,P., Zeng,X.M., Brosh,R.M. Jr, Hickson,I.D. and Bohr,V.A. (2002) Colocalization, physical, and functional interaction between Werner and Bloom syndrome proteins. *J. Biol. Chem.*, **277**, 22035–22044.
36. Ralf,C., Hickson,I.D. and Wu,L. (2006) The Bloom's syndrome helicase can promote the regression of a model replication fork. *J. Biol. Chem.*, **281**, 22839–22846.
37. Liberi,G., Maffioletti,G., Lucca,C., Chiolo,I., Baryshnikova,A., Cotta-Ramusino,C., Lopes,M., Pellicioli,A., Haber,J.E. and Foiani,M. (2005) Rad51-dependent DNA structures accumulate at damaged replication forks in sgs1 mutants defective in the yeast ortholog of BLM RecQ helicase. *Genes Dev.*, **19**, 339–350.
38. Zhang,S., Zhou,Y., Trusa,S., Meng,X., Lee,E.Y. and Lee,M.Y. (2007) A novel DNA damage response: rapid degradation of the p12 subunit of DNA polymerase δ. *J. Biol. Chem.*, **282**, 15330–15340.
39. Podust,V.N. and Hubscher,U. (1993) Lagging strand DNA synthesis by calf thymus DNA polymerases alpha, beta, delta and epsilon in the presence of auxiliary proteins. *Nucleic Acids Res.*, **21**, 841–846.
40. Maga,G., Villani,G., Tillement,V., Stucki,M., Locatelli,G.A., Frouin,I., Spadari,S. and Hubscher,U. (2001) Okazaki fragment processing: modulation of the strand displacement activity of DNA polymerase delta by the concerted action of replication protein A, proliferating cell nuclear antigen, and flap endonuclease-1. *Proc. Natl Acad. Sci. USA*, **98**, 14298–14303.

41. Kamath-Loeb,A.S., Johansson,E., Burgers,P.M.J. and Loeb,L.A. (2000) Functional interaction between the Werner syndrome protein and DNA polymerase δ. *Proc. Natl Acad. Sci. USA*, **97**, 4603–4608.
42. Kamath-Loeb,A.S., Loeb,L.A., Johansson,E., Burgers,P.M.J. and Fry,M. (2001) Interactions between the Werner syndrome helicase and DNA polymerase δ specifically facilitate copying of tetraplex and hairpin structures of the D(CGG)n trinucleotide repeat sequence. *J. Biol. Chem.*, **276**, 16439–16446.
43. Fry,M. and Loeb,L.A. (1999) Human Werner syndrome DNA helicase unwinds tetrahelical structures of the fragile X syndrome repeat sequence d(CGG)n. *J. Biol. Chem.*, **274**, 12797–12802.
44. Huber,M.D., Lee,D.C. and Maizels,N. (2002) G4 DNA unwinding by BLM and Sgs1p: substrate specificity and substrate-specific inhibition. *Nucleic Acids Res.*, **30**, 3954–3961.
45. Sun,H., Karow,J.K., Hickson,I.D. and Maizels,N. (1998) The Bloom's syndrome helicase unwinds G4 DNA. *J. Biol. Chem.*, **273**, 27587–27592.
46. Szekely,A.M., Chen,Y.H., Zhang,C., Oshima,J. and Weissman,S.M. (2000) Werner protein recruits DNA polymerase δ to the nucleolus. *Proc. Natl Acad. Sci. USA*, **97**, 11365–11370.
47. Schawalder,J., Paric,E. and Neff,N.F. (2003) Telomere and ribosomal DNA repeats are chromosomal targets of the bloom syndrome DNA helicase. *BMC Cell Biol.*, **4**, 15.